

Sheffield Hallam University

Chemical/thermal modification of poly(vinyl alcohol) film for enhanced water vapour barrier properties.

TRINH, Pham Thi Doan.

Available from the Sheffield Hallam University Research Archive (SHURA) at:

<http://shura.shu.ac.uk/20225/>

A Sheffield Hallam University thesis

This thesis is protected by copyright which belongs to the author.

The content must not be changed in any way or sold commercially in any format or medium without the formal permission of the author.

When referring to this work, full bibliographic details including the author, title, awarding institution and date of the thesis must be given.

Please visit <http://shura.shu.ac.uk/20225/> and <http://shura.shu.ac.uk/information.html> for further details about copyright and re-use permissions.

Assets Centre, City Campus
Sheffield S1 1WD

102 156 539 3



SHEFFIELD HALLAM UNIVERSITY
ADSETTS LEARNING CENTRE
CITY CAMPUS, SHEFFIELD
S1 1WB

REFERENCE

ProQuest Number: 10700870

All rights reserved

INFORMATION TO ALL USERS

The quality of this reproduction is dependent upon the quality of the copy submitted.

In the unlikely event that the author did not send a complete manuscript and there are missing pages, these will be noted. Also, if material had to be removed, a note will indicate the deletion.



ProQuest 10700870

Published by ProQuest LLC (2017). Copyright of the Dissertation is held by the Author.

All rights reserved.

This work is protected against unauthorized copying under Title 17, United States Code
Microform Edition © ProQuest LLC.

ProQuest LLC.
789 East Eisenhower Parkway
P.O. Box 1346
Ann Arbor, MI 48106 – 1346

**Chemical/Thermal Modification of
Poly(vinyl alcohol) Film for Enhanced Water
Vapour Barrier Properties**

Pham Thi Doan Trinh

A thesis submitted in partial fulfilment of the requirements of
Sheffield Hallam University
for the degree of Doctor of Philosophy

November 2015

DECLARATION

The work described in this thesis was carried out by the author in the Materials and Engineering Research Institute at Sheffield Hallam University, between March 2012 and April 2015. The author declares that this work has not been submitted for any other degree. The work is original except where acknowledged by reference.

Author

Director of Studies

(Pham Thi Doan Trinh)

(Dr. Francis Clegg)

ABSTRACT

Within the packaging industry, the increasing demand for sustainable packaging is driving research towards renewable coating materials for paper or paperboard with high barrier properties against gas, water vapour and odours. Poly(vinyl alcohol) (PVOH), a water soluble and biodegradable polymer, is a real option for sustainable packaging when applied as either a coating for paper and paperboard packaging or an independent packaging film. Since its application is limited in high humid environments, several modification methods including chemical crosslinking with glutaraldehyde (GA), salt treatment with sodium sulphate solution, heat treatment and nanoclay incorporation have been investigated in order to improve its barrier to water vapour and also thermal stability and mechanical properties. An extensive range of crosslinking times between GA and PVOH have been assessed. The crosslinked PVOH and salt treated films show an improvement in water vapour barrier properties by 60-70%. Whereas, heat treatment and clay addition show an improvement of 20-57%, in which the water vapour barrier properties increase with increasing heat treatment temperatures (40°C to 180°C) or clay contents (5 to 20 wt%). Additionally, crosslinking PVOH/Clay films with GA improves their water vapour barrier properties comparable to those of crosslinked PVOH films. Apart from the heat treated films, all the modified PVOH films possess higher thermal stability than neat PVOH films as evidenced by thermogravimetric analysis measurements. Combinations between heat treatment and crosslinking with GA as well as crosslinking on one side of PVOH films have been investigated. The films annealed at 180°C prior to crosslinking on both sides do not dissolve in hot water (90°C) even with short crosslinking time (5 minutes) and their water vapour barrier properties derive mainly from their enhanced crystallinity. The respective one-side crosslinked PVOH films show comparable water vapour barrier properties and thermal stability, but were dissolvable in hot water.

The diffusion of crosslinking solution into the PVOH films has been studied using in-situ FTIR. It has been shown that the crosslinking solution can rapidly penetrate and diffuse from the top to the bottom of the film (50-60 μm).

The crystallinity of PVOH films after subjection to different modification methods have been investigated using various techniques, including FTIR, Raman and XRD. It has been shown that the crystallinity increases with heat treatment whilst decreases after crosslinking with GA. On the contrary, treating PVOH films with sodium sulphate solution for different lengths of time did not change the crystallinity of the films. When clay is present in PVOH films with 5 wt%, the crystallinity is not affected but increases slightly and significantly with 10 and 20 wt% clay loading, respectively.

ACKNOWLEDGEMENT

First and foremost, I would like to express my sincere appreciation and thanks to my Director of Studies, Dr. Francis Clegg. Thank you for his advice, guidance, patience and persistent mentoring from the beginning until present. He always had time for me whenever I was struggling with my experiments, instruments or even with a scientific paper. He was also my English teacher and usually corrected my pronunciation as well as academic writing. It is him who nurtured my love of Peak District National Park and developed my knowledge about life and people in the UK. I also would like to thank Joanne for her kindness and friendliness when organised some trips to the Peak District with her and Francis in order to help me and friends release stress at work. Thank you Francis and Joanne!

I would also like to thank my second supervisor, Chris Breen, for his support and helping me evaluate my results from different angles. A big thank you is also directed to PCAS group for interesting and helpful discussions, advice in group seminars. Thank you Prof. Chris Sammon, Vicky, Hakan, Nikita! Especially, I would like to thank my two best friends Thomas and Kerstin for their encouragements and supports as well as happiness and sadness sharing during my PhD study. I feel lucky when having them with me in MERI.

For the technical support, I would like to thank Deeba and Bob. I will miss Deeba's morning salutation: "Hi Trinh! Are you alright?". I would also like to thank Oliver for training me the contact angle measurement and gave me opportunities to work for the university on Opening days.

Thank you MERI admin team for their helps and supports which made me feel comfortable during the time doing my PhD here.

Sincere thanks are sent to Daniel Loch, who is considered as a big brother among our friends. I never forget the first time I met him in our student office and he helped me to solve quickly all issues related to my settling in a new place. Thank you for his encouragement during my writing up time. Anna, Tom, Ronak,

Barnali, Paranjayee, Dignesh, Arun, Chinh and other friends and staffs in MERI, thank you for all the times we were hanging out together.

Pursuing a PhD in a foreign country is not easy since I was living far away from my family which sometimes made me feel very lonely. Thank you all my Vietnamese friends, whom I cannot list out all the names here, who were with me to cheer me up when I was in a bad mood or to share good food, beautiful sightseeing and happiness with me. I also would like to thank Ms Phuong Nguyen, my aunt-in-law, for her kindness to sponsor my stays and good food whenever I came to London.

Most importantly, I would like to thank Vietnamese Government who sponsored my study in the UK to pursuit a higher academic degree. Thank you VIED staff for your help and support during the time I was studying.

Above all, I would like to express my deepest gratitude and appreciation to my family and family-in-law as well as my husband, Thien Nguyen and my son, Minh Quan. Thank you my parent-in-law for taking care of my son during the time I was away and not with him. Thank you for always being my side and for your considerations. Thank you my father, mother, brothers and sisters for their encouragement. Also, thank you my husband for his love and endless supports and encouragements that without them, I cannot accomplish my thesis.

AWARD

❖ Runner up (2nd prize award) of the best PhD student talk - MERI symposium, Sheffield Hallam University, 13-14 May, 2014

ADVANCED STUDIES

❖ Research method units:

- English for research students
- MATLAB
- Project planning and management
- Laboratory management and operation training
- Finding information: data base and other online resources
- RefWorks: managing the information you find
- Health and Safety training: Fume cupboard/ Lab safety training
- e-Portal training.

❖ Associate lecturer course

❖ Workshop on advanced measurement technique (FTIR, SEM, X-ray, AFM)

❖ Thermal analysis training by Mettler Toledo, Manchester, 15 October, 2013

❖ Group seminars of the Polymer, Composites and Spectroscopy (PCAS) group within Materials, Engineering and Research Institute

❖ MERI seminars

ATTENDED CONFERENCES

- ❖ MERI symposium day - Sheffield Hallam University, 19-20 May, 2015.
- ❖ PhD and Knowledge transfer programme event - Sheffield Hallam University, 11 Mar, 2015, Poster presentation.
- ❖ BMRC/ MERI winter poster event - Sheffield Hallam University, 11 December, 2014, Poster presentation.
- ❖ MERI symposium day - Sheffield Hallam University, 13-14 May, 2014, Oral presentation.
- ❖ COST Action FB1003 meeting - Sheffield Hallam University, 05-06 March, 2014
- ❖ IRDG (204th) Christmas meeting and Poster session - University College London, 19 December, 2013, Poster presentation.
- ❖ BMRC/ MERI winter poster event - Sheffield Hallam University, 17 December, 2013, Poster presentation.
- ❖ POLYMAR 2013 for Early stage researchers - Barcelona, Spain, 3-7 November, 2013, Oral presentation.
- ❖ NewGenPak Optional Scientific training - Clay nanocomposite - Sheffield Hallam University, 12-13 September, 2013
- ❖ MacroGroup Young Researcher Meeting - Nottingham University, UK, 24-25 June, 2013, Poster presentation.
- ❖ Clay Minerals Group meeting (part of The Mineralogical Society of Great Britain and Ireland) - Durham University, UK, 26 March, 2013
- ❖ 7th Annual Meeting, RSC Biomaterials Chemistry Group - Sheffield Hallam University, 08-09 January, 2013
- ❖ BMRC/ MERI winter poster event - Sheffield Hallam University, 19 December, 2012, Poster presentation.
- ❖ MERI seminar day - Sheffield Hallam University, 21 June, 2012, Poster presentation.

CONTENTS

CHAPTER 1 Introduction	1
1.1 OVERVIEW	1
1.2 AIMS AND OBJECTIVES.....	7
CHAPTER 2 Theoretical aspects and characterisation methods	11
2.1 THEORETICAL ASPECTS OF MATERIALS AND TREATMENT METHODS USED	11
2.1.1 Poly(vinyl alcohol) (PVOH)	11
2.1.2 Glutaraldehyde and crosslinking reaction with PVOH	16
2.1.2.1 Glutaraldehyde (GA)	16
2.1.2.2 Crosslinking reaction between GA and PVOH	17
2.1.3 Sodium sulphate and its influence on the properties of PVOH.....	20
2.1.4 Heat treatment of PVOH	23
2.1.5 Montmorillonite (MMT) and PVOH/ MMT Nanocomposites	26
2.1.5.1 Montmorillonite (MMT).....	26
2.1.5.2 PVOH and Montmorillonite nanocomposites	28
2.1.6 Polyethylene glycol (PEG) as plasticiser	31
2.2 CHARACTERISATION METHODS	33
2.2.1 Water vapour transmission rate (WVTR)	33
2.2.2 Swelling test in water	37
2.2.3 Fourier transform infrared spectroscopy (FTIR).....	38
2.2.4 Raman spectroscopy	42
2.2.5 X-ray diffraction (XRD).....	45
2.2.6 Thermogravimetric analysis (TGA)	47
2.2.7 Dynamic mechanical analysis (DMA)	49
2.2.8 Contact angle measurement (CA)	51

CHAPTER 3 Crosslinking reaction between PVOH films and glutaraldehyde, and the effects of salt treatment on PVOH films	54
3.1 EXPERIMENTAL	54
3.1.1 PVOH film preparation	54
3.1.2 Crosslinking reaction between PVOH films and GA.....	55
3.1.3 Salt treatment of PVOH films	56
3.2 CHARACTERISATION METHODS	56
3.3 EFFECTS OF FILM THICKNESS, POLYMER MOLECULAR WEIGHT AND RELATIVE HUMIDITY ON THE WATER VAPOUR TRANSMISSION RATES (WVTR) OF PVOH FILMS	57
3.3.1 Effect of film thickness	57
3.3.2 Effect of molecular weight	60
3.3.3 Effect of relative humidity on WVTR of PVOH films.	62
3.3.4 Summary	63
3.4 CROSSLINKING REACTION BETWEEN PVOH FILMS AND GLUTARALDEHYDE.....	64
3.4.1 Changes in weight and thickness after crosslinking reactions	64
3.4.2 Degree of crosslinking (dCR).....	66
3.4.3 WVTR results.....	67
3.4.4 WVTR results of crosslinked films in different RH environments.....	69
3.4.5 Moisture content and swelling test results	71
3.4.6 Contact angle results	73
3.4.7 FTIR results.....	75
3.4.8 Raman spectroscopy results	80
3.4.9 XRD results	83
3.4.10 DMA results	86
3.4.11 Discussion	91
3.4.12 Summary	95

3.5 EFFECT OF SODIUM SULPHATE ON THE PROPERTIES OF PVOH FILMS	96
3.5.1 WVTR results	96
3.5.2 Swelling test results	97
3.5.3 FTIR results	97
3.5.4 Raman results	99
3.5.5 XRD results	100
3.5.6 DMA results	101
3.5.7 Discussion	103
3.6 CONCLUSIONS	105
CHAPTER 4 Heat treatment of poly(vinyl alcohol) films combined with chemical crosslinking	106
4.1 EXPERIMENTAL	106
4.1.1 Heat treatment of PVOH films	106
4.1.2 Heat treatment of high molecular weight PVOH and crosslinking reaction with GA	107
4.1.3 One-side crosslinking of PVOH31 films	107
4.1.3.1 In-situ FTIR measurements of crosslinking reaction	107
4.1.3.2 One-side crosslinking of PVOH31 films	108
4.2 CHARACTERISATION	109
4.2.1 Dissolution test	109
4.2.2 The other tests	109
4.3 EFFECT OF HEAT TREATMENT ON THE PROPERTIES OF PVOH FILMS	111
4.3.1 Dissolution test results	111
4.3.2 Swelling test results	112
4.3.3 Water vapour transmission rates (WVTR)	112
4.3.4 TGA results (water content)	113
4.3.5 Contact angle results	114
4.3.6 FTIR results	115

4.3.7 Raman results	119
4.3.8 X-ray diffraction.....	120
4.3.9 DMA results	123
4.3.10 Discussion	126
4.3.11 Summary	127
4.4 HEAT TREATMENT OF HIGH MOLECULAR WEIGHT PVOH AND CROSSLINKING REACTION WITH GLUTARALDEHYE.....	127
4.4.1 Heat treatment of PVOH124.	127
4.4.1.1 WVTR results	127
4.4.1.2 FTIR results	128
4.4.1.3 Discussion.....	130
4.4.2 Effect of combining heat treatment and crosslinking on the water vapour barrier properties of PVOH124.....	132
4.4.3 Summary	135
4.5 ONE-SIDE CROSSLINKING	136
4.5.1 The series FTIR results.....	136
4.5.2 One-side crosslinking of PVOH31	143
4.5.2.1 WVTR results	143
4.5.2.2 Swelling test results	146
4.5.2.3 FTIR results	148
4.5.2.4 Raman results.....	153
4.5.2.5 Discussion.....	155
4.6 CONCLUSION.....	157
CHAPTER 5 The incorporation of bentonite and plasticiser into poly(vinyl alcohol) films and subsequent chemical crosslinking	159
5.1 EXPERIMENTAL	159
5.1.1 PVOH/Clay film preparation.....	159
5.1.2 PVOH/PEG and NaCF10/PEG films preparation	160

5.1.3 Crosslinking reaction of PVOH/Clay, PVOH/PEG and NaCF10/PEG films .	160
5.2 CHARACTERISATION.....	161
5.3 EFFECT OF BENTONITE ON THE PROPERTIES OF PVOH FILMS	162
5.3.1 WVTR results.....	162
5.3.2 Water contact angle results.....	163
5.3.3 FTIR results	164
5.3.4 Raman spectroscopy results	168
5.3.5 XRD results	169
5.3.6 DMA results	170
5.3.7 Discussion	171
5.3.8 Summary	173
5.4 EFFECT OF CROSSLINKING ON THE PROPERTIES OF PVOH/CLAY FILMS	173
5.4.1 Water and water vapour barrier properties.....	173
5.4.2 FTIR results.....	177
5.4.3 Summary	180
5.5 EFFECT OF PLASTICISER ON THE PROPERTIES OF PVOH AND PVOH/CLAY FILMS	180
5.5.1 WVTR results.....	180
5.5.2 Water contact angle results.....	181
5.5.3 FTIR results.....	183
5.5.4 Raman spectroscopy results	185
5.5.5 XRD results	186
5.5.6 DMA results	187
5.5.7 Discussion	189
5.5.8 Summary	190
5.6 EFFECT OF CROSSLINKING ON THE PROPERTIES OF PLASTICISED PVOH AND PVOH/CLAY FILMS.	190
5.6.1 Weight change after crosslinking reaction	190
5.6.2 WVTR results.....	192

5.6.3 Summary	193
5.7 CONCLUSION	193
CHAPTER 6 Thermal stability of PVOH and its modified films	195
6.1 THERMAL STABILITY OF CROSSLINKED PVOH31 FILMS	195
6.2 THERMAL STABILITY OF PVOH31 FILM TREATED WITH SODIUM SULPHATE SOLUTION	198
6.3 THERMAL STABILITY OF ANNEALED PVOH31 FILM	199
6.4 THERMAL STABILITY OF PVOH31 FILMS AFTER BENTONITE AND/OR PLASTICISER WAS INCOPORATED AND SUBSEQUENT CROSSLINKED BY GA	200
6.4.1 Thermal stability of PVOH and crosslinked films containing NaMMT.	200
6.4.2 Effect of plasticiser on the thermal stability of PVOH and PVOH/Clay films.	204
6.5 CONCLUSION	206
CHATER 7 Conclusion and Future work	207
7.1 CONCLUSION	207
7.2 FUTURE WORK	214
REFERENCE	217
APPENDIX 1 Calculations for determining the crosslinking solution volume and degree of crosslinking	233
APPENDIX 2 Permeability coefficient calculation	237
APPENDIX 3 Crystallite size calculation	239

List of Abbreviations

DMA	Dynamic mechanical analysis
FWHM	Full width at half its maximum intensity
FTIR	Fourier transform infrared spectroscopy
GA	Glutaraldehyde
NaMMT	Sodium montmorillonite
PEG	Poly(ethylene glycol)
PVOH	Poly(vinyl alcohol)
PVOH31	PVOH material with a molecular mass of 31,000-50,000 g/mol
PVOH124	PVOH material with a molecular mass of 124,000-186,000 g/mol
RH	Relative humidity
TGA	Thermogravimetric analysis
WVTR	Water vapour transmission rate
XRD	X-ray diffraction

CHAPTER 1

Introduction

1.1 OVERVIEW

In recent years, the term "sustainability" has been widely used in our society. People describe a product or material as sustainable if it is environmentally, economically and socially sustainable [1]. Plastics can be considered as very positive sustainable materials because of their energy savings potential and intrinsic recyclability and energy recovery options. Plastics consume 4% of the world's oil production and use much less energy in their production compared to other materials. In addition, plastics have contributed to economic growth and offered a wide range of worthwhile careers together with training and development. Packaging is the largest end-use sector for plastic [2]. In comparison with other packaging materials, plastics have played very important roles in conventional packaging due to their lightweight, resource efficient and good barrier properties. For example, glass packaging is easily damaged and heavy, paper materials lack transparency as well as water resistance and metal packaging has transparency, damage and weight issues. There are wide varieties of plastics used in packaging such as the thermoplastics (polyethylene, polypropylene, polyvinyl chloride, polystyrene, nylons and polyester) and the thermosets (phenol-formaldehyde resins and glass fibre-reinforced polyesters) [3]. Some plastics used in packaging may be considered more sustainable than others. The problem being that packaging plastics are mainly based on petroleum resources and have triggered concerns within the environment because of their waste disposal problems [4,5]. According to Tolinski [2], the term "sustainability" is commonly used to represent environmental aspects, which relates to the use of renewable and natural materials that have no negative effects on human (or animal and plant) health. Also, any product that accumulates as waste in the environment is classified as unsustainable. The accumulation of plastics in the environment adversely affects land, waterways and oceans and

causes negative effects on wildlife, habitants and humans. In addition, oil resources are not infinite and their availability in nature is on the decrease leading to the increase in material costs. These are driving forces for the packaging industry to seek alternative materials to replace the traditional fossil fuel-based plastics with materials from agriculture and forest (plant starches and sugars, plant oils, plant protein, plants fibres and cellulose, etc.), those synthesised by bacteria (polylactic acid (PLA)) or animals (chitosan). Biopolymers can be divided into three main categories based on their origin which are described in Fig. 1.1 [5,6]

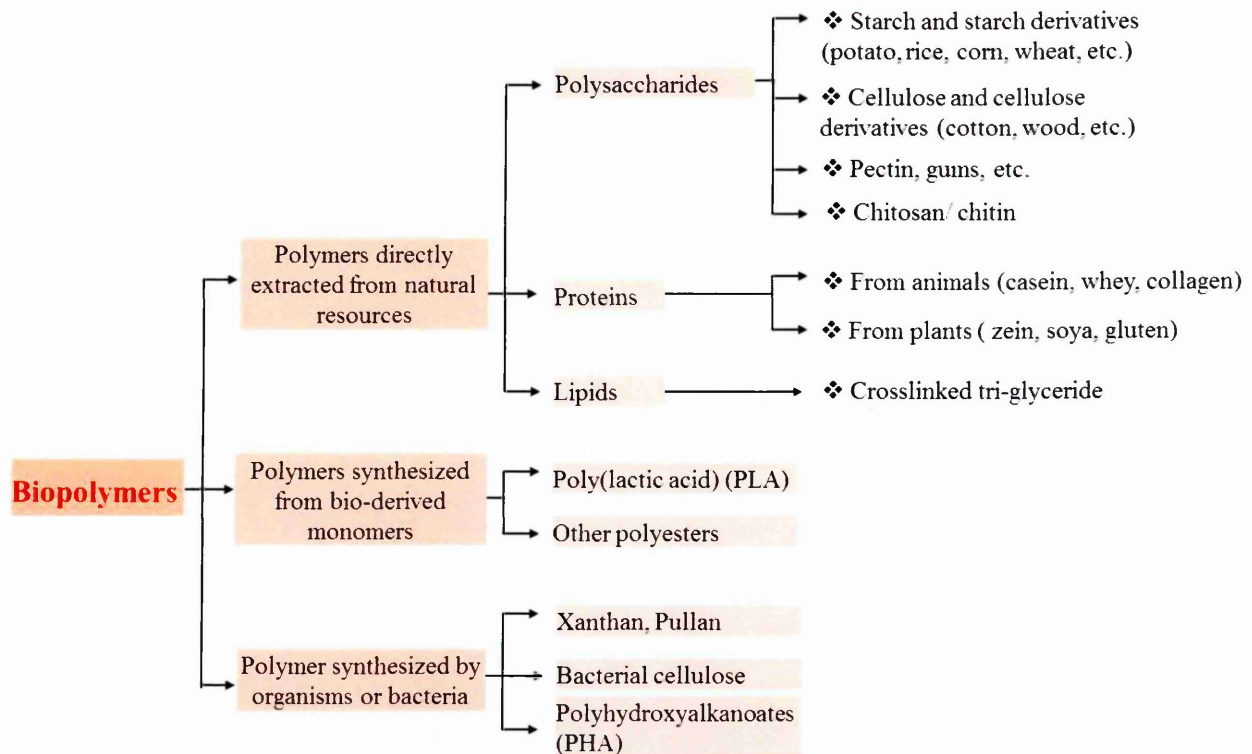


Figure 1.1 Classifications of biopolymers

A statistical report published by the World Packaging Organisation in 2008 stated that paper and paperboard accounted for the largest market share of global packaging materials which was 39% in 2003 [7] and is forecast to be valued at \$213.4 billion by 2020 (at a compound annual growth rate of 3.5% from 2015 to 2020) [8]. Paper and paperboard are also major packaging materials for food products around the world because of their lightweight, biodegradable and

recyclable properties, of which food packaging accounted for 40.7% of the total market in 2014 [8]. Nevertheless, paper has a porous structure, which can allow gas or water vapour to pass through. In food packaging, the barrier properties are focused on oxygen, water vapour and aroma permeability, which all contribute to prolonging the shelf life of food. Paine *et al.* [3] stated that among the vapours and odours which influence the nature of food products, water vapour is generally the most important vapour while flavourings and essential oils are the most important odours. In order to improve the barrier properties of paper against grease, gas, water vapour and odours as well as mechanical properties, it is often coated or laminated with plastics resulting in multi-layered packaging materials [3,5,9]. Typically coating materials are petroleum-based. Ethylene vinyl alcohol (EVOH) has been commonly used as an effective gas barrier as a coated material for paper in food packaging but its application is limited in high humid environments due to its hydrophilic character [5,10-15]. To overcome this issue, polyolefin is added as an additional layer to prevent water sorption [16]. However, these coating materials are petroleum-based and not biodegradable.

The increasing demand for sustainable paper packaging is driving research towards renewable and biodegradable coating materials which can be classified into three groups, including natural polysaccharides (starch, cellulose, chitosan and alginate), proteins (wheat gluten, whey and zein) and polyesters (polycaprolactone, polylactic acid) [13]. Coating materials are chosen depending on the desired functions. For gas and grease barrier properties, whey protein, sodium caseinate, corn zein and wheat gluten can be selected as effective coatings on paper. Paraffin wax or multilayer materials of paraffin wax and other renewable materials are good options for water vapour barrier coatings [12]. Khwaldia [17] was successful in reducing the water vapour permeability of paper coated with sodium caseinate by incorporating an additional paraffin wax layer which was resistant to moisture. Chitosan, a natural polysaccharide and a biodegradable material with excellent gas barrier properties has good compatibility with paper and has been used as paper coating for many years [12,13,18,19]. It is also used within multilayers with other hydrophobic materials, for example carnauba wax, on paper substrates to inhibit water sorption as well

as to preserve the gas barrier properties in relatively high humidity environments [11].

Coatings materials can be removed from paper. The recycling of a zein-wax-coated paper product was reported by Parris *et al.* [20]. The authors demonstrated, by using α -chymotrypsin enzyme to hydrolyse the zein present in the zein-wax-coated Kraft paper, the coating materials could be cleanly removed from the paper fibres (more than 97%). Moreover, Back [21] also reported the removal of dispersed wax under hot alkaline conditions for the recyclable packaging paper materials.

Biopolymers as renewable coatings have been widely developed in recent years although there has been no definitive agreement for their definitions. Biopolymers have been defined as polymeric biomolecules synthesised by living organism [22,23] or, in another description, biopolymers are polymers manufactured from renewable or biological resources using biological or conventional chemical processes [2]. Based on these definitions, biopolymers are not related to any petroleum-based resource. In addition, the property of biodegradability should be taken into account when considering whether a polymer is a biomaterial. The fact is that a fully biobased plastic may be non-biodegradable, and a 100 percent fossil fuel-based plastic can be biodegradable. According to European Bioplastics [24], biopolymers can be either biobased or biodegradable, or both and are classified into three main groups: 1) (partly) biobased resourced and biodegradable such as polylactic acid (PLA) synthesised by fermentation of maize or wheat, or polyhydroxyalkanoates (PHA) produced by bacterial fermentation, 2) fossil fuel resourced and biodegradable such as polycaprolactone (PCL) prepared from polymerisation of caprolactone, a petroleum-derived material [13] and 3) bio-resource and non-biodegradable such as bio-polyethylene (bio PE) manufactured from bioethanol made from various natural feedstock including sugar cane, sugar beet or rice. Fig. 1.2 describes in detail the classification as well as some example polymers.

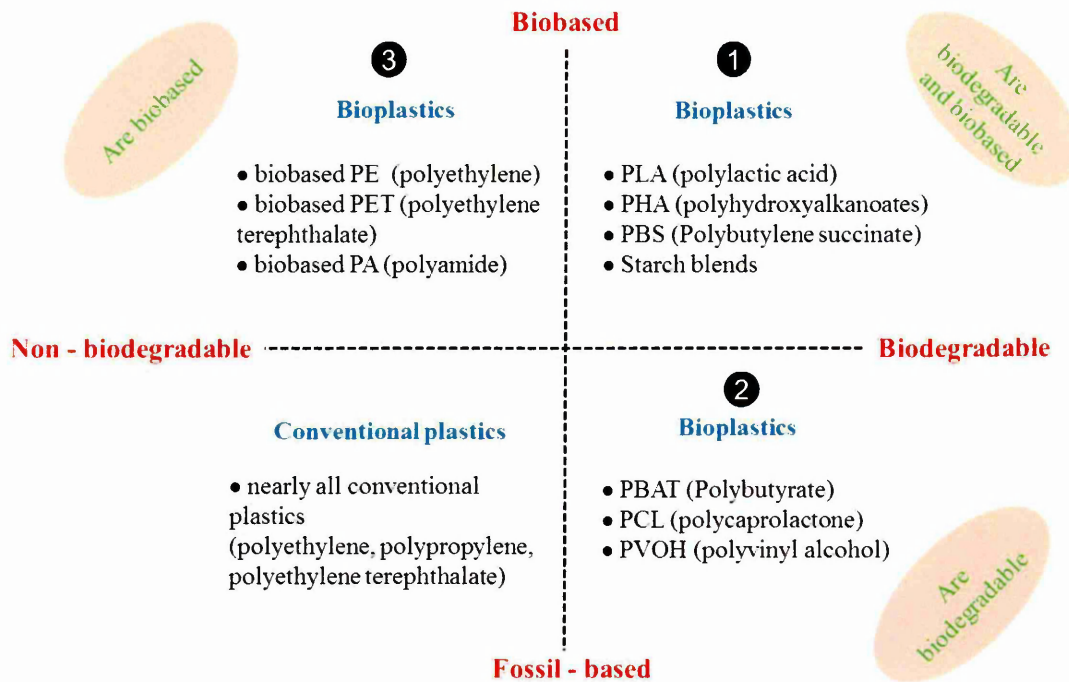


Figure 1.2 Three classified groups of bioplastics compared to the conventional polymers [24]

Poly(vinyl alcohol) (PVOH) is a biodegradable polymer synthesised from poly(vinyl acetate), a petroleum-derived polymer [13,25]. PVOH is soluble in water and has excellent oxygen and aroma barrier properties, and so can keep foods fresher or stop the release of aromatics. Apart from its convenience, performance and safety, the outstanding property that makes PVOH unique is its biodegradability and therefore a real option for sustainable packaging solutions. It has been widely used as water-soluble film or coating since its dissolution rates can be controlled and also optimised for use in hot or cold water [26]. Typical packaging applications can range from high selling commodities such as liquid detergent capsules for automatic dishwashers to anglers' bait bags. In addition, PVOH has been used in the paper industry for a long time as paper adhesives, paper coatings and a good binder for ink jet coating on paper [27]. However, the hydrophilic character of PVOH makes it a poor barrier to water and water vapour which limits its packaging applications [13]. To improve the water vapour barrier properties, PVOH has been modified under different processes. Excelval™ and

Kuraray R-Polymers, trading products of Kuraray Europe, are good examples of PVOH modified with ethylene groups and silanol groups, respectively, which give the films significant water resistance but still maintain the gas and oil barrier properties [28].

PVOH can be crosslinked to create a more tightly-held polymer chain network, thus reducing its swelling properties and the number of pathways for water to navigate through. Chemical cross-linking methods for PVOH have been extensively studied in the field of membrane technology for the selective removal of water from aqueous organic mixtures (pervaporation or permeation) [29]. In membrane technology a relatively small number of cross-links ensure that the structure is maintained and prevents complete dissolution. This reduces the flux of water, but still allows sufficient amounts to pass with high separation factors from attendant organics. An important consequence of the cross-links is that the membranes become more rigid and hydrophilicity is reduced because some of the hydroxyl groups are consumed in the cross-linking process. Non-chemical methods of improving barrier properties includes annealing, this acts to increase crystallinity and thus reduce the permeation of water [30,31]. However effective thermal treatment is problematic since degradation occurs at temperatures lower than the melting point (or at preferential annealing temperatures) [32] and in addition the effect is reversible because over time water penetrates the crystalline regions converting them to water permeable amorphous regions.

The addition of salts to PVOH solution can help to increase the crystallinity of PVOH film upon drying, thereby increasing its water resistance. A variety of salts have been investigated including Na_2SO_4 , CH_3COONa [33], NaCl , Na_2CO_3 and NH_4Cl [34,35]. Tretinnikov *et al.* [35] stated the addition of salts such as Na_2SO_4 , Na_2CO_3 and NH_4Cl allowed PVOH films to achieve a degree of crystallinity when prepared at room temperature equal to that obtained when heating a film higher than 120°C .

Recently, PVOH, starch and clay composites have been successfully developed as barrier coatings on paper and board (in the absence of water protecting laminates), but their potential and practical use is currently limited to relatively

dry products and in locations with relatively low average humidity and low temperatures (23°C, 50% Relative Humidity (RH)), as opposed to tropical conditions (35°C, 90% RH) [5]. The amount of PVOH used can be minimised when applied as a coating on paper or board (as opposed to films) because the mechanical strength of the package, and hence the protection it provides, is provided by the paper or board.

1.2 AIMS AND OBJECTIVES

Aims:

To enhance the water vapour barrier as well as mechanical properties of PVOH when applied as either a coating for paper and paperboard packaging or an independent packaging film.

It should be noted at this stage that PVOH coatings onto paper have not yet been studied but are a real potential application. The additional complications derived from PVOH coated paper such as, thickness variations throughout the coating due to uneven cellulose fibres of the paper or increased chance of pinholes in the coating have been eliminated from the investigation, this allows a more thorough understanding of the coating itself rather than any influence from the paper/paperboard.

Objectives:

- ❖ To critically assess the effectiveness of the crosslinking mechanism between PVOH films and glutaraldehyde (GA) and any subsequent changes in water vapour barrier and mechanical properties

- ❖ To characterise the effect of salt treatment on PVOH films towards improving water vapour barrier properties and also its role within the crosslinking process with GA.

- ❖ To heat treat PVOH in order to control the extent of crystallinity and then assess any further changes when undergoing crosslinking reactions with GA.

❖ To investigate the presence of nanoclay in PVOH films affecting the water vapour barrier properties. In addition, effects of crosslinking with GA on the properties of PVOH/Clay films are also assessed.

❖ To characterise the effects of poly(ethylene glycol) as a plasticiser in PVOH and PVOH/Clay films on the water vapour barrier and mechanical properties and then evaluate further changes when the plasticised films are crosslinked with GA.

Layout of thesis:

To aid comprehension the aims and objectives are described below with reference to their location within the thesis

1) The crosslinking reaction between PVOH films and GA was studied and its effects on the films properties in terms of water and water vapour barrier and mechanical properties were evaluated. GA was chosen because it has been considered an effective and efficient crosslinker for PVOH and would provide a number of crosslinks to act as barrier to the diffusion of water vapour through the films. Extents and location of modification were carefully controlled in order to determine the optimum balance between improved barrier properties whilst minimising any possible adverse effects such as flexibility or biodegradability. An underlying theme of the crosslinking process was to ascertain whether it could be achieved effectively at only the uppermost surface of the PVOH film in order to reduce the amount of crosslinking required and cost. The information gained is also relevant to the preparation of membranes for pervaporation application. The location of the crosslinks within the film may help to optimise the transport of one species over another and the integrity of the film [29,36].

This treatment method is reported in Chapter 3.

2) Modification of PVOH films using salt treatment with sodium sulphate was investigated and is described in Chapter 3. In previous work reported by several authors [34,35,37,38], salt treatment was performed by adding salt with different amounts to PVOH in solution which was then dried to form films. In this

research, aqueous salt solution was used to treat the surface of PVOH films for specified lengths of time. Sodium sulphate (Na_2SO_4) was selected since it is also used as part of the crosslinking solution for reaction between PVOH and GA, it therefore also allows an important investigation into any effect of the salt during the crosslinking process.

3) The annealing of PVOH films at selected temperatures for specified lengths of time was carried out in order to investigate any impact on their water vapour barrier and mechanical properties. This treatment method is presented in Chapter 4.

4) In addition to the surface modification methods mentioned above, composite films comprised of PVOH and different amounts of sodium bentonite were prepared. Clay particles in PVOH films act as barriers to diffusion molecules by a tortuous path effect, thereby allowing a means to increase their water vapour barrier properties (Chapter 5)

5) Good film/coating flexibility is often essential for some packaging forming processes. To achieve this, poly(ethylene glycol) with molecular weight $M_w = 400$ (PEG400) was used as a plasticiser and its influence on the properties of PVOH films were observed and presented in Chapter 5.

6) Combinations of the different treatment methods above (1-5) were also investigated in order to assess any synergistic/combined effects or the resulting properties of one treatment (e.g. enhanced crystallinity) on the influence of another treatment (e.g. crosslinking). The influence of annealing on the crosslinking between PVOH and GA was investigated and reported in Chapter 4. This chapter also presents the crosslinking reaction on one side of PVOH films, which were annealed at different temperatures prior to crosslinking. Additionally, the effect of clay and/or plasticiser in the PVOH films and their influence on crosslinking was also studied and described in Chapter 5.

An overarching aim of the research was to utilise a wide range of characterisation techniques to assess and understand the effects of the different treatment methods. Water vapour transmission rate (WVTR) measurement was considered the most important test to evaluate the water vapour barrier of PVOH and its modified

films. The other techniques used include Fourier transform infrared spectroscopy (FTIR), Raman spectroscopy, X-ray diffraction (XRD), contact angle measurement and dynamic mechanical analysis (DMA). Furthermore, the thermal stability of films was taken into account using thermogravimetry (TGA).

Subsequently, poly(vinyl acetate) is dissolved in methanol in the presence of a catalyst (usually sodium hydroxide) and converted to PVOH. This is called the hydrolysis (or alcoholysis) process (Fig. 2.2). The major impurity in PVOH is sodium acetate which has to be removed following the hydrolysis process [39-42]. This by-product in commercial PVOH is typically low and may reach several percentages (0.11% to 9.6%) [43].

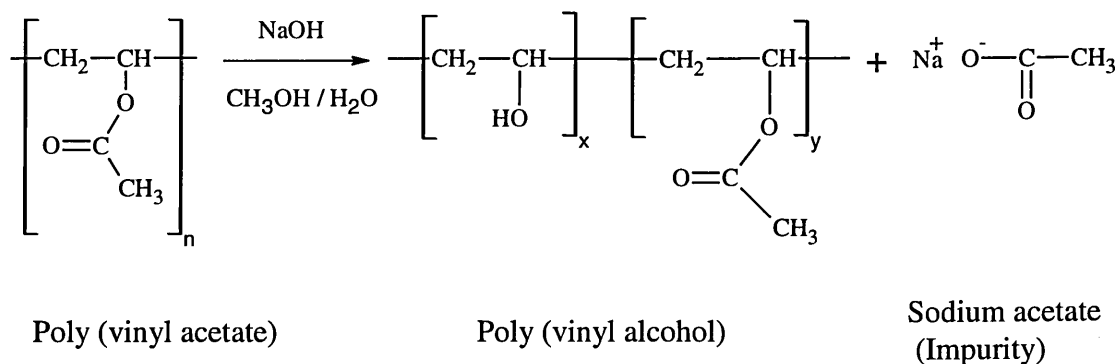


Figure 2.2 PVOH preparation via base-catalysed hydrolysis process.

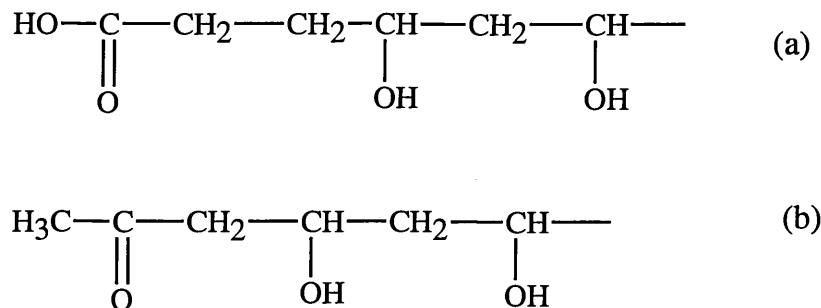


Figure 2.3 End structures of PVOH which contain (a) carboxyl group and (b) carbonyl group

The end structures of PVOH may contain carboxyl, carbonyl or benzoyl groups depending on the manufacturing process. If PVOH is produced from a polymerisation of vinyl acetate polymer in methanol solution, the end structure contains carboxyl groups while PVOH obtained from the polymerisation initiated by benzoyl peroxide has a benzoyl end structure. In addition, impurities of the monomer (for example, acetaldehyde impurity in vinyl acetate) during the

polymerisation process can result in a ketone-type end group of PVOH [41]. Fig. 2.3 illustrates the carboxyl and carbonyl end-group structure of PVOH.

Since the hydrolysis reaction does not occur completely, PVOH still contains an amount of residual acetyl groups which may be adjusted as low as possible by controlling the concentration of catalyst, reaction temperature and time. In fact, PVOH could be considered a copolymer of PVOH and poly(vinyl acetate) [31]. Based on the content of acetyl groups remaining in the product after hydrolysis, PVOH is classified into partially hydrolysed and fully hydrolysed grades. The physical properties of PVOH, especially solubility and swellability depend on the degree of hydrolysis of the polymer. Partially hydrolysed PVOH has higher solubility and swellability in water than fully hydrolysed materials, whereas fully hydrolysed PVOH generally has higher crystallinity, tensile strength and tear resistance. During the hydrolysis process, the hydroxyl groups replace the acetate groups of poly(vinyl) acetate making the material more sensitive to water. However, a higher degree of hydrolysis which results in a higher concentration of O-H groups actually reverses the solubility in water due to strong hydrogen bonding formed between O-H groups producing crystalline zones in the polymer [44]. Maximum solubility can be found in 88% hydrolysed PVOH and PVOH ranging from 87-89% of hydrolysis are soluble in cold water. To dissolve fully hydrolysed PVOH, it is required that water be heated to higher temperature, approximately 90°C.

PVOH is a semi-crystalline polymer. Structures of PVOH can be atactic, syndiotactic or isotactic where atactic polymers expose highest crystallinity and isotactic-rich polymers show poor crystallinity. Bunn [45,46] denied all former assumptions about the crystalline structures of PVOH which had O-H groups placed on the same side of the plane of the carbon chains (isotactic). According to the author, by using X-ray diffraction, in the high crystalline PVOH structure, the O-H groups were randomly placed in left- and right-hand positions of the zigzag plane of the carbon chains (atactic). That crystallinity is affected by stereoregularity was reported to be associated with differences in hydrogen bonding. In comparison with atactic PVOH, the syndiotactic polymer has more regular arrangement of O-H groups along the polymer chains leading to a higher

number of intermolecular hydrogen bonds which reduce chain mobility and orientation. Therefore, the atactic PVOH, with fewer hydrogen bonds and greater chain mobility should have higher tendency to crystallise than syndiotactic polymer resulting in higher crystallinity. In isotactic PVOH, more intramolecular hydrogen bonds are created between adjacent O-H groups leading to stiffening of the chains, decreasing in intermolecular forces and lower crystallinity [47].

Hydrogen bonding has a significant impact on the properties of PVOH as it contributes to the crystallinity of the polymer and thus controls the water solubility of the material. There are two kinds of hydrogen bonds between O-H groups in PVOH, intermolecular and intramolecular hydrogen bonding. Increasing intramolecular hydrogen bonding will reduce the intermolecular forces between O-H groups which results in the decrease in crystallinity [31]. PVOH is fully dissolved when the crystal structure is disrupted as a result of a replacement of polymer-polymer bonds with polymer-water hydrogen bonds [48]. X-ray diffraction is an effective method to analyse the crystal structure of PVOH [45,48] while Fourier transform infrared spectroscopy (FTIR) has been used to evaluate the crystallinity degree by analysing the relevant peaks present in the spectra [37,49-51].

The glass transition temperature of PVOH typically ranges from 40-60°C [39] and can reach 85°C for fully hydrolysed PVOH with high molecular weight, for example $M_w = 89,000-98,000$ [52,53]. PVOH decomposes before reaching its melting temperature (~230°C for fully hydrolysed grades whilst 180-190°C for partially hydrolysed PVOH) [54]. Therefore, PVOH is usually processed in solvents or in the presence of plasticisers, although their presence could result in a decrease in the melting temperature of PVOH [55]. Only hydrophilic compounds with highly polar groups can be used as plasticisers for PVOH to ensure good compatibility between materials. Water can act as plasticiser for PVOH but it is not an ideal option as water can easily evaporate from the polymer. Common plasticisers for PVOH are ethylene glycol, di- and tri-ethylene glycol, etc. with the amount not exceeding 30% relative to PVOH [39,56,57]. Apart from water, there are some other solvents that can dissolve PVOH such as polyhydroxy compounds (ethylene glycol, glycerol), amides (formamide,

acetamide) and amines (diethylenetriamine, triethylenetetramine) [25,58-60]. Some solvents can dissolve PVOH at ambient temperature while others need to be heated.

PVOH can have excellent resistance to oxygen, aroma and odour but this is subject to its water content. It is almost not affected by hydrocarbons, carboxylic acid esters, grease or oils. The oxygen barrier properties of PVOH are excellent at low humidity below 60% where the oxygen permeability can be from $0.2-0.4 \times 10^{-13} \text{ cm}^3 \cdot \text{cm}/(\text{cm}^2 \cdot \text{kPa})$ [52]. To improve the oxygen barrier performance of PVOH films, mixtures between PVOH and poly(methyl vinyl ether-*co*-maleic acid) was developed by Labuschagne *et al.* [61]. The authors found that the hydrogen bonding complexation between these two polymers could form coatings with oxygen barrier properties much higher than those of each individual polymer. With 20 wt% of poly(methyl vinyl ether-*co*-maleic acid) present in the film, the oxygen transmission rate was 4.43 times lower than that of neat PVOH. The incorporation of clay into PVOH can also contribute to the overall property improvement of PVOH, including mechanical, thermal and barrier properties [62-64]. In addition, in order to improve its properties, PVOH can be either physically crosslinked by annealing or chemically crosslinked with other chemicals such as glyoxal, GA, boric acid, maleic acid [29,65,66].

The outstanding properties of PVOH are its biodegradability and solubility in water. The microorganisms which can degrade PVOH are comprised of bacteria, moulds, yeast and fungi and at least 55 species have been identified that are able to decompose or take active roles in the degradation of PVOH [52]. The biodegradable mechanism of PVOH is proposed to occur in two steps; the first step is the decomposition of C-C linkages of PVOH either by the enzymes dehydrogenase or oxidase. In the second step, the structures are further degraded by involving in a hydrolase or aldolase action to form simple compounds [67,68]. The degradation products can be hydrogen peroxide, a carboxylic acid, and a ketone or alcohol [69,70].

With its favourable nature, PVOH has been applied extensively in several industries, including automotive, packaging and medicine. Bait bags containing oil-based bait for anglers, packaging for detergent capsules, protective coatings

for glass, mould release agents for mould construction and casting, paper coatings or paper adhesive are some of PVOH's applications [26,27,71]. PVOH is also used as a disintegrating agent [72], bio-membrane, as part of biomaterials for synthetic articular cartilage application [73] or drug delivery [74,75].

2.1.2 Glutaraldehyde and crosslinking reaction with PVOH

2.1.2.1 Glutaraldehyde (GA)

GA is an organic compound which is mainly used as an aqueous solution within the concentration range from 50% w/w to less than 1% w/w [76]. It is a colourless oily liquid with a pungent odour. GA is non-flammable, non-explosive and has a lower volatility than water.

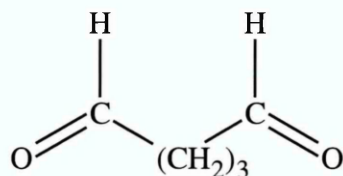


Figure 2.4 Structure of glutaraldehyde

Fig. 2.4 shows that GA is an aliphatic dialdehyde, it can undergo most of the typical aldehyde reactions. It is soluble in water, ethanol, benzene and ether. GA tends to polymerise in solution or rather partially polymerise to form oligomers with variable compositions. When heated to high temperature, GA thermally decomposes to form carbon oxides and hydrocarbons. GA is a toxic and strong irritant chemical and classified as high risk of exposure to human health or the environment, however, when crosslinked, its hazardous nature is nullified.

The applications of GA in different industries have flourished all over the world, including water treatment, X-ray film processing and leather tanning. Acting as a hardening agent in developing solutions for black-and-white X-ray photography, GA helps to make the drying cycle in film processing shorter. In the tanning industry, GA is incorporated into soaking solutions for leathers to make them softer and more resistant to water, alkalis and mould. GA also has wide

applications in the healthcare industry as disinfectant for instruments such as endoscopes, surgical instruments and dental equipment where these instruments are immersed in an aqueous GA solution for a specific length of time then rinsed with clean water [76]. In biological electron microscopy, GA acts as a fixative by crosslinking proteins and enzymes to kill cells quickly in order to prevent their decay [77].

2.1.2.2 Crosslinking reaction between GA and PVOH

In recent years, GA has been broadly used as a crosslinking agent to improve the properties of PVOH films in terms of chemical, thermal, mechanical stability and barrier properties. Bolto *et al.* [29] has highlighted and reviewed the crosslinking reactions with different ratios between PVOH and GA which were performed by previous authors. It was concluded that in comparison with other crosslinking agents, GA was more effective than formaldehyde or glycidyl acrylate. In addition, crosslinked products from GA and PVOH swelled less in water than those obtained by heat treatment processes to increase crystallinity.

There are three recognised methods to produce crosslinked PVOH films using GA:

- 1) The first method is termed the phase inversion technique [78] which consists of casting, precipitation and crosslinking. In this technique, aqueous PVOH solution is cast on a support (metal, glass plate or non-woven cloth) before being precipitated in a non-solvent bath (for example, acetone, sodium sulphate solution) to form a porous membrane [66,79]. Then the porous membrane is crosslinked with GA in a crosslinking solution.
- 2) The second method to generate crosslinked PVOH films using GA is to initially form the films on a support then immerse the dry films in a crosslinking solution to induce the acetalisation [80]. This method is employed in this research
- 3) For the third method, GA is introduced directly into the aqueous PVOH solution with or without the presence of a catalyst, followed by film casting. The

dry films without catalyst are subsequently immersed in an aqueous acid catalyst solution to induce the crosslinking [81,82].

An aqueous crosslinking solution typically contains GA, acid catalyst and salt. The salt solution creates a reaction medium for the crosslinking to take place. It does not take part in the reactive process but functions to "salt out" or insolubilise PVOH, i.e., it causes the PVOH to precipitate out of solution [82]. Various unreactive salts can be used, including sodium sulphate, potassium sulphate and sodium phosphate to prevent the dissolution of PVOH. The most common salt used is sodium sulphate. Catalyst can be any acid such as sulphuric acid, hydrochloric acid, etc., where the former is more commonly used than others.

Aqueous salt solutions can be replaced by acetone. Yeom and Lee [80] successfully fabricated crosslinked PVOH membranes using GA in acetone solution. The crosslinked films were reported to be very stable in aqueous solutions and could be applied in the pervaporation separation of water-acetic acid mixtures.

During the crosslinking reaction, O-H groups of PVOH are consumed by GA producing crosslinked products with acetal linkages (Fig. 2.5). The crosslinking makes the polymer network more tightly compact, resulting in less space for species to permeate through the membrane. The resistance to permeation is also higher for larger species [29].

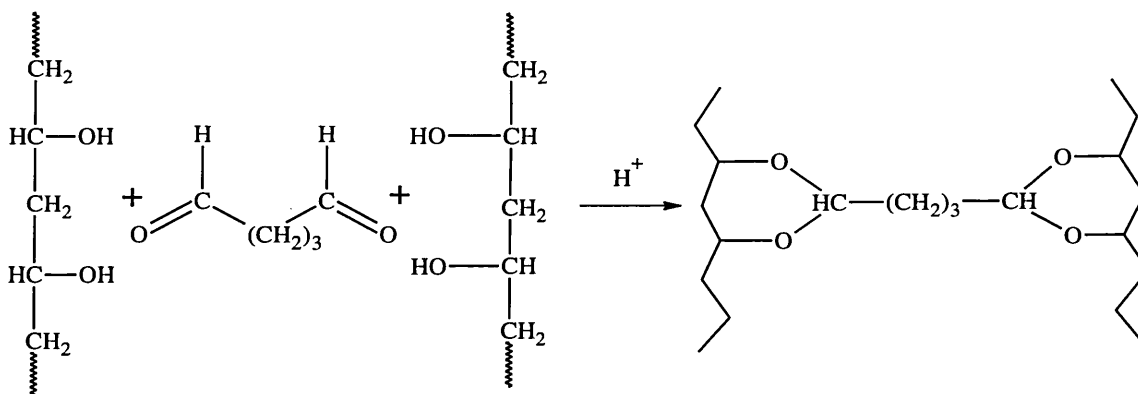


Figure 2.5 Crosslinking reaction between PVOH and GA

The reaction between GA and PVOH can be bi-functional or mono-functional where for the latter, PVOH chains react with only one aldehyde group of GA resulting in an unreacted aldehyde pendent to the polymer chains. An increase in GA content in the crosslinking solution (beyond 10 vol%) was found to have a negative effect on the swelling behaviour of crosslinked films as more acetal and pendent aldehyde groups were present making the films have more affinity to water [80].

Differences between PVOH and crosslinked films in terms of swellability in water, thermal and mechanical properties have been investigated [53]. Crosslinked PVOH films (99% hydrolysed, $M_w = 89,000-98,000$) were obtained by casting an aqueous solution containing PVOH, GA and HCl on a glass plate. The final crosslinked films had thicknesses of 50-80 μm . It was observed that the swelling of crosslinked films decreased when GA amount increased while the untreated films totally dissolved in water. Increasing the GA amounts resulted in the increase of crosslinking density and a corresponding decrease in melting temperature and extent of crystallisation.

PVOH crosslinked films have mainly been applied in the pervaporation separation process, which aims to separate liquid mixtures. The feed solution is in contact with one side of a membrane while the permeate is removed as a vapour from the other side [36]. The pervaporation characteristics are closely related to the swelling properties of the materials involved. PVOH membranes (98% hydrolysed) prepared by the phase inversion technique and crosslinked with GA contained in an aqueous sodium sulphate and sulphuric acid crosslinking solution bath at 40°C were shown to achieve a maximum crosslinking degree of ~75% [66]. The degree of crosslinking was proved to have an influence on the swelling behaviour in water and pervaporation separation of ethanol-water mixtures, both the swelling degree and permeate flux decreased with increasing crosslinking degrees. It was also observed that their wetting behaviours were not affected by the degree of crosslinking.

Porous PVOH membranes (99% hydrolysed) have been prepared via the phase inversion technique and post-treated by either heating to 120°C or by

crosslinking with GA [83]. Chemically crosslinked PVOH films exhibited higher tensile strength (~1.5 times) than those prepared by heat treatment. However, this was applicable just in the dry state of the materials. When in wet conditions, crosslinked membranes were fragile while the heat treated films were more flexible indicating better elasticity. When extending the post-treatment time, the morphology of crosslinked membranes did not change as significantly as those of the heat treated membranes; the porosity degree was nearly constant for the former yet decreased for the latter. This was explained by the nature of the different post-treatment methods. In the crosslinking process, polymer chains were fixed by GA while in the heat treatment process, the PVOH molecules gained sufficient energy to re-arrange the polymer structure to be less porous. However, Ahmad *et al.* [79] showed the morphology changed in porous PVOH membranes when crosslinking with different GA amounts. It was also found that when increasing the crosslinking time, the morphology changed and the pore size distribution decreased.

Drug release from swellable PVOH has been shown to be controlled by crosslinking density and PVOH content [74]. PVOH (97.5-99.5% hydrolysed, $M_w = 72,000$) hydrogel was prepared by a crosslinking reaction with GA. The crosslinking density was increased when increasing the GA/PVOH ratio resulting in a decrease of swelling degree which helped to prolong the drug release process.

2.1.3 Sodium sulphate and its influence on the properties of PVOH

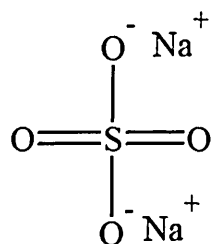


Figure 2.6 Structure of sodium sulphate

Sodium sulphate is a neutral salt of strong acid (H_2SO_4) and strong base (NaOH). It is a white crystal solid when in anhydrous state and is sometimes referred to as "salt cake". It has a molecular weight of 142.04 g/mol and melting point at 884°C [84]. Mostly, sodium sulphate is found from natural resources and exists in a decahydrated crystalline state with the formula $\text{Na}_2\text{SO}_4 \cdot 10\text{H}_2\text{O}$ which is known as Glauber's salt. Industrially, it can be produced as a by-product in various chemical and metallurgical processes including the manufacturing of HCl or from the reaction between sulphuric acid and sodium hydroxide [85].

Sodium sulphate, regarded as non-toxic, is soluble in water but the solubility is limited at ambient temperature (13.9g/ 100 mL (20°C)). Heating water from 0 to $\sim 32^\circ\text{C}$ will increase the solubility more than tenfold. Sodium sulphate has wide application in industry, mainly in the detergent, glass and paper industries. Detergent application is the largest use of sodium sulphate where the chemical is used as filler in powder detergent to bulk up the product, making the product less costly to produce per unit weight [86]. Sodium sulphate can be used as a fining agent in the glass industry as it helps to remove small bubbles from molten glass and prevent scum formation. In paper pulp manufacturing, sodium sulphate is used in the Kraft process which is a conversion process to change wood into wood pulp. The wood chips, after impregnation with sodium sulphate, are heated to cause a reduction of sodium sulphate into sodium sulphide to treat the chips.

Other applications of sodium sulphate although used in smaller quantities can be found in the fibre industry, textile dyeing, electroplating and in the production of animal feedstuffs and chemicals (for example sodium sulphide). Sodium sulphate was used as a coagulant agent in the production of polyvinyl alcohol fibres or filaments using a wet spinning technique [87,88]. To form the fibres or filaments with a homogeneous cross section, an aqueous PVOH solution including additives was extruded through a multi-hole spinneret into an aqueous coagulating bath containing sodium sulphate, this was done at a specific temperature for a duration of time before the produced fibres were dried and treated at high temperature. Then, the fibres were crosslinked with formaldehyde in the presence of sulphuric acid and sodium sulphate in water.

In waste water treatment, sodium sulphate can be used to remove/recover PVOH present in solutions [89]. By mixing sodium sulphate (salting agent) with salts of boric acid (gelling agent) in the form of an aqueous solution or solid into the waste water to be treated, PVOH is precipitated into particles and then removed from the vessel.

Immobilising enzymes or bacteria entrapment is another function of sodium sulphate. PVOH-alginate beads containing enzyme/bacteria were crosslinked with boric acids then treated with an aqueous sodium sulphate solution in order to obtain stable and more hydrophobic beads that could be applicable in aqueous solution [90-94].

Recently, sodium sulphate has attracted interest in medical applications. The presence of very low level of sodium sulphate promotes the physical crosslinking of PVOH enough to produce a hydrogel with a suitably strong network to potentially act as an artificial knee meniscus [95]. It was formed by adding sodium sulphate to an aqueous PVOH (10% w/v) solution to precipitate the PVOH followed by a number of freeze and thawing cycles at -80°C and room temperature, respectively. Furthermore, the PVOH hydrogels exhibited less water absorption, was more thermally stable and also resistant to breakdown by compressive force than unmodified PVOH. Tretinnikow *et al.* [35] reported that PVOH/salt films which were formed from an aqueous solution containing sodium sulphate and PVOH with concentrations of 0.1 mol/L and 4 wt%, respectively, possess crystallinity at room temperature which could be achieved in films with no salt by heating at temperatures above 120°C .

As a coagulant agent, sodium sulphate has been used in phase inversion techniques to form PVOH membranes [66,79,96] or as previously described used as an aqueous medium for the crosslinking reaction between PVOH and glutaraldehyde [81,82,97]. When PVOH solution droplets are added into an aqueous salt solution, the sulphate ion SO_4^{2-} , which has a very good affinity to water immediately penetrates into the PVOH solution and polarises the water molecules; this results in the destabilisation of hydrogen bonding between O-H groups of PVOH and water and so in effect the SO_4^{2-} ions remove the water

associated with the PVOH molecules via hydrogen bonding. This allows "free" PVOH molecules to form inter- and intra-hydrogen bonds through their O-H groups and form PVOH crystallites.

2.1.4 Heat treatment of PVOH

Freezing-thawing of a PVOH solution has been proved as an effective method to increase the properties of PVOH in terms of crystallinity and swellability [30,31,73]. This process includes a number of cycles of cooling the solution to a very low temperature (below freezing) then thawing at room temperature or higher. During ice formation, the PVOH molecules are aggregated and hydrogen bonding is developed between molecular chains (crystallite formation). Repeating the freezing-thawing process produces materials with higher crystallinity and lower swellability in water. It is believed the crystallite zones act as crosslinks between the amorphous regions.

Heating (annealing) introduces crystallites in the polymer resulting in the increase of the crystallinity. Heat treatment of PVOH membranes has been used to create high crystalline polymers for application in drug release [98], pervaporation and ultrafiltration [83]. Mallapragada *et al.* [98] reported that when the annealing conditions were controlled well, the crystallinity of PVOH and the drug release rate could be adjusted. Increasing the annealing temperature or time would result in an increase in degree of crystallinity and water resistance leading to a decrease of drug released rate. For example, PVOH ($M_w = 35,240$) heated at 110°C for 10 minutes released the drug much faster than one crystallised at 120°C for 1 hour due to lower crystallinity in the former. The degrees of crystallinity achieved during heat treatment of PVOH can be very different. Wang *et al.* [83] obtained a crystallinity degree of 18.7% for PVOH membrane annealed at 120°C for 1 hour while in Mallapragada's study, heating the sample at lower temperature and shorter time (90°C for 30 minutes) obtained a higher value of 38%. This might be due to the differences in PVOH preparation, PVOH molecular weight and more importantly, the calculation method for crystallinity

degree; for example, Wang *et al.* used infrared spectra whilst Mallapragada used differential scanning calorimetry (DSC).

The crystallinity of PVOH can be determined using different methods, including X-ray diffraction, density measurements, DSC and infrared spectroscopy [51]. From DSC measurements, the degree of crystallinity is calculated based on the ratio between the heat of melting of PVOH crystals and the heat needed to melt a 100% crystalline PVOH sample [98]. Infrared spectroscopy (IR) has been used as an effective method to investigate the crystallinity of PVOH. The peak at 1141-1145 cm^{-1} represents the crystallinity of PVOH [99] and efforts have been made to determine the degree of crystallinity of PVOH based on this specific peak. Peppas [49,51] was one of early authors who proposed Equation 2.1 for calculating the degree of crystallinity based on FTIR spectra wherein the peak at 1425 cm^{-1} was used as a reference peak:

$$D_c (\%) = A (a/b) - B \quad (2.1)$$

Where D_c – degree of crystallinity (%); a and b – peak heights at 1141 and 1425 cm^{-1} , respectively and A, B – coefficients which were calculated via calibration. The authors did not describe the calibration method but stated that the value of A was 102.6, but reported different values of B in two separate reports (63.6 [49] and 10.236 [51]).

Another expression for the degree of crystallinity using a relationship between band intensities at 1144 and 1097 cm^{-1} was reported by Korodenko [40] when investigating the effect of sodium acetate on the structure of PVOH with reference to density measurements, Equation 2.2

$$D_c (\%) = 0.82 (A_{1144} / A_{1097}) \quad (2.2)$$

was suggested to compare the crystallinity between different samples. However, issues associated with choice of baselines were not clearly explained.

A peak at 854 cm^{-1} may also be utilised as a reference peak for determining the crystallinity using Equation 2.3:

$$D_c (\%) = A (a/b) + B \quad (2.3)$$

where a and b are the heights of absorbance bands at 1141 and 854 cm^{-1} , respectively [100]. Unfortunately, the values for the coefficients A and B were not reported.

One of the most recent studies by Tretinnikov and Zagorskaya [37] determined the crystallinity of PVOH films using FTIR. PVOH films were heated to various temperatures to induce crystallinity and accessed by both X-ray diffraction and infrared analysis. The intensities of the absorbance bands at 1144 cm^{-1} relative to those at 1094 cm^{-1} (Fig. 2.7) were measured and then plotted against the crystallinity degrees calculated from XRD data. An equation to calculate the crystallinity degree was established using Equation 2.4:

$$D_c (\%) = 89.5 (a/b) - 13.1 \quad (2.4)$$

Where D_c – degree of crystallinity (%), a – intensity of the peak at 1144 cm^{-1} , b – intensity of the peak at 1094 cm^{-1} .

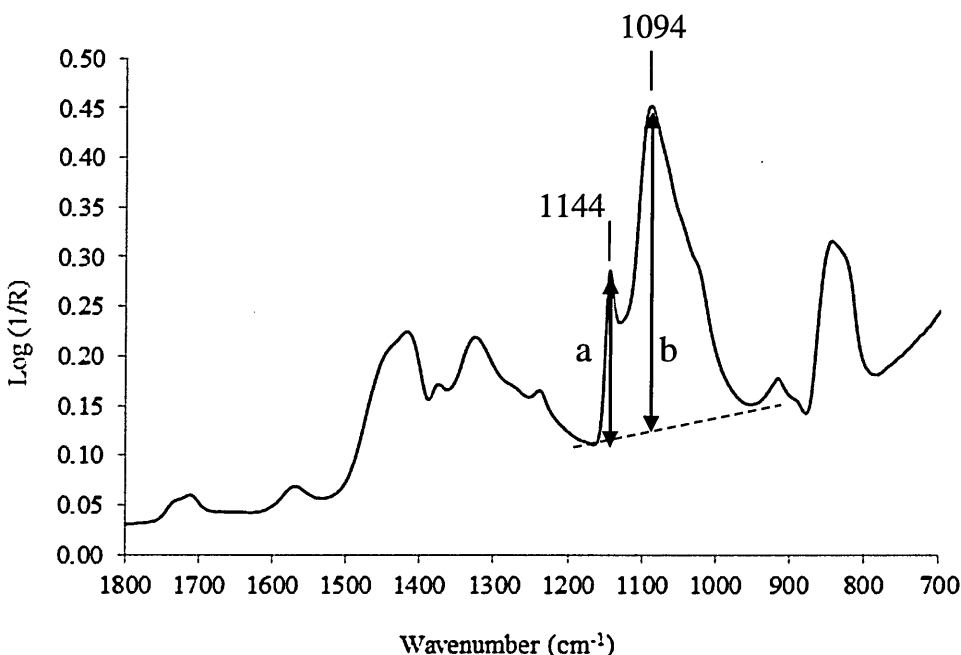


Figure 2.7 Diagrammatic representation for calculation of peak intensities for determining crystallinity of PVOH based on Tretinnikov and Zagorskaya studies [16]. The peak at 1094 cm^{-1} is used as the reference peak.

Water absorption within a PVOH film has a relationship with crystallinity. When the crystallinity degree increases, the water permeation decreases. Also, the

mechanical properties of PVOH increase with an increase in degree of crystallinity [83].

Care should always be exercised during the heat treatment of PVOH since above a certain range of temperatures over certain time periods, PVOH decomposes. This can occur before reaching the melting point temperature [67,68].

2.1.5 Montmorillonite (MMT) and PVOH/ MMT Nanocomposites

2.1.5.1 Montmorillonite (MMT)

Clay minerals are layered silicates which are used popularly in polymer nanocomposite preparations. Layered silicates or phyllosilicates are natural or synthetic minerals consisting of aluminosilicate layers stacked together [101,102]. The layer thickness of clay is in the nanoscale, about 1 nm and the lateral dimension varies from 30 nm to several micrometers or larger [103]. The layered structures of clays are constructed from silicon tetrahedral sheets and aluminium octahedral sheets [104-107]. A tetrahedral sheet is composed groups of four oxygen ions at four tips surrounding a silicon ion at the centre while the octahedral sheet is built from groups of six oxygen ions or hydroxyl groups occupying six tips and an aluminium ion at the centre. The tetrahedral and octahedral sheets are joined together by sharing of the oxygen atoms. Unshared oxygen atoms are present in hydroxyl form. When a single tetrahedral sheet is fused with a single octahedral sheet, a 1:1 layered silicate structure is formed. A 2:1 layered silicate structure is created from two tetrahedral sheets fused to and sandwiching an octahedral sheet of aluminium (Fig. 2.8). Clays consist of many silicate layers stacked together and separated by regular van der Waals gaps which are called the interlayer space or gallery. In the dry state, clay layers exist in face-to-face stacks like a deck of playing cards. The forces that hold the stacks together are relatively weak, thus allowing small molecules including water, solvents and monomer as well as polymer to enter into the galleries, causing the lattice to expand.

A moderate surface charge characterising the layered silicates is called the cation exchange capacity (CEC), generally expressed as meq/100g and is the maximum quantity of total cations, of any class, that a layered silicate is able to hold and be available for exchange with other cations. The negative surface charge in MMT arises from the isomorphous substitution of aluminium cations with iron or magnesium. Each type of layered silicate has a characteristic d-spacing value which is a repeat unit in the crystalline structure including the 1nm-thick silicate layer and the gallery [62].

The 2:1 layered silicates are the most commonly used in preparation of polymer nanocomposites. In this family, montmorillonite, hectorite and saponite are the most popular species. They are hydrophilic and only miscible with hydrophilic polymers. To be miscible with other polymer materials, the hydrophilic silicate surface should be converted to an organophilic surface by ion-exchange reactions with cationic surfactants. Alkylammonium or alkylphosphonium based surfactants are generally used which help to reduce the surface energy of the clay layers and thus improving the miscibility with polymer matrix and also enlarging the interlayer spacing. The exchange ability of clay with cationic surfactants depends on the cation exchange capacity (CEC) which characterises the clay itself (Table 2.1).

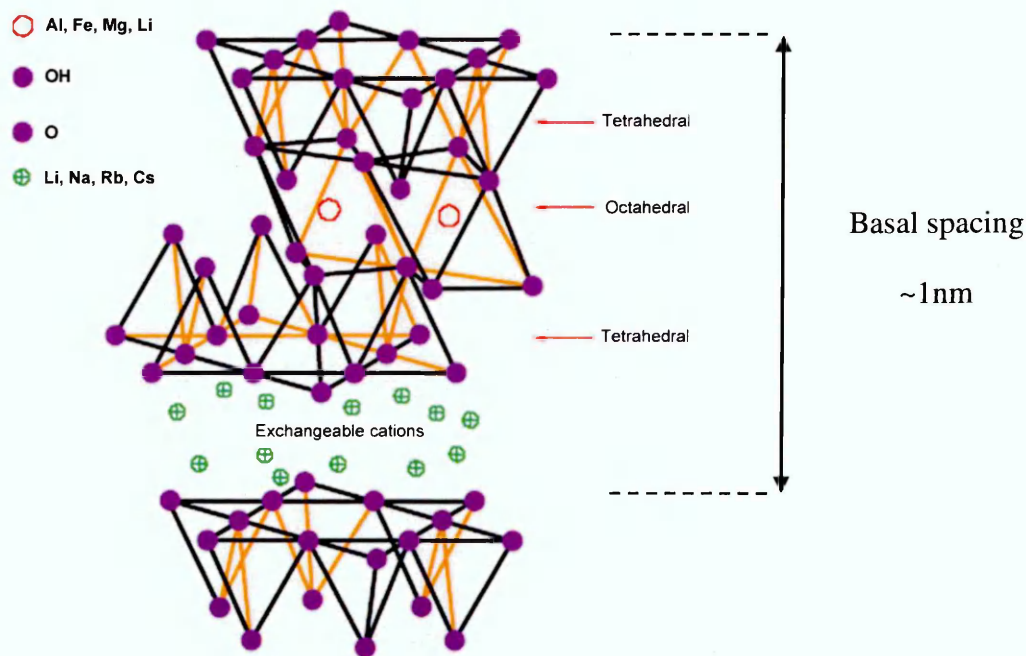


Figure 2.8 Structure of the 2:1 layered silicates [101]

Table 2.1 Characteristics of montmorillonite, hectorite and saponite [105]

2:1 layered silicate	Typical chemical formula ^a	Typical CEC (meq/100 mg)	Typical clay layer length (nm)
Montmorillonite	$M_x(Al_{4-x}Mg_x)Si_8O_{20}(OH)_4$	110	100-150
Hectorite (Laponite)	$M_x(Mg_{6-x}Li_x)Si_8O_{20}(OH)_4$	120	200-300 20-30
Saponite	$M_xMg_6(Si_{8-x}Al_x)Si_8O_{20}(OH)_4$	86.6	50-60

^a M = monovalent cation; x = degree of isomorphous substitution (between 0.3 and 1.3)

Among the 2:1 layer silicates family, montmorillonite (MMT) is the best-known member in its clay mineral group and widely used in many application, especially in polymer nanocomposite synthesis. Its structure usually contains hydrated Na^+ , Ca^{2+} or K^+ as the exchanged cations. MMT (CEC of 80-120 meq/100g [105]) is relatively cheap, abundant in nature in large quantities and environmentally friendly as it is derived from volcanic ash and rocks. In addition, it has a potentially high-aspect ratio and high surface area that can lead to materials exhibiting significant property enhancement.

2.1.5.2 PVOH and Montmorillonite nanocomposites

PVOH/MMT nanocomposite materials have attracted strong interest in today's materials research [108-111]. When clay is introduced to a polymer, three main types of composite are obtained: tactoid, intercalated and exfoliated [62,101,105,111,112].

❖ Tactoid (phase separated structure): Here polymer is unable to intercalate within the silicate layers and the obtained composite structure is in the range of a traditional microcomposite (Fig. 2.9a).

❖ Intercalated composite: Here polymer can penetrate between the silicate layers and cause the expansion of the interlayer spacing resulting in well-ordered multilayers of alternating polymer and silicate layers with a repeat distance of few nanometers (Fig. 2.9b).

❖ Exfoliated nanocomposite: Here extensive polymer penetration in between the silicate layers results in their complete separation from one another. This disordered delamination produces exfoliated nanocomposites consisting of individual silicate layers dispersed in the polymer matrix (Fig. 2.9c).

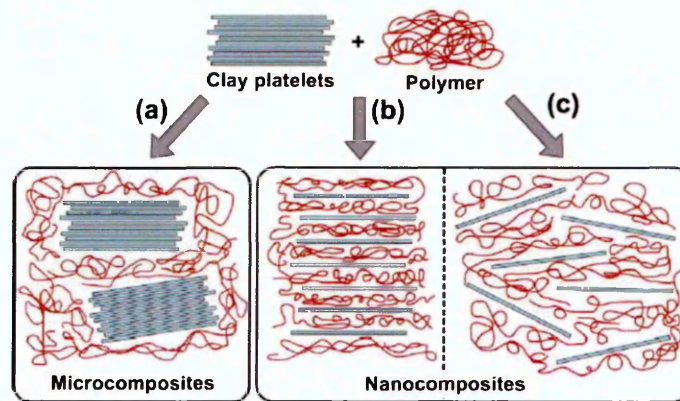


Figure 2.9 Schematic diagram of different composite types obtained from the interaction of clay with polymer: (a) tactoid (phase separated microcomposite) (b) intercalated nanocomposite and (c) exfoliated nanocomposite [106]

Since PVOH and MMT clay are hydrophilic, the MMT can disperse very well and homogeneously in the polymer, this can produce enhanced properties when compared with the pure polymer. For example, when clays are present in the PVOH matrix they introduce a tortuous path effect (Fig. 2.10), in which the particles can hinder any diffusing molecules by forcing them to follow longer and more tortuous paths resulting in the improvement of their barrier properties [62,102,113,114].

The "tortuous path" effect was first proposed by Nielson [115]. The rectangular nanoclay platelets were assumed to be oriented parallel to the polymer film surface and aligned perpendicular to the diffusion direction which could

maximised the traveling distance of diffusing molecules. The Nielson equation is given in Equation 2.5

$$\frac{P_{\text{NaCF}}}{P_{\text{Po}}} = \frac{1 - V_{\text{F}}}{1 + (L/2W)V_{\text{F}}} \quad (2.5)$$

Where

- P_{NaCF} the permeability of nanocomposite film
- P_{Po} the permeability of unfilled polymer
- V_{F} volume fraction of filler
- L length of a nanoclay platelet
- W thickness of a nanoclay platelet
- L/W aspect ratio

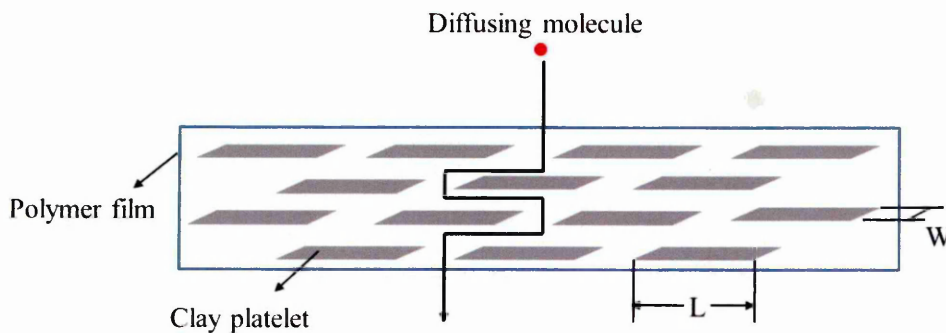


Figure 2.10 Tortuous path effect when clays are present in a polymer matrix

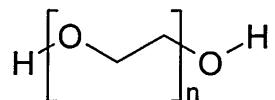
When relatively small amounts of clay are present in PVOH, enhancements in other material properties can be achieved, including thermal stability, mechanical properties, solvent resistance and a decrease in gas and liquid permeabilities. Grunlan *et al.* [114] reported the incorporation of 3 wt% clay into modified PVOH (comprised of 97 wt% vinyl alcohol, 2 wt% vinyl acetate and 1 wt% itaconic acid) could reduce the oxygen permeability at 23°C, 35% relative humidity from 0.006 cc.mil/(m².day) in the absence of clay to an undetectable

value ($<0.001 \text{ cc.mil/m}^2\text{.day}$). In addition, the glass transition temperature of the modified PVOH containing 10 wt% clay also increased by 10°C in comparison with a sample without clay. However, there was a decrease in transparency with the increase of clay content, the % transmission decreased 30% and the haze degree increased $\sim 80\%$ when the amount of clay increased from 0 to 10 wt%. Effects of clay on the properties of PVOH were also reported by Sapalidis *et al.* [62]. A series of PVOH/NaMMT films prepared by a solvent casting technique showed significant improvements in mechanical strength and gas barrier properties as well as an increase in heat resistance while retaining the optical transparency even at high clay loadings of 20 wt%. Recently, Breen *et al.* [116] investigated the diffusion of acetone: water mixtures through PVOH films. By using ATR-FTIR spectroscopy, the authors reported a significant reduction in the diffusion of the mixture through the film in the presence of clay proving the significance of the tortuous path effect of the clay particles. More significantly, the diffusion of acetone was only shown to occur after the PVOH film had become fully saturated/ swollen with water. In terms of water permeability, a small amount of clay present in PVOH can significantly reduce the rates of water/water vapour transmitting through the films. Yeh *et al.* [117] showed that the water vapour transmission rate decreased by 43% when 1-3 wt% clay was incorporated into PVOH films but increased with increasing clay contents (more than 4 wt% clay). When investigating the effects of nanoclay on the physical and mechanical properties of PVOH/chitosan mixtures as well as individual polymer, Mahdavi *et al.* [118] found that the water vapour barrier properties improved when clay was present in which the improvements were 27% and 67% for PVOH/Clay films containing 23 and 54 wt% clay, respectively.

2.1.6 Polyethylene glycol (PEG) as plasticiser

PVOH films have relatively high stiffness and brittleness and decompose before melting. Therefore, plasticisers are used either to aid the manufacturing process, or decrease stiffness and brittleness and generally allow PVOH products to be used in a wider variety of applications. PEG with up to molar masses of ~ 400

g/mol are common plasticisers used in PVOH and are typically used not in excess of 30 wt% relative to PVOH [39]. PEG has the following chemical structure:



PEG is the name used to refer to oligomers and polymers with molecular masses below 20,000 g/mol. For molecular masses above 20,000 g/mol, the name poly(ethylene oxide) (PEO) is used. Poly(oxy ethylene) (POE) is used to refer to a polymer of any molecular mass. Depending on their molecular weights, PEG and PEO are liquid or low-melting solids. PEGs are synthesised by polymerisation of ethylene oxide and are commercially available over a wide range of molecular masses from 200 to 10,000,000 g/mol.

PEG is readily soluble in water but its solubility decreases with increasing molecular mass. It also dissolves in other solvents such as methanol and benzene. Plasticising effects of PEG on PVOH films in comparison with other plasticisers were studied by Lim and Wan [56]. The authors found PEG600 had less compatibility with PVOH ($M_w = 14,000$ g/mole) than propylene glycol and glycerol resulting in more translucent and heterogeneous films with increasing amount of PEG600. Generally, when plasticiser is incorporated into PVOH, the flexibility increases and water resistance decreases. Also, it reduces the crystallinity degree of the sample and lowers the melting temperature of PVOH. However, Lim and Wan reported that the presence of PEG600 did not significantly affect the melting temperature of PVOH due to its large size and lower incompatibility with PVOH. Li *et al.* [57] investigated the interaction between PVOH and different PEGs with low molecular weights of 200, 400 and 600 g/mol. TGA, DSC and DMA were used to characterise the PVOH/PEG samples. When the PEGs were incorporated into the polymer network, two effects were described that occurred concurrently: (i) PEG hydrogen bonded with PVOH to form a physical network resulting in an increase in the glass transition

temperature, and (ii) PEG enlarged the distance among PVOH intersegment leading to a decrease in glass transition temperature. PEG200 was proved to form unstable PVOH/PEG systems while PEG with higher molar mass was effective on the plasticisation of PVOH.

2.2 CHARACTERISATION METHODS

2.2.1 Water vapour transmission rate (WVTR)

In the British Standard, BS 2782-8:1996 [119], water vapour transmission rate is defined as;

"the mass of water vapour transmitted through a unit area in a unit time under specified conditions of temperature and humidity"

and

"is expressed in grams per square metre per 24 hours [$\text{g}/(\text{m}^2 \cdot \text{d})$]" .

The WVTR depends on several factors such as material properties (e.g. thickness or composition), the temperature and relative humidity conditions at which the measurement is performed. For sheet materials, the thickness should be less than 3 mm and the expected transmission rate not less than $1 \text{ g}/(\text{m}^2 \cdot \text{day})$.

Sometimes the WVTR value is desirably related to the thickness of the materials in the case of homogeneous films, in which, the WVTR value obtained for a given thickness is multiplied by the thickness in thousandths of an inch ($\text{g} \cdot \text{mil}/(\text{m}^2 \cdot \text{day})$) (British standard 3177:1959 [120]).

Relative humidity (RH) represents the amount of water vapour the air contains. In other words, it is defined as the ratio of the partial pressure of water vapour in the air to the partial pressure of saturated water vapour at the same temperature [121]. Chen *et al.* [122] reported that the WVTR values of PVOH films increase exponentially with both relative humidity and temperature although the effect of temperature was not as noticeable as that of RH. Increasing the RH to more than 70% led to a rapid increase in WVTR values, this was due to the plasticising

effect of water which caused the films to swell resulting in the increased diffusion of water through the films.

The gas or water vapour transfer to a film by a diffusion process which follows Fick's Law of Diffusion [3]:

$$Q = -\frac{S \times t \times D}{\ell} \times \frac{dc}{dx} \quad (2.6)$$

Where

Q	the mass of gas or vapour passing through a film
S	area of the film
t	time
D	diffusion constant
ℓ	film thickness
dc/dx	concentration gradient

The relationship between transmission rate and permeability coefficient is described in the following equation:

$$Q = P \times \frac{p_1 - p_2}{\ell} \times S \times t \quad (2.7)$$

Where Q is the mass of gas or vapour passing through a film of area S after time t, therefore $Q/(S \times t)$ is defined as transmission rate; $(p_1 - p_2)$ is the different pressure between two sides of the film; ℓ is the film thickness and P is the permeability coefficient [123].

According to the British standard BS EN 20187:1993 [124], samples should be pre-conditioned in the specified testing atmosphere before measurement. The standard atmosphere for testing pulp, paper and paperboard is $23^\circ\text{C} \pm 1^\circ\text{C}$ and $50 \pm 2\%$ RH. In tropical countries an atmosphere of $27^\circ\text{C} \pm 1^\circ\text{C}$ and $(65 \pm 2)\%$ RH is preferably used. For WVTR tests for paper and plastic in general and when

using Payne cups, there are five established environmental conditions used, they are shown in Table 2.2 [119].

Table 2.2 Standard conditions for WVTR testing

Condition types	Temperatures (°C)	Relative humidity (%)
A	25 ± 1	90 ± 2
B	38 ± 1	90 ± 2
C	25 ± 1	75 ± 2
D	23 ± 1	85 ± 2
E	20 ± 1	85 ± 2



(a)



(b)

Figure 2.11. Water vapour transmission rate measurement system. (a) Humidity chamber (b) Sample preparation using Payne cups

For determining water vapour transmission rates in our study, the procedure followed the British standard BS 2782-8: Method 820A:1996 [119]. Before the measurement, all films were pre-conditioned at the desired temperature and relative humidity (RH) for at least 20 hours (i.e. until no further gain in mass was observed) in a humidity oven supplied by Sharetree Limited Company (Fig. 2.11a). The humidity chamber is designed to maintain temperature and RH at set points controlled by the operator at the front panel. Air is circulated through the chamber and monitored. A low-pressure vapour generator discharges water

vapour into the chamber through a small orifice to induce the required humidification.

WVTR investigation of polymer thin films produced in this current work was conducted at 23°C and 85% RH (Condition D – Table 2.2) using Payne cups (Sheen Instruments) which are made from aluminium and resistant to corrosion under the test conditions (Fig. 2.11b). Each dish contained an equivalent amount of silica gel as desiccant (about ~9g) which was dried overnight in an oven at 100°C. The dishes were covered by the polymer thin films with an exposure surface of 25 cm² and placed in the humidity oven during the measurement. At suitable time intervals, the dishes were weighed and the total increase in mass for each dish was plotted graphically as a function of exposure time. The test was completed when at least four data points lay on a straight line showing a constant rate of water vapour passage (Fig. 2.11c). The WVTR result was an average of 3 WVTR values from 3 different test pieces of the same sample type.

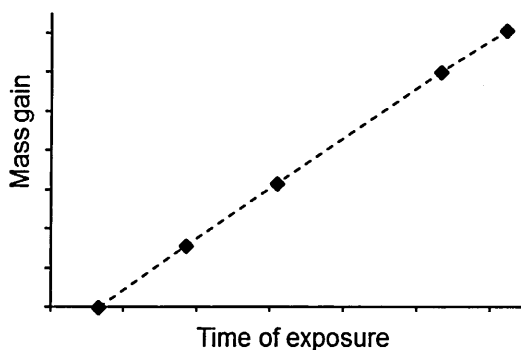


Figure 2.11c A schematic increase in mass as a function of exposure time

The WVTR value for each test piece was calculated based on the straight line using the following formula:

$$\frac{240 \times Q}{S \times t}, [\text{g}/(\text{m}^2 \cdot \text{day})] \quad (2.8)$$

Where

- t the total duration, in *hrs*, of the exposure periods where the straight line is plotted.

- Q the increase in mass, in mg , during the time t .
- S the exposed surface area of the test piece, in cm^2 .

2.2.2 Swelling test in water

Swelling can change the physical and chemical structure of polymers and plays an important role in the transport of molecules through membranes [125]. In dense polymer, swelling leads to an increase in the free volume and so membranes become more open and allow more liquid to pass through. An increase in affinity between solvent and polymer will increase the swelling degree of the polymer. The mechanism of polymer swelling includes three processes:

1. Absorption: solvent molecules are absorbed into the membrane surface
2. Penetration: the solvent molecules penetrate into the membrane, occupy the free volume and then diffuse further into the polymer membrane
3. Expansion: the polymer expands to allow more or bigger molecules to penetrate. The solvent molecules which are held in the pores continue penetrating into other pores present in the network resulting in the polymer swelling.

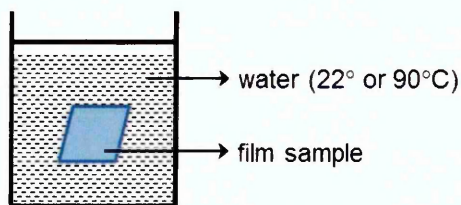


Figure 2.12 Swelling test in water

The swelling tests of PVOH films in this thesis were conducted in water at two different temperatures which were 22 and 90°C. Films were cut into squares (2.5 cm x 2.5 cm) and immersed in water for 24 hours in order to reach an equilibrium (Fig. 2.12). After the films were taken out of water, they were

immediately wiped with soft paper to remove any surface water and then their wet weights were recorded. To obtain the dry film weights, they were dried under vacuum at 40°C for 48 hours in order to remove the majority of water present.

The swelling degrees were attained from the average values of three films and were calculated as following:

$$SW = \frac{W_w - W_d}{W_d} \times 100, (\%) \quad (2.9)$$

Where SW is the swelling degree, in %; W_w and W_d are the weights of wet and dry films, respectively, in *grams*.

2.2.3 Fourier transform infrared spectroscopy (FTIR)

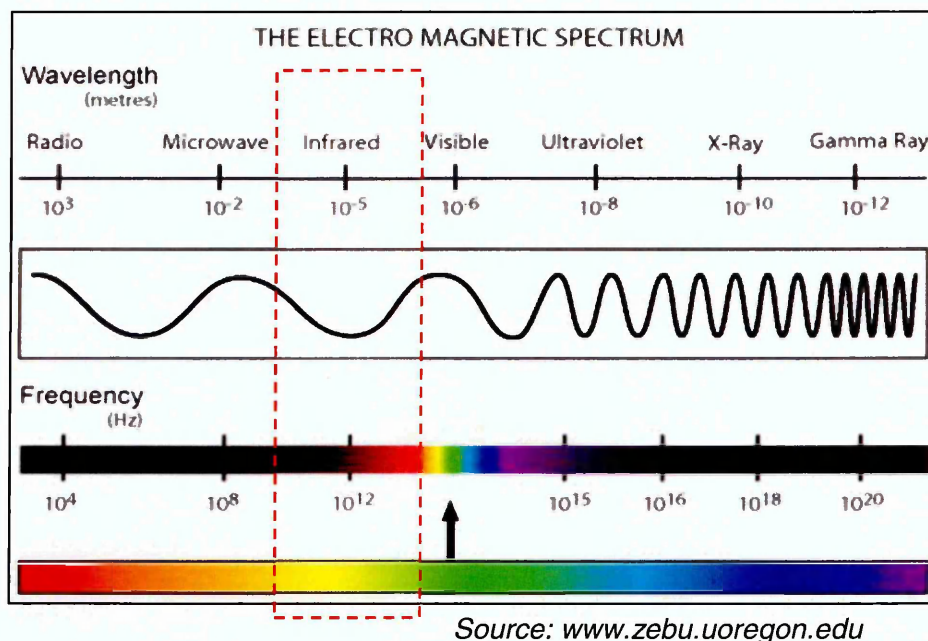


Figure 2.13 Electromagnetic system

Infrared spectroscopy (IR spectroscopy) is a technique that deals with the infrared region of the electromagnetic spectrum (Fig. 2.13). There are three IR radiation regions obtained from a typical IR source which are the near-IR region ($14,000 - 4,000 \text{ cm}^{-1}$), the mid-IR region ($4,000 - 400 \text{ cm}^{-1}$), and the far-IR region ($400 - 10 \text{ cm}^{-1}$).

IR spectroscopy is also referred to as vibrational spectroscopy as it investigates the interaction between IR radiation and molecular vibrations by measuring the transitions between molecular vibrational energy levels. A molecule can vibrate in many ways, for example, a water molecule has 3 vibrational modes which are shown in Fig. 2.14 and each vibration can absorb a certain frequency of IR radiation. Therefore, in IR spectroscopy specific functional groups of a molecule absorb infrared light at unique frequencies and show specific absorbance bands in an IR spectrum. These act like a finger print and allow the identification of substances.

The mid-infrared region is the most commonly used for the investigation of materials. This mid-IR spectral region historically was measured with a dispersive instrument. Today, most of the commercially available mid-IR instruments are (Fourier Transform) FTIR spectrometers which use interferometers [126].

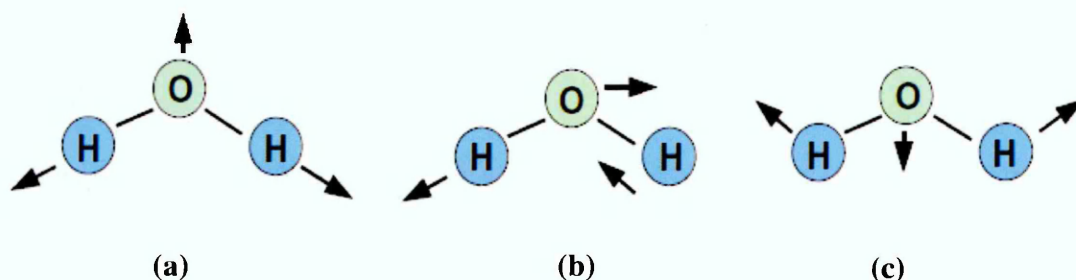


Figure 2.14 Three vibration modes of H₂O molecules

- (a) **Symmetric stretching vibration**
- (b) **Asymmetric stretching vibration**
- (c) **Deformation vibration**

Fourier transform spectrometer is based on the Michelson interferometer which includes a beam splitter, a fixed and a moving mirror (Fig. 2.15). The light from the source is split by the beam splitter into two equal beams. One beam is reflected off a fixed mirror and the other is reflected off a moving mirror. When the beams recombine, any time delay creates constructive or deconstructive interference depending on the component frequency of the radiation. The intensity of the radiation after passing through a sample can be expressed as a

function of the time delay i.e. displacement of the moving mirror. The recorded interferogram is transformed into a single beam spectrum using the Fourier transformation. The ratio between the single beam of a sample and that of the background, which is measured under the same condition but without the sample, produces the absorbance (or transmittance) spectrum of the sample.

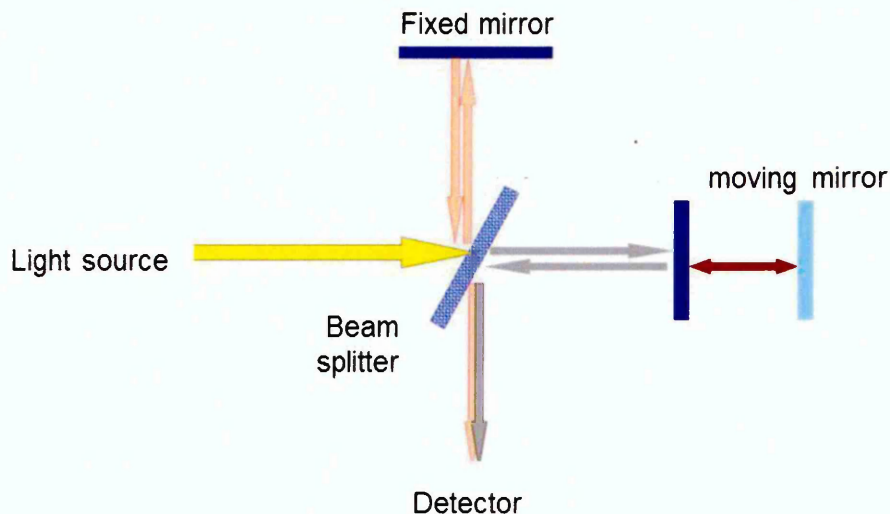


Figure 2.15 A Michelson interferometer

An IR spectrum describes the absorption of light (electromagnetic radiation) from a sample at different wavenumbers. The energy E of the absorbed electromagnetic radiation can be related to the frequency ν and the wavelength λ in the following way:

$$E = h\nu = h\frac{c}{\lambda} \quad (2.10)$$

$$\nu = \frac{c}{\lambda} \quad (2.11)$$

Where c is the speed of light ($2.99793 \times 10^8 \text{ m s}^{-1}$) and h is the Plank constant ($6.624 \times 10^{-34} \text{ Js}$)

The wavelength in turn can be related to the wavenumber, $\bar{\nu}$, of an IR spectrum:

$$\bar{\nu} = \frac{1}{\lambda} = \frac{\nu}{(c/n)} \quad (2.12)$$

Where n is the refractive index of the medium the light is passing through.

FTIR spectroscopy provides a spectrum over a wide wavenumber range. The spectrum is attained by plotting the intensity (absorbance or transmittance) versus the wavenumber.

Among sampling techniques used by FTIR spectroscopists, attenuated total reflectance (ATR) is becoming the most popular as it is quick, relatively non-destructive and requires only minimal or no sample preparation. It is a contact sampling method which involves a crystal with a high refractive index and excellent IR transmitting properties [126]. In ATR-FTIR spectroscopy, the IR beam is directed onto a ATR crystal and is reflected on the internal surface in contact with the sample. This internal reflection creates an evanescent wave that extends beyond the surface of the crystal into the sample. Absorption of IR radiation of the evanescent wave occurs in the sample and the remaining radiation towards the detector is collected by the detector after it exits the crystal (Fig. 2.16). Since the evanescent wave penetrates only a few microns (0.5 – 5 μm) [127] into the sample there must be good contact between the crystal and the sample to assure a constant penetration depth of light into the sample. Furthermore, this technique is mainly for surface measurement.

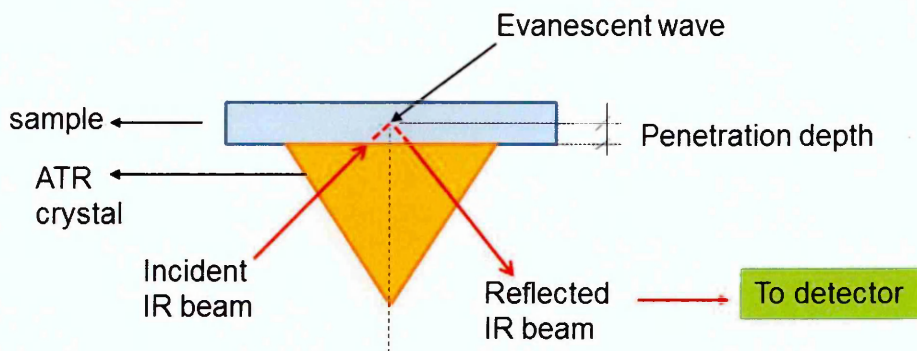


Figure 2.16 A schematic of an ATR-FTIR system

A very wide range of sample types can be measured by IR. Samples can be organic or inorganic, liquids, solids or gases, and analysed over a wide range of temperatures

In this study, a Thermo Nicolet NEXUS spectrometer equipped with a mercury cadmium telluride (MCT) detector which is cooled by liquid nitrogen was used for all the FTIR analysis. A single reflection diamond ATR cell (Graseby Specac,

UK) was used, which has the trade name “Golden gate”. Film samples were pressed on top of the diamond ATR crystal and their spectra were collected.

Since the amount of water in PVOH is dependent on atmospheric conditions (especially humidity), before any FTIR analysis, samples were dried in an oven at 40°C overnight to desorb the majority of water present in the films. Each sample was analysed at three different positions on both upper and lower surfaces. The spectral range analysed was between 4000 and 650 cm^{-1} . The number of sample scans and the resolution were 64 and 4.0 cm^{-1} , respectively. To collect and analyse the spectra, OMNIC software (version 7.3) was used.

2.2.4 Raman spectroscopy

Like IR spectroscopy, Raman is also a vibrational spectroscopy technique involving the interaction between radiations and molecular vibrations in which “the finger prints” of molecules /materials are identified. Therefore, Raman is used for characterising molecular structures and properties of materials. A typical Raman experiment involves the radiation of the sample by a laser with monochromatic radiation [126]. Laser sources (785 and 1064 nm) are available for excitation in the UV (10-400 nm), visible (380-800 nm) and near-IR (700-2500 nm) spectral region. Therefore, when a visible excitation is used, the Raman scattered light will also be in the visible region

While several vibrations are active with both IR and Raman, some vibrations are simply selective with Raman and not IR, and vice versa. Therefore, Raman and IR spectroscopy are different in processes and selection rules. Table 2.3 briefly summarises some of the differences between the two techniques. In general, Raman spectroscopy is best with symmetric vibrations of non-polar groups while IR spectroscopy is best with the asymmetric vibrations of polar groups. That is why Raman is very convenient for measuring samples containing a relatively high amount of water due to its polar structure. The absence of dominant water bands in the Raman spectrum allow other bands to be observed in the same region.

Table 2.3 Comparison of Raman and mid-IR spectroscopy [126]

	Raman	Infrared
Ease of sample preparation	Very simple	Variable
Suitability for		
Liquid	Very simple	Very simple
Powder	Very simple	Simple
Polymers	Very simple*	Simple
Gases	Simple	Very simple
Fingerprinting	Excellent	Excellent
Best vibrations	Symmetric	Asymmetric
Group frequencies	Excellent	Excellent
Aqueous solution	Very good	Very difficult
Quantitative analysis	Good	Good
Low frequency mode	Excellent	Difficult

* True for FT-Raman at 1064 nm excitation

IR absorption is a one-photon event [128] where a molecule is elevated in vibrational energy after encountering and receiving energy from an IR photon at the frequency of vibrational resonance. In other words, the IR absorption process occurs when the frequency of the absorbed IR matches the natural frequency of a particular normal mode of vibration, which causes a change in the dipole moment of the molecule. Raman spectroscopy, on the contrary, is a two-photon event. A photon of an incident laser is absorbed by a sample molecule and moved from the ground state into a virtual state. At this virtual state, a new photon is created and scattered. The scattered light consists of both Rayleigh scattering and Raman scattering (Fig. 2.17). Rayleigh scattering corresponds to the light scattered at the same frequency as that of the incident radiation, i.e. no energy is lost, whereas, the photons of Raman scattered light can lose or gain some energy, which is relative to the exciting energy and the specific vibrational modes of the samples. In order for Raman bands to be observed, the molecular vibration must cause a change in the polarisability.

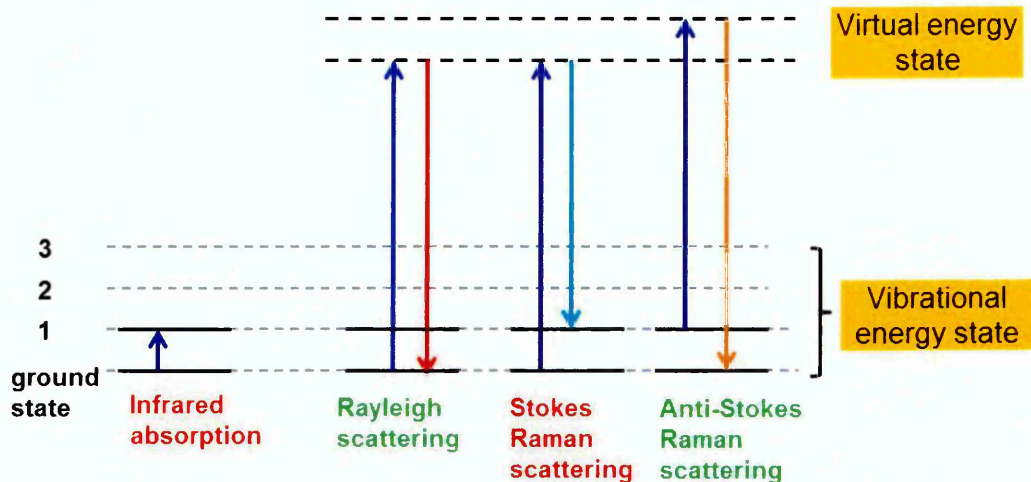


Figure 2.17 Diagram of energy-level changes for IR absorption and Raman or Rayleigh scattering.

There are two types of Raman scattering which are Stokes and anti-Stokes, these are related to the loss or gain in energy of the photon, respectively. The amount of energy lost is seen as a change in energy of the photon of the incident radiation. This energy loss is characteristic for a particular bond in the molecule

For the work presented in this thesis, Raman measurements were carried out using a Renishaw inVia Raman Microscope with WiRE 3.4 software. The laser source was a near infrared diode laser (785 nm). Settings for these runs are summarised in Table 2.4. Each sample was analysed at three points on both upper and lower surfaces.

Table 2.4 Settings for Raman analysis

Spectral range	100 - 4000 cm^{-1}
Exposure time	10s
Accumulation	4
Objective	x50
Laser power	100%
Detector	Renishaw CCD Camera 578 x 400 Laser name 785 nm edge (mode Regular)

2.2.5 X-ray diffraction (XRD)

X-ray diffraction is a non-destructive analytical technique used for identification and quantitative determination of various crystalline forms of compounds present in powder or solid samples. It is also used for determination of structure, phase analysis, solid solution analysis, determination of particle size, chemical identifications, etc.

X-rays are a form of electromagnetic radiation with high energies and short wavelengths (100 to 0.1 Å). X-rays were discovered by Wilhelm Conrad Rontgen, a German physicist in 1895. X-rays are generated when high speed electrons are abruptly stopped by a solid target [129]. To produce X-rays, an X-ray tube is needed; this must consist of three important factors; namely, an electron source, a means of accelerating electrons and a target to stop them. As a result, X-rays are emitted in all directions from the target surface with a continuous range of wavelengths which form a continuous spectrum called "white radiation" or "background radiation".

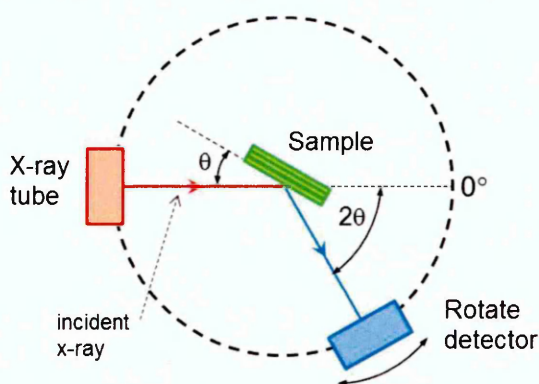


Figure 2.18 Schematic diagram of an X-ray diffractometer

Fig. 2.18 schematically describes an X-ray diffractometer, an apparatus for determining the angles at which diffraction occurs for a specimen. The monochromatic X-ray beam is generated from the X-ray tube and impinges on a flat sample; its diffracted beams have intensities recorded by a rotate detector. The sample is supported so that its rotation through θ angle is accompanied by a 2θ rotation of the detector.

For crystallographic work, a monochromatic X-ray beam is preferable. A crystal is composed of a regular three dimensional array of atoms, ions or molecules. When a monochromatic X-ray beam is incident on a crystal, the scattered X-rays from the atoms (1' and 2' in Fig. 2.19) constructively interfere with each other, giving strong diffractions [130]. Diffraction only occurs if the Bragg equation is obeyed for a particular family of planes:

$$2d \sin\theta = n\lambda \quad (2.13)$$

Where n is an integer (1, 2, 3, etc.) called the order of reflection; d is the spacing of atomic net planes which are defined as the parallel planes of regular arranged atoms; θ is the angle between the X-ray beam and the planes and λ is the wavelength of incident X-ray.

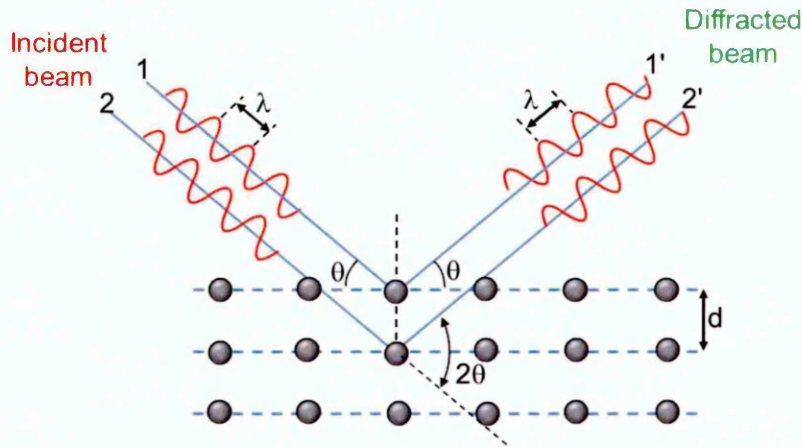


Figure 2.19 Bragg's condition

If Bragg's law is not obeyed, the interference will be non-constructive in nature, therefore producing a very low-intensity diffracted beam. The high intensity diffracted peak results when the Bragg condition is satisfied by some set of crystallographic planes.

In this study, X-ray diffraction data were collected using an X'Pert Pro Diffractometer (Philips). Films of ~3cm diameter were placed in a sample holder incorporating a background-free silicon wafer disk. A copper tube (Cu K α λ = 1.541 Å), a minipro detector and configuration of spinner were used. The measurements were conducted under 40 mA and 40 kV. The scan range was from 2° to 45° with step size of 0.04° and a scan time of 2s per step. The sizes of mask, anti-scatter slit and divergent slit were 10 mm, 1° and 1/2°, respectively. Before measurement, samples were dried overnight at 40°C then kept over a silica gel desiccant in order to minimise any rehydration.

2.2.6 Thermogravimetric analysis (TGA)

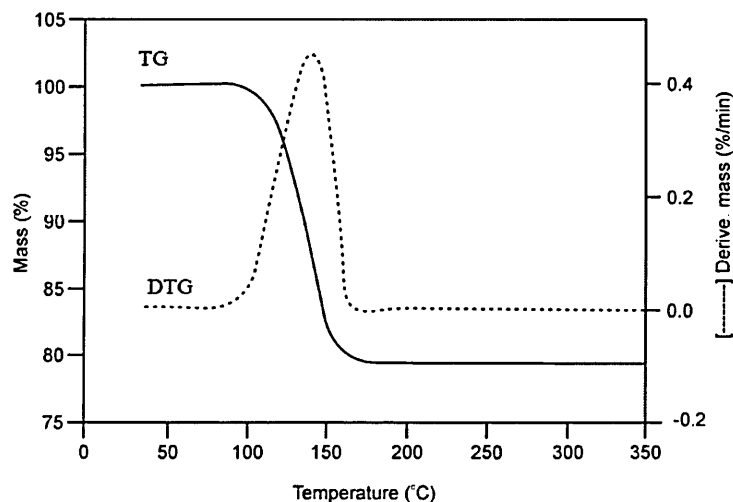


Figure 2.20 Typical TG and DTG curves

TGA is the most widely used thermal method and measures sample mass as a function of temperature and/or time [131]. Most TGA curves display weight losses though a gain in weight can be observed if for example oxidation occurs [132]. In most cases, TGA curves are plotted with weight (W) decreasing downwards on the y axis and temperature (T) increasing to the right on the x axis. Sometimes, for expressing the results of TGA, the negative first derivative curve,

-DTG (Derivative Thermogram) is used. The -DTG plots $-dW/dT$, i.e. the rate of weight loss divided by the rate of temperature change (T) (Fig. 2.20).

The instrument for thermogravimetry is called a thermobalance which comprises several basic components such as the balance, furnace, programmer for temperature measurement and control, and a recorder which is used for recording the changes in mass and temperature (Fig. 2.21). A crucible containing sample is placed in a furnace of which the temperature is controlled and monitored by the programmer. The analysis is carried out by increasing the temperature of the sample in a flow of air or inert gas such as N_2 , Ar or He and the sample mass against temperature is recorded and plotted. Some factors that affect the TGA includes heating rate, amount of sample, carrier gas flow, type of gas flow, etc.

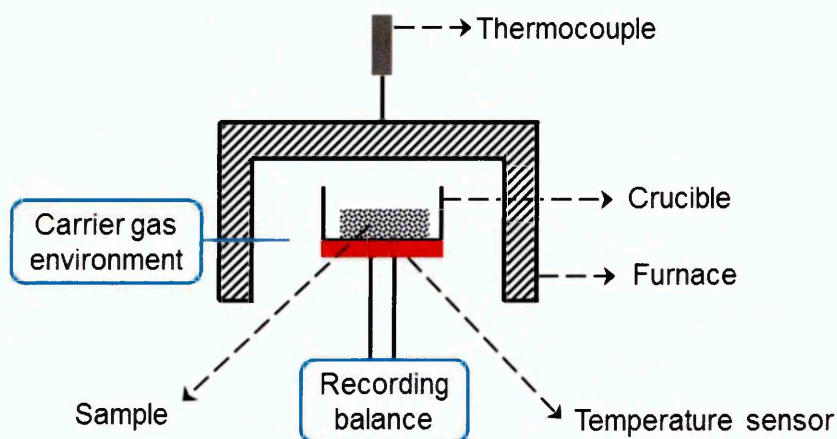


Figure 2.21 A schematic diagram of a TGA instrument

TGA is used to detect any thermal process associated with a change in mass. Therefore there is a wide range of applications of TGA including the determination of thermal stability of a particular sample or understanding about the chemistry of decomposition of a compound. TGA is also used to determine the content of moisture and volatile materials present in samples, composition of a mixture, reaction kinetics, corrosion of metals in various atmospheres, oxidative and reductive stability. For polymer materials, TGA is mostly used to study their thermal stability in order to understand the decomposition

mechanisms which may be characteristic for each type of polymer, in some cases, it can be used for identification purposes [133]. There are six main mechanisms in which a polymer degradation route can be categorised:

1. main-chain scission
2. side group scission
3. elimination
4. depolymerisation
5. cyclisation
6. cross-linking

Mass change is rarely seen during cyclisation and cross-linking steps so they are not usually detected by TGA while routes 1-4 usually results in the development of volatile products which are accompanied by mass change. If the measurement process is carried out under air atmosphere, oxidation processes may occur resulting in the formation of oxide products of the constituent elements present in samples.

In this study, a Mettler Toledo TG50 Thermogravimetric analyser was used with crucibles made from alumina. Samples with mass ~5 mg were heated from 35 to 800°C at a rate of 20°C/min under nitrogen with a flow rate of 40 mL/min. An initial isothermal stage was used where the sample was kept at 35°C for 15 minutes before following the set temperature programme. This was performed in order to "normalise" any amounts of water between samples.

2.2.7 Dynamic mechanical analysis (DMA)

DMA is a widely used technique to characterize the material properties by measuring the response of a sample to an oscillatory force applied on it [134]. DMA data can inform the stiffness of materials and their ability to relax and regain shape when deformed. The most important information for this study that was obtained from DMA is the glass transition temperature (T_g) of a material.

DMA is said to be a more sensitive technique for obtaining T_g data than Differential Scanning Calorimetry (DSC).

When an oscillatory force is applied to a sample of known geometry, a sinusoidal stress is generated and causes a sinusoidal strain. The material will deform a certain amount relating to its stiffness [135] (Fig. 2.22). DMA investigates viscoelastic materials (polymers) which are the combinations of two characters: viscous and elastic behaviours. From DMA, three values are obtained: storage modulus (E'), loss modulus (E'') and $\tan \delta$ which is defined as the ratio of the loss (E'') to the storage (E') modulus. The storage modulus (E') represents the solid-like property (elastic) of materials and demonstrates how stiff the materials behave when pushed and how well they store the energy of the input stress. Materials that are stiff have high storage modulus. The loss modulus (E'') represents the liquid-like behaviour (viscous) which is an ability to dampen the force or stress, or the loss of impact. Thus, soft materials have high loss modulus. At glass transition temperatures, materials change their properties with E' and E'' changing rapidly, giving a peak at the $\tan \delta$ curve.

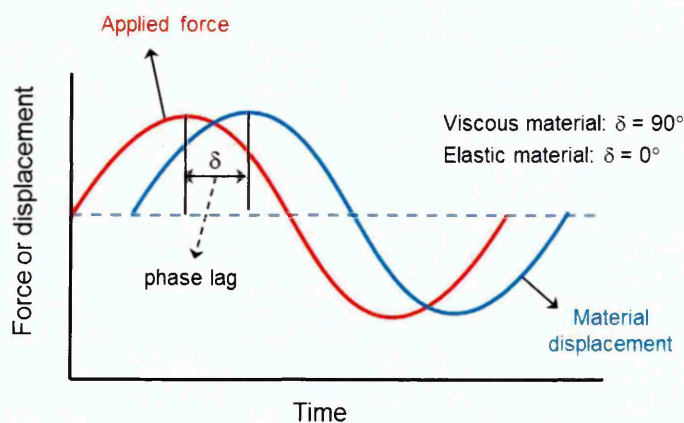


Figure 2.22 A relationship of the applied sinusoidal stress to strain results in a phase lag (δ) and sample deformation

All DMA measurements in this study were performed on a Perkin Elmer DMA8000 instrument. Tension mode was used with a ratio tension of 1.2. Samples were run at 2 frequencies (multi frequency scan), which were 1 and 10 Hz under a nitrogen purge. The heating rate was $2^\circ\text{C}/\text{minute}$ and the

displacement was set at 0.01 units. Samples were heated from -50°C to a final temperature depending on the thermal properties of the samples. Samples were cut into rectangular strips of 4-5 mm width and the measurement length was 6-7 mm.

2.2.8 Contact angle measurement (CA)

Contact angle (θ) is a measurement of the wettability of a solid by a liquid. It is defined as an angle existing at the contact surface between solid and the liquid [136]. Fig. 2.23b shows that a small contact angle is observed when the liquid spreads on the surface ($0^{\circ} < \theta < 90^{\circ}$) and the solid is wettable. An angle with a value of 0° occurs when the solid is completely wet (Fig. 2.23c). Also, a larger contact angle is observed when the liquid beads on the surface ($\theta > 90^{\circ}$) (Fig. 2.23a).

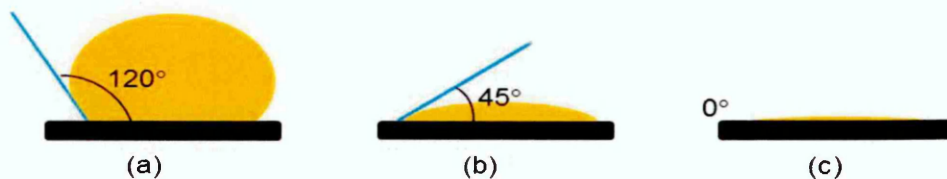


Figure 2.23 Different contact angles from different materials

(a) $\theta = 120^{\circ}$ - poor wetting (b) $\theta = 45^{\circ}$ - good wetting

(c) $\theta = 0^{\circ}$ - complete wetting

In hydrophilic or hydrophobic coatings, paintings, printing and bondings, the contact angle is very important since it describes the applicability of the materials. In fact, the shape of a liquid droplet is determined by the surface tension of the liquid. Surface tension is the energy, or work, required to increase the surface area of a liquid due to intermolecular forces. In a pure liquid, there are intermolecular forces between neighbouring liquid molecules. However, when the liquid is in contact with a solid surface, the liquid molecules at the surface don't have neighbouring molecules in all directions so they are only pulled

inward to the centre of the liquid droplet. This creates an internal pressure which is responsible for the shape of the liquid droplet [137].

The relationship between contact angle θ and the surface tension of the liquid (Fig. 2.24) is expressed in Young's equation:

$$\sigma_s = \gamma_{sl} + \sigma_l \cdot \cos\theta \quad (2.14)$$

Where σ_s the surface free energy of the solid

γ_{sl} the interfacial tension between liquid and solid

σ_l the surface tension of the liquid

θ the contact angle

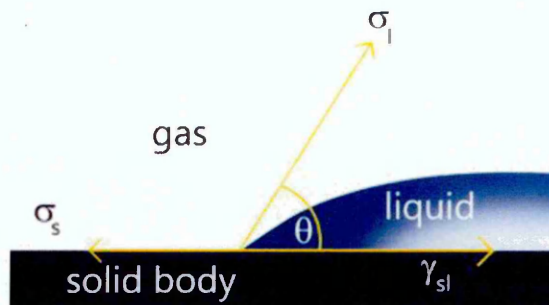


Figure 2.24 Schematic diagram of contact angle and surface tension [136]

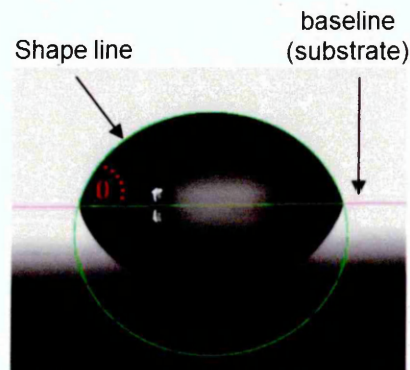


Figure 2.25 Drop shape analysis using sessile drop for contact angle measurement. The fitted contour is shown in green [138]

One of the common methods to measure the contact angle is drop shape analysis which is an image analysis method for determining the contact angle from the shadow image of a sessile drop, a standard arrangement for optical measurement of the contact angle is shown in Fig. 2.25. When a liquid is dropped on the surface of a solid, an image of the drop is recorded with the help of a camera and transferred to the drop shape analysis software. A geometrical model describing the drop shape is fitted to the contour which is recognised based on the image. Then the contact angle is given by the angle between the calculated drop shape function and the solid surface which is called the baseline [138]

To determine the contact angle, the fitting methods available for modelling the drop shape on the solid surface are; circle method, conic section method (eclipse fitting), polynomial method (tangent fitting), and Young-Laplace fitting. The choice of the fitting method for calculating the contact angle is based on the measuring range, drop weight, liquid dosing and contour shape.

The static contact angle measurement in this study was conducted using an optical contact angle meter (Dataphysics - OCA 15) with software SCA20. A 1 μ L drop of distilled water with dosing rate of 1 μ L/s from a syringe Hamilton 500 μ m was placed on the polymer film surface. The drop type was sessile drop and calculation method used eclipse fitting. The atmosphere temperature was 20-22°C. For each analysis, the contact angle measurements were performed every 30 seconds after initial drop formation until the droplet was deformed. The contact angle values were the mean of 5-10 analyses and at the same interval.

Crosslinking reaction between PVOH films and glutaraldehyde, and the effects of salt treatment on PVOH films

In this chapter, the influence on water vapour barrier properties of PVOH films by film thickness, polymer molecular weight and relative humidity are reported. In addition, the effects of crosslinking reactions with glutaraldehyde (GA) on the properties of PVOH films are investigated. Last but not least, sodium sulphate, an integral part of the crosslinking reaction, is also taken into account in determining the improved properties of the films.

3.1 EXPERIMENTAL

3.1.1 PVOH film preparation

PVOH (98-99% hydrolysed, $M_w = 31,000-50,000$, melting point = 200°C and density = 1.26 g/cm^3), purchased from Sigma-Aldrich and used as received, is the primary material used throughout this study. For PVOH film preparation, a desired amount of PVOH was added to a round-bottom flask containing water at a weight ratio of 1:20 (PVOH : water). The mixture was magnetic stirred at 90°C for 6 hours before being cast in Petri dishes. The solution was dried at room temperature for 48 hours to form solid films (size of Petri dish, 89 mm in diameter) which were then stored in closed containers at room temperature. To prepare PVOH films with different thickness, the amount of hot solution cast in Petri dishes was adjusted so as to obtain dry films with thickness varying from 21 ± 3 to $182 \pm 3 \mu\text{m}$ (Table 3.1). Film thickness was measured using a Mitutoyo ball micrometer (resolution of 0.01mm, made in Japan, Identity number 53018). The mean thickness value was taken from five random positions on the film.

Table 3.1 Thickness differences of PVOH films ($M_w = 31,000-50,000$) obtained from different amounts of casting solution

Weight of solution (g)	5	10	15	20	25	30
Dry film thickness (μm)	21 ± 3	54 ± 4	84 ± 6	121 ± 7	154 ± 5	182 ± 3

PVOH of higher molecular weight (98-99% hydrolysed, $M_w = 124,000-186,000$, melting point = 200°C and density = 1.26 g/cm^3) was also used for comparison in addition to the PVOH mentioned above ($M_w = 31,000-50,000$). Different denotations are used to distinguish them which are PVOH124 and PVOH31, respectively.

3.1.2 Crosslinking reaction between PVOH films and GA

For the crosslinking reaction of PVOH films, a crosslinking solution was prepared. This aqueous solution contained GA, sulphuric acid and sodium sulphate at a ratio of 1:5:32 in molarity. GA solution (25% in water), sodium sulphate powder (Na_2SO_4 , ReagentPlus $\geq 99.0\%$, $M_w = 142.04$ and density = 2.68 g/cm^3) and sulphuric acid (conc.) were purchased from Sigma-Aldrich. Before any crosslinking reaction, PVOH films were dried at 40°C for 3 hours to release the majority of un-bound water. The dry films were then immersed in the crosslinking solution which was also kept at 40°C . The molar ratio between PVOH repeat units and GA was kept at 4:1. The calculations for the amount of crosslinking solution required for a reaction corresponding to the required PVOH/GA ratio are described in Appendix 1.

After specified lengths of time, the films were taken out of the crosslinking solution, thoroughly washed with water and then washed with acetone. Finally, films were dried in an oven at 40°C for 48 hours. Weights of films before and after crosslinking reaction were recorded.

3.1.3 Salt treatment of PVOH films

An aqueous salt solution was prepared by mixing the salt and water at the same ratio used in the crosslinking solution preparation (see Section 3.1.2) without the presence of GA and sulphuric acid. PVOH films ($M_w = 31,000-50,000$, 50-58 μm) were conditioned at 40°C for 3 hours before being immersed in the aqueous sodium sulphate solution which was also at 40°C. After specified lengths of time, the films were taken out of the salt solution and washed quickly and thoroughly with water. Finally, films were dried in an oven at 40°C for 48 hours.

3.2 CHARACTERISATION METHODS

Table 3.2 Characterisation methods and sample preparations

No.	Techniques	Sample preparation
1	Water vapour transmission rate (WVTR)	- Before measurements, samples were conditioned in a humidity chamber set at a specified temperature and relative humidity for at least 20 hours before measurement (i.e. after which no change in weight was observed)
2	Swelling test	- Samples were cut into squares (2.5 x 2.5 cm) and immersed in water for 24 hours
3	Contact angle measurement (CA)	- Samples were stored in a sealed container at room temperature after film preparation
4	Fourier transform infrared spectroscopy (FTIR)	- Samples were dried at 40°C in an oven overnight before spectra were collected.
5	Raman spectroscopy	- Samples were stored in a sealed container at room temperature after film preparation
6	X-ray diffraction	- Samples were dried at 40°C in an oven overnight before analysis
7	Dynamic mechanical analysis (DMA)	- Samples were cut into rectangular strips. Measurement areas were 4-5 mm width and 6-7 mm length. - Samples were dried at 40°C in an oven overnight before measurement

The instrumental set up for sample characterisations in this chapter are described in detail in Section 2.2, Chapter 2. Table 3.2 describes the sample preparations undertaken before each type of characterisation.

3.3 EFFECTS OF FILM THICKNESS, POLYMER MOLECULAR WEIGHT AND RELATIVE HUMIDITY ON THE WATER VAPOUR TRANSMISSION RATES (WVTR) OF PVOH FILMS

3.3.1 Effect of film thickness

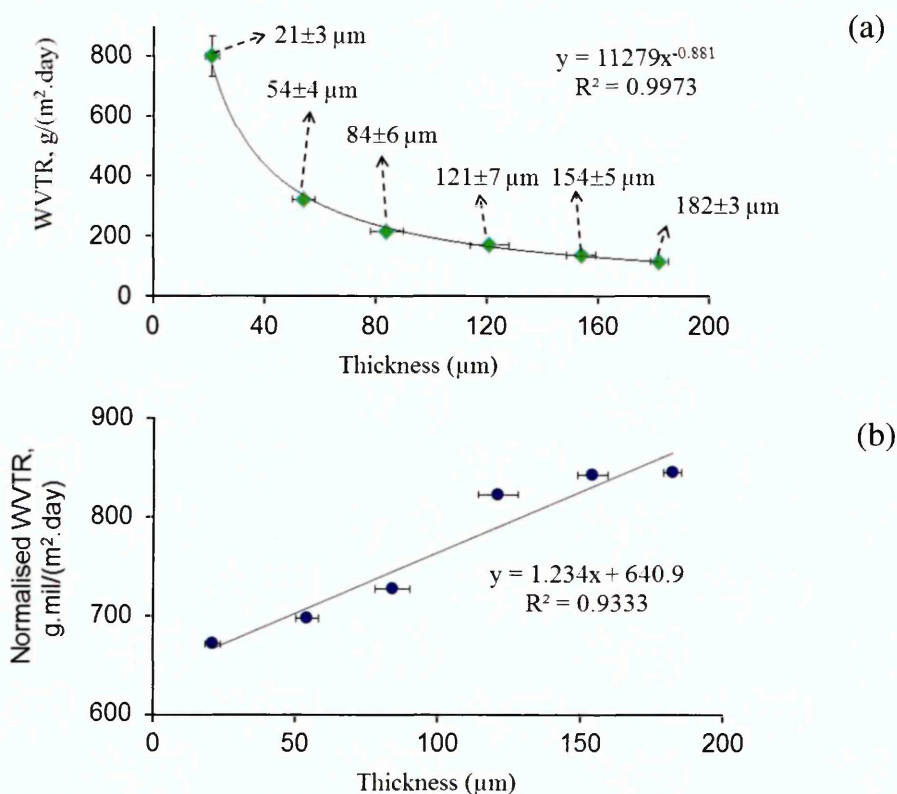


Figure 3.1 Water vapour transmission rates of PVOH films ($M_w = 31,000-50,000$) at 23°C and 85% RH as a function of film thickness

(a) A power regression line between WVTR values and film thickness

(b) Normalised WVTR to a film thickness of $25\ \mu\text{m}$

A decrease in WVTR values was observed when the film thickness increased, the relationship of which can be presented with a power function as shown in Fig.

3.1a. WVTR in the literature can be expressed as normalised data [139] to a film thickness of 25 μm and Fig. 3.1b shows the normalised data for PVOH films of various thicknesses. It can be observed that the normalised WVTR increases from 671 to 823 $\text{g.mil}/(\text{m}^2.\text{day})$ as the film thickness increases from 21 to 121 μm , but then tends to plateau as the thickness is increased further to 182 μm . This shows that the passage of water is dependent on film thickness when the film thickness is below 121 μm , but independent when above this thickness. Since the typical film thickness used within the data herein was $\sim 54 \mu\text{m}$ and within the region where WVTR values are dependent on thickness, it was decided to express all the data as raw data and not normalised.

Fig. 3.1a shows that for the thinner films a film thickness increase by ~ 2.6 times (from $21 \pm 3 \mu\text{m}$ to $54 \pm 4 \mu\text{m}$) results in a significant WVTR decrease by a similar factor of ~ 2.5 . With the thicker films, the WVTR values decreased relatively less. Taking two pairs of thickness values as examples, (54 ± 4 and 121 ± 7) and (84 ± 6 and 154 ± 5) where the increased thickness factors were 2.24 times for the former and 1.84 times for the latter, the corresponding decreases in the WVTR values for each pair were 1.9 and 1.57 times, respectively. Typically, the water vapour transmission rate of polymer is inversely proportional to thickness, i.e. $\text{WVTR} \propto \text{thickness}^{-x}$, where x is in a range of 0.8-1.2 [140,141]. The x values herein ranged from 0.8 to 1 and therefore in agreement with literature. According to Ashley [142], x was assumed to have a value of 1 because the permeability coefficient was independent of the film thickness. However, this assumption was simply for a perfect theoretical case and was thus not truly applicable for the empirical data herein.

Permeability coefficient is an alternative means to present WVTR data by taking into account the film thickness. It is similar to normalised WVTR but also accounts for differences in water vapour pressure below and above the film. Whether the permeability coefficient depends on the barrier thickness has been a controversy for a long time. Some authors reported the thickness dependence of permeability while others found it to be independent of the membrane thickness [143-145]. Fig. 3.2 illustrates the relationship between permeability coefficients of water vapour passing through PVOH and the film thickness and to some

extent resembles the normalised WVTR data presented in Fig. 3.1b. The calculation method used for the permeability coefficient is described in Appendix 2. It is observed that the permeability coefficients increased when the thickness increased from 121 to 182 μm but then became plateau up to 182 μm and the values ranged from 12,700 to 16,000 Barrers or $10^{-10} \text{ cm}^3(\text{at STP})\cdot\text{cm}/(\text{cm}^2\cdot\text{s}\cdot\text{cmHg})$. That the permeability coefficient is higher in thicker films is in agreement with Xianda *et al.* [146] who reported an increase in film thickness from 10 to 60 μm resulted in an increase in permeability coefficient by 95%.

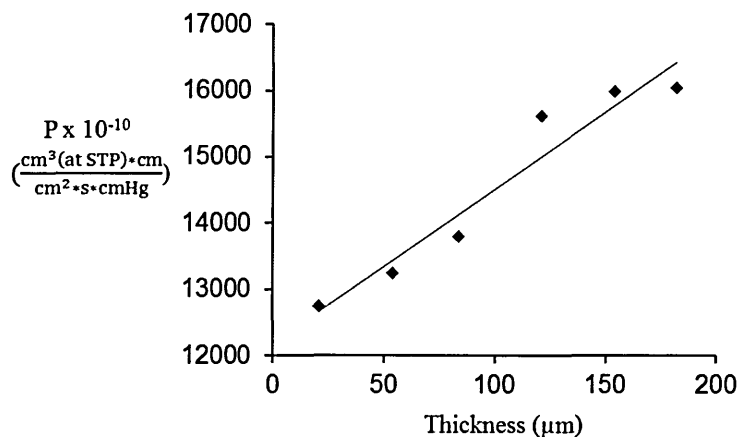


Figure 3.2 Changes of water vapour permeability coefficient at 23°C and 85% RH when thickness of PVOH films increases

Table 3.3 lists some permeability coefficients taken from the literature. It can be observed that the permeability coefficients vary greatly and this is due to the differences in measurement conditions, PVOH molecular weight, grade, and sample preparation method. The permeability coefficients herein (at 23°C, 85% RH) are different but sometimes comparable to the referenced data. Unfortunately, due to the vastly different experimental parameters and lack of information used within the literature (e.g. PVOH materials and preparation methods), a direct comparison cannot be sensibly achieved.

Table 3.3 Permeability coefficients of water vapour in PVOH membranes obtained from the literatures.

PVOH and test conditions		$P \times 10^{10} \left(\frac{\text{cm}^3(\text{at STP}) \cdot \text{cm}}{\text{cm}^2 \cdot \text{s} \cdot \text{cmHg}} \right)$	Ref.
25°C, 50% RH		2,900-14,900	[147]
23°C, p = 2.3 cm Hg		42,000	[123,141]
23°C, 85% RH		24,400	[122,148]
40°C, 90% RH		608	[122]
Biaxially-oriented film (12.2 ± 3 μm)	23°C, 50% RH	2.41-2.74	[122]
M _w = 74,800, films (10 - 60 μm) were prepared at 120°C/2hrs	38°C, 90% RH	5,354 - 10,458	[146]

3.3.2 Effect of molecular weight

PVOH films of two different molecular weights having the same degree of hydrolysis and film thickness (between 50-60 μm) were prepared via the same process. Based on a visual observation, the solution containing the higher molecular weight PVOH was more viscous than that containing the low molecular weight PVOH. In addition, there was no difference in the visual appearance of the two different film types. Fig. 3.3 shows the WVTR results obtained at 23°C and 85% RH for PVOH31 and PVOH124. The higher variability for PVOH31 is possibly due to a higher number of films being measured (21 compared to 3). It can be observed that when the molecular weight increased, the WVTR decreased by a factor of 30% from ~310 g/(m².day) for PVOH31 to 215 g/(m².day) for PVOH124.

Molecular weight has been stated to have little effect on diffusion rates and permeability of frequently used polymers in packaging [123]. However, according to data herein, a change in molecular weight has had significant

contribution to the WVTR. The effect of molecular weight will be discussed in detail in Chapter 4, section 4.4, page 127.

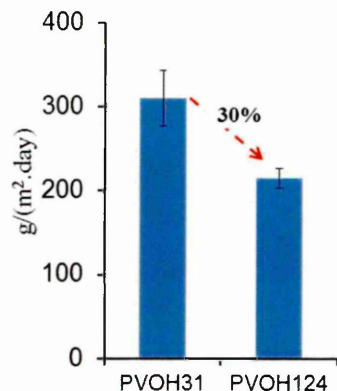


Figure 3.3 Water vapour transmission rates (23°C, 85% RH) of PVOH films with two different molecular weights: 31,000-50,000 (PVOH31) and 124,000-186,000 (PVOH124)

In correlation with the water vapour barrier property results, the water contact angles of PVOH124 films as a function of drop formation time are shown to have higher values than those of PVOH31 films (Fig. 3.4). This shows that water can wet the surface of PVOH31 films more easily than that of the PVOH124 films.

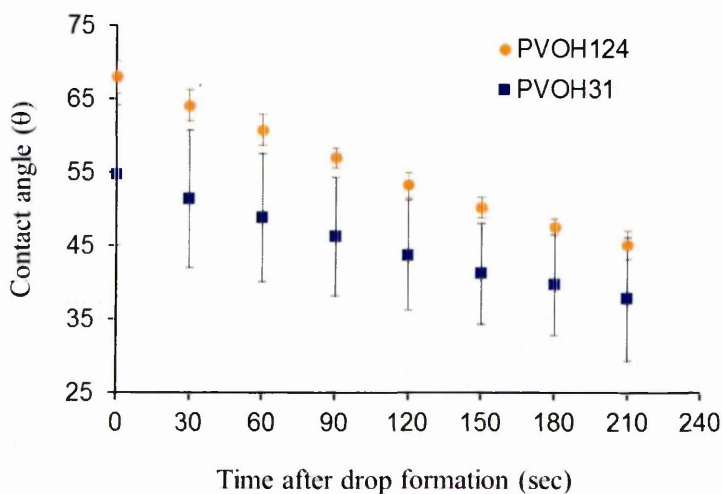


Figure 3.4 Water contact angle values versus time after drop formation for PVOH31 and PVOH124. The drop type was sessile and the testing atmosphere was 20-22°C and atmospheric humidity. Each value was a mean of 5-10 measurements at the same condition.

3.3.3 Effect of relative humidity on WVTR of PVOH films.

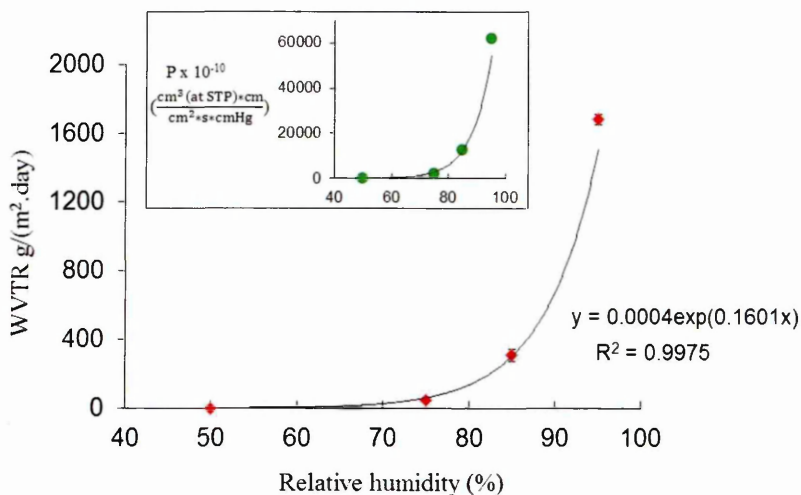


Figure 3.5 WVTR (♦) and permeability coefficient (●) of PVOH films ($M_w = 31,000 - 50,000$, $54 \pm 4 \mu\text{m}$) at different relative humidity and 23°C .

Xianda *et al.* [146] performed water vapour barrier for PVOH films (99% hydrolysis, $M_w = \sim 74,800$, $20 \mu\text{m}$) at 38°C and reported WVTR increased from 17.6 to $1350 \text{ g}/(\text{m}^2.\text{day})$ and permeability coefficients from 199 to $8217 \times 10^{-10} \text{ cm}^3(\text{at STP}).\text{cm}/(\text{cm}^2.\text{s}.\text{cmHg})$ when the RH increased from 50 to 90%. Fig. 3.5 shows that the WVTR values of PVOH films ($M_w = 31,000-50,000$) herein also increased with the increase of relative humidity and likewise the permeability coefficient. At 23°C , when the RH increased from 50 to 95%, the WVTR values increased from 1.2 to $1683 \text{ g}/(\text{cm}^2.\text{day})$ while the permeability coefficient increased from 84 to $61770 \times 10^{-10} \text{ cm}^3(\text{at STP}).\text{cm}/(\text{cm}^2.\text{s}.\text{cmHg})$. Therefore, whilst our WVTR values are perhaps comparable to Xianada's values, the coefficients are quite different. It may be due to differences in molecular weight, PVOH film preparation and measurement temperature. The exponential relationships shown between WVTR and RH in Fig. 3.5 are also in agreement with Mo *et al.* [122] who investigated the effect of RH (at 23°C) on the WVTR of biaxially-oriented PVOH (thickness $\sim 12 \mu\text{m}$, no molecular weight and hydrolysis provided). According to the authors, the increase in WVTR values of PVOH films with RH was due to a change in the hydrogen bonding between O-H groups of polymer chains and water molecules. The water had a plasticising

effect on PVOH which swelled the films. The extent of swelling in PVOH films increased with the increase of RH allowing the water vapour to diffuse through the films more quickly.

3.3.4 Summary

Either increasing the molecular weight of PVOH or film thickness did lead to a decrease in the water vapour transmission rates of the polymer films resulting in better water vapour barrier properties. The normalised WVTR and permeability coefficient, P , were shown to be thickness dependent when the film thickness was below 121 μm . PVOH with $M_w = 31,000 - 50,000$ was chosen to be the primary material for further exploration in this study as low molecular weight is preferred for coating purposes [39]. Specifically, a film of $54 \pm 4 \mu\text{m}$ in thickness was selected in order to be comparative to that of commercial PVOH films (for example, Kuraray Poval film with thickness $\sim 35\text{-}40 \mu\text{m}$). Furthermore, at this thickness any positive or negative changes in WVTR values due to any subsequent treatment would be more pronounced compared to thicker films (Fig.3.1a). Since this film thickness is within the region where WVTRs are dependent on thickness, the onwards WVTR data are expressed as raw data and not normalised.

On the contrary, an increase in relative humidity led to a corresponding increase in water vapour transmission rates as well as the permeability coefficient. With low RH's of 50 and 75%, films showed good resistance to water vapour with WVTR values below $50 \text{ g}/(\text{m}^2.\text{day})$. The environment with 95% RH produced the highest WVTR value; however these conditions are not common in product storage. Therefore, water vapour barrier properties of PVOH films at 23°C and 85% RH were required to be improved.

3.4 CROSSLINKING REACTION BETWEEN PVOH FILMS AND GLUTARALDEHYDE

3.4.1 Changes in weight and thickness after crosslinking reactions

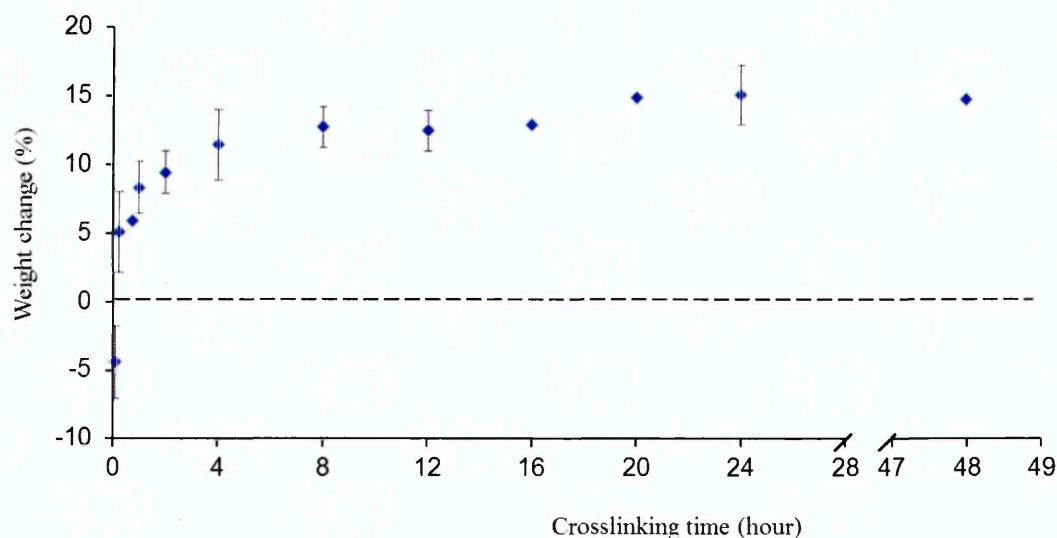


Figure 3.6 Weight change of PVOH films after crosslinking time increased. The reaction ratio was 4 moles of PVOH repeat units per 1 mole GA

Fig. 3.6 shows that apart from the samples crosslinked for 5 minutes, the weight of PVOH films increased when the crosslinking time increased. A negative value was observed for samples crosslinked for 5 minutes, this decrease maybe due to the loss of some PVOH molecules which were dissolved by water in the crosslinking solution before being stabilised by Na_2SO_4 and crosslinked with GA. Alternatively, some PVOH molecules may have been removed during the washing stage for the same reason. To support this, Table 3.4 shows that a decrease in sample weight was also observed when PVOH films were immersed in an aqueous Na_2SO_4 solution without the presence of GA and sulphuric acid (see Section 3.1.3). The weight loss change values displayed for PVOH films submerged in Na_2SO_4 solution for > 15 minutes (-0.38 to -1.78%) are not as great as those for the sample crosslinked for 5 minutes (~-4.5%) and therefore do not fully account for the larger decrease in the latter sample. Unfortunately, the data for 5 minutes treatment with salt solution could not be achieved since the produced films dissolved partially during the water washing stage.

Table 3.4 Weight change of PVOH films after immersion in Na₂SO₄ solution for different lengths of time.

Time in salt solution	Weight change (%)
15 minutes	-0.5
1 hour	-1.78
2 hours	-0.38
4 hours	-1.43
24 hours	-0.59

For the case of the 5 minutes crosslinked sample, more PVOH could have been lost from the sample due to less stabilisation from Na₂SO₄, but it is not possible to state with certainty at this stage. If one considers that the small amount of weight loss which occurred for the samples immersed in Na₂SO₄ solution for > 15 minutes (-0.38 to -1.78%) is only a small fraction of the weight change after crosslinking (and also within the distribution of weights increase after crosslinking), these weight increases can be used with more confidence to calculate the degree of crosslinking. Furthermore, any amounts of water present in the films before crosslinking were negligible and also accounted for in the weight gains calculations.

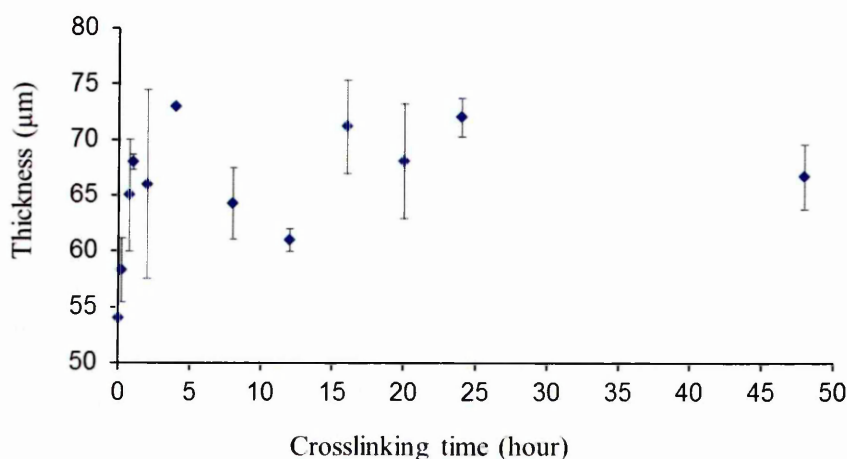


Figure 3.7 Changes of PVOH film thickness with crosslinking times. The reaction ratio was 4 moles of PVOH repeat units per 1 mole of GA

After the crosslinking reaction, the thickness of PVOH films varied but in general they increased after the crosslinking (Fig. 3.7). The biggest increase was

noticeable after 15 minutes and prolonging the crosslinking time did not show any significant change in the film thickness.

3.4.2 Degree of crosslinking (d_{CR})

The degree of crosslinking was calculated based on the weight gain of PVOH films after the crosslinking reaction. As previously explained, the weight change at 5 minutes was negative (Fig. 3.6) so the degree of crosslinking at this point of time could not be determined. The calculation for the crosslinking degree based on the weight increases of PVOH films, which were considered to equal the amount of GA consumed during the crosslinking, is described in Appendix A1.2 with a hypothesis that no PVOH was lost during the reaction due to the dissolution.

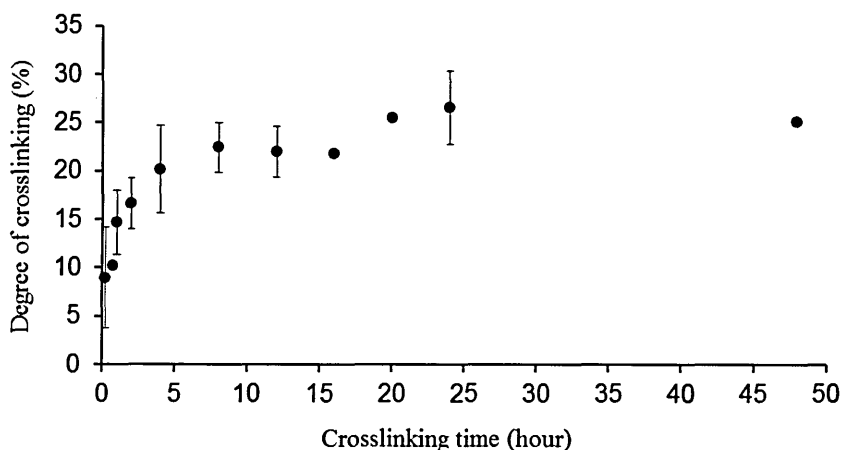


Figure 3.8 Degree of crosslinking as a function of crosslinking time. Values were calculated from the weight gain of PVOH films. The crosslinking ratio of PVOH repeat units and GA was 4:1

Fig. 3.8 shows an increase in the crosslinking degree with crosslinking time, having a maximum value of 26.5% achieved with 24 hours of treatment. From 15 minutes up to 4 hours, the degree of crosslinking increased gradually from 9% to 20.2%, respectively. After 4 hours of crosslinking time, the degree of crosslinking plateaued until a crosslinking time of 20 hours where a stepped

increase was observed, no further significant changes were observed in the following 24 hours.

3.4.3 WVTR results

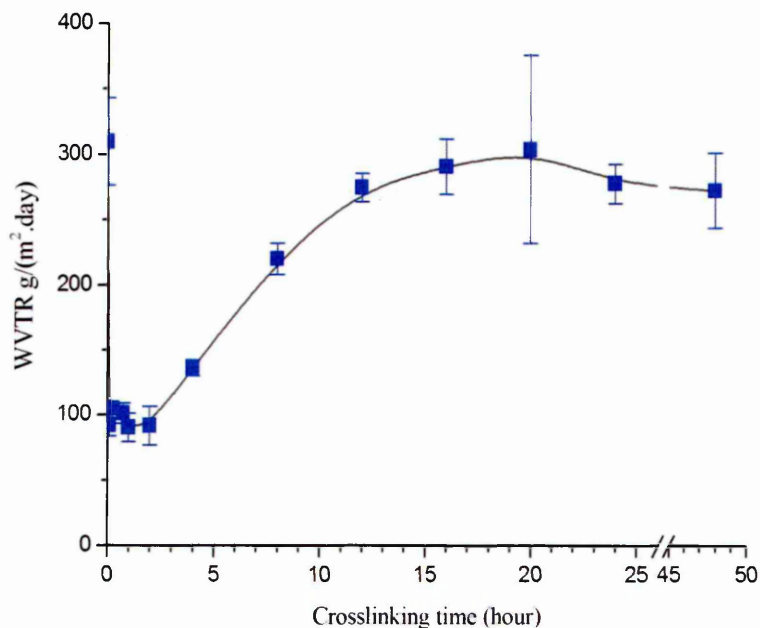


Figure 3.9 WVTR results (23°C, 85% RH) of crosslinked PVOH films at different crosslinking times. The ratio of PVOH repeat units and GA was 4:1.

The WVTR results obtained from the various PVOH films crosslinked using a molar ratio of PVOH repeat unit : GA of 4 : 1 are shown in Fig. 3.9. A significant improvement in water vapour barrier properties can be observed with low crosslinking times (5 minutes up to 2 hours) since WVTR values decrease between 66-70% in comparison with that of un-crosslinked film. For example, the WVTR value of un-crosslinked film (310 g/(m²·day)) decreased to 92 g/(m²·day) and 91.8 g/(m²·day) after the films were crosslinked with GA for 5 minutes and 2 hours, respectively. After 2 hours of treatment, the WVTR values started to increase gradually representing a worsening of water vapour barrier properties and when prolonging the crosslinking time after 16 hours and up to 48 hours no notable differences in the WVTR values were observed.

Based on the thickness and WVTR values of the crosslinked films, the water vapour permeability coefficient was determined and its relationship with the degree of crosslinking is exhibited in Fig. 3.10b. This shows a similar pattern to that of the WVTR values which are also presented as a function of crosslinking degree in Fig. 3.10a. It can be observed that the increase in both WVTR values and permeability coefficients occur after a crosslinking degree of 16.6%, which corresponds to 2 hours of crosslinking time.

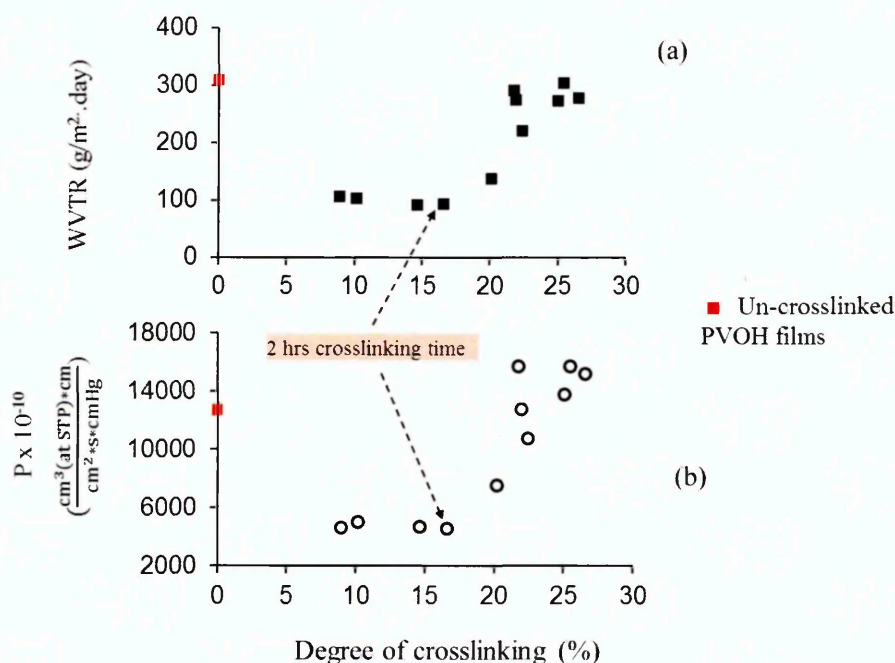


Figure 3.10 Relationship between (a) WVTR values and (b) permeability coefficients as a function of the degree of crosslinking. Conditions: 23°C, 85% RH

Incidentally, when changing the molar ratio, the WVTR values are very similar for the three different molar ratios at short crosslinking times (up to 2 hour) (Fig. 3.11). After 15 minutes of crosslinking time, the WVTR values of the PVOH films decreased sharply from ~ 310 g/(m².day) to 118, 105 and 111 g/(m².day) for ratios of 4/0.5, 4/1 and 4/2, respectively, and these improvements equate to an improvement between 62 to 66%. When extending the treatment time to 24 hours, the WVTR values increased markedly and the lowest value was observed for the ratio of PVOH repeat unit/ GA of 4/0.5 (217 ± 0.5 g/(m².day)).

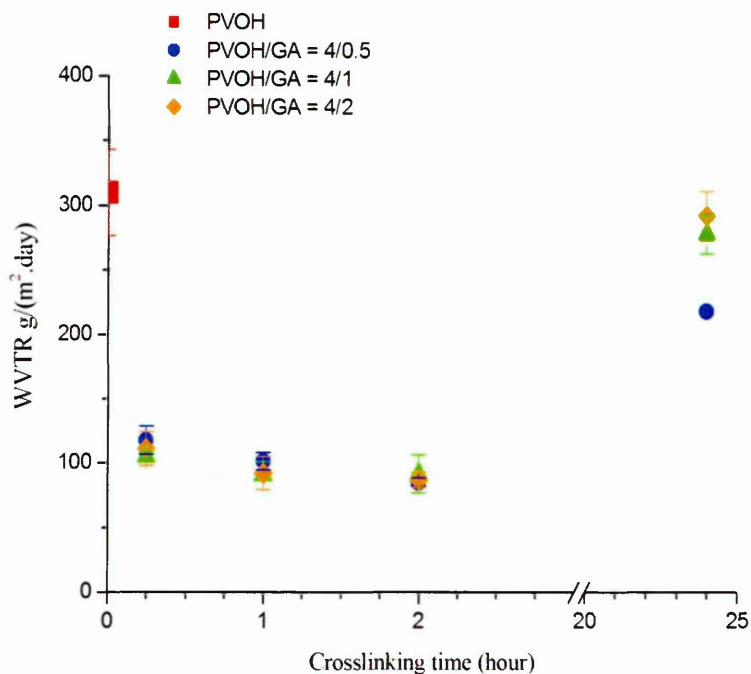


Figure 3.11 A comparison of WVTR results (23°C, 85% RH) from PVOH and crosslinked PVOH films when using three different molar ratios of PVOH repeat units to GA, which were 4/0.5, 4/1 and 4/2.

3.4.4 WVTR results of crosslinked films in different RH environments

The effects of RH on the water vapour barrier properties of crosslinked PVOH films were investigated. Here, only the crosslinked films produced at low and medium crosslinking times (5 and 15 minutes, 1 and 2 hours) were investigated as these showed the best improvement in water vapour barrier properties (at 23°C, 85% RH) in comparison with untreated PVOH films (see Section 3.4.3). Like the untreated PVOH films (see Fig. 3.5), the WVTR values of each crosslinked films increased with increasing RH, this exponential relationship is shown in Fig. 3.12.

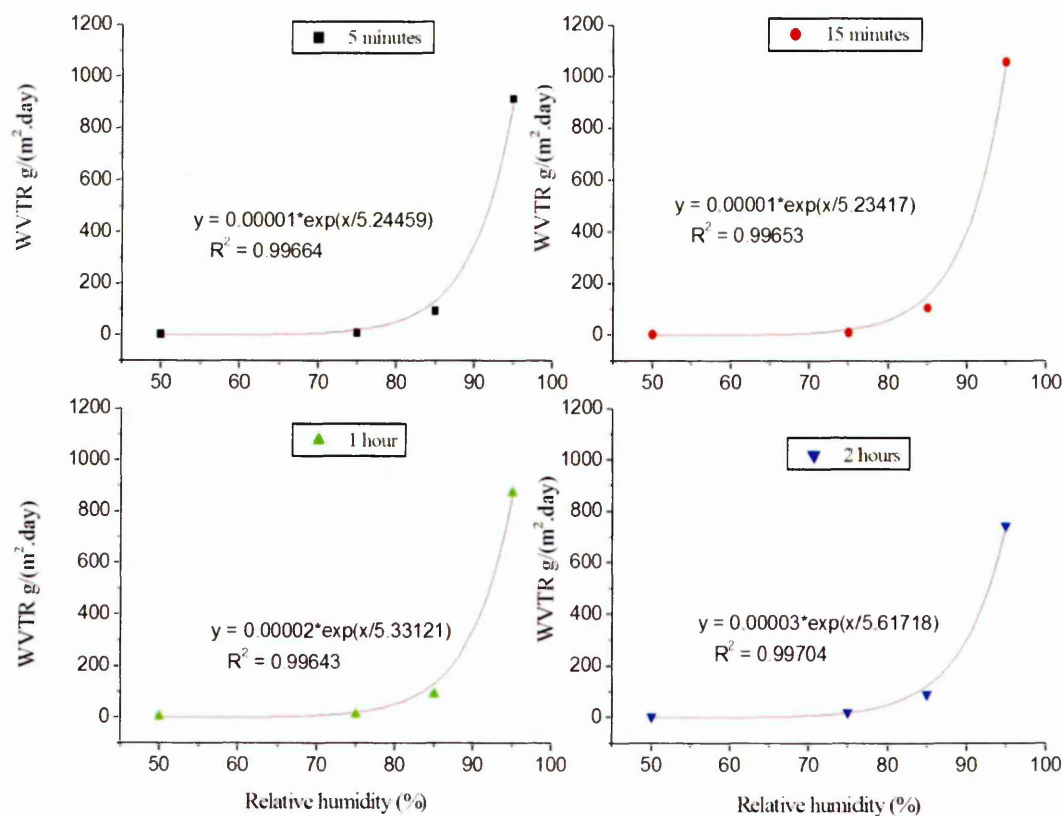


Figure 3.12 Relationship between WVTR values and RH for PVOH films crosslinked for 5, 15 minutes, 1 and 2 hours. The temperature for WVTR experiments was 23°C

Fig. 3.13 illustrates the WVTR values of crosslinked film at different RH as a function of crosslinking time. Fig 3.13a shows that at with RH's of 50 and 75%, the WVTR values of crosslinked films were very low, less than 5 g/(m².day) and 25 g/(m².day), respectively. At 50% RH, the WVTR value of the untreated PVOH (1.2 g/(m².day)) was below those of the respective crosslinked films at the same RH. However, with the other RH's, the crosslinked films always provided lower WVTR values than those of the un-crosslinked PVOH films at the respective RH's. The low WVTR values for films treated at 50% RH reflect the limits of the test at these conditions and an inability to distinguish any difference. With RH's of 85 and 95%, the WVTR values of PVOH films decreased significantly with any crosslinking and for any particular time (Fig. 3.13b). The highest WVTR values were obtained at 95% RH with the values of 913, 1057, 873 and 743 g/(m².day) for films crosslinked at 5, 15 minutes, 1 and 2 hours, respectively.

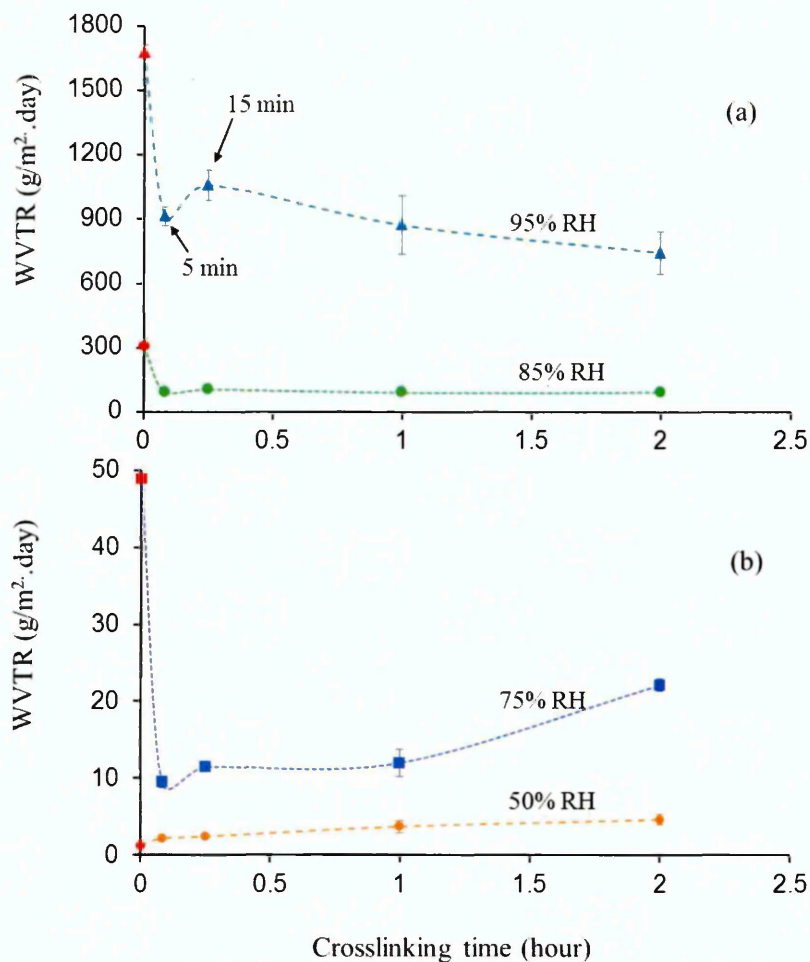


Figure 3.13 WVTR results (at 23°C) for PVOH and crosslinked films at different RH as a function of crosslinking time

In summary, the crosslinking reaction between PVOH and GA can help to improve the water vapour barrier properties of PVOH films significantly at high RH environments (75-95%). At low RH (<50%), PVOH does not absorb much water vapour and crosslinking the films does not contribute to the improvement in the water vapour barrier properties.

3.4.5 Moisture content and swelling test results

The moisture contents in neat PVOH and crosslinked films after conditioning in a humidity chamber for 24 hours at 23°C , 85% RH were investigated. Increasing the conditioning time to 48 hours did not change the weight of the films indicating that 24-hour conditioning was enough to reach an equilibrium state.

This data reflects the amount of water present in the films during the film preconditioning before WVTR experiment. Fig. 3.14 illustrates a decrease in the amount of absorbed water after PVOH films were crosslinked with GA. The amount of absorbed water was highest for the neat PVOH films, which then gradually decreased with short crosslinking times up to 2 hours. Extending the crosslinking times led to no further significant change in the moisture contents.

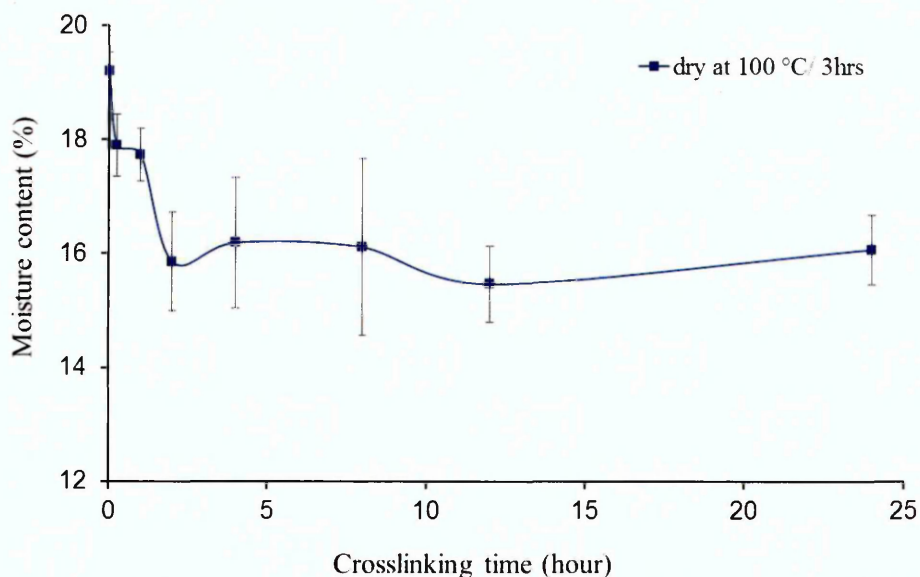


Figure 3.14 Moisture contents in neat PVOH and crosslinked films after being kept in a humidity oven for 24 hours at 23°C, 85% RH. Moisture values were determined after drying the films 100°C for 3 hours.

The swelling properties of PVOH and crosslinked PVOH in water when kept at 22°C and 90°C were also investigated; the former is considered room temperature while the latter is that used for PVOH film preparation. When an untreated PVOH film is immersed in water, it fully dissolves after 15 minutes which reflects its hydrophilic nature. Thus, it can be inferred that the swelling degree of PVOH film has an infinite value. Fig. 3.15 shows that the degree of swelling of the crosslinked films in water kept at either 22°C or 90°C decreased with increasing crosslinking time. With short crosslinking times (< 1 hour) the decrease was sharp, but then continued to decrease only slightly as the

crosslinking time increased above 2 hours. It can be seen from the graph that the relative swelling degrees of the films in water kept at 90°C were higher than those at 22°C, but only for those with short crosslinking times (< 2 hours). Above 2 hours, there were no significant differences between the relative swelling degrees when kept in water at 22°C or 90°C indicating no matter what temperatures the water was at, after a certain extent of crosslinking time, the swelling degree of the crosslinked films could no longer be increased.

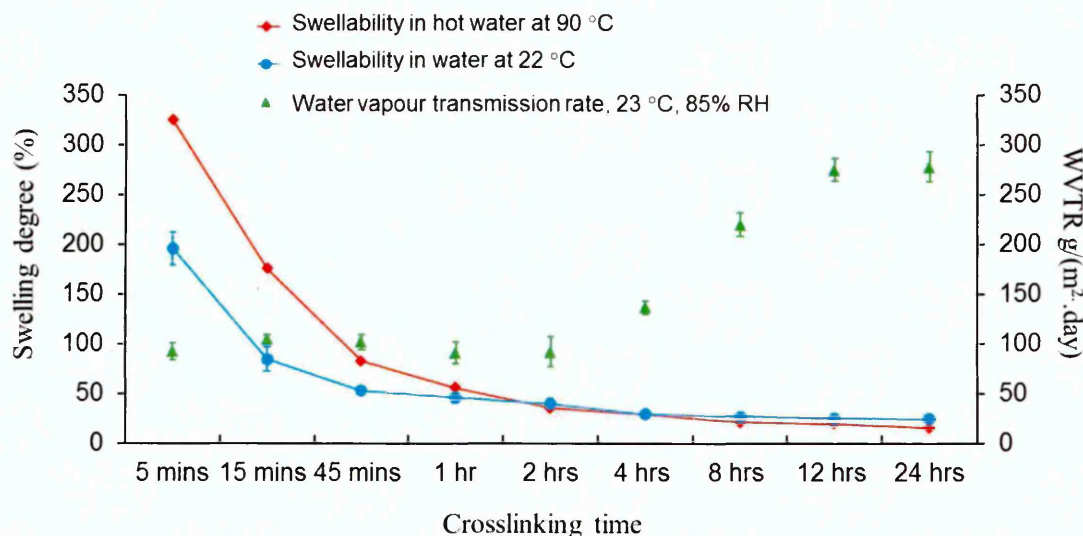


Figure 3.15 Degree of swelling in water at 22°C and 90°C for crosslinked PVOH films prepared with different crosslinking times in comparison with respective WVTR values.

It is interesting to observe that while the swelling in water of the crosslinked PVOH films decreased with crosslinking time and reached a minimum point of swelling at 2 hours, the water vapour transmission rates (WVTR) behaved in an opposing way since before 2 hours of treatment time a plateau was observed and after 2 hours, the values started increasing.

3.4.6 Contact angle results

Fig. 3.16 pictures the shape changes of liquid water on the surface of the PVOH films with time after drop formation as a function of crosslinking time. The

measurement time was below and up to 240 seconds since water evaporates with longer time. It can be observed that the longer the liquid drops remained on the film surfaces, the more the water wetted the films resulting in the reduction of the droplet volumes. As crosslinking time increased the wetting of water on the film surfaces decreased as seen by less spreading of the water droplets on the surfaces.

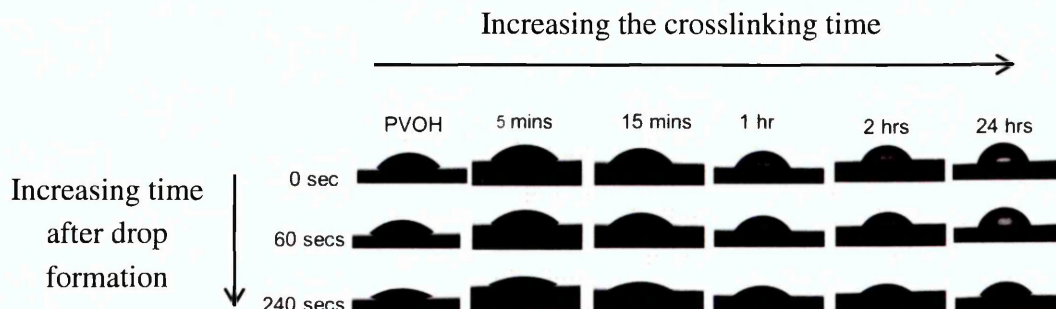


Figure 3.16 Water droplet shapes on the surfaces of PVOH and crosslinked films obtained via contact angle experiments

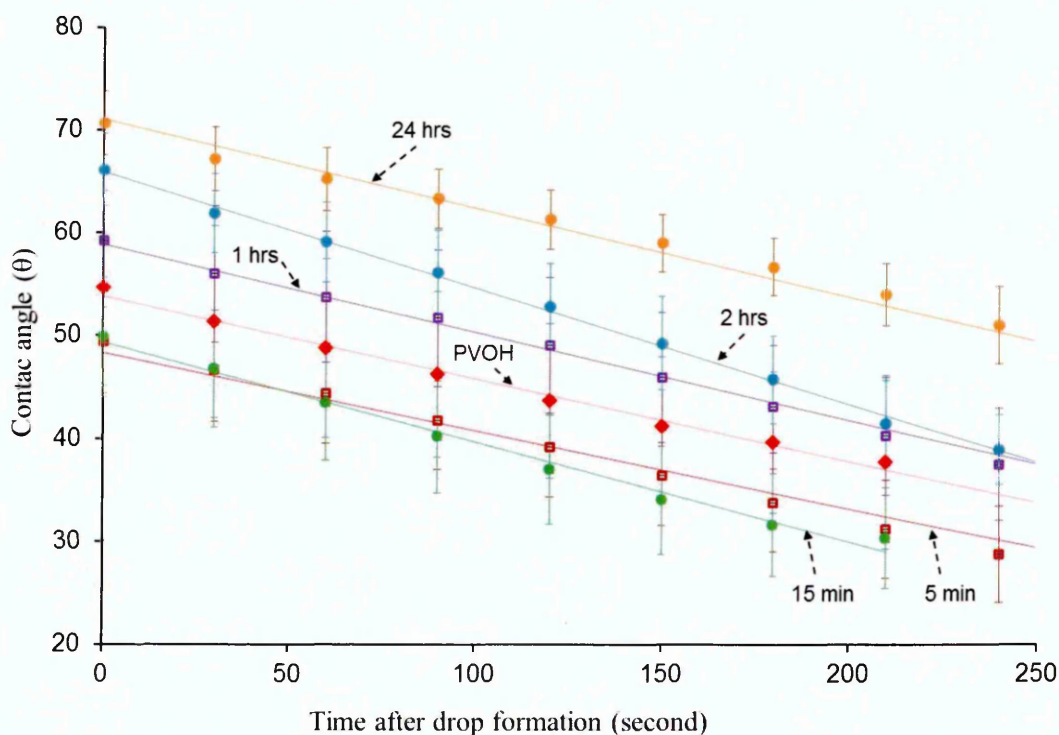


Figure 3.17 Water contact angle values versus time after drop formation obtained from neat PVOH film and crosslinked films prepared with different crosslinking time. The drop type was sessile and the testing atmosphere was 20-22°C and atmospheric humidity. Each value was a mean of 5-10 measurements at the same condition.

The contact angle values from films crosslinked at 5 and 15 minutes were similar and lower than those of neat PVOH films (Fig. 3.17). At the initial point (0 sec), the neat PVOH films had a contact angle value of $\sim 55^\circ \pm 9$, which was comparable to some values described in the literature ($\theta = 51^\circ$ at 25°C [149], $\theta = 74^\circ$ [150], 57 ± 1 [151]). The corresponding values for films crosslinked at 5 and 15 minutes were $\sim 50^\circ \pm 5$ and $50^\circ \pm 6$, respectively. Films crosslinked for 24 hours exhibited the highest contact angles which were $\sim 71^\circ \pm 3$ at 0 sec and $\sim 51^\circ \pm 4$ at 240 sec.

3.4.7 FTIR results

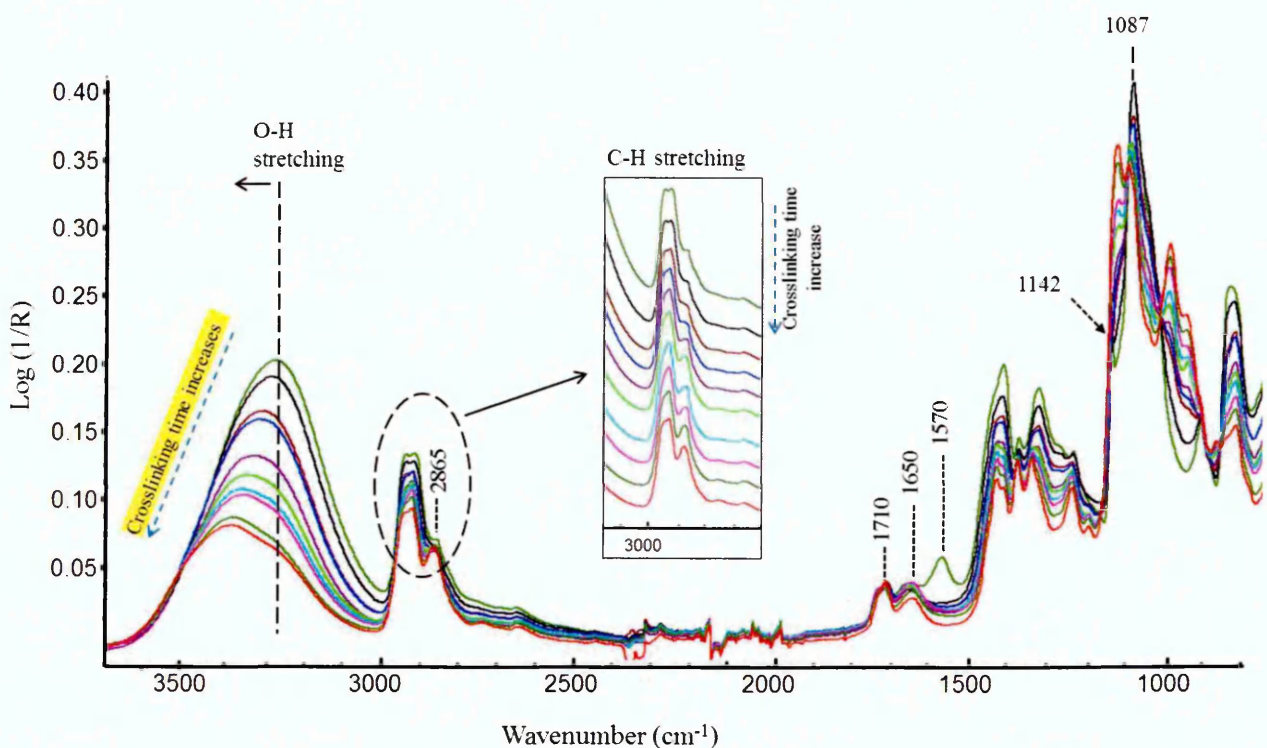


Figure 3.18 ATR-FTIR spectra of PVOH and crosslinked films from using different crosslinking times (5 minutes to 48 hours)

FTIR spectroscopy was used to monitor the molecular changes of the PVOH films after crosslinking. The spectrum of PVOH film exhibits several specific absorption bands of interest (Fig. 3.18). The broad O-H stretching band in the range $3000 - 3600\text{ cm}^{-1}$ includes contributions from PVOH and absorbed water

while the peak at 1650 cm^{-1} derives from the O-H bending mode of absorbed water [65,152]. The two peaks within the region 2890 to 2950 cm^{-1} are assigned to C-H stretching. The carbonyl group (C=O) of unhydrolysed poly(vinyl acetate) is represented by the band at 1710 cm^{-1} while the band at 1570 cm^{-1} is from sodium acetate impurity formed during the manufacturing process of PVOH from poly(vinyl acetate) [40]. The two absorption bands at 1142 cm^{-1} and 1087 cm^{-1} are assigned to the C-C skeleton stretching mode and C-O stretching of C-OH, respectively.

When PVOH films are crosslinked with GA, O-H groups are consumed as GA forms acetal linkages, this leads to a decrease in the peak intensity of the O-H stretching band. When crosslinking time was increased, an increase in the intensity of the band at 2865 cm^{-1} is observed, which is due to the C-H stretching of the aldehyde. These changes prove that the crosslinking reaction between PVOH and GA has occurred [66,80,153]. It can be observed that when increasing the crosslinking time, the O-H band shifts from 3270 cm^{-1} for untreated PVOH to higher wavenumber for crosslinked films indicating weaker hydrogen bonding networks in the crosslinked systems [59,60]. In addition, the 1710 cm^{-1} peak which represents the C=O stretching of carbonyl groups is practically unchanged when extending the crosslinking time up to 24 hours (Fig. 3.19a). With 48 hours crosslinking time, the intensity of this peak increases indicating the presence of aldehyde peaks. Yoem and Lee [80] mentioned the existence of pendant aldehydes in their fully crosslinked product. When PVOH films were crosslinked with GA for longer times, there was a strong likelihood that pendant aldehyde groups were present leading to the increase in the intensity of the 1710 cm^{-1} peak. Presumably, as fewer and fewer hydroxyl groups remain, the likelihood of a GA molecule bridging across two PVOH chains decreases.

A decrease of the 1142 cm^{-1} peak and an increase of the 1129 cm^{-1} peak are observed in Fig. 3.19b when the crosslinking time increases. With 15 minutes crosslinking time, the intensity of the peak at 1142 cm^{-1} decreases but after 45 minutes crosslinking time it is not clearly present due to the growth of the 1129 cm^{-1} peak. The growth of the 1129 cm^{-1} peak, assigned to C-O stretching groups of acetal linkages formed as a result of crosslinking reaction, indicates more

acetal linkages are generated when increasing the crosslinking time [80,153]. There is a likelihood that the increase in the intensity of the 1129 cm^{-1} peak makes this peak become so dominant that it overlays and hides the peak at 1142 cm^{-1} . Calculating the degree of crystallinity of crosslinked films using the 1142 cm^{-1} peak and Eq.2.4 (Section 2.1.4) as proposed by Tretinnikov *et al.* [37] is not possible at higher crosslinking times due to the increasing C-O stretching absorbance band making it very difficult to obtain values for its relative intensity.

There is evidence however to show that the 1142 cm^{-1} peak is still present in the spectra of longer-crosslinking-time samples by using the second derivative spectra (Fig. 3.19c). OMNIC software was used to convert the original spectra to their second derivatives using the Savitzky-Golay filter set with 5 data points and a polynomial order of 3. Theoretically, the second derivative shows the change in rate of change across the spectra and can help to locate the centre of shoulders or overlapping and hidden peaks in the original spectra [154,155]. In addition, the second derivative has been most commonly used for detecting trace components in the presence of a strong background [156].

Fig. 3.19c shows that the 1142 cm^{-1} peak (observed in the derivative spectra as a trough) is still present in all the spectra collected from the crosslinked films. It is more prominent in the derivative spectra for PVOH and the 15-minute crosslinked film, the depth of the trough then appears almost unchanged in those crosslinked for 45 minutes or longer. It can however be observed in Fig. 3.20 that there is actually a significant decrease in the absolute height of 1142 cm^{-1} (in the derivative spectra) with the crosslinking time from 5 minutes to 1 hour, which plateaus up to 4 hours and then continues to decrease gradually to 12 hours crosslinking time

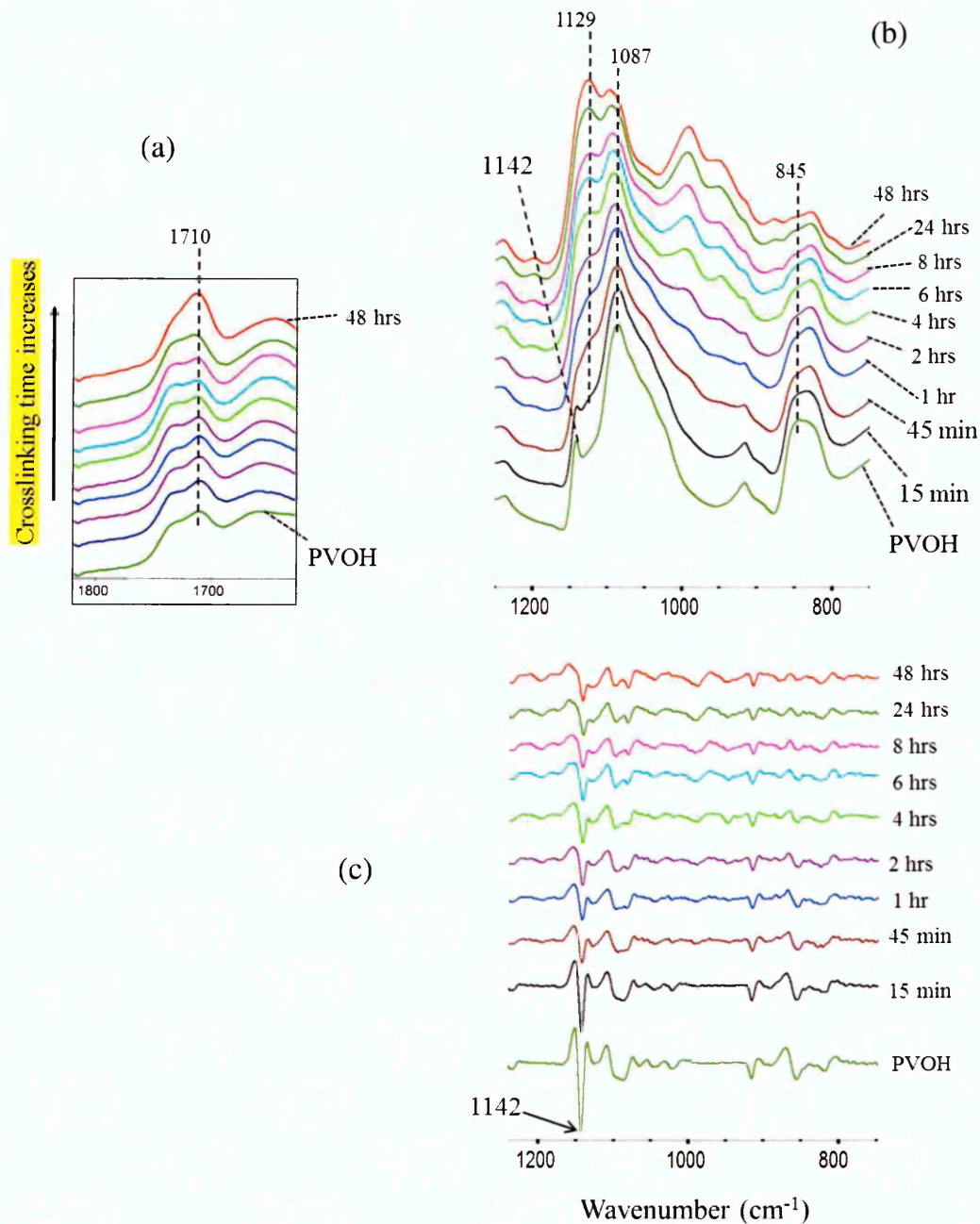


Figure 3.19 (a) Changes in the absorption band at 1710 cm⁻¹ with increasing crosslinking times

(b) ATR-FTIR spectra (1200-800 cm⁻¹) of PVOH and crosslinked films prepared with different crosslinking times.

(c) Corresponding second derivative spectra. The Savitzky-Golay smooth was used and set with 5 data points and polynomial order of 3. Spectra are shifted vertically for better clarity

The derivative of a peak is said to be proportional to its peak height in the original spectra [156]. Therefore, the decrease in the amplitude of the trough at

1142 cm^{-1} in the derivative spectra of the crosslinked films reflects a decrease in the intensity of this peak in the original spectra, suggesting a decrease in the crystallinity of PVOH films after crosslinking with GA [37,49,51,99]. In Fig. 3.20, the decrease in the absolute height is 17% with 5 minutes crosslinking time and reached 70 - 71% from 1 to 4 hours of treatment. With 24 and 48 hours of crosslinking time, the decreases are 77 and 78%, respectively which indicates that extending the crosslinking time resulted in very low crystallinity. This is in agreement with Peppas *et al.* [50] who reported that highly and moderately crosslinked PVOH possessed very little crystallinity when investigating the crystallisation kinetic of PVOH using DSC and FTIR.

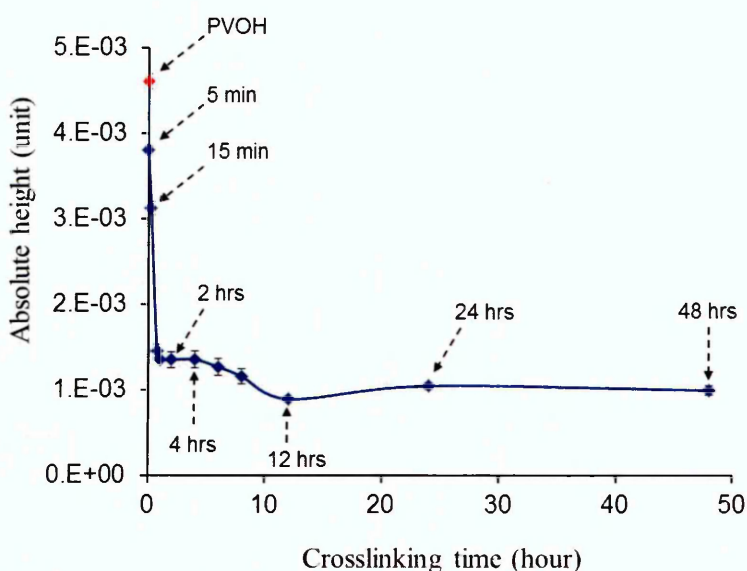


Figure 3.20 Absolute heights of the 1142 cm^{-1} peak obtained from the second derivative spectra of PVOH and crosslinked films as a function of crosslinking time.

The absorption band at 845 cm^{-1} assigned to the C-C skeletal bending mode [43,157] has also been reported to be crystallinity sensitive [99]. Fig. 3.21a shows the peak height ratio H_{845}/H_{1710} decreases when the crosslinking time is increased, here the absorption band at 1710 cm^{-1} is used as a reference because it is unaffected by changes in crystallinity. This indicates a decrease in crystallinity when the films were crosslinked. A steep decrease was observed for samples treated with increasing crosslinking times up to 2 hours, and with longer

crosslinking times the decrease was less pronounced. In addition, the peak height ratio H_{845}/H_{1710} is also observed to be inversely proportional to the degree of crosslinking (Fig. 3.21b) showing that the number of crosslinks directly related to a decrease in the crystallinity. The data calculated from the peak height ratio of H_{845}/H_{1710} shows very similar trends to that obtained from the derivative data utilising the 1142 cm^{-1} peak (Fig. 3.20). This therefore provides some credence to the latter data which was more troublesome to obtain due to the overlapping band at 1129 cm^{-1} .

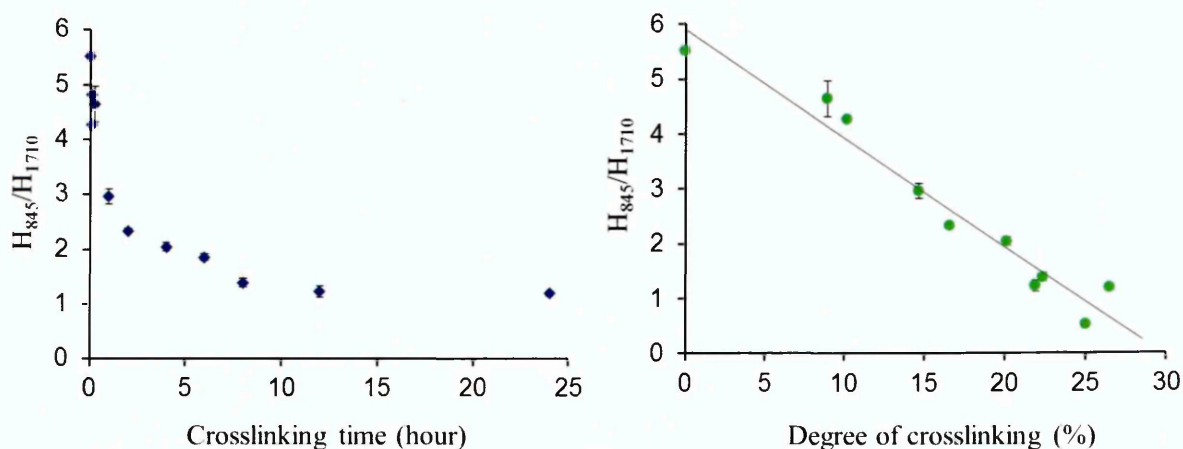


Figure 3.21 Peak height ratio for H_{845}/H_{1710} with respect to (a) crosslinking time and (b) degree of crosslinking. The degree of crosslinking was determined by mass gain measurements.

3.4.8 Raman spectroscopy results

Fig. 3.22 exhibits a typical Raman spectrum collected from a PVOH film and is in agreement with other published data [158,159]. The $1200 - 1000\text{ cm}^{-1}$ region is reported to be crystallinity-dependent and in particular for peaks at 1148 and 1094 cm^{-1} [159]. The assignments for peaks observed in the Raman spectrum are listed in Table 3.5 and were obtained from references in the literature [158-161].

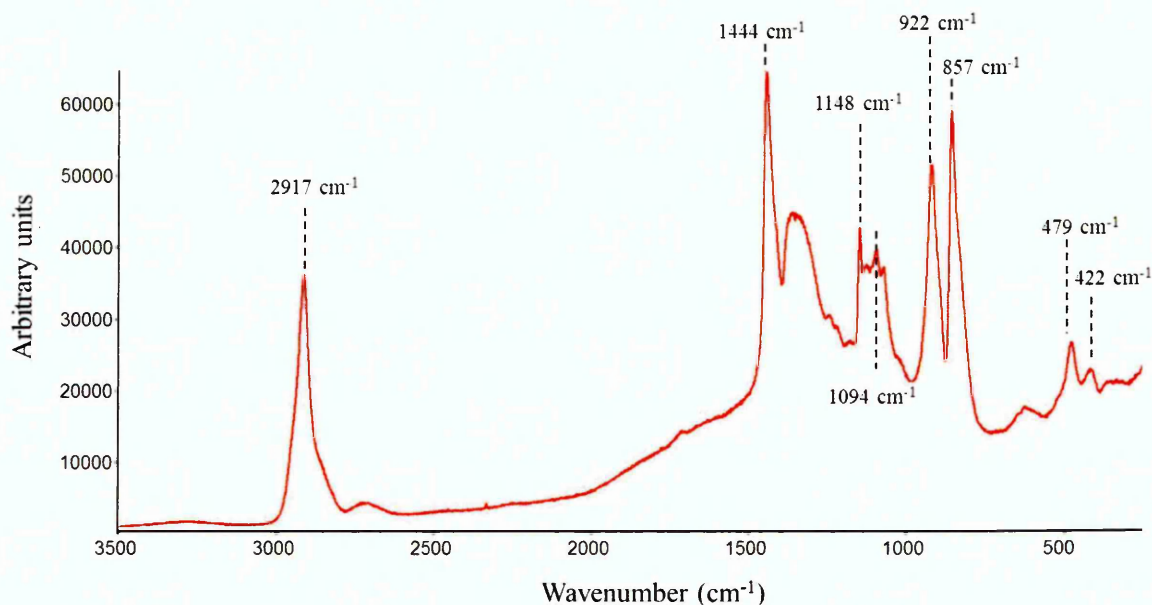


Figure 3.22 Raman spectrum of PVOH film

Table 3.5 The assignments of Raman bands of PVOH

Wavenumbers (cm ⁻¹)	Assignments
422	C-O wagging
479	C-O bending, C-H out of plane
627	O-H wagging, O-H twisting
857	C-C stretching
922	C-C stretching or C-H rocking
1072	C-O stretching
1094	C-O stretching; C-O and O-H bending
1148	C-O-C stretching, C-C and C-O stretching
1244	C-H wagging; C-OH valence asymmetric ring vibration
1300 - 1382	C-H bending, O-H bending
1444	C-H bending
2917	C-H stretching

The Raman spectra for the crosslinked PVOH films are shown in Fig. 3.23 and present some significant changes in the 1400 - 600 cm⁻¹ region. When these are compared to the spectrum of the untreated PVOH film, decreases in the intensity of the crystallinity bands at 1148 and 1094 cm⁻¹ are observed as the crosslinking

time increases, this supports the FTIR data presented above. Moreover, the decreases in the C-C stretching bands at 857 and 922 cm^{-1} are indicative of some conformational changes in the backbone [162]. The broad band between 1382 and 1300 cm^{-1} , which is ascribed to the C-H and O-H deformation vibrations [163,164] in the spectrum of untreated film, decreases in intensity and is replaced by four visible bands at 1382, 1348, 1331 and 1302 cm^{-1} upon crosslinking which are complicated to assign due to the many overlapping bands in this region [164]. It is however noted that GA also has an absorption band of medium intensity in this region due to C-H bending rather than C=O stretching.

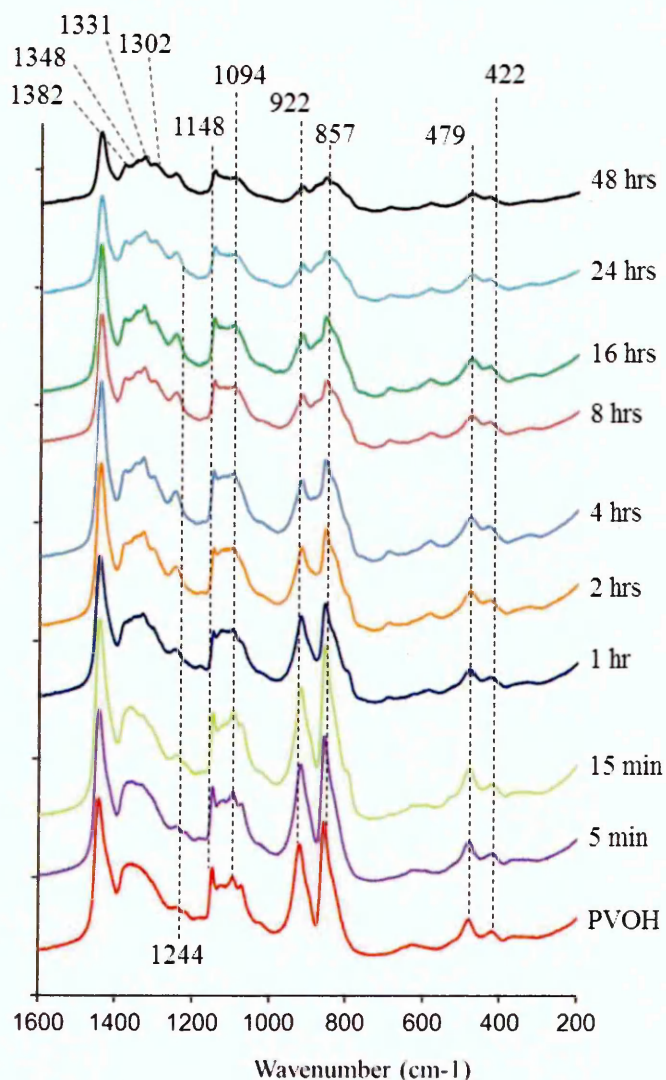


Figure 3.23 Raman spectra of PVOH films after crosslinking with GA for different crosslinking times. Spectra are off-set vertically for clarity

Another significant change is an increase in the intensity and a shift to higher wavenumber for the band at 1244 cm^{-1} . This is likely to be attributed to an increase of C-O stretching through acetal group formation although this has previously been assigned to C-H bending elsewhere. In the crosslinked films, the C-O stretching of the cyclic ether groups, which is reported to be present at $1270\text{--}1030\text{ cm}^{-1}$ in literature [164], is more likely to absorb radiation much stronger than the C-O stretching groups of PVOH and so could be the reason it becomes more dominant as crosslinking increases. In addition, the shift of the 1244 cm^{-1} to the higher wavenumber (1255 cm^{-1}) as the films are crosslinked for longer indicates a decrease in H-bonding strength. Martinelli *et al.* [162] reported additional and intense bands at 980 and 1120 cm^{-1} representing C-O-C stretching in the crosslinked network of PVOH and GA. However, in the Raman spectra herein, these bands were not clearly present. This may be due to the differences in materials and/or sample preparation since the authors mixed GA with PVOH before film casting wherein herein the PVOH films were immersed in the crosslinking solution.

3.4.9 XRD results

Fig. 3.24 shows the diffraction traces of the PVOH and crosslinked films over the angular range $8\text{--}25^\circ 2\theta$. The principle crystal diffraction peak is positioned at $19.18^\circ 2\theta$ for the untreated PVOH films and slightly shifts to a lower Bragg angle with increasing crosslinking time indicating an increase in the spacing between the planes in the lattices as well as a less tightly packed crystal network. Also, the broadening of this crystal diffraction peak and a decrease in peak height with increased crosslinking times corresponded to a decrease in crystallinity. The decrease in crystallinity of PVOH after crosslinking with GA was also reported by Mansur *et al.* [165] who characterised the structure of PVOH-derived hybrids using small-angle X-ray scattering. These XRD results are consistent with the FTIR and Raman results.

Table 3.6 highlights the slight decrease in position of the principle crystal diffraction peak as well as the increase in FWHM values when PVOH films experience increased crosslinking times.

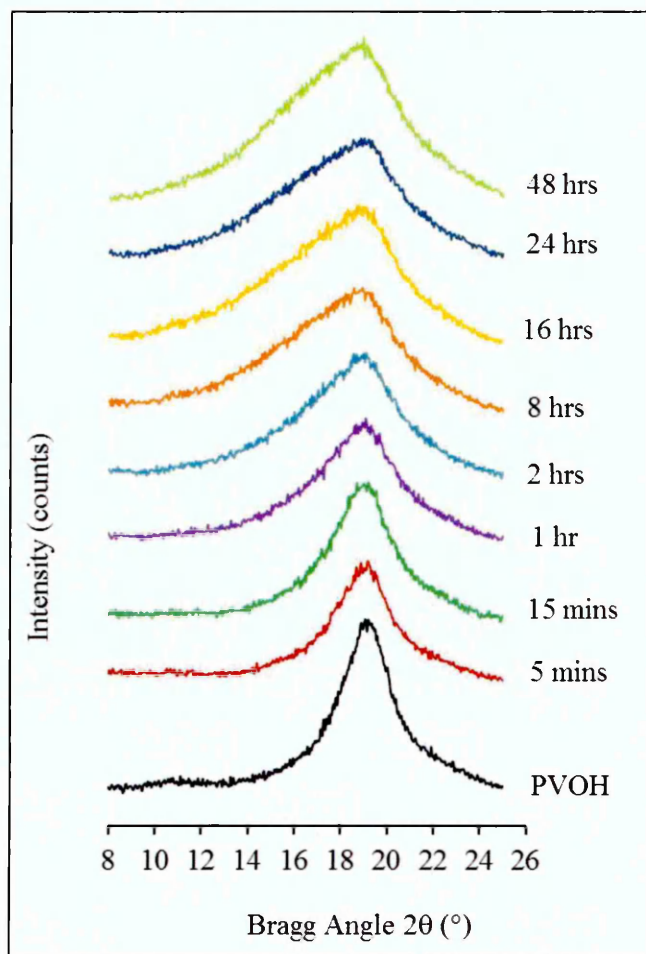


Figure 3.24 X-ray diffractograms of PVOH and crosslinked films prepared using different crosslinking times. The patterns are shifted along the ordinary for more clarity.

Crystallite sizes of PVOH and crosslinked films of different crosslinking times were calculated using Scherrer's equation (See Appendix 3). The crystallite size calculated for PVOH herein is 3.51 nm, which is much smaller in comparison with the 15 nm size reported by Mansur *et al.* [165] and the 15.6 nm size for PVOH film obtained from melting PVOH powder and reported by Ricciardi *et al.* [166]. A decrease in the size of crystallites when films were crosslinked herein is shown in Fig. 3.25. A significant fall in size is observed when the neat PVOH films are crosslinked for up to 2 hours wherein the crystallite size decreases from

3.51 nm to 2.21 nm. When extending the crosslinking time from 2 hours to 48 hours, there is only a moderate decrease in the size values indicating that longer crosslinking time does not lead to a significant change in the structure of the sample. Presumably, as the crosslinking solution enters the PVOH film, all the crystallites are either reduced in size or the larger crystallites are removed leaving the smaller crystallites.

Table 3.6 Peak positions ($^{\circ}2\theta$) and full width at half maximum (FWHM) values of PVOH and its crosslinked films after experiencing different crosslinking times. These values were taken from the original XRD diffractograms using the X'Pert Data Viewer

Sample names		Values	
		Peak position, 2θ (degree)	FWHM (degree)
PVOH films		19.18	2.3
Crosslinked films	5 min	19.09	2.53
	15min	19.05	2.52
	1 hr	18.96	3.16
	2 hrs	18.93	3.66
	8 hrs	18.84	4.46
	16 hrs	18.81	4.61
	24 hrs	18.90	4.49
	48 hrs	18.73	5.08

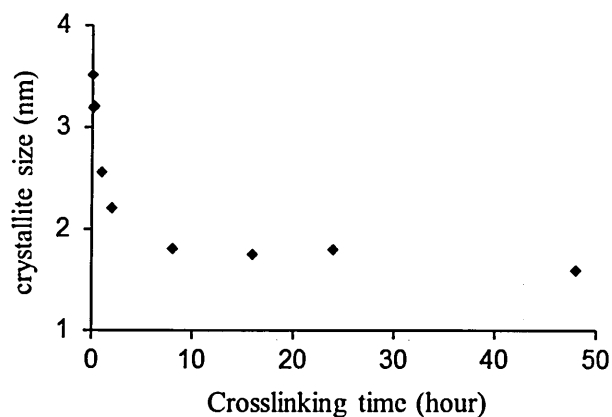


Figure 3.25 Crystallite sizes in PVOH and crosslinked films obtained from XRD data and using Scherrer's equation

3.4.10 DMA results

The mechanical properties of PVOH and crosslinked films of different crosslinked times were investigated using DMA in tension mode. $\tan \delta$ as a function of temperature is illustrated in Fig. 3.26. For neat PVOH film (red curve), there are two peaks in agreement with Peng *et al.* [167]. The first peak at around 50°C is the glass transition temperature T_g (α transition) of PVOH since there is a shift of the $\tan \delta$ peak to higher temperature with higher frequency (from 1 Hz to 10 Hz) due to the frequency-dependent property of T_g (data not shown). The peak at approximately 120°C which is far below the melting temperature of PVOH (~230°C) is termed the alpha star transition, T_{α}^* which is associated with the slippage between crystallites (PVOH is a semicrystalline polymer) [134]. When PVOH films were crosslinked with GA using short crosslinking times (5 minutes up to 1 hour) (Fig. 3.26a), peaks around 0°C are observed which can be ascribed to the beta transition T_{β} , this always appears at a lower temperature than the T_g and is related to the movement of whole side chains or localised groups of adjacent atoms in the main chains [134]. It can also be observed that the sample with 15 minutes crosslinking time has a broad α transition with two $\tan \delta$ peaks at ~81°C and ~108°C.

When extending the crosslinking time (from 2 hours), the $\tan \delta$ curves change considerably to those with lower treatment times. Fig. 3.26b shows that additional peaks at 65-70 °C below the T_g appear in the $\tan \delta$ curves of samples treated with longer time. These peak may be assigned to beta transitions T_{β} while the peaks at ~0°C are now possibly gamma transitions, T_{γ} , which correspond to the solid-state transition [134,168]. Below T_{γ} , the polymer molecules are highly compact. When material warms and expands, there is an increase in free volume inducing the movement of localized bonds (bending and stretching) and some side chains which are expressed as the peak at T_{γ} in $\tan \delta$ curve.

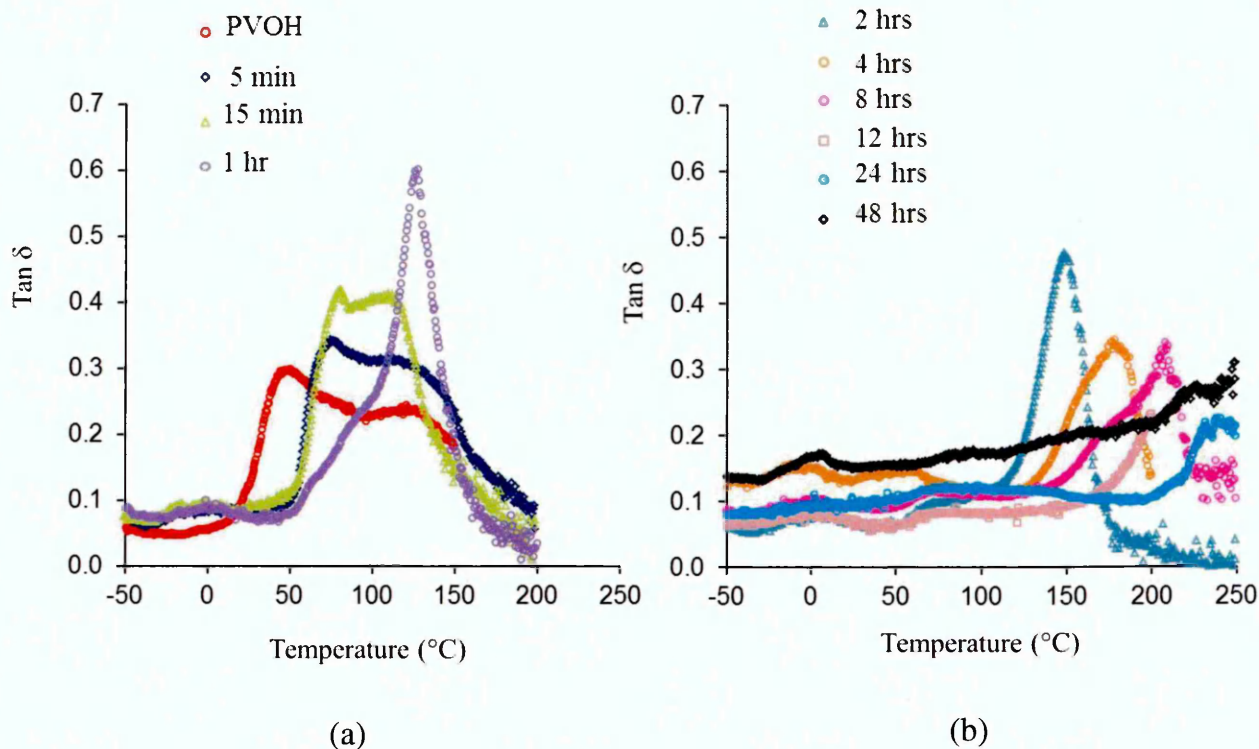


Figure 3.26 Tan δ of PVOH and crosslinked films prepared using different crosslinking times. DMA was conducted in tension mode with the frequency 1 Hz and temperature scanning rate of 2°C/min.

T_g is affected by the molecular weight of polymer, moisture content, frequency and operation method. Different T_g values obtained from DMA measurement of PVOH have been reported in the past, which are 60°C ($M_w = 94,000$) [169], 65°C ($M_w = 67,000$) [170], 82°C ($M_w = 75,000$) [57] and 85°C ($M_w = 89,000$ -98,000) [53], measurements by DSC investigation have given 50-60°C [171]. When the crosslinking times between PVOH and GA were increased, the T_g shifted to higher temperature. Fig. 3.27a shows the increase in the T_g value of PVOH film when crosslinked with increasing crosslinking times. A significant increase was observed when going from the untreated PVOH to the 4-hour crosslinked film in which T_g increased from ~50°C to ~179°C, respectively. After 4 hours of crosslinking time, the T_g values only increased gradually up to 48 hours crosslinking and no remarkable change in T_g values are observed. For the tan δ amplitude at T_g (Fig. 3.27b), the maximum intensity at T_g increased

from 0.30 for PVOH film to a maximum at 0.55 for 1-hour crosslinked film, the values then decreased to that of neat PVOH until 48 hours of crosslinking time.

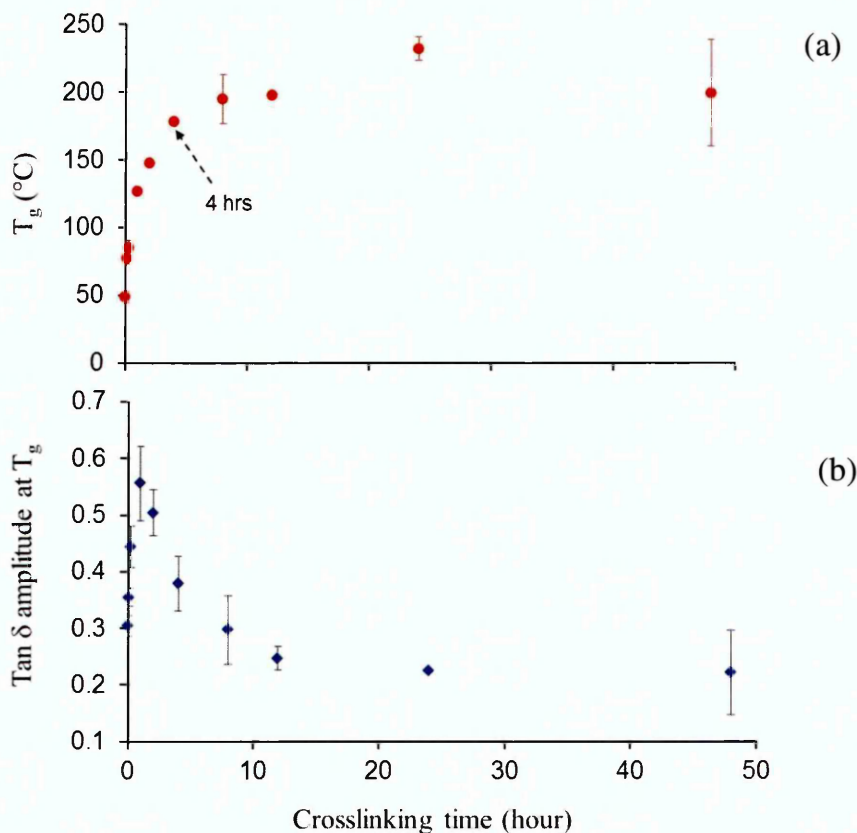


Figure 3.27 a) An increase in T_g with crosslinking times. T_g was taken from the peak of $\tan \delta$ curve b) Changes in the maxima at T_g position when crosslinking time increased. Each value is a mean value taken from three samples.

The tensile storage modulus (E') as a function of temperature is shown in Fig. 3.28a. $\log E'$ is also illustrated in Fig. 3.28b with the curves shifted vertically for clarity. Fig. 3.28b shows that for the neat PVOH, $\log E'$ gradually decreases when being heated from -50°C to 25°C , which is followed by a sudden drop to 70°C that corresponds to the α transition. The curve then plateaus and starts increasing again as the temperature increases to 120°C . This increase of $\log E'$ is ascribed to the loss of tightly bound water. When the sample is heated above 120°C , $\log E'$ decreases due to slippage of the crystallites past each other making

the material softer. This is quite consistent with the $\tan \delta$ data of PVOH (Fig. 3.26).

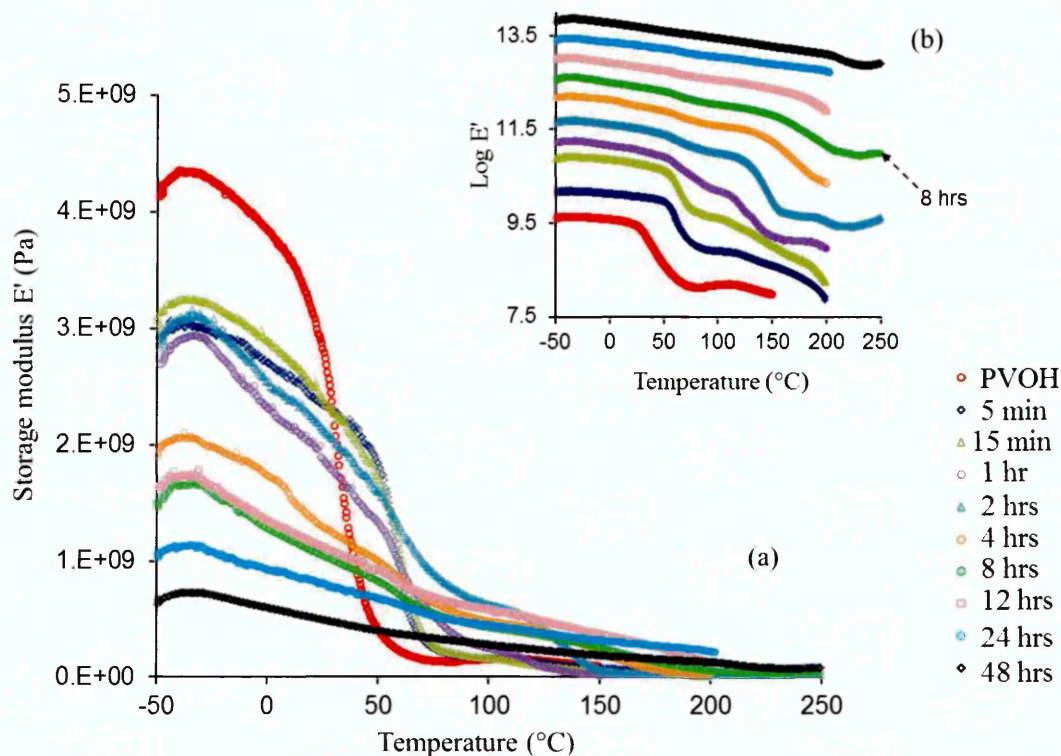


Figure 3.28 a) Tensile storage modulus (E') and b) $\log E'$ of PVOH and crosslinked films prepared using different crosslinking times. $\log E'$ curves are shifted along the ordinary axis for clarity. DMA was conducted in tension mode using a frequency of 1 Hz and temperature scanning rate of 2°C/min.

When PVOH films were crosslinked with GA, the $\log E'$ curves of the crosslinked samples below 8 hours of crosslinking time showed similar trends to that of neat PVOH films (although at different temperature) with visible decreasing steps relating to the α , β transitions or softening points of materials. However, for films crosslinked for 12, 24 and 48 hours, the $\log E'$ curves are straighter with no significant decreasing steps observed. In addition, the extents of decrease of $\log E'$ from -50°C to the end of the heating process (200°C) were smaller than those of lower crosslinking time samples. It is noted that the region above T_g is known as the rubbery plateau, in which the alpha star transition T_{α}^*

occurs due to the crystal-crystal slip. With higher crosslinking times (from 1 hour), the T_{α}^* is not observed in the $\tan \delta$ curves which may be attributed to the increase in the number of crosslinks in the PVOH which hinder the movement of the polymer chains.

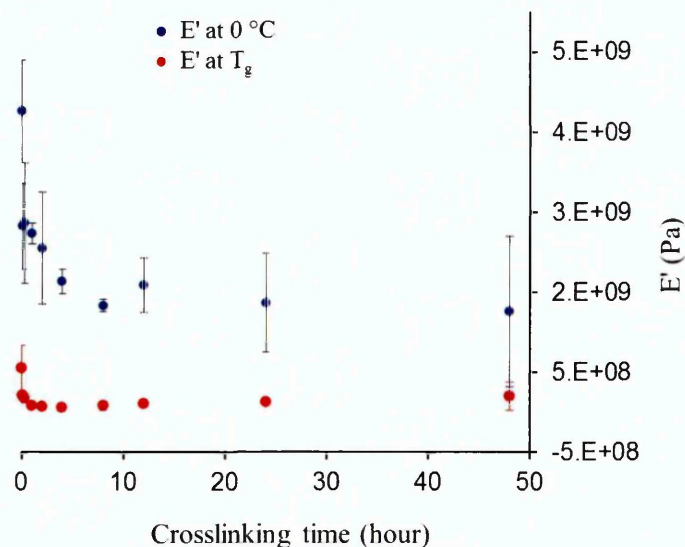


Figure 3.29 Storage modulus at 0°C and at T_g position of PVOH and crosslinked films as a function of crosslinking time

Furthermore, Fig. 3.28a shows that in general, E' decreases when PVOH was crosslinked with GA, this is also described in Fig.3.29 where E' values taken at 0°C and at T_g position are plotted. In both cases, the E' values of PVOH are the highest. At 0°C, E' decreases significantly from 3.7×10^9 Pascal for neat PVOH to 2.3×10^9 for just 5-minute crosslinked films, of which the decrease is $\sim 38\%$. The differences between E' of low crosslinking time samples (5 minutes to 2 hours) are not considerable. After 2 hours of crosslinking time, E' decreases gradually. The same trends were apparent for E' at T_g . However, after 1 hour of crosslinking time, there is no significant change in E' up to 4 hours crosslinking and only a slight increase followed when extending the crosslinking time to 48 hours.

In summary, when PVOH films were crosslinked with GA, the glass transition temperature T_g increased while the tensile storage modulus decreased with increasing crosslinking time. The crosslinked samples exhibited higher α

transition ranges indicating that they can be operated in a higher range of temperature than that of neat PVOH, in other words the crosslinked films have better thermal stability. In addition, the reduction of E' in the crosslinked films proved that the crosslinking reaction increased the flexibility of the polymer or lower stiffness properties. This is in agreement with Park *et al.* [53] who confirmed a more flexible structure in the crosslinked films which were cast from a solution of PVOH, GA and a catalyst. According to the authors, O-H groups were consumed due to the crosslinking reaction leading to a decrease in hydrogen bonding and thus a decrease in stiffness. However, Park *et al.* reported a decrease in T_g when PVOH was crosslinked while in this current work, T_g increased with crosslinking time. The increases in T_g were not significant for longer-crosslinked samples (after 4 hours crosslinking time) indicating that prolonging the crosslinking time did not provide significant changes in the mechanical properties of the films.

3.4.11 Discussion

The maximum degree of crosslinking achieved in the current work was 26.5% and occurred over 24 hours crosslinking (Fig. 3.8), this is lower than that reported by Kim *et al.* [66,96] who obtained a 75% degree of crosslinking within 1 hour of a crosslinking reaction. As PVOH films produced by Kim had porous structures, the GA present in the crosslinking solution may find it easier to access a larger surface area by passing through the sample pores and enhancing the degree of crosslinking. PVOH films in the current work, on the contrary, were dense films providing less surface area for the crosslinking solution to penetrate resulting in lower effectiveness of crosslinking between PVOH and GA. This is believed to be the main reason why the degree of crosslinking was lower even though the crosslinking time was much longer than that in Kim's work. After 4 hours and up to 48 hours of crosslinking time, the degree of crosslinking (Fig. 3.8) did not show any significant increase indicating that when the crosslinking reaction reached a certain degree after a certain time, prolonging the crosslinking reaction time did not result in any higher degree of crosslinking. It also means

that there was a limited extent for the crosslinking reaction between GA and PVOH dense film. This is supported by the WVTR results of crosslinked films prepared from different ratios between PVOH repeat units and GA (Fig. 3.11). One may anticipate that more GA present in the crosslinking solution would lead to higher crosslinking effectiveness resulting in a higher crosslinked network and lower WVTR. However, in spite of the difference in the reaction ratios, the WVTR values of the three crosslinked film types at the same crosslinking time were not much different at low crosslinking times. It is likely that there is only a certain amount of GA that could penetrate into the PVOH films after a certain time and this amount is low, no matter what the ratio is. Nevertheless, with longer treatment time (24 hours), the PVOH films crosslinked with the lowest ratio (4:0.5) between PVOH repeat unit and GA possessed the lowest WVTR value. It might be due to a lower number of acetal groups (discussed later) present in these crosslinked films which attracts less water than those crosslinked with higher ratios (4:1 and 4:2).

The WVTR results of crosslinked films (ratio 4:1 between PVOH repeat unit and GA) in Fig. 3.9 shows that below 4 hours of crosslinking reaction, the effectiveness of the crosslinked network in Fig. 3.8 was demonstrated well by the significant decrease of WVTR values. However, prolonging the crosslinking time led to a decrease of water vapour barrier properties. When PVOH is crosslinked with GA, O-H groups of the polymer are consumed by GA resulting in a more hydrophobic character. Yeom and Lee [80] mentioned the affinity of acetal groups to water. According to the authors, acetal groups were formed during the crosslinking reaction by the bridging of GA across two PVOH chains, in addition to GA molecules in which only one half reacts with a PVOH chain to produce an acetal group and the other half creates pendant aldehyde group. In our FTIR results (Fig. 3.18 and 3.19a), except for the sample treated for 48 hours, there were no peaks suggesting the existence of pendant aldehydes. When the extent of crosslinking increased beyond 2 hours crosslinking time, more acetal groups were generated and so potentially affecting the water vapour barrier properties of the crosslinked films. Despite the fact crosslinks make the films better barriers to water vapour, there becomes a point where too many acetal groups produced

con-currently with crosslinks have an adverse effect on this property. When reaching a certain degree of crosslinking, the latter effect becomes dominant and induces a decrease in water vapour barrier properties.

Another explanation for the increase in WVTR values with higher crosslinking time is the decrease in crystallinity during crosslinking. FTIR and Raman provided evidence of such a decrease by a decrease in the intensity of crystallinity peaks in the respective spectra of crosslinked films. XRD results also supported this point of view where the crystallite sizes were described to decrease as the crosslinking time increased. The XRD results were in agreement with the study by Mansur *et. al.* [165] who stated the crosslinking between PVOH and GA caused the re-arrangement of the PVOH molecules not in an ordered manner, thus reducing the crystalline domain formation of PVOH. Furthermore, GA consumed O-H groups of PVOH thereby reducing probability of a hydrogen bonding network being formed within the system and so contributing to a decreasing probability of crystallinity in the materials. This was evidenced in FTIR spectra with a decrease in peak intensity and also a shift of the O-H stretching band to higher wavenumber (Fig. 3.18) as the crosslinking time was increased.

The swelling results in water for PVOH and crosslinked films reflected the WVTR results in that both factors decreased when the crosslinking time increased up to 2 hours. However, after 2 hours crosslinking, the WVTR values increased while the swelling reached an equilibrium and practically stayed unchanged thereafter (Fig. 3.15). In addition, there was no considerable difference between the swelling extents in hot and cold water after this point of crosslinking time. This indicated that with 2 hours crosslinking, the crosslinked films contained a certain amount of free volume which allowed a certain amount of water to be absorbed. The free volume in the polymer network can create channels for water molecules to penetrate into the films. When water is absorbed at the polymer surface, the water molecules penetrate into the polymer, occupy the free volume and then diffuse into the polymer leading to the expansion of polymer (swelling). As PVOH is hydrophilic, the water molecules are easily absorbed and form hydrogen bonding with PVOH molecules via hydroxyl

groups; thus the intra- and intermolecular forces between PVOH molecules in the film are broken leading to their solubility in water. When PVOH films are crosslinked with GA, the polymer networks become more compact (less free volume) which limits the penetration of water and film expansion. When increasing the crosslinking time, more crosslinks are produced making the polymer difficult to expand when water is present leading to a decrease of the degree of swelling. In hot water, the polymer chains obtain enough energy to move and expand in the polymer resulting in the higher swelling degree than polymer in cold water. In addition, if there were still crystalline domains present in the below-2-hour crosslinked samples, then the hot water could dissolve these and lead to an increase in swelling when compared to in cold water where the crystallites act like crosslinks between the amorphous regions stopping the film from swelling. However, at 2 hours crosslinking, the amount of free volume in the film reached an equilibrium and extending the crosslinking time could not contribute to the free volume reduction. Therefore beyond this crosslinking time, the swelling degrees of polymer in hot and cold water were not much different.

The opposing behaviours of crosslinked PVOH in WVTR and swelling tests can also be explained by the difference in operating process. For the swelling test, water can be absorbed into the films thanks to the free volume availability and hydrogen bonding between water and O-H groups of the polymer. For the WVTR test, water transfers to the film by a diffusion process (see Section 2.2.1, Equation 2.6) in which the concentration gradient is very important as it is the driving force for the whole diffusion process. In WVTR analysis, there existed a concentration gradient between 2 surfaces of the film of which one surface was in contact with water vapour whereas the other was in contact with low pressure (~ 0) medium since the silica gel at the bottom of the Payne cup could adsorb the water vapour. So in this case, the diffusion occurred following 3 steps: 1. The water vapour was absorbed at the film surface 2. The vapour penetrated into the film and occupied the free volume 3. The water vapour diffused through the film to the other surface and then was adsorbed by silica gel. Therefore, in the WVTR test, water vapour was transferred through the film not only thanks to free volume, but also through hydrogen bonding with hydroxyl groups like in the

swelling test. As mentioned above, acetal groups formed during the crosslinking have affinity to water. When the crosslinking time is increased, more acetal groups are present resulting in more sites for water vapour to be absorbed by the films. These sites are perhaps the leading cause for an increase in the WVTR values.

The water wettability of PVOH films tends to increase with increasing crosslinking time (Fig. 3.17) proving that crosslinking with GA made the film surfaces become more hydrophobic to resist the wetting by water. The water contact angle values were highest for the films crosslinked at 24 hours while lowest for those at 5 and 15 minutes. To understand thoroughly why the contact angles values for neat PVOH film were higher than those crosslinked for 5 and 15 minutes, it is suggested to condition all the films at the same certain temperature and duration before measurements in order to remove significantly the effect of water present on the film surface so that better comparison can be achieved.

The DMA results showed a dramatic increase in the glass transition temperature after PVOH films were crosslinked with GA. With the formation of crosslinks, the polymer chains become more compact and the material needs higher energy to expand in order to provide enough space for the side chains and localised groups of some backbone atoms to begin to move and to break out of the rigid glassy state. This explains the increase in β transition (T_{β}) and α transition temperatures (T_g) with the increasing crosslinking time. However, the DMA results confirmed a more flexible structure in crosslinked films when compared with the neat PVOH.

3.4.12 Summary

It can be concluded that when PVOH was crosslinked with GA, the crystallinity decreased. When the crosslinking time increased, there was an increase in the crosslinking degree but a decrease in the crystallinity. The GA is effective in improving the water vapour barrier properties of PVOH films by crosslinking the films with low and medium crosslinking times (5 minutes to 2 hours). Extending

the crosslinking time has a negative effect on the water vapour barrier properties of PVOH. The crosslinked PVOH films have higher T_g thus possessing a higher operating temperature range than the neat PVOH which means they can be used at higher temperature without loss in properties of the films. In addition, a more flexible structure was observed in the crosslinked films in comparison with neat PVOH films.

3.5 EFFECT OF SODIUM SULPHATE ON THE PROPERTIES OF PVOH FILMS

3.5.1 WVTR results

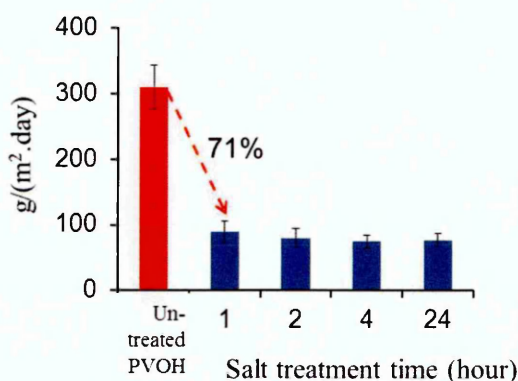


Figure 3.30 WVTR results at 23°C, 85% RH for salt treated PVOH films as a function of treatment time

Fig. 3.30 shows there is an improvement in water vapour barrier properties of PVOH films after treatment with sodium sulphate solution. It was noted that the 15-minute treated films shrunk and distorted and did not have a good shape for WVTR testing. This was due to a swelling of the films during the water washing step after the salt treatment. With 1 hour of salt treatment, the WVTR decreased markedly from ~310 g/(m²·day) for neat PVOH films to ~89 g/(m²·day), of which the improvement in the water vapour barrier properties equates to about 71%. This was very comparable to the improvement obtained when PVOH was crosslinked with GA for between 5 minutes and 2 hours which was 66-70%.

Extending the salt treatment time beyond 1 hour did not show any considerable differences in the WVTR of the PVOH/salt film.

3.5.2 Swelling test results

In water at 90°C, the salt treated PVOH films dissolved completely. However, unlike PVOH films, the salt treated films did not dissolve in water at 22°C after 24 hours immersion. Fig. 3.31 shows that the degree of swelling at 22°C decreased with increasing salt treatment times. Films treated in sodium sulphate solution for 15 minutes showed the highest degree of swelling which was about ~730% while that for the 24-hour treated sample was the lowest (~150%). The degrees of swelling between 1 to 4 hours treatment were not much different and varied from 200 - 260%.

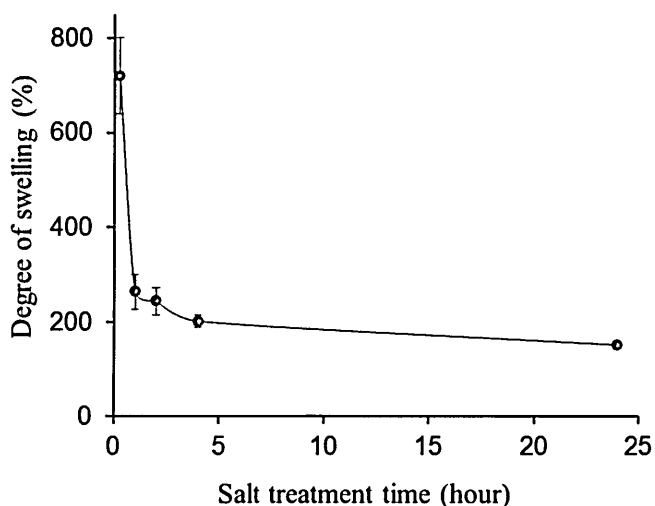


Figure 3.31 Swelling test results in water at 22°C for salt treated PVOH films

3.5.3 FTIR results

After PVOH films were treated by sodium sulphate solution for different time lengths, their FTIR spectra exhibited no new absorption bands or band shifting when compared with the spectrum of the neat PVOH suggesting that there was no chemical interaction between PVOH film and salt. Fig. 3.32 shows that the peak intensities at 1142 cm^{-1} and 845 cm^{-1} practically unchanged after the salt treatment which indicates that modifying the PVOH films using sodium sulphate

solution did not affect the film crystallinity. Sodium salts have been shown by other researchers to induce the crystallinity of PVOH [34,35,40] by an increase in the intensity of the crystallite peak at 1142 cm^{-1} of FTIR spectra. In all of the cases, films were cast from an aqueous solution containing both PVOH and salt. However, in this current work, sodium sulphate solution was simply used to immerse the dry PVOH film before being washed thoroughly with water. Therefore, the different approaches strongly influenced the crystallinity of the films.

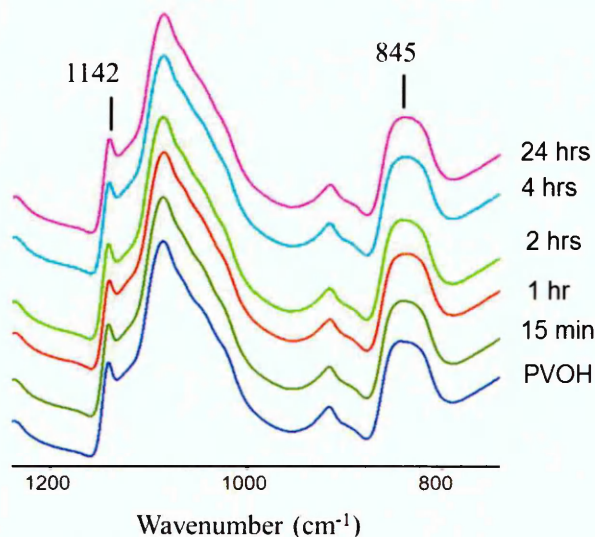


Figure 3.32 FTIR results from PVOH and salt treated films

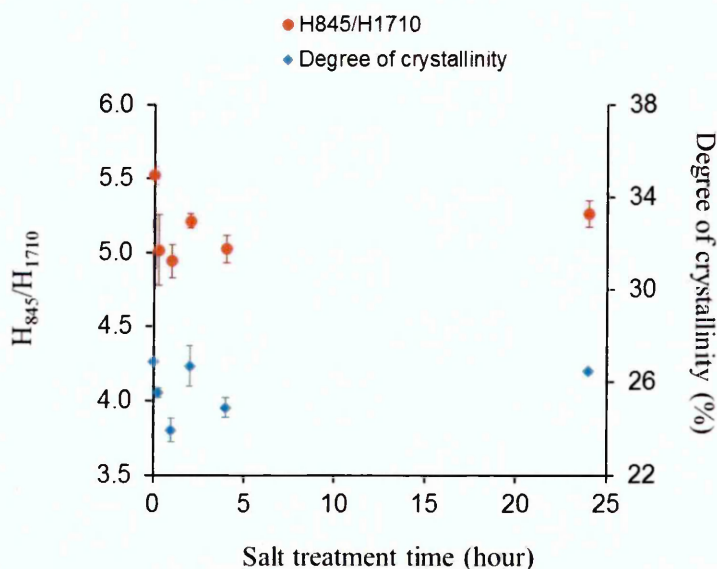


Figure 3.33 Changes in degree of crystallinity and peak height ratios H_{845}/H_{1710} when increasing the treatment time between PVOH films and sodium sulphate solution

The degree of crystallinity can be calculated based on the intensity of the 1142 cm^{-1} peak relative to that at 1087 cm^{-1} (Eq. (2.4), Section 2.1.4, Chapter 2) [37]. Fig. 3.33 shows how the degree of crystallinity changed when PVOH films were treated with sodium sulphate solution for different time durations. The peak height ratios between the 845 cm^{-1} (C-C bending) and 1710 cm^{-1} bands (C=O stretching) are also plotted to evaluate the crystallinity change for comparison since the 845 cm^{-1} band was proved previously to be sensitive to the crystallinity of the sample. It can be observed that treating the PVOH films with sodium sulphate solution did not significantly increase the degree of crystallinity nor the peak height ratio between the 845 and 1710 cm^{-1} bands. No trend was recognised for the changes of crystallinity degree and the peak height ratio as a function of the treatment time due to the minor changes.

3.5.4 Raman results

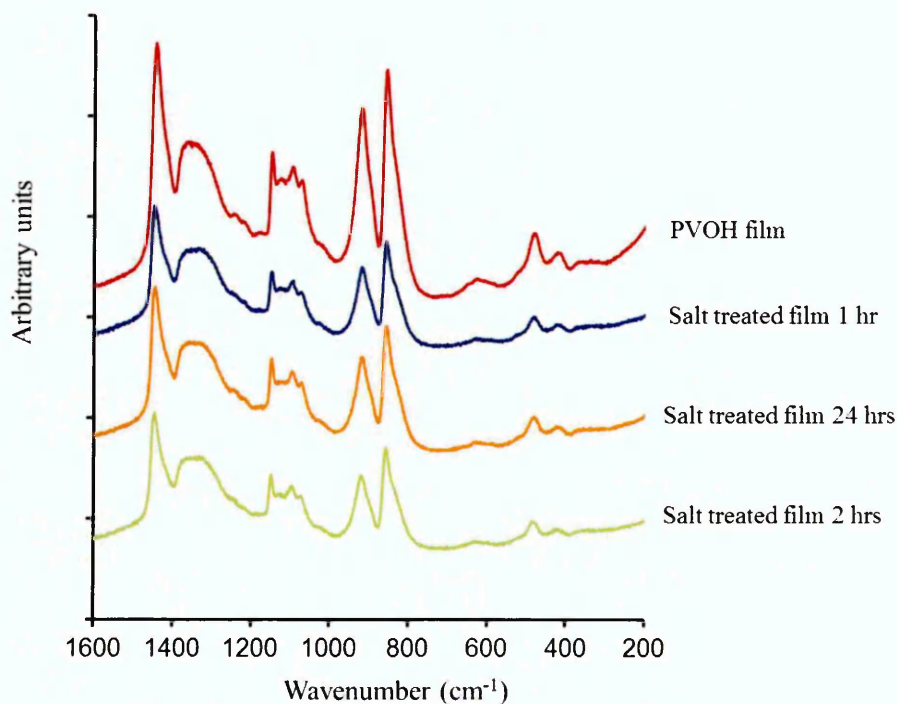


Figure 3.34 Raman spectra from PVOH and films treated with salt for 1, 2 and 24 hours

Like the FTIR spectra, the Raman spectra of the different salt treated films were very similar (Fig. 3.34). The spectra were shifted vertically for clarity. There were no new absorption bands or band shifts in the spectra of the salt treated films. In addition, the crystallinity peaks at 1148 and 1094 cm^{-1} were mostly unchanged between samples of different treated times.

3.5.5 XRD results

Fig. 3.35 shows the diffraction patterns for the samples over an angular range $2 - 25^\circ 2\theta$ which are displaced vertically for better clarity. Samples treated with sodium sulphate solution for 2 and 24 hours were analysed to compare with the neat PVOH. The three diffractograms are very similar with the principle crystal diffraction peak at $19.18^\circ 2\theta$. No peak broadening or peak shifting was observed.

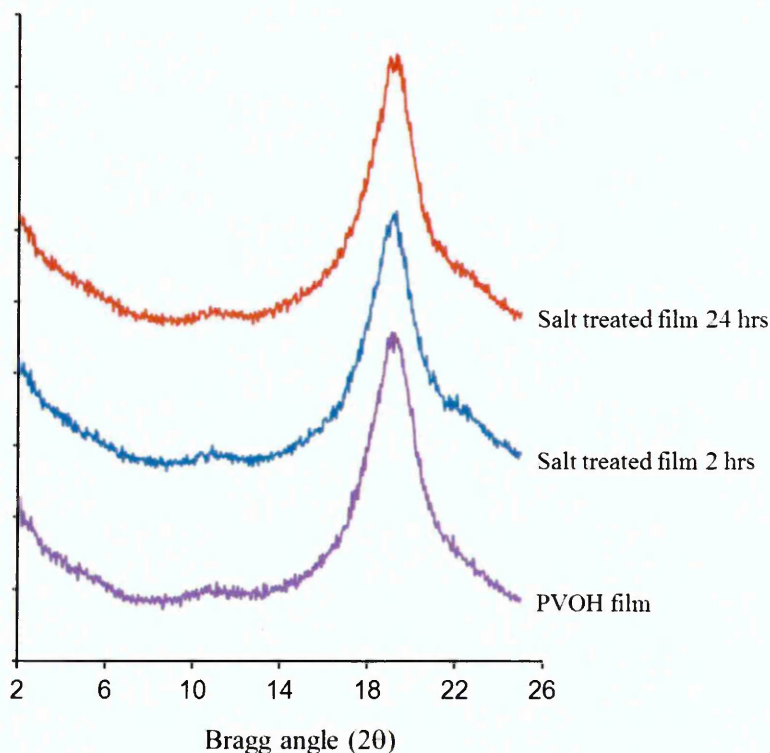


Figure 3.35 X-ray diffractograms of PVOH films treated with sodium sulphate solution for 2 and 24 hours in comparison with neat PVOH film.

3.5.6 DMA results

The $\tan \delta$ values as a function of temperature for the salt treated films and PVOH are presented in Fig. 3.36. There were no significant differences between the α transition temperatures (T_g) of samples treated with sodium sulphate solution for different durations of time, as shown in Fig. 3.37, of which the values were about 75-80°C but they were higher than that of neat PVOH (~50°C). After PVOH films were treated with sodium sulphate solution, minor peaks between -5 to -10°C were observed, which could be ascribed to the beta transition T_β and related to the movement of whole side chains or localised groups of adjacent atoms in the main chains. The peaks representing the slippage of crystallites were located at the same temperature for PVOH and for samples treated with salt solution for 1 and 2 hours (120°C), whereas those treated for 4 and 24 hours were higher (about 135-140°C).

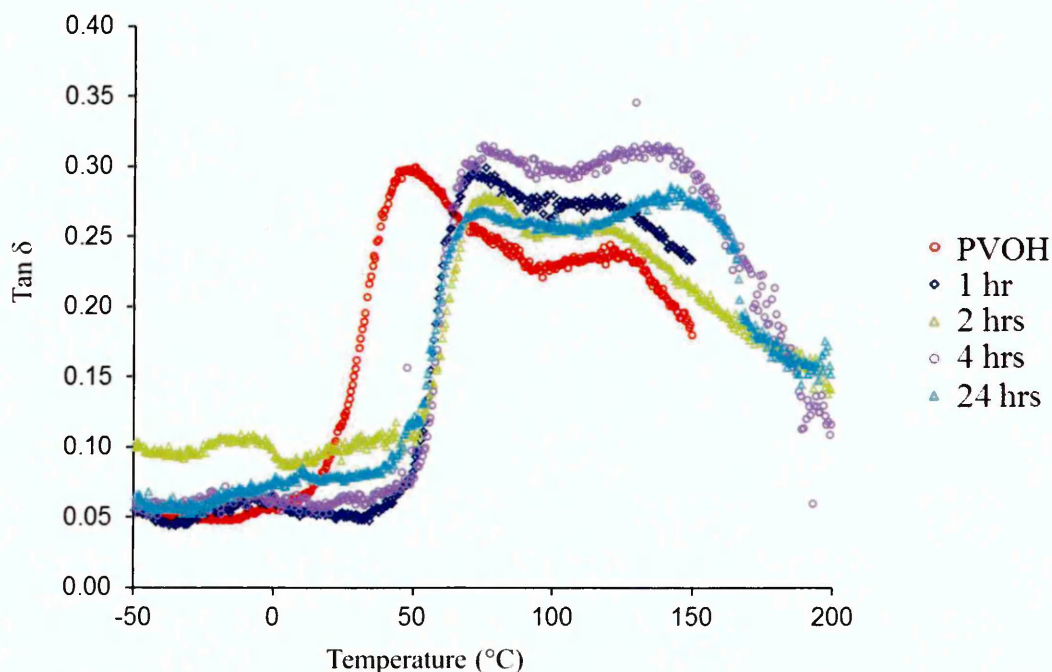


Figure 3.36 $\tan \delta$ curves for PVOH and films treated with salt for different time lengths. DMA was conducted in tension mode at the frequency 1 Hz, temperature scanning rate 2°C/min.

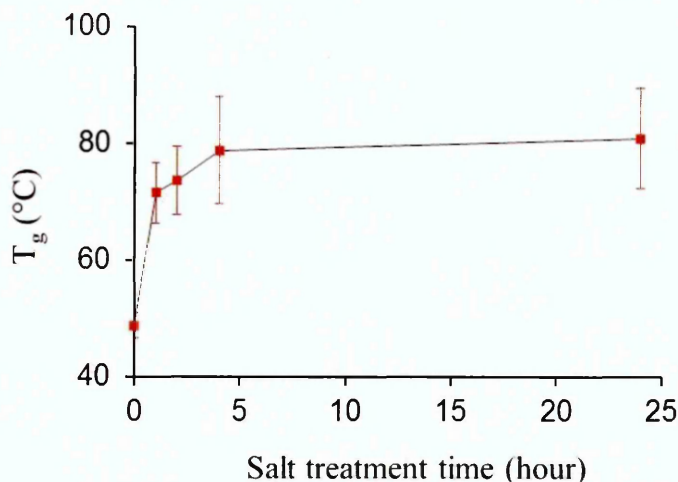


Figure 3.37 An increase in T_g with salt treatment times. T_g was taken from the peak of $\tan \delta$ curve

The tensile storage modulus (E') decreased when PVOH films were treated with sodium sulphate solution suggesting lower stiffness in the salt treated films. Fig. 3.38 shows the E' values taken at 0°C and at the T_g position, where in both cases, E' values were highest for PVOH films and decreased when increasing the treatment time. At 0°C , E' decreased significantly from 3.7×10^9 Pa for neat PVOH to 2.2×10^9 for the 1-hour-treatment sample, of which the decrease was $\sim 40.5\%$. When extending the treatment time up to 24 hours, the E' value decreased slightly but the extent of reduction was not as great. From 1 hour to 24 hours of treatment, the E' decreased approximately 13.6%.

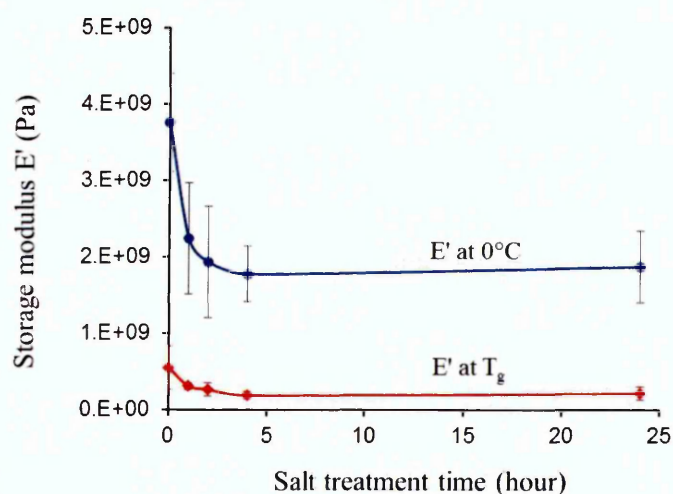


Figure 3.38 E' values at 0°C and at T_g positions as a function of salt treatment time

3.5.7 Discussion

The FTIR, Raman and XRD results provided no evidence that any chemical interactions between PVOH and sodium sulphate occurred after PVOH films were treated with aqueous salt solution. In addition, there were no significant differences between samples treated with salt solution for different lengths of time in terms of chemical structure. In fact, there was no evidence indicating that the crystallinity of PVOH increased when PVOH films were treated with sodium sulphate. For mechanical properties, the DMA results showed lower stiffness but a higher thermal operating range for the salt treated films than for untreated PVOH films. The effects of salt treatment on the swelling and water vapour barrier properties of PVOH films were quite obvious. After treatment with sodium sulphate, the films did not dissolve in water at 22°C and maintained their shapes. Warm water (~45°C) however could induce the dissolution of these salt treated films. More significantly, the water vapour barrier properties of PVOH films improved markedly to a level (~71%) which could be achieved by the crosslinking reaction with GA for low crosslinking times. While the WVTR values of the salt treated samples did not change much when prolonging the treatment time, those of crosslinked films did increase with increasing crosslinking times. In the crosslinking reaction between PVOH and GA, sodium sulphate not only acts to destabilise the hydrogen bonding between PVOH and water, it may also contribute to the water vapour barrier improvement of the films. However, with the production of more acetal linkages when increasing the crosslinking times, the WVTR of the crosslinked films increased. This did not happen to the films treated with salt only when extending the treatment time, which supported the previous arguments about the effects of acetal linkages in increasing the WVTR values in the high crosslinked PVOH films. Nevertheless, GA was important in that it crosslinked PVOH molecules creating a crosslinked network which helped the crosslinked films not dissolve in hot water (90°C) (even for samples with a very low crosslinking time of 5 minutes). Note that, without GA, the salt treated films could be dissolved immediately in warm water. The question is how salt treatment could help to improve the water vapour barrier as well as the swelling properties of PVOH. Based on the results found,

crystallinity is not the answer. When PVOH solution is in contact with aqueous sodium sulphate solution, a "salting-out" effect happens which depends more on the nature of the anion than that of the cation (Hofmeister series) [172]. The SO_4^{2-} anion is classified as a kosmotrope, which is strongly hydrated and has strong salting-out effects (aggregation) on proteins and macromolecules. By polarising the water molecules that hydrogen bond with the polymer molecules, the kosmotrope anions increase the hydrophobic interface between the polymer and water resulting in the stabilisation of the polymer in water. In the case of dense PVOH films in this current study, when in salt solution, water molecules immediately penetrate into the amorphous regions or free volume of the PVOH films making the films swell. Concurrently, the water molecules are pulled back by the SO_4^{2-} anions as these anions have high affinity to water. This presumably facilitates the rearrangement and packing of PVOH molecules leading to better resistance to water molecules but not enough to gain higher crystallinity or at least to a level detected by the techniques used herein (FTIR, XRD).

Sodium sulphate molecules could be confined in the PVOH films after both salt treatment and crosslinking with GA. Table 3.7 shows the contents of Na^+ and SO_4^{2-} present in the crosslinked films of 15 minutes, 4 and 24 hours and salt treated films of 4 hours. The ion-chromatography (IC) and inductively coupled plasma-optical emission spectrometry (ICP-OES) analyses were used for determining the SO_4^{2-} and Na^+ , respectively and were performed by Medac Ltd in the UK. It can be observed that the sulphate contents in the crosslinked films and salt treated films at the same 4 hours were not much different. For crosslinked films, a longer crosslinking time led to higher contents of sulphate ion in the samples.

Table 3.7 Contents of sodium cation and sulphate anion in the crosslinked films and salt treatment films

Sample		Contents (ppm)		Ratio Na ⁺ / SO ₄ ²⁻
		Na ⁺	SO ₄ ²⁻	SO ₄ ²⁻
Crosslinked PVOH film	15 minutes	36.7	63.2	1 : 1.72
	4 hours	12.3	124.5	1 : 10.1
	24 hours	513.7	1536.8	1 : 2.99
Salt treatment PVOH films	4 hours	187	118	1 : 0.63

3.6 CONCLUSIONS

GA as a crosslinker can help to improve the properties of PVOH films including water/water vapour barrier properties and flexibility. The crosslinked films also have higher thermal operating ranges than those of the neat PVOH. The crosslinking reaction is fast and effective in just 5 minutes (if not at shorter times). In addition, the amount of GA consumed in the crosslinking reaction is small. Extending the crosslinking time more than 2 hours leads to a decrease in water vapour barrier properties. Crosslinking is effective with low and medium levels of crosslinking time (5 minutes to 2 hours).

In comparison with in-situ crosslinking in which the GA crosslinking agent and acid are mixed with PVOH in solution, the immersion of the dry PVOH films in the crosslinking solution is better in reducing any possible trace of un-reacted GA since the crosslinked films are washed thoroughly with water after the crosslinking reaction and evidenced by the FTIR spectra.

Sodium sulphate contributes to the water/water vapour barrier improvement of the PVOH films, but in the absence of GA, the salt treated films readily dissolve in warm water (45°C). Through treatment of the PVOH films with sodium sulphate solution, there is no increase in crystallinity detected.

Heat treatment of poly(vinyl alcohol) films combined with chemical crosslinking

In this chapter, the effects of annealing PVOH films on water vapour barrier properties, mechanical properties and crystallinity are reported.

In the previous chapter, crosslinking with GA was proved to be effective for improving the water resistance of PVOH films even when exposed to hot water (90°C) (see Section 3.4.5). This chapter continues to report the effects of the crosslinking reaction, but after annealing high molecular weight PVOH.

Last but not least, crosslinking reactions were performed on only one side of the PVOH31 films. The aim of this investigation was to reduce the amount of crosslinking agent required to obtain a system with good water barrier, but also to limit any potential loss of biodegradability.

4.1 EXPERIMENTAL

4.1.1 Heat treatment of PVOH films

PVOH films (98-99% hydrolysed, $M_w = 31,000-50,000$, 50-58 μm) were annealed at selected temperatures for specific lengths of time. The heating duration at high temperature was strictly controlled in order to avoid thermal degradation as indicated by a yellow or brown discolouration. For example, heating films at 180°C for longer than 10 minutes would lead to the colour changing. Films annealed at 120, 150 and 180°C were interleaved between two PTFE sheets placed in an oven in order to achieve flat surfaces, the heating time was kept the same at 10 minutes. At lower treatment temperatures such as 40, 60 and 90°C, films were simply placed in the oven for 3 hours. After heat treatment, films were cooled in a closed vessel, containing silica gel as desiccant, before further measurements were taken.

4.1.2 Heat treatment of high molecular weight PVOH and crosslinking reaction with GA.

PVOH124 films (98-99% hydrolysed, $M_w = 124,000-186,000$, 50-60 μm) were annealed at different temperatures prior to crosslinking with GA. Three methods of film annealing in the oven were used; i) 40°C for 3 hours, ii) 90°C for 3 hours and iii) 180°C for 10 minutes followed by 40°C for 5 minutes. For the crosslinking reaction, an aqueous crosslinking solution was prepared which contained GA, sulphuric acid and sodium sulphate as described in Section 3.1.2. PVOH124 films after heat treatment were immersed in the crosslinking solution at 40°C which was also the reaction temperature. The ratio between PVOH124 repeat unit and GA was kept at 4:1. After specified lengths of time, the films were taken out of the crosslinking solution and thoroughly washed with water then washed with acetone. Finally, films were dried in an oven at 40°C for 48 hrs.

4.1.3 One-side crosslinking of PVOH31 films.

4.1.3.1 In-situ FTIR measurements of crosslinking reaction

In order to understand further the crosslinking mechanism of PVOH31 with GA and to determine whether the crosslinking solution could pass through the film thickness, a series of FTIR spectra were collected overtime from the film whilst exposed to the crosslinking solution. A PVOH31 film was placed on the ATR crystal mounted in tungsten carbide which was heated at 40°C. A stainless steel cylinder was used as a crosslinking solution reservoir and device to ensure a good contact between a PEEK frit, the PVOH film and the ATR crystal (Fig. 4.1). The PEEK frit with pore size of 20 μm and dimensions 0.188" x 0.74" x 0.254" was supplied by VWR International Ltd. The crosslinking solution was introduced to the cylinder via a syringe which then passed through the frit to contact the PVOH film. The spectra were effectively collected from the bottom surface of the film, whereas the crosslinking solution entered from the top surface. Since the PVOH film is 55-60 μm thick and the FTIR sampling depth is ~0.5-5 μm the experiment allows the diffusion of the crosslinking solution to be

monitored overtime as the components pass through the films and are detected spectroscopically. The added advantage is that spectral changes in the polymer and for components can provide chemical information. The spectral range was 4000 to 650 cm^{-1} . The number of sample scans and the resolution were 64 and 4.0 cm^{-1} , respectively. Spectra were recorded after specified time period and are described in the relevant results section.

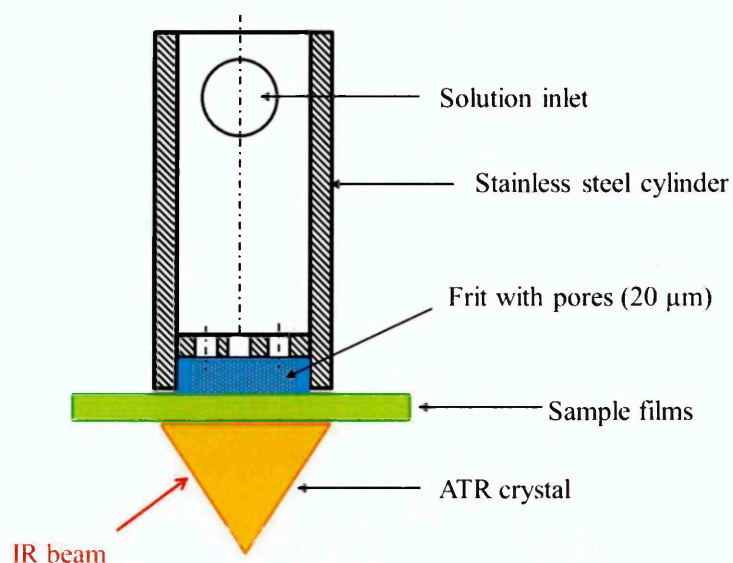


Figure 4.1 Schematic of the series FTIR system

4.1.3.2 One-side crosslinking of PVOH31 films

PVOH films (98-99% hydrolysed, $M_w = 31,000-50,000$, 50-58 μm) were annealed at selected temperatures for specified lengths of time, which were 40, 60 and 90°C for 3 hours and 120, 150 and 180°C for 10 minutes as described in Section 4.1.1. After heat treatment, films were placed and secured in the Payne cups (Sheen Instruments) (Fig. 4.2). A silicon ring was placed between the film and the cup ring to avoid any leaking passage of the crosslinking solution around the sides of the film. The space above the film and inside the lid of the Payne cup was used to contain the crosslinking solution. Then the system was placed in an oven set at 40°C.

The crosslinking solution, which was also pre-heated at 40°C, was poured onto the lid of the Payne cup on top of the film. The required volume of crosslinking solution was calculated based on the mass and surface area of the PVOH films in contact with the solution. After specified durations of time, the crosslinking solution was removed and the film surface was washed thoroughly with water and then acetone before the film was removed from the Payne cup and dried at 40°C for 48 hours. Three crosslinking times were investigated, including 5, 15 and 60 minutes.

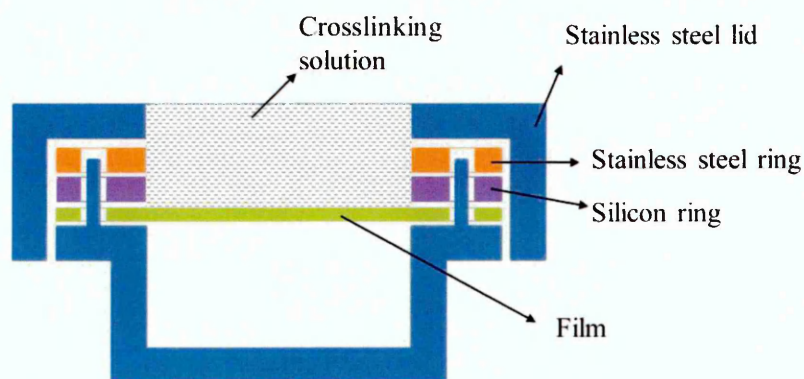


Figure 4.2 Schematic of the one-side crosslinking system using Payne cup

4.2 CHARACTERISATION

4.2.1 Dissolution test

The PVOH31 films after being annealed and placed in the desiccant container were cut into pieces 2 cm x 2 cm and immersed in water at selected temperatures in the range 22 to 50°C for 15 minutes. Their behaviours in water were observed and recorded. The experiment was repeated 3 times.

4.2.2 The other tests

The instrumental set up for techniques used here are described in Section 2.2, Chapter 2. For heat treated PVOH films, the FTIR spectra and X-ray

diffractograms were collected immediately after cooling in a container for 10 minutes. Samples for FTIR and X-ray diffraction were taken from separate halves of the same film. Table 4.1 summarises some of the characterisation techniques as well as sample preparations before measurements.

Table 4.1 Characterisation methods and sample preparations

No.	Techniques	Sample preparations
1	Water vapour transmission rate (WVTR)	- Before measurements, samples were conditioned in a humidity chamber set at 23°C and 85% RH for at least 20 hours before measurement.
2	Swelling test	- Samples were cut into squares (2.5 cm x 2.5 cm) and immersed in water for 24 hours
3	Thermogravimetry analysis (TGA)	- Samples were analysed immediately after annealing to determine water content.
4	Contact angle measurement (CA)	- Measurements were taken from cooled films stored in a container
5	Fourier transform infrared spectroscopy (FTIR)	- Heat treated samples were analysed immediately after being cooled for 10 minutes. - For the other films, before FTIR measurement, films were dried at 40°C in an oven for overnight.
6	Raman spectroscopy	- Measurements were taken from cooled films stored in a container
7	X-ray diffraction	- Heat treated samples were analysed immediately after being cooled for 10 minutes.
8	Dynamic mechanical analysis (DMA)	- Samples stored in a container were cut into rectangle strips. Measurement areas were 4-5 mm width and 6-7 mm length.

4.3 EFFECT OF HEAT TREATMENT ON THE PROPERTIES OF PVOH FILMS

4.3.1 Dissolution test results

From the dissolution test, three types of film status in water were observed, these were: i) swollen (films expanded and increased in dimensions), ii) disintegrated (films separated into pieces and remained in the water) and iii) dissolved (films became incorporated into water so as to form a solution) (Table 4.2). When immersed in water at room temperature (~22°C) for 15 minutes, only the un-heated films dissolved whereas films treated at 40 and 60°C disintegrated and the others simply became swollen. Films heated at either 90 and 120°C dissolved in water at 45°C, which was only 5°C higher than the dissolution temperature of those heated at 40 and 60°C. Films treated at elevated temperatures (150 and 180°C for 10 minutes) were swollen in water and dissolved when water temperature increased to 65°C.

Table 4.2 Behaviour of annealed PVOH31 films after 15 minutes in water at different temperatures

Annealed PVOH31 films	Water temperature (°C)						
	Room Temp.	40	45	50	55	60	65
Un-heated	DS						
40°C/ 3 hrs	Disint	DS					
60°C/ 3 hrs	Disint	DS					
90°C/ 3 hrs	S	Disint + DS	DS				
120°C/ 10 min	S	Disint	DS				
150°C/ 10 min	S	S	S	S	S	Disint	DS
180°C/ 10 min	S	S	S	S	S	S	DS

S - swollen

Disint - disintegrated

DS - dissolved

4.3.2 Swelling test results

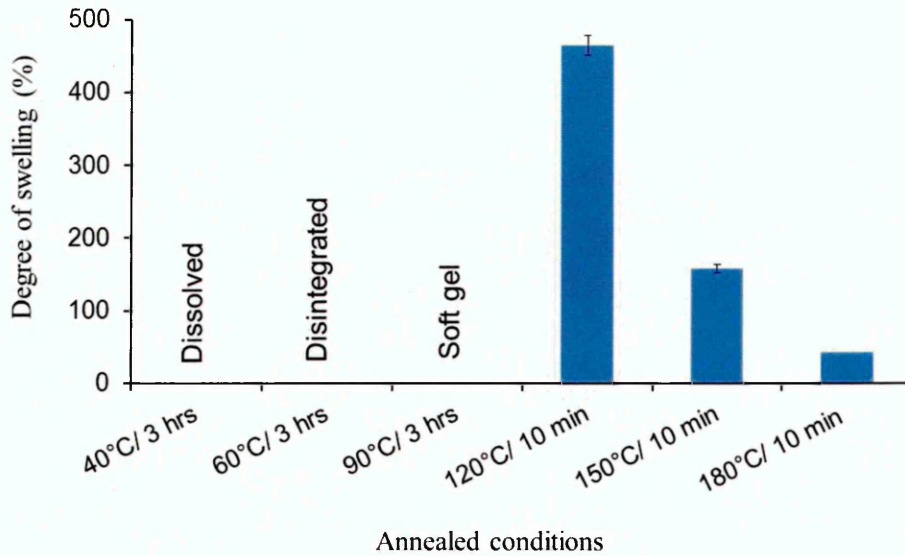


Figure 4.3 Degree of swelling in water (22°C) of PVOH films annealed at different temperatures

In water at room temperature (22°C), only films heated at 40°C completely dissolved after 24 hours while those treated at 60°C disintegrated. For films annealed at 90°C and immersed in water, their shapes were maintained but then the films disintegrated and stuck together when being blotted with soft paper which made it difficult to obtain their correct weights. Therefore, the swelling test results for films annealed at low temperatures were impossible to calculate. For samples treated at higher temperatures (> 90°C), films became just swollen in water. The degree of swelling in water of the film treated at 180°C/ 10 min was the lowest (~43%) in comparison with 465% and 158% for those treated at 120°C and 150°C, respectively (Fig. 4.3).

4.3.3 Water vapour transmission rates (WVTR)

Fig. 4.4 shows a decrease in WVTR values as annealing temperature for PVOH is increased. With a heat treatment of 40°C/ 3hrs, the WVTR of PVOH decreased to ~247 g/(m².day) from ~310 g/(m².day) for un-heated films, which related to an improvement of 20.3%. Annealing the films at 60°C/ 3hrs did not show

considerable change in the WVTR relative to the values at 40°C/ 3hrs whilst increasing the annealing temperature from 90°C to 180°C led to further gradual decreases in WVTR values. The lowest WVTR was achieved with an annealing temperature of 180°C (145 g/(m².day)) expressing an improvement of 53% in water vapour barrier property in comparison with the untreated PVOH film.

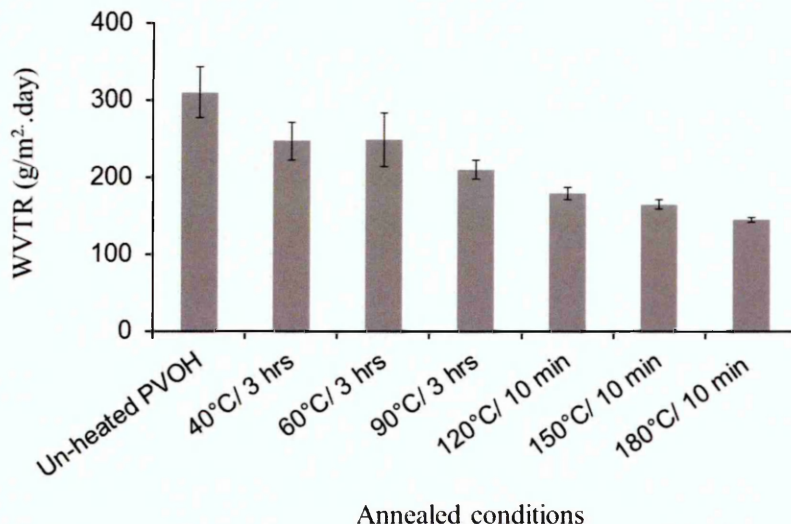


Figure 4.4 WVTR results (23°C, 85% RH) from PVOH films ($M_w = 31,000-50,000$) annealed at different temperatures and duration of times.

4.3.4 TGA results (water content)

TGA was used to compare the amounts of water remaining in the PVOH films after heat treatment at different temperatures (i.e. water content was calculated from the weight loss up to 185°C). When PVOH films were annealed, water evolved from the films, the higher the annealing temperature, the more water was removed (Fig. 4.5). It can be observed that most of the water was removed after heating the films at 120°C for 10 minutes. The amount of water remaining in the films heated at 120, 150 and 180°C was quite low (below 0.7 wt%) while the value in unheated film was ~7.3 wt%.

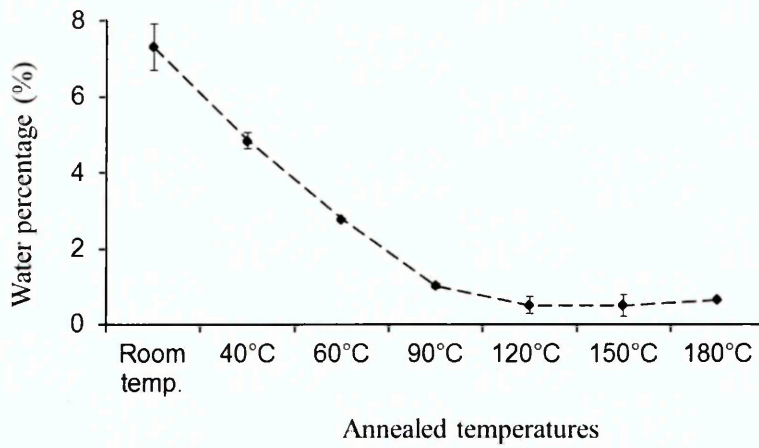


Figure 4.5 Water content in PVOH films after annealed at different temperatures (from TGA results)

4.3.5 Contact angle results

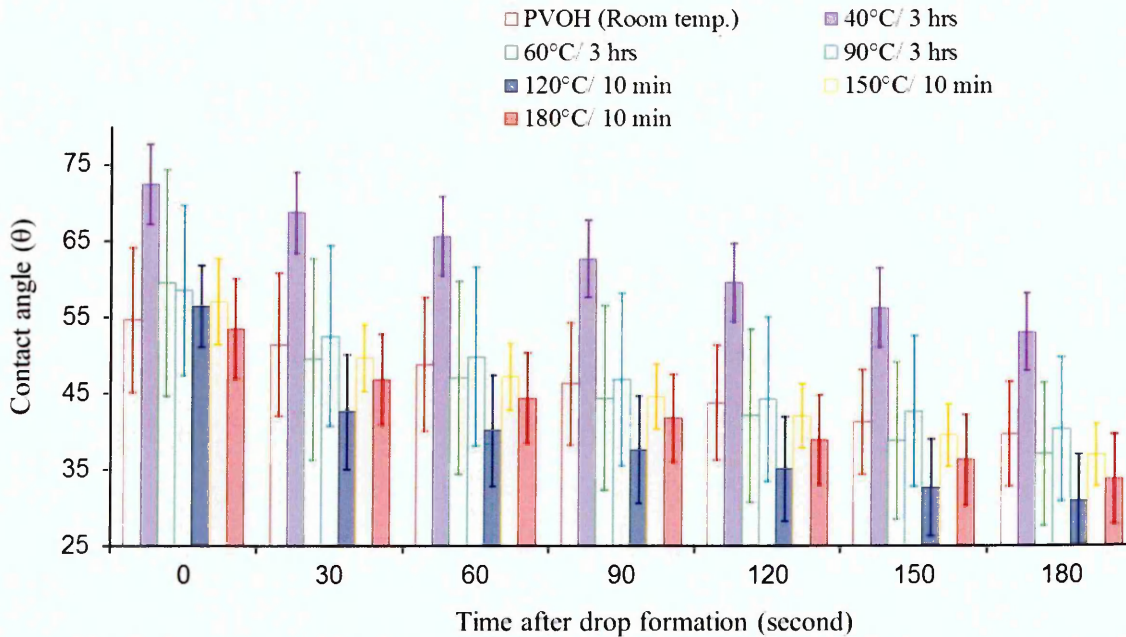


Figure 4.6 Water contact angle values versus remaining time after drop formation on neat PVOH film and heat treated films. The drop type was sessile drop and the testing atmosphere was 20-22°C. Each value was a mean of 5-10 measurements at the same condition.

It is noted that the PVOH at room temperature was prepared by casting method from the PVOH solution and kept in a close container after atmospheric drying, i.e. no heat treatment before the contact angle experiment. Fig. 4.6 shows that at the initial point (0 sec), its contact angle values were comparable to those of PVOH films annealed at 60, 90, 120, 150 and 180°C. Since there is a large spread within each data bar it is difficult to ascertain with certainty any clear trends. However, when extending the time after the drop formation on the film surface, films annealed at 120°C possessed the lowest contact angle values. Also, in general, the contact angle values of PVOH films treated at 40°C/ 3hrs were always higher than those of the other annealed films.

4.3.6 FTIR results

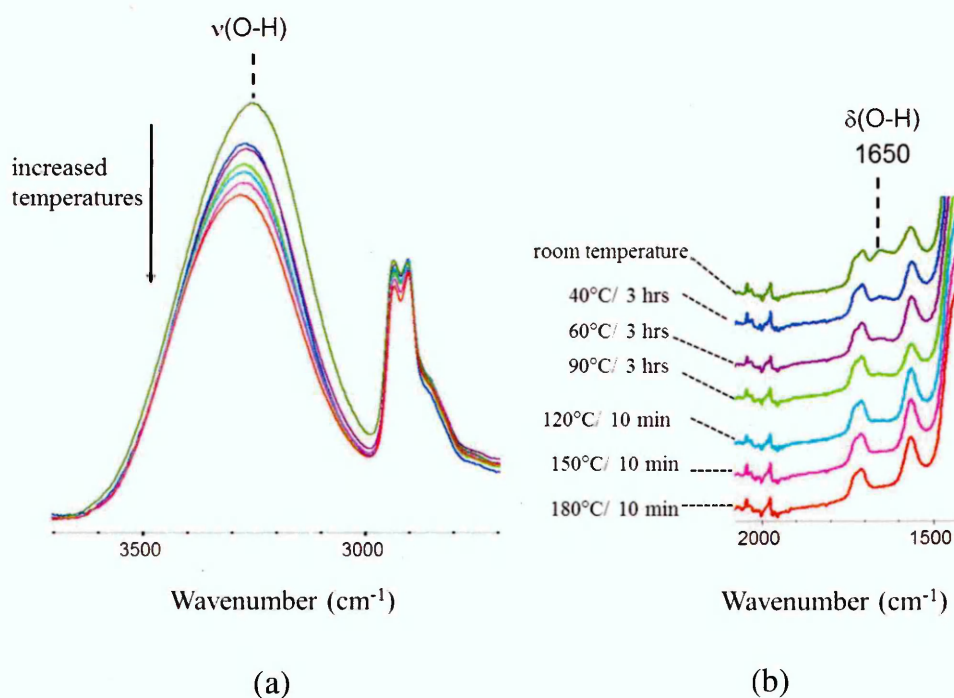


Figure 4.7 Changes in absorption intensities of (a) O-H stretching and (b) O-H bending vibrations after PVOH films were annealed at different temperatures. Spectra in (b) are offset for clarity

Heat treatment of the PVOH films resulted in some significant changes to their FTIR spectra. A decrease in intensities with increasing annealing temperature for

two absorption bands at 3260 cm^{-1} and 1650 cm^{-1} was observed which are attributed to O-H stretching and O-H bending, respectively confirming a removal of water present in the films [152]. It can be observed in Fig. 4.7a that the intensity of the O-H stretching band decreased significantly when PVOH film was annealed at 40°C indicating a considerable removal of the amount of water. Films treated at 40 and 60°C for 3 hours did not show any significant differences in their O-H stretching band intensity, while that annealed at 180°C showed the lowest O-H stretching intensity. Fig. 4.7b shows that the O-H bending peak (1650 cm^{-1}) peak was substantially reduced when films were heated at 120°C for 10 minutes and at higher temperatures confirming that most of the water was removed. This is consistent with the TGA results reporting the content of water present in the films heated at the higher temperatures is very low ($< 0.7\%$).

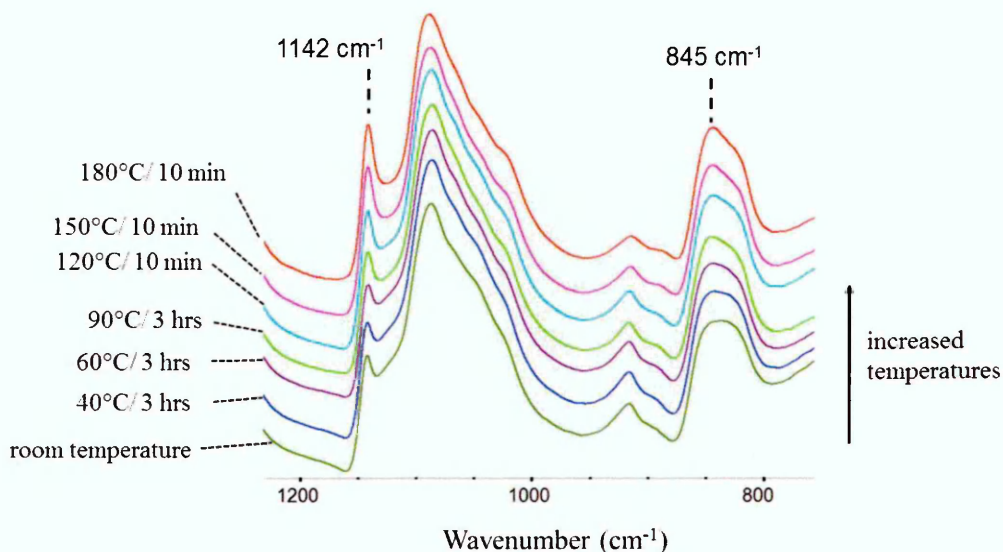


Figure 4.8 Changes in the absorbance intensities of 1142 cm^{-1} and 845 cm^{-1} peaks in FTIR spectra of PVOH films after heat treatment. Spectra are offset for clarity.

The increase in the intensity of the 1142 cm^{-1} peak with temperature (Fig. 4.8) indicated a corresponding increase in crystallinity [35,37,51,99]. The intensities of the 1142 cm^{-1} peak obtained from films annealed at 40 and 60°C were not much different from that belonging to the non-heated film (room temperature). Increasing the heating temperature further resulted in a more intense and sharper 1142 cm^{-1} peak.

Table 4.3 demonstrates an increase in the degree of crystallinity of PVOH films when heated at increasing temperatures, the values relate to the intensity of the 1142 cm^{-1} band relative to that at 1087 cm^{-1} (Section 2.1.4, Equation 2.4) [37].

Table 4.3 Changes in the degree of crystallinity of PVOH films after heat treatment. The relative intensities of absorbance bands at 1142 and 1087 cm^{-1} were taken with the baselines starting from 952.6 to 1159 cm^{-1} (see Fig.2.9, Section 2.1.5)

Treated temperature	Exposed time	Degree of crystallinity D_c (%)
Room temperature	n/a	23.2 \pm 0.8
40°C	3 hours	24.9 \pm 0.3
60°C	3 hours	25.0 \pm 0.2
90°C	3 hours	27.4 \pm 0.3
120°C	10 minutes	31.1 \pm 0.4
150°C	10 minutes	36.4 \pm 0.4
180°C	10 minutes	39.2 \pm 0.5

The degrees of crystallinity of PVOH films derived from utilising the 1142 cm^{-1} peak in IR spectra have been reported by several authors and are listed in Table 4.4. It can be observed from Tables 4.3 and 4.4 that, the degrees of crystallinity of herein annealed samples are lower than those stated in the literature. This may be due to the differences in PVOH molecular weight, sample preparation, the calculated equation, IR technique operation, etc. For example, Korodenko *et al.* [40] confirmed a degree of crystallinity of ~42 % was obtained when treating PVOH at 120°C for 10 minutes using the same reference peak at 1097 cm^{-1} (equivalent to herein 1087 cm^{-1}) but a different equation. Peppas [49] used the 1425 cm^{-1} band as the reference peak to calculate degrees of crystallinity of 31.1% and 51.6% for PVOH films heated at 90°C for 0.5 and 1.5 hours, respectively, these are higher than the value obtained at 90°C for 3hrs in this current work (~27.5%). In addition, the crystallinity equation proposed by Tretinnikov [37] was obtained from the IR spectra using FTIR transmission

while herein the ATR-FTIR was applied. The non-porous films in this current work were also shown to have a higher degree of crystallinity (31.1% at 120°C/ 10min) than the porous films of Wang [83] (18.7% at 120°C/ 1hr).

Table 4.4 Literature values of degrees of PVOH crystallinity obtained using the 1142 cm⁻¹ peak in IR spectra

M _w	Annealed temperature	Exposed time	Reference peak (cm ⁻¹)	Degree of crystallinity (%)	Ref.
88,800	90 °C	0.5 hr	1425	31.1	[49]
	90 °C	1.5 hrs	1425	51.6	
133,000	90 °C	1 hr	1094	38.8	[37]
	120 °C	1 hr	1094	46.2	
	150 °C	1 hr	1094	60.2	
38,800	120 °C	10 min	1097	42	[40]
77,000	120 °C	1 hr	1425	18.7	[83]

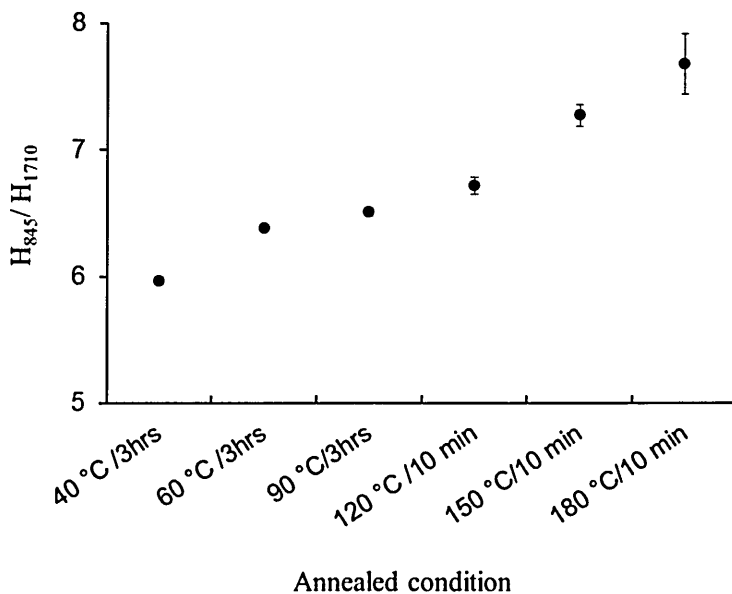


Figure 4.9 Peak height ratio between FTIR bands at 845 cm⁻¹ and 1710 cm⁻¹ for annealed PVOH films.

Lebeda *et al.* [99] related an increase in intensity and a narrowing contour of the absorbance band at 845 cm^{-1} , assigned to C-C skeletal bending [43,157] to the increasing crystallinity of PVOH samples. Therefore, the crystallinity of the PVOH films can be able evaluated from the 845 cm^{-1} peak. When the annealing temperature increased for the samples herein, the 845 cm^{-1} peak became narrower and increased in intensity indicating increased crystallinity (Fig. 4.8). The absorption band of C=O group at 1710 cm^{-1} was used as a reference peak because no considerable change was observed upon heat treatment (Fig. 4.7b). It is shown in Fig. 4.9 that the peak height ratio H_{845}/H_{1710} increases with increasing annealing temperatures and can be expressed in a linear relationship with the degree of crystallinity, D_c , in Fig. 4.10

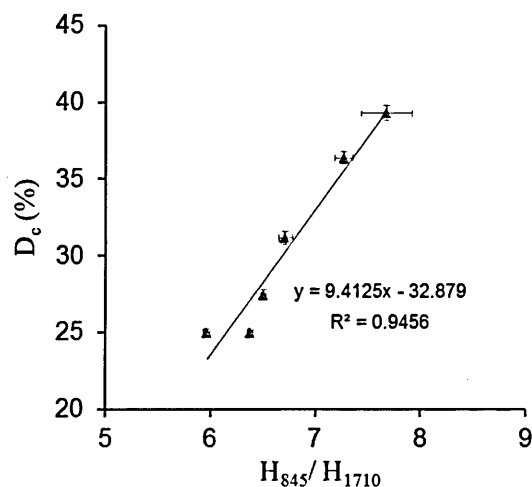


Figure 4.10 A linear relationship between the peak height ratio H_{845}/H_{1710} and the degree of crystallinity (D_c) derived from using the 1142 cm^{-1} peak.

4.3.7 Raman results

The underlying background of Raman spectra increased as the annealing temperature increased, which has also been previously reported by Iwamoto *et al.* [159]. Therefore, automatic baseline correction was used (OMNIC software) to normalise the changes. The spectra in Fig. 4.11 were baseline corrected and then

offset for clarity. Some significant changes were observed: an increase in the intensity of the crystallinity representative bands at 1148 cm^{-1} (C-O-C and C-C stretching) and 1094 cm^{-1} (C-O stretching), whilst the 1072 cm^{-1} band (C-O stretching) remained unchanged. In addition, the absorption band at 857 cm^{-1} which is ascribed to C-C stretching also increased when the annealing temperature increased. These results indicate an increase in the crystallinity of PVOH films after heat treatment and are consistent with Raman results reported by Iwamoto *et al.* [159] and Thomas *et al.* [158].

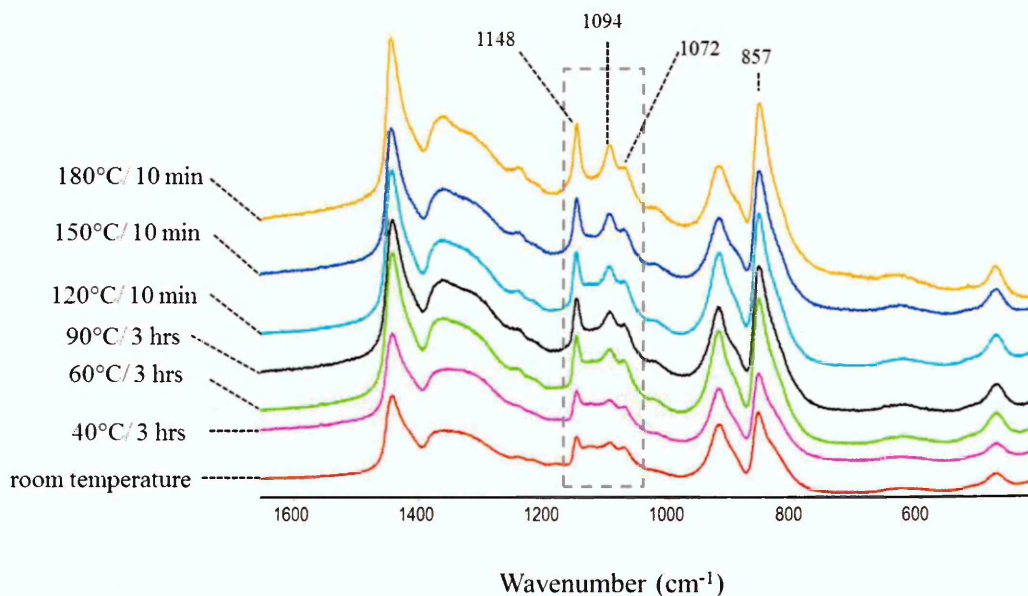


Figure 4.11 Raman spectra of PVOH films annealed at different temperatures

4.3.8 X-ray diffraction

The XRD patterns collected between $2\text{-}45^\circ 2\theta$ from PVOH films annealed at different temperatures are shown in Fig. 4.12. The diffraction profiles are in agreement with Assender and Windle [48] and Ricciardi *et al.* [166] who investigated the crystallite structure of PVOH based on the theory regarding the monoclinic structure of unit cells of PVOH which was proposed by Bunn [45]. These authors reported a presence of a doublet at $19.4^\circ 2\theta$ and $20^\circ 2\theta$ ($10\bar{1}$ and 101 reflections, respectively) in highly crystalline PVOH.

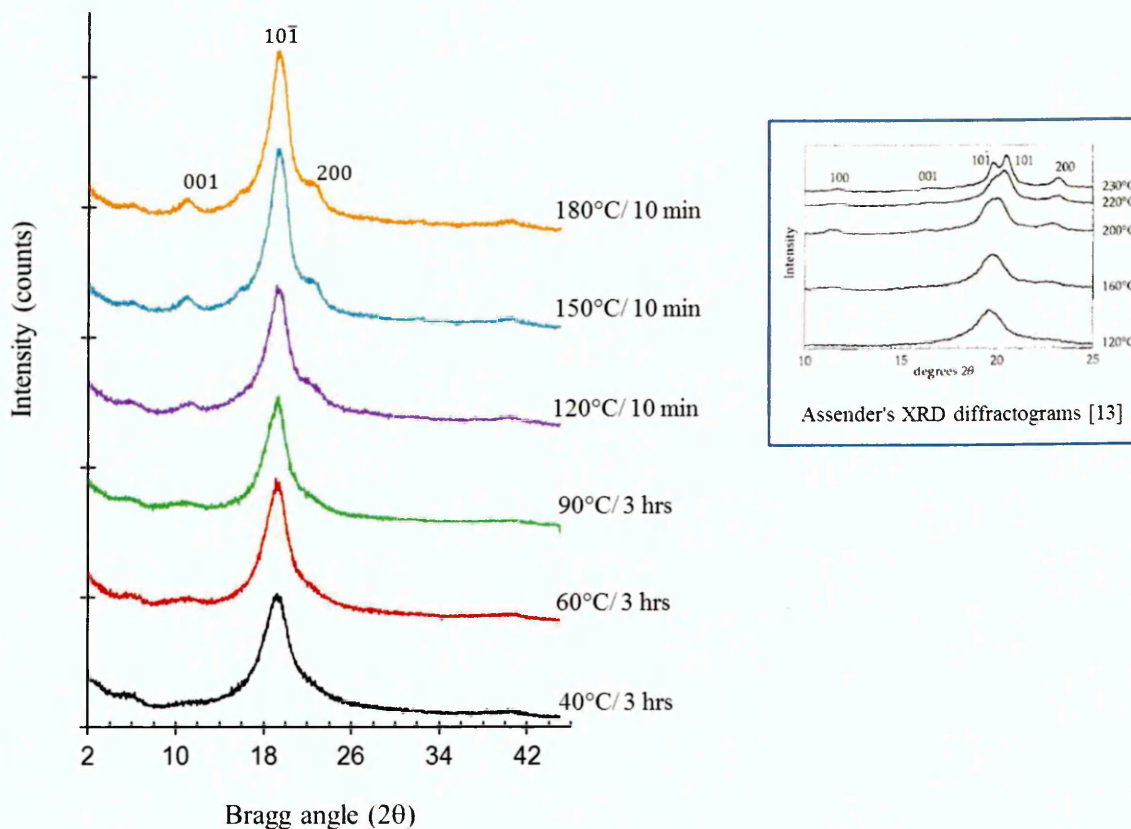


Figure 4.12 X-ray diffraction traces from PVOH31 films annealed at different temperatures. The diffractograms are shifted vertically for clarity

However, in the diffractograms herein, the diffraction peak at $20^\circ 2\theta$ was not present. According to Assender and Windle, heating the sample at 220°C for 1 hour did not reveal the doublet but was present in a very high crystalline polymer prepared at 230°C for 4 minutes. This was supported by XRD results of Ricciardi *et al.* which demonstrated the doublet and a very high crystallinity degree (64%) in PVOH films prepared from melting PVOH powder at 230°C and then slowly cooling to room temperature. Herein the heating temperatures were below the melting point of PVOH and the heating durations were controlled so that the films did not turn brown due to thermal degradation. Therefore, it is likely that the crystallinity of our PVOH films was not high enough to induce the presence of the $20^\circ 2\theta$ peak.

Fig. 4.12 shows that there were two small diffraction peaks at $11.3^\circ 2\theta$ and $22.5^\circ 2\theta$ that became prominent and increased in intensity at higher treatment temperatures (120° to 180°C). These peaks are believed to be associated with crystallinity since they were also present in Assender and Windle data for high crystalline samples and assigned as 001 and 200 reflections, respectively (although the 200 peak was at slightly higher angle, $23.5^\circ 2\theta$).

There was an increase in the sharpness and intensity of the crystalline peak at $\sim 19.2^\circ 2\theta$ ($10\bar{1}$ reflection) when PVOH was heated at the higher temperatures (150°C and 180°C). In addition, no shift to higher Bragg angle was observed when increasing the annealing temperature as stated by Assender and Windle [48]. Crystallite sizes of annealed PVOH films are observed to increase with increasing temperature (Fig. 4.13). The highest value was 4.7 nm for the sample heated at $180^\circ\text{C}/10$ minutes.

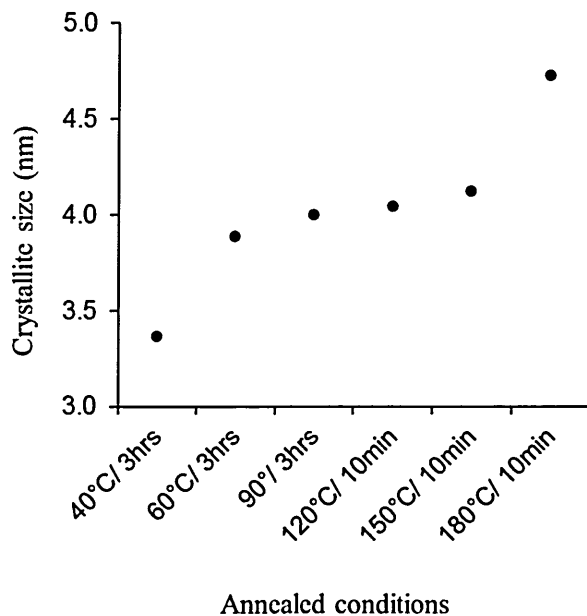


Figure 4.13 Crystallite size of PVOH31 films annealed at different temperatures

4.3.9 DMA results

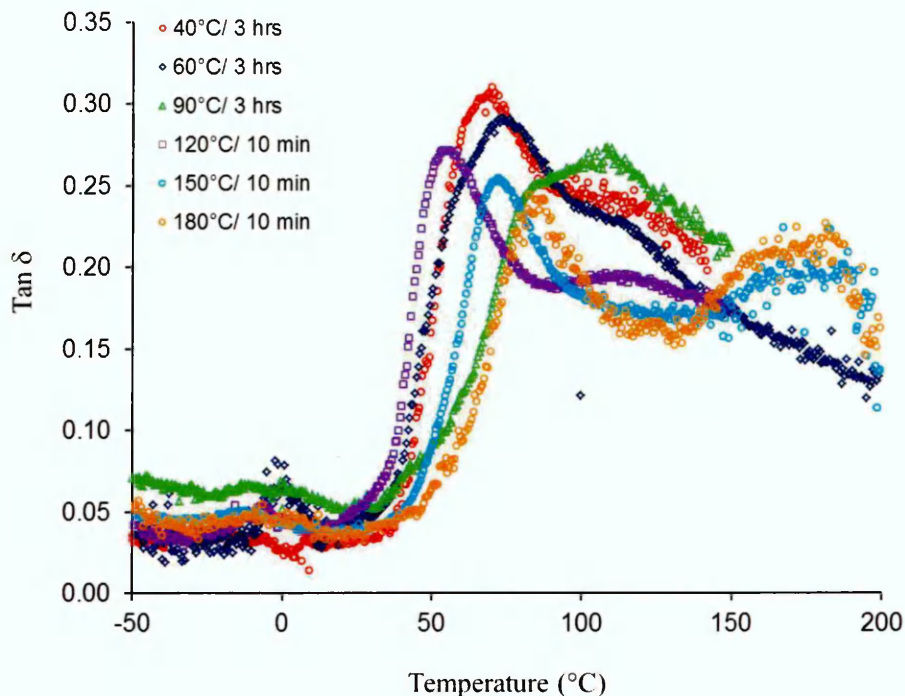


Figure 4.14 Tan δ curve for annealed PVOH31 films. DMA was conducted in tension mode with frequency 1 Hz and temperature scanning rate of 2°C/min.

Tan δ damping factors for annealed PVOH films as a function of temperature are illustrated in Fig. 4.14. In general, the tan δ curves for all the annealed PVOH films exhibited 3 relaxations of which the first one at around 0°C can be assigned to β relaxation which is related to the movement of the whole side groups (hydroxyl and acetate groups) and localised groups of 4-8 backbone atoms [53,134,173]. Gonzalez-Campos *et al.* [173] reported a relation between β relaxation and moisture content in that samples annealed at higher temperature (120°C) did not exhibit the β transition. However, it is unlikely to be applicable herein where β transitions were present in all tan δ results.

The second relaxation from 50 to 100°C (varied between samples) is related to the α transition (glass transition) which is indicative of movement of the large segments of polymer chains. The third relaxation above 100°C is related to the slippages of crystallites past each other (alpha star transition T_{α}^*) [134]. This relaxation was stated by Nishio and Manley [174] to relate to the degree of

crystallinity (crystalline relaxation) and increase with increasing crystallinity. Fig. 4.14 shows that when the annealing temperature increased from 40 to 120°C, there were no significant changes in this relaxation temperature (from 110 to 120°C). For samples annealed at 150 and 180°C, the T_{α}^* relaxation shifted to higher temperature (~180°C) corresponding to the higher degrees of crystallinity in these films.

In theory, when PVOH is subjected to a higher annealing temperature, a corresponding decrease in the water content present in the sample occurs leading to an increase in crystallinity due to the formation of intermolecular and intramolecular hydrogen bonding between the polymer molecules. This affects the crystalline and amorphous phases in the polymer as well as restricts movement of the polymer chains resulting in an apparent increase in the glass transition temperature [173]. Herein the T_g achieved from different annealed PVOH films did not show an increasing trend with increasing temperature. However, the results can be divided into two annealing temperature groups which are 40, 60 and 90°C for 3 hours and 120, 150 and 180°C for 10 minutes. In each group, the T_g increased with increasing temperature (Fig. 4.15). The T_g values of samples treated at 40 and 60°C were not vastly different and in the range of 65-74°C, whilst that belonging to the film annealed at 90°C was at ~84°C. This glass transition temperature was not clearly defined in the graph (Fig. 4.14) but its position was supported by the shift of the $\tan \delta$ peak to higher temperature when measured using a higher frequency (10 Hz). Increasing the annealing temperature did not necessarily lead to an increase in the T_g value. On the contrary, PVOH film heated at 120°C had the lowest T_g (55°C) while the T_g values at 150 and 180°C heat treatment were shown to be relative to those treated at 60 and 90°C, respectively.

The tensile storage modulus (E') values of different annealed PVOH films were taken at 0°C and at T_g position and shown in Fig. 4.16. It can be observed that both E' values increased when the heating temperature increased from 40 to 120°C and then decreased at 150 and 180°C. The increase in E' values when heating the films up to 120°C/ 10 min is ascribed to the removal of water present

in the films which caused the films more compact and restricted the movement of the polymer chains. Whereas, treating the films at 150 and 180°C, which were close to an initial decomposition point of the films, could cause some chemical destruction in the polymer resulting in a decrease in E' values.

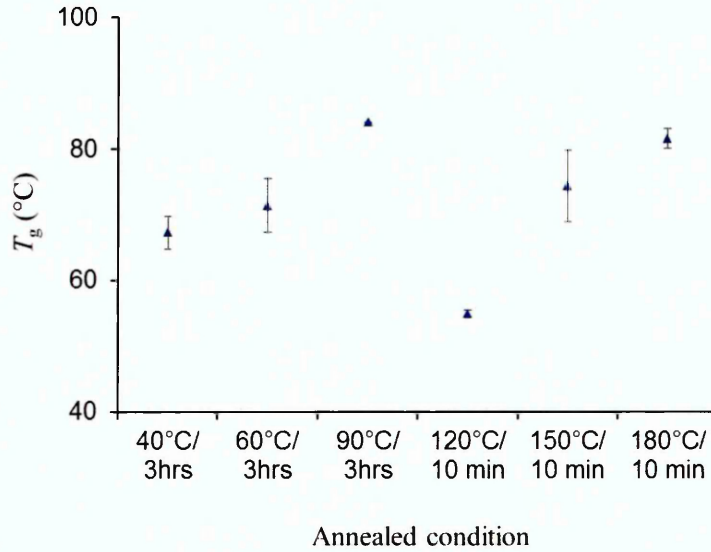


Figure 4.15 Glass transition temperatures (T_g) of heat treatment PVOH films

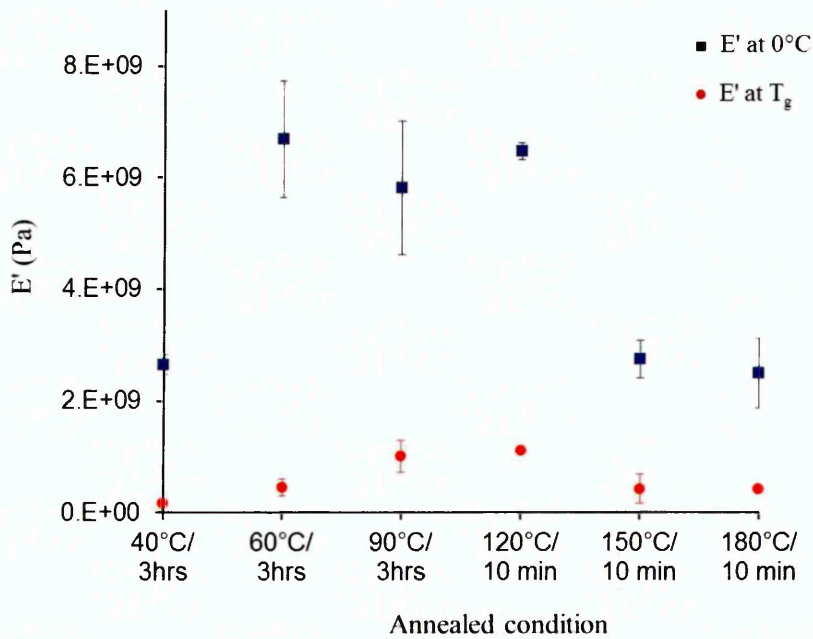


Figure 4.16 Storage modulus (E') at 0°C and at T_g position for PVOH31 films annealed at different temperatures.

4.3.10 Discussion

FTIR, Raman and XRD results showed that when PVOH films are subjected to high temperature, their crystallinity increased. During the heating of the films, the removal of water occurred and the polymer chains gained enough energy to rearrange to form inter- and intramolecular hydrogen bonds between their O-H groups and thus crystalline regions and crystallinity [83,173]. As the polymer became more crystalline (compact), less free volume was present in the films leading to a better resistance to water and water vapour. The higher the annealing temperature, the higher the barrier properties to water. The WVTR and swelling test results confirmed an increase in the water vapour barrier properties and a decrease in the degree of swelling in water of PVOH films with increasing annealing temperature. In the dissolution test, films of lower crystallinity (i.e. 40, 60, 90 and 120°C) dissolved at lower water temperature (i.e. $\leq 45^{\circ}\text{C}$). Films heated at 150 and 180°C for 10 minutes only swelled in water at temperatures below 60°C, which is owing to the higher crystallinity formed in the films during annealing. However, they dissolved when the dissolution temperature increased to 65°C indicating that the crystallites formed in the films could still be dissolved. This also applied to the swelling test in water at 90°C where all the films completely dissolved. In cold water (22°C), the films annealed at low temperatures (40, 60 and 90°C) dissolved or disintegrated because of their low crystallinity making it easier for water to penetrate into the amorphous regions to form hydrogen bonds with PVOH hydroxyl groups, here any hydrogen bonds between the polymer chains were broken.

It is noteworthy that the degree of crystallinity in current work was calculated utilising the 1142 cm^{-1} absorption band in FTIR and using an equation from literature (Section 2.1.4, Equation 2.4) in spite of differences in the instrumental set up and PVOH materials. Therefore, the obtained values herein are simply used for reference and for comparison between different samples in this thesis. Ideally, an independent technique is required with known calibration standards.

According to the WVTR, XRD and FTIR results, the samples annealed at 40 and 60°C were similar in their properties while the films at 180°C possessed the

highest degree of crystallinity and barrier properties to water and water vapour. The low-temperature annealed films (40°C) showed lower wettability to water than the high-temperature annealed films (150 and 180°C). In addition, films annealed at 120°C/ 10 min had the lowest contact angle values and the lowest glass transition temperature (~55°C). The DMA results did not show an increasing trend in glass transition temperature with increasing annealing temperature. In addition, the storage modulus increased when heating the films from 40 to 120°C then decreased when at 150 and 180°C. This decrease in E' is possibly due to chemical destruction in the films at high temperatures.

4.3.11 Summary

Heating PVOH31 films induces crystallinity resulting in lower WVTR values and degrees of swelling in water. The higher the annealing temperature, the better the water and water vapour barrier properties. Treating the films at 180°C for 10 minutes led to an improvement in the water vapour barrier properties by 53% and a crystallinity degree of 39.2%, without any visual thermal degradation effects. However, heating PVOH films at high temperature (150 and 180°C) could cause some chemical destruction leading to a decrease in the storage modulus values.

4.4 HEAT TREATMENT OF HIGH MOLECULAR WEIGHT PVOH AND CROSSLINKING REACTION WITH GLUTARALDEHYDE

4.4.1 Heat treatment of PVOH124.

4.4.1.1 WVTR results

In the previous section, two groups of annealing temperatures/times were investigated, which included 40, 60 and 90°C for 3 hours and 120, 150 and 180°C for 10 minutes. When heating PVOH31 films at 40 and 60°C, no significant differences in the film properties were observed and likewise when

annealing at 150 and 180°C for 10 minutes. Therefore, the selected annealing temperatures used to treat PVOH124 films were 40 and 90°C for 3 hours and 180°C for 10 minutes.

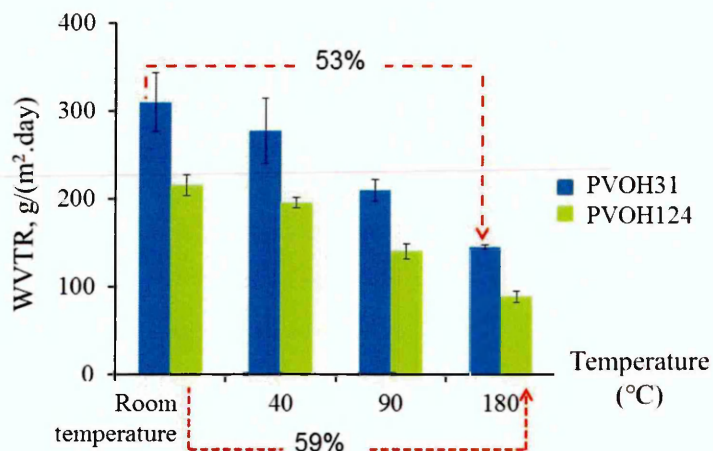


Figure 4.17 Comparison between WVTR (23°C, 85% RH) values from PVOH124 and PVOH31 films before and after heat treatment

It can be observed in Fig. 4.17 that, like PVOH31, when PVOH124 films were annealed at elevated temperatures, the WVTR decreased. Heating the PVOH124 films from room temperature to 180°C resulted in a decrease of WVTR from 215 to 88 g/(m².day), in which the improvement of the water vapour barrier properties was 59%, this was slightly higher than that for PVOH31 (53%). Overall, with the same treatment condition, respective WVTR values for PVOH124 were lower than those for PVOH31 indicating that PVOH124 exhibited higher water vapour barrier properties than PVOH31 regardless of the treatment temperature.

4.4.1.2 FTIR results

The FTIR spectra of annealed PVOH124 films showed significant changes when compared with the spectrum of unheated film (room temperature) (Fig. 4.18). Like in the respective spectra for PVOH31 (Fig. 4.8), there was an increase in the

intensity of the 1142 cm^{-1} (C-C stretching band) as well as an increase and narrowing contour of the 845 cm^{-1} peak (C-C bending) when the annealing temperature increased from 40°C to 180°C . These changes indicated an increase in the crystallinity during the heat treatment.

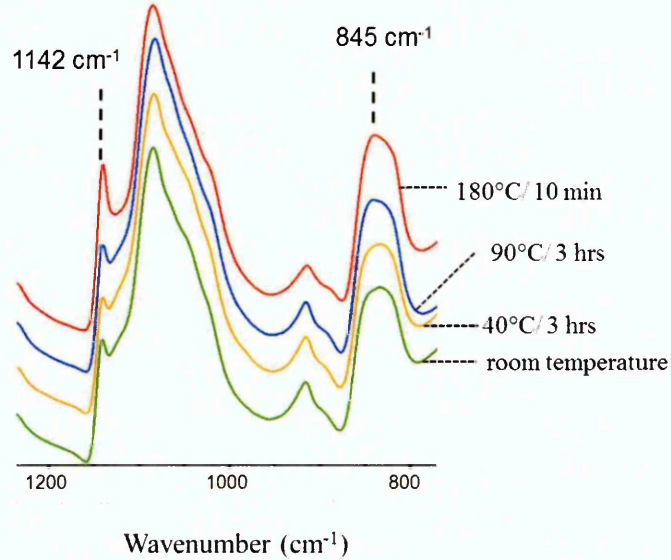


Figure 4.18 FTIR spectra of neat PVOH124 and its annealed films

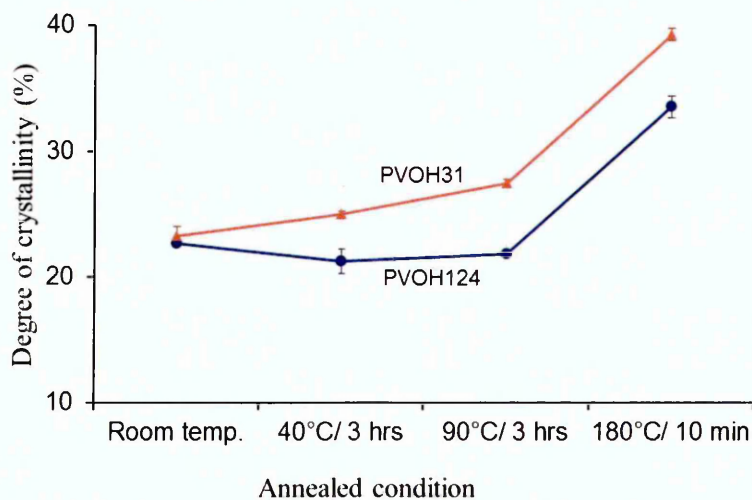


Figure 4.19 The degrees of crystallinity of annealed PVOH124 films compared with those of PVOH31 films

The degree of crystallinity of the annealed films was calculated utilising the intensity of the 1142 cm^{-1} peak relative to that at 1087 cm^{-1} (Section 2.1.4, Equation 2.4) [37]. A comparison between the degrees of crystallinity between PVOH124 and PVOH31 is shown in Fig. 4.19. A lower degree of crystallinity was observed for all the annealed PVOH124 films relative to those for PVOH31. The degrees of crystallinity between the two unheated films (room temperature) were not much different (23.2% for PVOH31 and 22.6% for PVOH124). When the temperature was increased from 40°C to 90°C , the PVOH31 films exhibited an increase in the degree of crystallinity from $\sim 25\%$ to $\sim 27.5\%$, respectively, while the PVOH124 films did not show a significant change in crystallinity (i.e. 21.2% and 21.8% for films heated at 40°C and 90°C , respectively). Annealing at 180°C induced a dramatic increase in the degree of crystallinity in which the value for PVOH124 was 33.5% and lower than that for PVOH31 (39.2%).

4.4.1.3 Discussion

When annealing PVOH124 films at 180°C , a significant increase in crystallinity relative to that at 40°C was observed, whereas when heated at 90°C , no significant change occurred, but the WVTR values decreased by $\sim 28\%$ (Fig. 4.17). A possible explanation for this phenomenon is related to the long chains of PVOH124 not having sufficient energy at 90°C to support the alignment of the amorphous polymer chains to form crystallites. A reduction in the free volume present in the films annealed at 90°C would still occur (more so than at 40°C) due to the removal of more water making the polymer films more compact. As a result, the water vapour barrier properties of films heated at 90°C were higher than those of 40°C .

The unheated PVOH124 films were shown to exhibit higher water vapour barrier properties than the respective PVOH31 films with a WVTR difference of about 30%. Heating both types of PVOH films at respective temperatures also produced similar results in that the annealed PVOH31 films showed water vapour barrier properties 30-39 % lower than those of PVOH124 films. The

diffusion process in polymer is influenced by the polymer molecular weight [175,176]. Berens *et al.* [176] reported a decrease in the diffusion coefficients of some organic vapours such as acetone and benzene in polystyrene when the polymer molecular weight increased. For example, the diffusivity decreased by a factor of ~10 when the molecular weight increased by 30 times. This was explained by a chain end effect of the polymer. Within the polymer structure exists a number of chain ends of which the concentration (number of end groups per unit volume) is inversely proportional to the molecular weight [177]. The presence of chain ends in the polymer can interrupt the packing of the molecules leading to more free volumes being generated. This may form more sites for the permeant molecules to accumulate and enhance diffusion [178]. Therefore, when the molecular mass of PVOH increases, the number of chain ends decreases resulting in less free volume being present and contributing to lower water vapour transmission rates. Another factor that could account for this is the polarity of the end groups. According to Sakurada [41], carboxyl and carbonyl groups, which are polar, are common end groups in PVOH. The carbonyl groups are found in the acetaldehyde impurities in PVOH and their amounts are usually small. In the low molecular weight PVOH, more end groups are present making the film more polar which can attract more polar water; this results in an increase in the water vapour diffusion.

The FTIR results revealed lower crystallinity for PVOH124 than for PVOH31. This can be explained by the polymer morphology in that the longer chains of the higher molecular weight polymer require more energy to become aligned and produce ordered regions, i.e. to form crystallites [100].

Therefore, when the molecular mass of PVOH is increased, there are two opposing effects occurring concurrently. The first is an increase in the water vapour barrier properties due to the chain ends effects, whilst the second is a decrease in the crystallinity because of the effects of longer polymer chains, which might result in a negative effect on the water vapour barrier properties. As a result, it can be inferred that the impact of the chain ends in polymer structure on the transportation of the water vapour in the PVOH films is dominant in comparison with that of the polymer crystallinity.

It is interesting to observe that the intervals between WVTR values for different annealing temperatures for each respective pair of PVOH124/ PVOH31 films were very close and so were the differences between the degrees of crystallinity. This may indicate that when films are subjected to higher temperatures, a similar number of amorphous chains are re-arranged to form crystallites, despite their different molecular weights.

In summary, PVOH124 possess lower crystallinity but higher water vapour barrier properties than those of PVOH31. The concentration of end groups in the polymer structure presumably has higher impact on the water vapour barrier properties than the crystalline structure. When PVOH films are subjected to higher temperatures, the degree of crystallinity increases while the water transmission rate decreases.

4.4.2 Effect of combining heat treatment and crosslinking on the water vapour barrier properties of PVOH124.

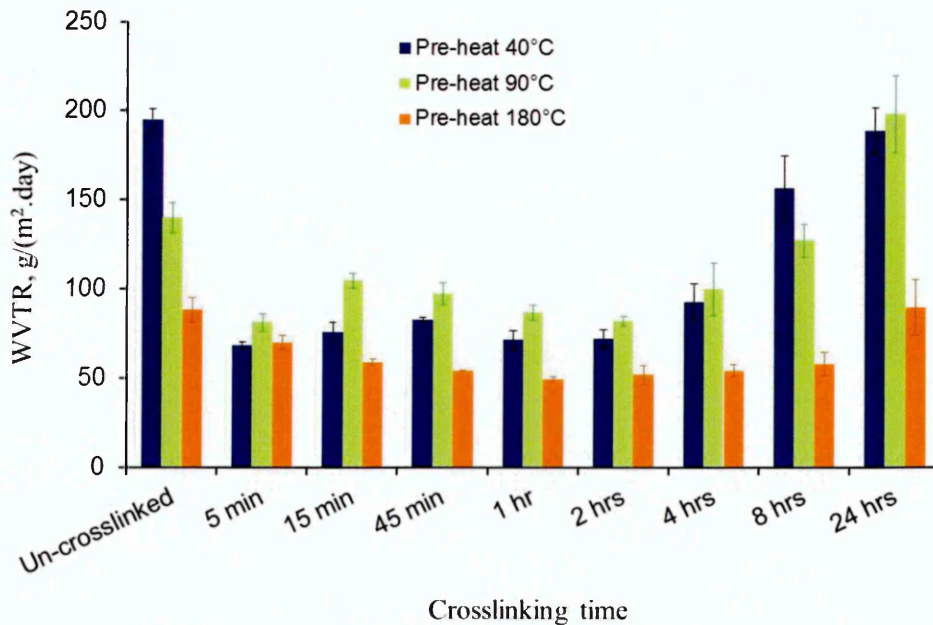


Figure 4.20 WVTR results at 23°C ad 85% RH of crosslinked PVOH124 films. Before crosslinking reactions, films were pre-treated at 3 different temperatures which were 40°C, 90°C for 3 hours and 180°C for 10 minutes. The ratio between PVOH124 repeat units and GA was 4:1.

One of the aims for this study was to create a high crystalline polymer system by heat treatment which could hinder the penetration of the crosslinking agent so that the crosslinking reaction occurred only at the outermost surfaces. The resulting polymer film may therefore show good resistance to water and water vapour but could also be dissolved in hot water. Previous results showed that no crosslinked PVOH31 films dissolved in hot water (90°C) including those crosslinked for very short crosslinking times (5 minutes) (see Section 3.4.5). The same phenomenon was also observed for all crosslinked PVOH124 films in this current study regardless of the annealing temperatures prior to the crosslinking with GA. Therefore, it is believed that the crosslinking reaction occurs effectively through out the neat and annealed films.

The WVTR results for the annealed and crosslinked PVOH124 films are shown in Fig. 4.20. After any crosslinking reaction, the WVTR values generally decreased. Like previous WVTR results for PVOH31 films (Fig. 3.9, Section 3.4.3), when extending the crosslinking time from 4 hours, the WVTR values started increasing indicating a decrease in the water vapour barrier properties. The reason for this is believed to be due to the dominance of acetal linkages formed as part of the crosslinks which have an affinity with water vapour (see Section 3.4). For PVOH124 films annealed at 40°C/3 hours and then treated with the crosslinking solution for 5 minutes, a large improvement in the water vapour barrier property was observed by about 68%. When increasing the crosslinking time up to 2 hours, the WVTR values varied but not greatly. For films heated at 90°C/3 hours prior to crosslinking for 5 minutes, the water vapour barrier property improved approximately 42% relative to un-crosslinked films, i.e. the WVTR decreased from ~140 to 81 g/(m².day), respectively. When PVOH124 films were heated at 180°C/10 minutes prior to the crosslinking reaction, smaller changes in the WVTR values were apparent due to the already decreased value because of the annealing process. The WVTR values for the PVOH124 films heated at 180°C/10 minutes decreased gradually from 88 g/(m².day) for the un-crosslinked film to 54 g/(m².day) for the 45-minute-crosslinked films and then remained steady with up to 8 hours of crosslinking time before starting to rise at 24 hours (89 g/(m².day)).

It can be observed that with the 3 different preconditioning temperatures, the films heated at 90°C, in general, possessed the highest WVTR values after being crosslinked, i.e. the poorest water vapour barrier properties apart from those obtained with 8 hours of crosslinking time. It could be assumed that a greater free volume is present in the PVOH124 films heated at 40°C than those at 90°C making it more susceptible for the crosslinking agent to penetrate into the films to create more crosslinks and reduce free volume. Consequently, films annealed at 40°C showed higher water vapour barrier properties after crosslinking than those treated at 90°C. In addition, it can be postulated that those treated at 180°C exhibited the lowest WVTR values due to their significant increase in the crystallinity after annealing (see Section 4.4.1.2). During the crosslinking process, the high crystalline structure of these films disrupted the penetration of the crosslinking agent into the films leading to fewer crosslinks being formed. The WVTR values for different crosslinking times (below 24 hours) were very similar and not too different from the values for un-crosslinked films. One possible explanation is that crosslinking was limited in the films annealed at 180°C relative to the lower temperatures, and that the films after crosslinking still maintained a certain level of crystallinity which had a major contribution to the water vapour barrier properties.

Fig. 4.21 compares the WVTR values for crosslinked PVOH124 and PVOH31 films that were annealed at 40°C for 3 hours prior to being crosslinked. As for the un-crosslinked films, the crosslinked PVOH124 films exhibited better water vapour barrier properties than those of the crosslinked PVOH31 films. The differences in WVTR values of both crosslinked films were similar within 4 hours of crosslinking time, within 26 to 32%. However with 8 hours and greater crosslinking times, the differences increased, for example, the differences were 50% and 47% with 12 and 16 hours of crosslinking time, respectively.

When extending the crosslinking times, more acetal groups which have an affinity to water vapour are generated leading to an increase in WVTR values. Since more chain end groups are present in PVOH31 than in PVOH124 then more free volume is created and more channels are available for the crosslinking

agent to penetrate the polymer to create more crosslinks in the PVOH31 films. A possibility is that with high crosslinking time (after 4 hours), more acetal groups are present in the crosslinked PVOH31 films than in the respective crosslinked PVOH124 films leading to the higher differences between WVTR values

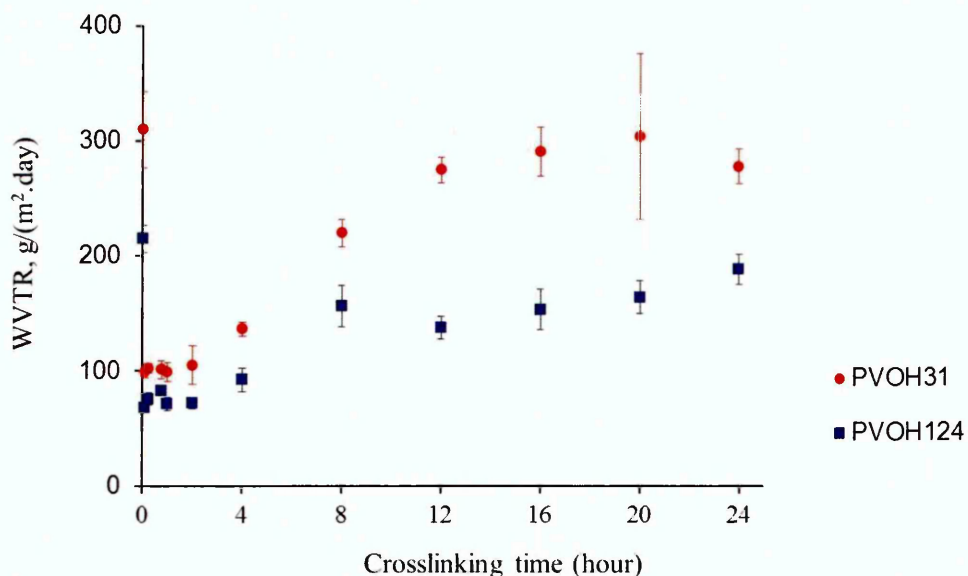


Figure 4.21 WVTR values for crosslinked PVOH124 and PVOH31 films. All films were treated at 40°C for 3 hours before crosslinking.

4.4.3 Summary

The high molecular weight PVOH films showed higher crystallinity and improved water vapour barrier properties after heat treatment. Heating films at 90°C for 3 hours did not show any significant increases in crystallinity in comparison with those heated at 40°C for the same duration. In comparison with PVOH31, PVOH124 films exhibited higher water vapour resistance but poorer crystallinity. This is in part due to fewer chain end groups present in the PVOH124 films resulting in reducing free volume and polarity of the polymer. The longer molecular chains of PVOH124 make it more difficult for adjacent polymer chains to align in order to create crystallites resulting in lower crystallinity when compared with PVOH31 films produced using the same heating conditions.

After crosslinking, PVOH124 films also exhibited higher water vapour barrier properties than the respective crosslinked PVOH31 films. The crosslinking between PVOH124 and GA was effective in improving the water vapour barrier properties when the crosslinking times were low (≤ 2 hours). Extending the crosslinking time led to negative effects in the water vapour resistance of the films.

The PVOH124 films heated at 180°C had the highest crystallinity and lowest WVTR values for the crosslinked and un-crosslinked films which was believed to be due mainly to the contribution from the crystallinity of the films. Films heated at 90°C prior to crosslinking showed the poorest water vapour resistance in comparison with the crosslinked films of those pre-treated at 40°C and 180°C.

4.5 ONE-SIDE CROSSLINKING

4.5.1 The series FTIR results

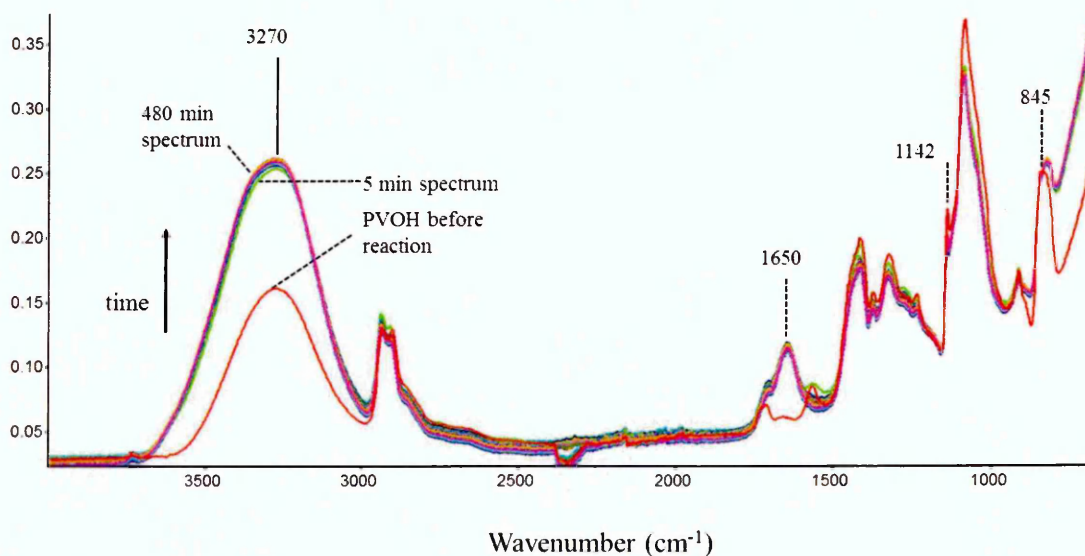


Figure 4.22 FTIR spectra collected during the diffusion of the crosslinking solution into the PVOH31 film. The spectra were recorded for 480 minutes every 5 minutes, only a selected number are presented.

The spectrum coloured red in Fig. 4.22 was collected from the PVOH film prior to any contact with the crosslinking solution. When the crosslinking solution was

injected into the cylinder, the first spectrum collected immediately after (~40 seconds to collect) was quite similar to that of the original PVOH, thus it is not presented here. However, the next spectrum collected after 5 minutes showed two significant changes: an increase in the intensities of the O-H stretching and O-H bending bands at 3270 and 1650 cm^{-1} , respectively together with a decrease in intensities of C-O stretching band at 1087 cm^{-1} and C-C bending band at 845 cm^{-1} . In addition, the 1142 cm^{-1} peak which represents the crystallinity of the sample also slightly decreased. These changes proved the diffusion of water into the film. The shift of the O-H stretching band from 3270 cm^{-1} to higher wavenumbers 3280 cm^{-1} indicated that in general the inter- and intramolecular hydrogen bonds in PVOH were weakened due to the interaction with water or the consumption of O-H groups by GA. The following spectra (up to 480 minutes collection time) did not show significant differences in comparison with the one collected at 5 minutes. Also, no obvious changes indicating the occurrence of the crosslinking between PVOH and GA were observed as reported in the previous chapter (Section 3.4.7). When the crosslinking solution penetrated into the sample film, the first thing to happen was that the water swelled the film leading to an increase in the O-H absorption band which was initially predominant to the hydroxyl groups of PVOH. The decrease in intensity of the bands at 1087, 845 and 1142 cm^{-1} are due to a decrease in polymer volume at the ATR crystal contact surface due to the swelling of the polymer by water. Fig. 4.23 compares the FTIR spectrum of the PVOH film before in contact with the crosslinking solution (film surface in contact with the ATR crystal) with those after 480 minutes treatment (film surface in contact with the crosslinking solution and ATR crystal) and washing and drying.

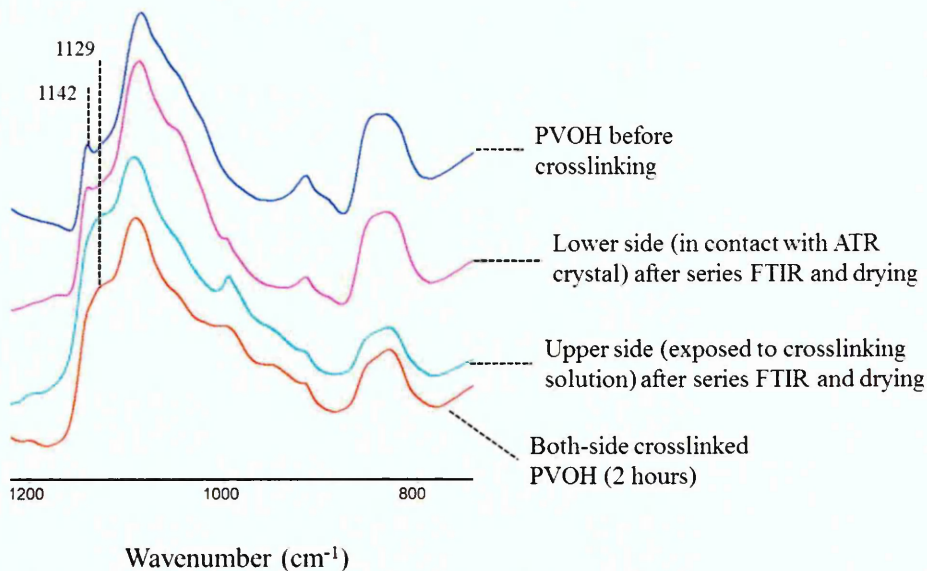


Figure 4.23 FTIR spectra of PVOH film before and after series experiment (480 minutes) in comparison with the spectrum from the both-side crosslinked PVOH31 film for 2 hours.

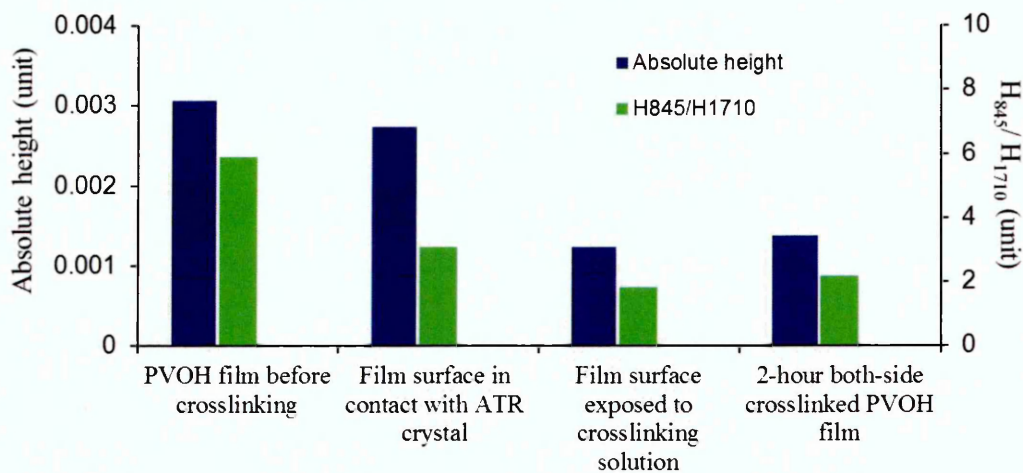


Figure 4.24 Absolute heights of the peaks located at 1142 cm⁻¹ in the second derivative FTIR spectra and peak height ratios H₈₄₅/H₁₇₁₀ of PVOH films before and after the series FTIR experiment (480 minutes) in comparison with those of the both-side crosslinked film (2 hours)

It can be observed in the spectrum of the PVOH surface in contact with the ATR crystal after treatment (pink curve) that the peak intensity at 1142 cm⁻¹ appears lower than that in the initial untreated PVOH while in the spectrum of the film directly in contact with the crosslinking solution is not clearly present. More

importantly, there is an increase in the C-O stretching band of acetal groups (1129 cm^{-1}) in the spectrum of the upper side (in contact with crosslinking solution) which is similar in intensity to that of the both-side crosslinked PVOH31 films treated for 2 hours (red curve) (see Section 3.4.7). There is also a slight increase in this region for the spectrum collected from the lower side (in contact with the ATR crystal). Although the 1142 cm^{-1} band does appear to decrease in intensity, it is not with certainty, possible to state whether there is a decrease in the crystallinity due to the overlapping band due to the C-O stretching of acetal groups. Fig. 4.24 shows that after the PVOH film experienced the series FTIR, the absolute height at 1142 cm^{-1} peak (in second derivative spectra) and H_{845}/H_{1710} decreased in both surfaces in contact with ATR crystal and the crosslinking solution, suggesting a decrease in the crystallinity of the films (see Section 3.4.7). In addition, the values of the upper side were comparable with those of PVOH films crosslinked on both sides for 2 hours.

Another series experiment using the same method but with a threefold increase in the amount of GA in the crosslinking solution was conducted. Spectra were collected every 2 minutes.

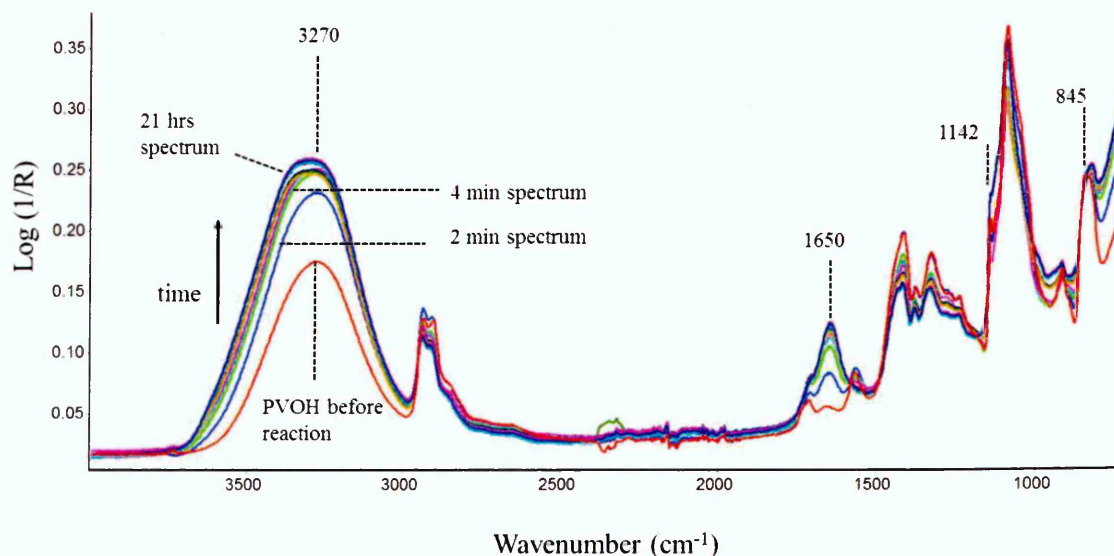


Figure 4.25 FTIR spectra collected during the diffusion of the crosslinking solution into the PVOH31 film. The GA amount in crosslinking solution was increased 3 times. The total duration was 21 hours. The spectra were collected every 2 minutes.

Fig. 4.25 shows the FTIR results from a series of spectra collected at periods up to 21 hours of reaction time. It can be observed that the penetration of the crosslinking solution into the film (or at least water) occurred very fast which is evidenced by an increase in the O-H stretching and O-H bending bands after 2 minutes. To understand how these bands changed in the spectra collected from the film surface in contact with the ATR crystal, their areas were plotted as a function of the reaction time. Fig. 4.26a shows that after the PVOH film was in contact with the crosslinking solution for 6 minutes, the areas of the O-H stretching (3650 to 2992 cm^{-1}) and bending (1691 to 1610 cm^{-1}) bands in the spectra collected from the surface in contact with the ATR crystal increased significantly, 55% and 773%, respectively and increased slowly up to ~50 minutes before the area of the O-H stretching band decreased gradually while that of the O-H bending band levelled. This indicates that at 50 minutes the crosslinking reaction between PVOH and GA started to occur on the bottom side of the film resulting in the decrease of the O-H stretching band. This happened more so when extending the exposure time between the film and the crosslinking solution. The O-H bending band, which represents only water in the film, was unchanged after 50 minutes and shows it reached its maximum.

For PVOH film in contact with the normal crosslinking solution (GA amount of 0.03 mol/L) in the first series FTIR (Fig. 4.22), areas of the O-H stretching and O-H bending bands were also shown to increase significantly after 6 minutes of the reaction time (Fig. 4.26b), however, they were practically unchanged up to 480 minutes. It is hard to state whether the crosslinking occurred at the surface in contact with the ATR or not as changes occurring in the O-H stretching region were found to be complex as the band is due to several overlapping bands arising from stretching vibrations of the PVOH hydroxyl groups, water penetration into the sample film and PVOH-GA interaction. However, Fig. 4.26b shows no or very small amount of crosslinking occurred at the untreated side of the film. A possible reason to explain this is that the amount of GA in the crosslinking solution was too small (0.03 mol/L) to "compete" with water during the diffusion process. When in contact with the crosslinking solution, water penetrates into the film from the top to the bottom first then the GA, suggesting that the crosslinking

reaction occurs more at the surface directly in contact with the crosslinking solution than at the surface in contact with the ATR crystal.

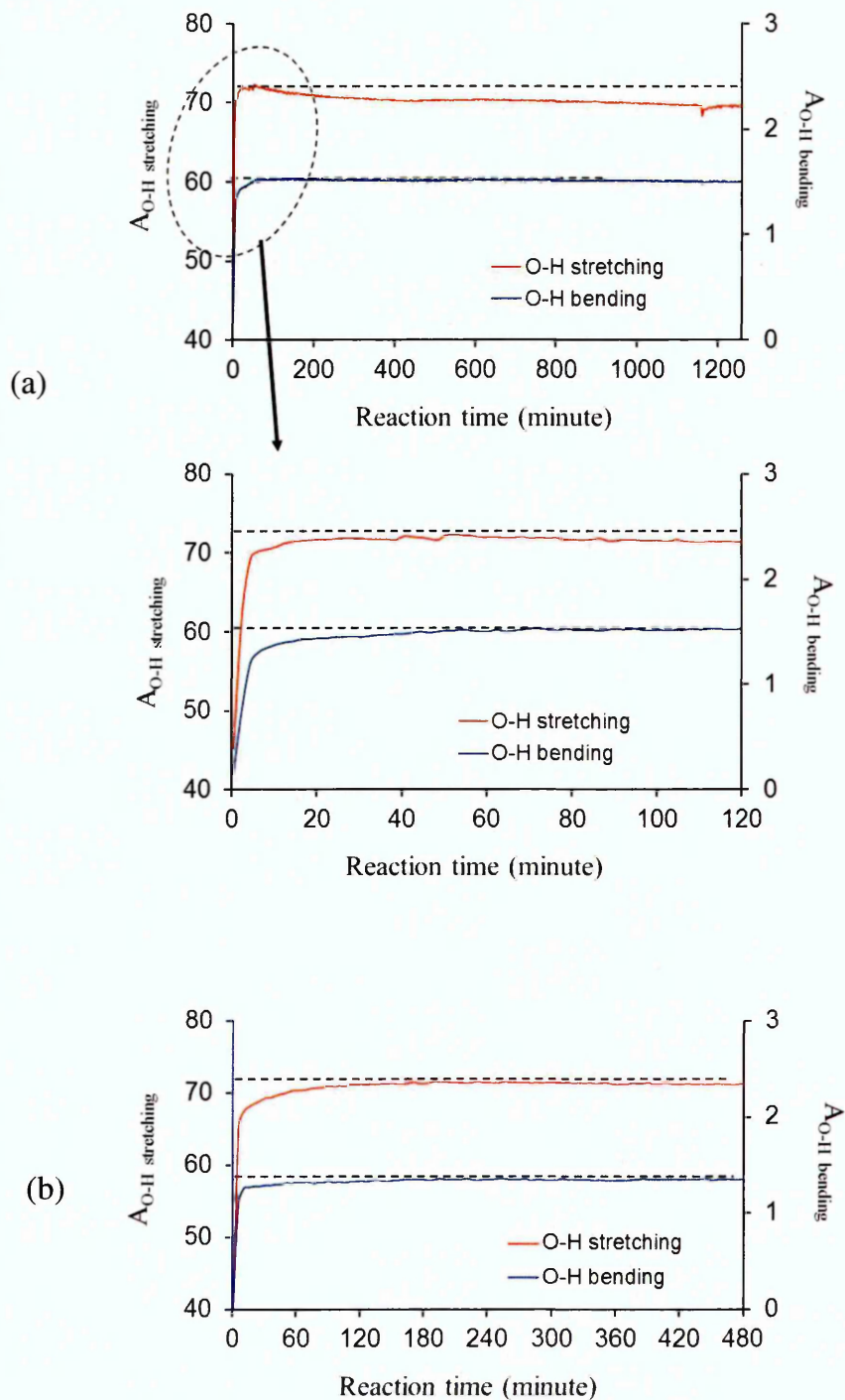


Figure 4.26 Areas of the O-H stretching and O-H bending as a function of the reaction time.

(a) Spectra were collected every 2 minutes from the film surface in contact with the ATR crystal. The amount of GA in the crosslinking solution was 3 times higher than that in the normal solution

(b) Spectra were collected every 5 minutes. The amount of GA in the crosslinking solution was 0.03 mol/L as normal

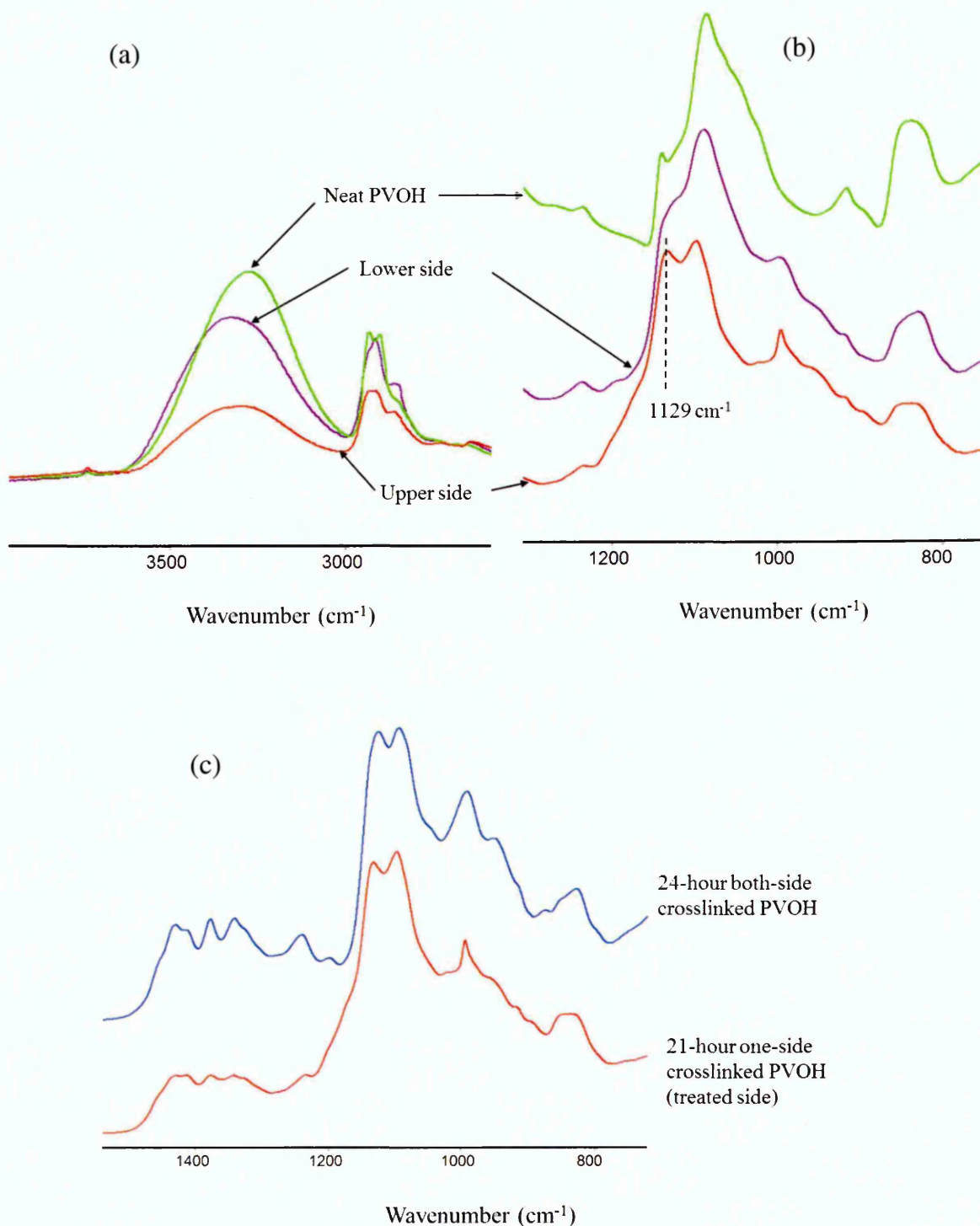


Figure 4.27 FTIR spectra collected from the PVOH films treated on one side with GA for 24 hours and subsequently washed and dried
(a) A decrease in the O-H stretching absorption and **(b)** an increase in the C-O stretching of acetal groups in the spectra of upper and lower sides of the sample film in comparison with neat PVOH.
(c) Similar absorption band at C-O stretching group between the upper side of sample film and the films crosslinked both sides for 24 hours.

The spectra collected from both sides of the film after the 2nd series experiment and washing and drying show large changes in the O-H stretching band compared to the initial PVOH (Fig. 4.27a). The decrease in the intensity of the O-H stretching band as well as the shifts to higher wavenumber in the spectra of the upper and lower sides indicate that a lot of crosslinking has occurred on both sides of the sample and that on the upper side (that in contact with crosslinking solution) is obviously more so. Further evidence to support this are the changes in the intensity of the crystallite band at 1142 cm⁻¹ and C-O stretching band at 1129 cm⁻¹ (Fig. 4.27b). The 1142 cm⁻¹ band was not visible in the spectra of upper and lower sides but could be masked by the now stronger and overlapping 1129 cm⁻¹ band. The increases in intensities of C-O stretching bands at 1129 cm⁻¹ on both sides of the sample indicate the production of acetal linkages in the films. It is also found that the absorptions of C-O stretching of acetal group were of similar intensity for the upper side spectra and the 24-hour both-side crosslinked PVOH31 (Fig. 4.27c)

It can be concluded that when in contact with one surface of the PVOH film, the crosslinking solution can diffuse from the top to the bottom of the film. Although salt present in the crosslinking solution can stop the PVOH film from dissolving in water, some water is still able to penetrate into the film followed by the GA diffusion to crosslink PVOH. The extent of crosslinking reaction is low due to its competition with water in the diffusing process. The higher the GA amount in the crosslinking solution, the more the crosslinking occurs.

4.5.2 One-side crosslinking of PVOH31

4.5.2.1 WVTR results

As can be seen in Fig. 4.28, for PVOH31 films pre-heated at different temperature, and then undergoing crosslinking treatment on only one side with GA, the WVTR values decreased significantly in comparison with those of the un-crosslinked films at the same respective annealing temperature. With 1 hour of crosslinking time, the WVTR values did slightly increase to those of lower crosslinking treatment times, however the differences were not considerable. It

can also be observed that with 1 hour of crosslinking time, films pre-treated at 40, 60, 90 and 120°C exhibited very similar WVTR values. In addition, the WVTR values were lowest for films pre-heated at 150 and 180°C but for the crosslinked films these were very similar.

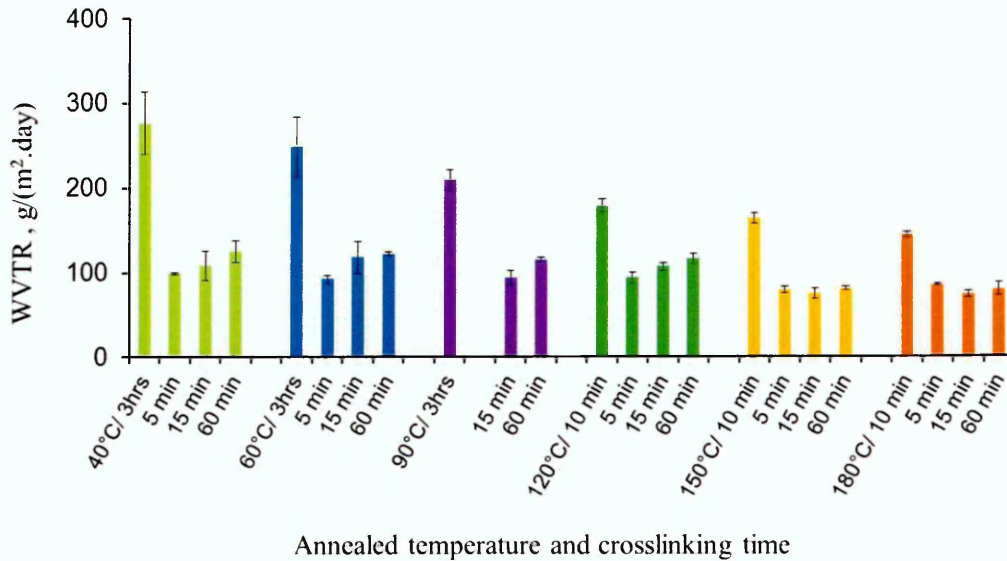


Figure 4.28 WVTR results of one-side crosslinked films at 5, 15 and 60 minutes. PVOH31 films were pre-heated at different temperatures before the crosslinking reactions with GA. The reaction temperature was 40°C.

The improvements in the water vapour barrier properties of crosslinked films are expressed as the percentage decreases in WVTR values relative to those of un-crosslinked films (Fig. 4.29). It shows that films pre-treated at 40°C for 3 hours gained the highest improvement in water vapour barrier properties, i.e. 64, 61 and 55% for films crosslinked at 5, 15 and 60 minutes, respectively. Films pre-treated at 60°C also showed a significant decrease in WVTR after crosslinking in that the WVTR values decreased to 51 and 63% with 5 and 60 minutes crosslinking, respectively. The improvement in the water vapour barrier properties after crosslinking was lowest for the films pre-heated at 120°C for 10 minutes. Films heated at 150°C showed better improvements in water vapour barrier properties after crosslinking than those heated at 180°C.

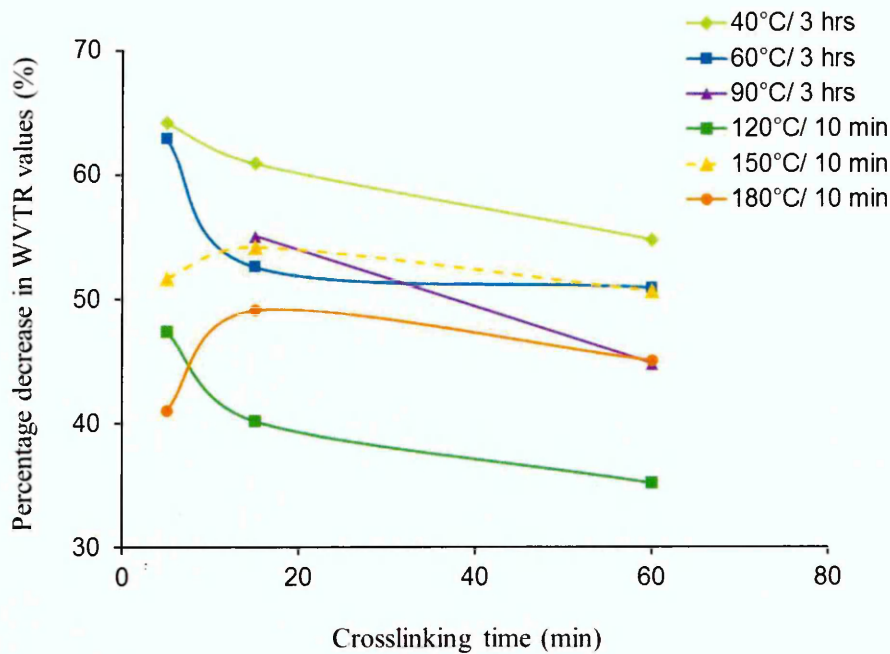


Figure 4.29 Percentage decreases in WVTR values (compared to those of un-crosslinked films) for one-side crosslinked PVOH films at different crosslinking times. Films were treated at different temperatures before the crosslinking reactions with GA

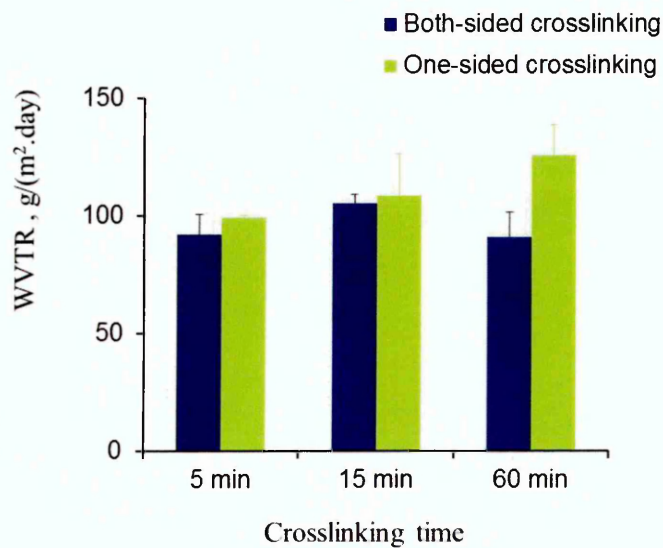


Figure 4.30 A comparison between the WVTR values of PVOH31 films crosslinked with GA on one side or both sides. PVOH31 films were pre-heated at 40°C for 3 hours before the crosslinking reaction.

Fig. 4.30 compares the WVTR values of PVOH31 films crosslinked on one side and both sides. In general, the both-side crosslinked PVOH films had better water vapour barrier properties than the films crosslinked on one side. However, the differences between WVTR values were not considerable (3-7%), except for those with 60 minutes of crosslinking, in which it was about 28% lower for the both-side crosslinked films.

4.5.2.2 Swelling test results

When placed in cold water (22°C), all the one-side crosslinked samples swelled and increased in weight. Fig. 4.31a shows that the degree of swelling decreased when the crosslinking time increased, the values were highest for films crosslinked for 5 minutes and lowest for those crosslinked for 60 minutes. For PVOH films crosslinked for 15 and 60 minutes and placed in cold water, the degree of swelling decreased gradually when the heat treatment temperatures increased. However, for the respective films crosslinked on one side for 5 minutes, the swelling degree increased slightly from 254 to 285% for films pre-heated from 40 to 60°C, then decreased gradually to 123% with 150°C pre-treatment, and increased to 210% with 180°C of heat treatment.

It was not possible to obtain the degree of swelling in hot water (90°C) for films crosslinked on one side for 5 minutes, the films heated at 40, 60 and 90°C prior to crosslinking became a soft gel and were easily broken and stuck to the blotting paper. Those treated at 120, 150 and 180°C before the crosslinking reaction either dissolved partially, majorly or completely, respectively. With films crosslinked for 15 minutes and placed in hot water, only those pre-heated at 150 and 180°C became a soft gel and stuck to the blotting paper tissue, no results are shown for these samples. The degree of swelling in hot water for the one-side crosslinked PVOH films described in Fig. 4.31b are higher than those in the cold water. As in the cold water test, the degrees of swelling for films crosslinked for 15 minutes were higher than those crosslinked for 60 minutes. It can be observed that unlike the swelling properties in cold water, the swelling degrees of the 60

minutes crosslinked films increased when the treatment temperature prior to crosslinking increased.

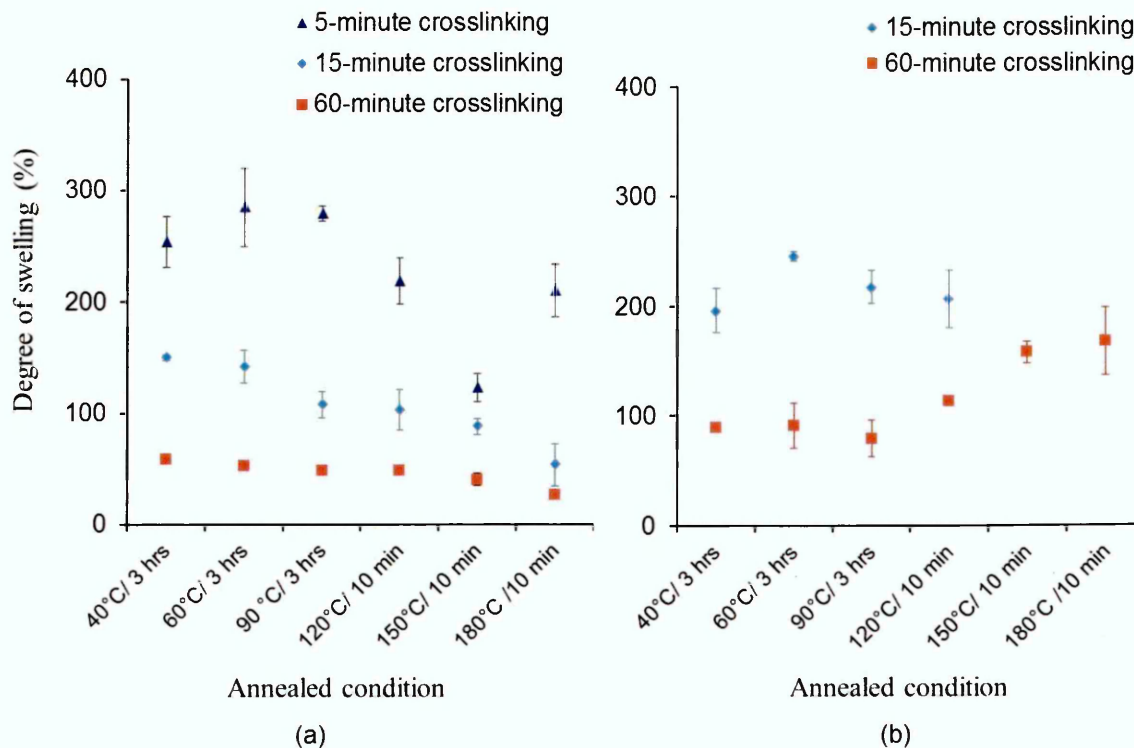


Figure 4.31 Degree of swelling in water at (a) 22°C and (b) 90°C for one-side crosslinked PVOH films. PVOH films were pre-heated at different temperatures prior to the crosslinking reaction.

When comparing both-side crosslinked PVOH31 films with those crosslinked on one side, the latter always exhibited higher degrees of swelling when placed in either cold or hot water (Fig. 4.32). When placed in hot water, the films crosslinked on one side for 5 minutes deformed and turned into a soft gel while the both-side crosslinked films swelled (an increase in weight of ~324%) but maintained their shape.

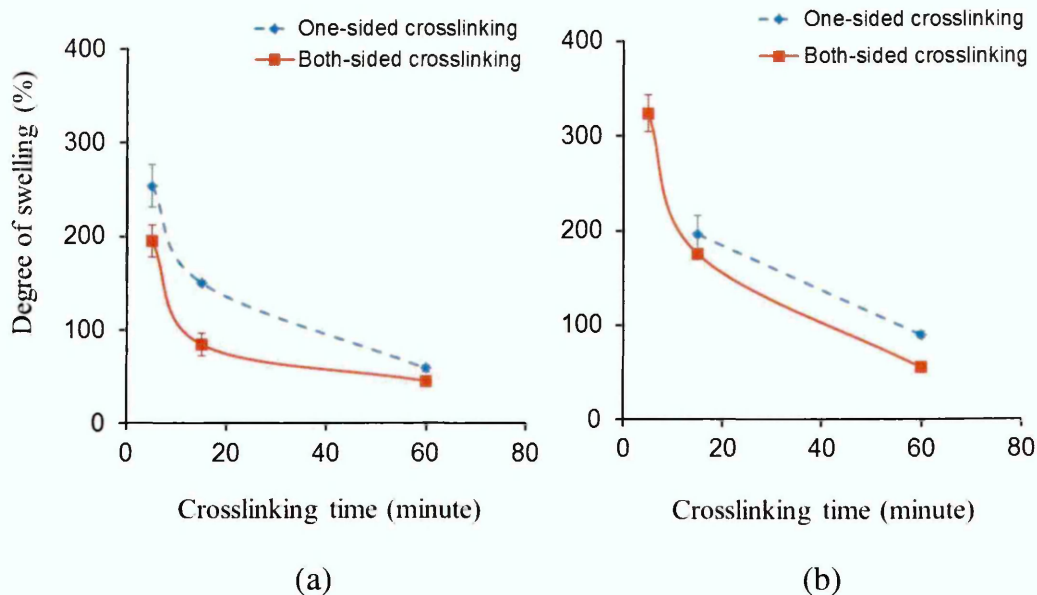


Figure 4.32 Comparisons between the degrees of swelling in (a) cold water (22°C) and (b) hot water (90°C) of both-side and one-side crosslinked PVOH31 films. Films were heated at 40°C for 3 hours prior to the crosslinking reaction

4.5.2.3 FTIR results

In Chapter 3 (Section 3.4.7), the differences in the FTIR spectra of PVOH films before and after crosslinking were described. The decreases in the peaks representing O-H stretching ($3000\text{-}3600\text{ cm}^{-1}$), C-C stretching (or the crystalline peak, 1142 cm^{-1}), and the C-C skeleton bending (845 cm^{-1}) or the increase in the C-O stretching (1129 cm^{-1}) of acetal groups were the main changes observed in the crosslinked films. For the one-side crosslinked films, similar changes were also observed in the spectra collected from the treated side. However, whether these changes were obvious or not depended on the annealing temperature prior to crosslinking and crosslinking time. Take the films heated at 40°C before crosslinking as an example. Since changes occurring in the O-H stretching region were complex due to the multiple contributions from the stretching vibrations of the PVOH hydroxyl groups, the water present in the film and the PVOH-GA interaction, the spectral range from $800\text{ to }1200\text{ cm}^{-1}$ was investigated.

Fig. 4.33 shows that the C-O stretching band at 1129 cm^{-1} was not clearly present in 5 minutes crosslinked spectra. The spectra in the region between $800\text{-}1200\text{ cm}^{-1}$ collected from the treated side of films crosslinked on one side for 15 minutes or 1 hour were quite similar to those collected from the both-side crosslinked films with the same respective crosslinking times. It can be observed the intensities of the 1142 cm^{-1} peak in the spectra collected from the treated sides always appeared lower than those from the un-treated sides. This peak was almost unresolved in 60-minute crosslinked film. As the crosslinking reaction was accompanied by a decrease in the intensity and overlapping of the 1142 cm^{-1} peak by the increasing of the 1129 cm^{-1} peak, it can be inferred the crosslinking did happen moreso on the film surface in contact with the crosslinking solution. Extending the crosslinking time from 5 to 60 minutes resulted in the gradual increase in the 1129 cm^{-1} peak (although only apparent as a shoulder) leading to it almost completely overlapping the 1142 cm^{-1} peak. However, from the spectra collected from the untreated surfaces it could not tell whether the crosslinking occurred for the 5 and 15 minutes crosslinked films, though it is more obvious to occur on the untreated side of the film in contact with the crosslinking solution for 60 minutes. Similar changes were observed in the spectra collected from the one-side crosslinked films of samples pre-heated at 60°C and 90°C prior to crosslinking.

The crystallinity induced in the films pre-heated at 150 and 180°C was retained after one-side crosslinking as evidenced by the sharpness and intensity of 1142 cm^{-1} peaks in the respective spectra from treated and untreated sides (Fig. 4.34). This was still the case for the sample undergoing 60 minutes of crosslinking time though the intensities of the 1142 cm^{-1} peak were slightly lower than those in the un-crosslinked films indicating that the crosslinking reaction had slightly reduced the crystallinity. These results indicate that there was very little crosslinking on the treated side of the films annealed at 150 and 180°C . The spectra collected from treated and untreated films annealed at 120°C and subjected to crosslinking for 60 minutes were similar to the respective films annealed at 90°C , but the 1142 cm^{-1} peak in the spectrum from the treated side of the film annealed at 120°C was more intense.

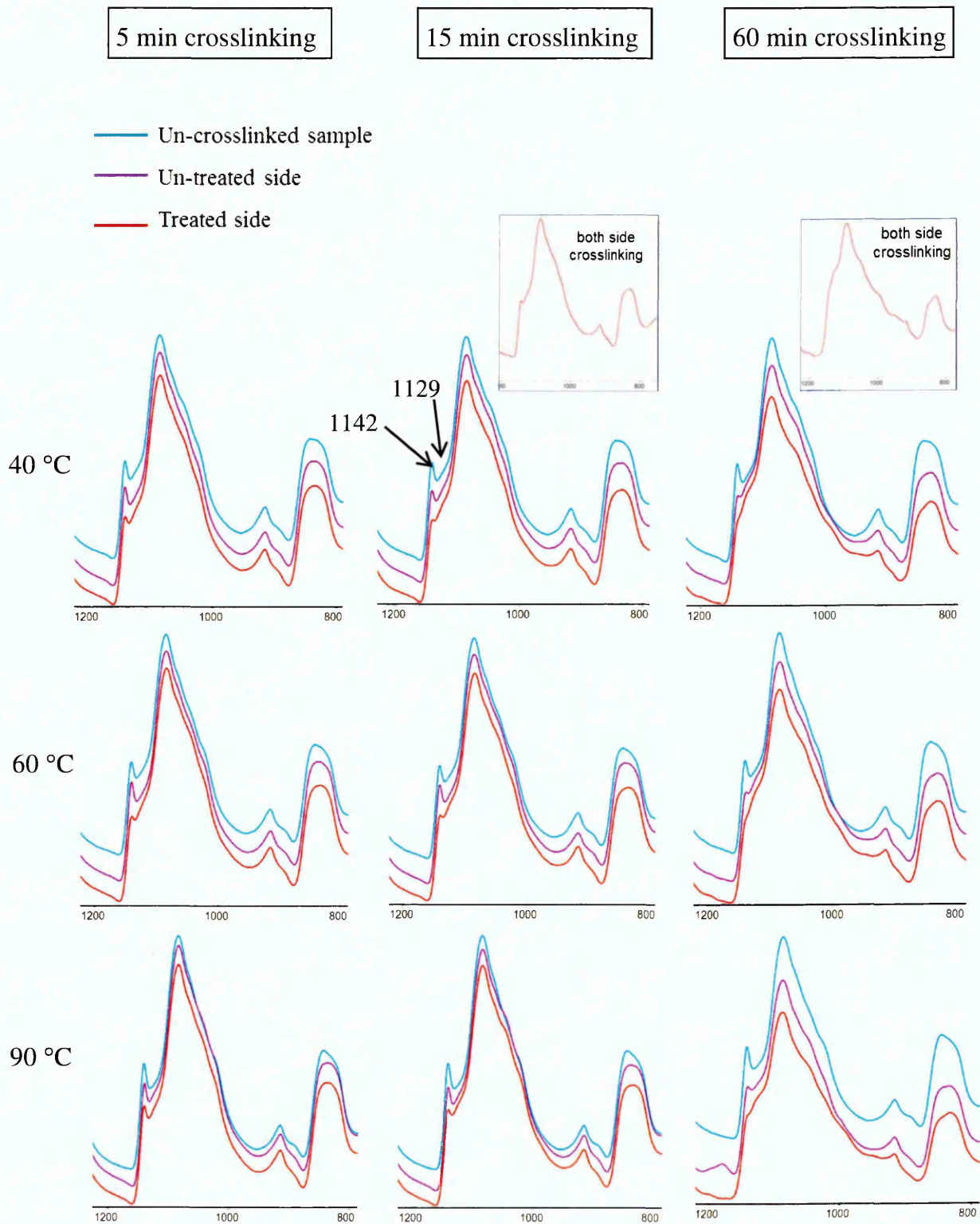


Figure 4.33 Changes in the 1142 and 1129 and 845 cm^{-1} peaks in the FTIR spectra of treated and un-treated side in comparison with those of un-crosslinked samples when PVOH films were one-side crosslinked with GA. Films were pre-heated at 40, 60 and 90 °C for 3 hours before crosslinking

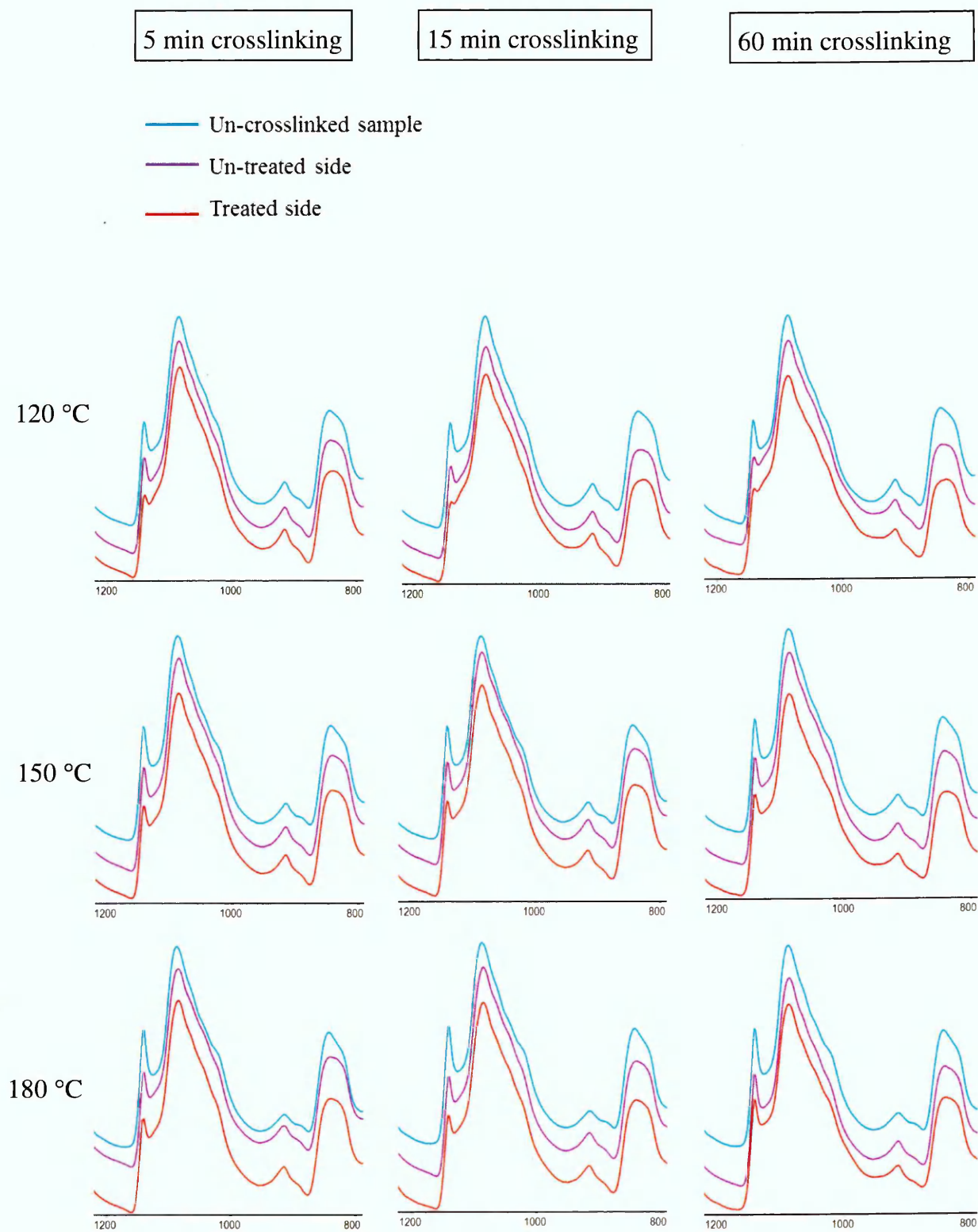


Figure 4.34 Changes in the 1142 and 1129 and 845 cm^{-1} peaks in the FTIR spectra of treated and un-treated side in comparison with those of un-crosslinked samples when PVOH films were one-side crosslinked with GA. Films were pre-heated at 120, 150 and 180 °C for 10 minutes before crosslinking

To compare the changes in crystallinity of the films after crosslinking and between different pre-heated temperatures, the absolute heights of the 1142 cm^{-1} peak in the second derivative spectra were accessed (Fig. 4.35). It is clear to see that the peak heights for the un-treated sides are higher than those for the respective treated sides. As the crosslinking time increased, the intensities decreased for films pre-heated at 40 and 90°C indicating lower crystallinity in the highly crosslinked films. For films annealed at 180°C prior to one-side crosslinking, the differences in the peak intensities between the different crosslinking times were not significant for both treated and untreated sides. It is noted that the data in Fig. 4.35 is within the error, but it is difficult to image that the films heated at 180°C prior to one-side crosslinking undergo a decrease in crystallinity after one side crosslinking. This is due to the FTIR spectra of un-crosslinked films were collected after the films were annealed, i.e. very high crystallinity.

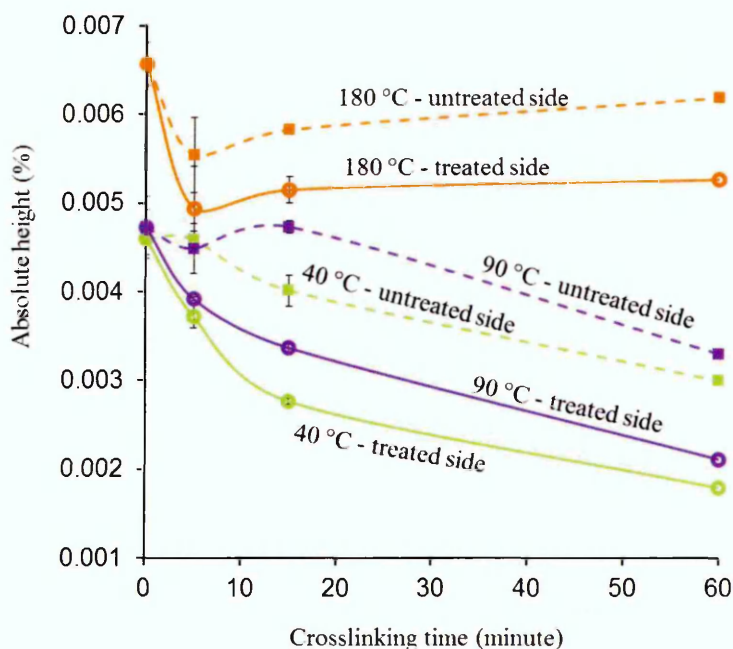


Figure 4.35 Changes in the absolute heights of the peaks located at 1142 cm^{-1} in the second derivative FTIR spectra of the films crosslinked with GA on one side. Films were pre-heated at 40 , 90°C for 3 hours and 180°C for 10 minutes prior to the crosslinking reaction. FTIR spectra were taken from both sides of the one-side crosslinked films (i.e. treated and untreated)

Changes in the C-C skeleton bending bands (around 845 cm^{-1}) were also observed after the one-side crosslinking reaction with a decrease in intensity and a shift to 825 cm^{-1} indicating more amorphous zones being present [99]. At low pre-heated temperatures ($40\text{-}90^\circ\text{C}$), the changes were obvious at 60 minutes of crosslinking time while they were not as pronounced in the spectra of the one-side crosslinked films which were annealed at higher temperatures (120 to 180°C) prior to crosslinking.

4.5.2.4 Raman results

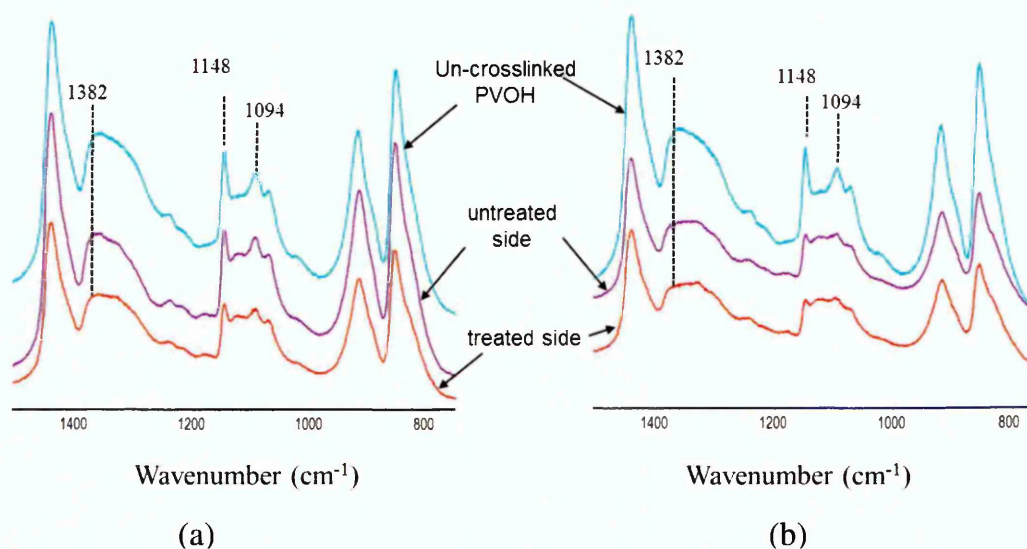


Figure 4.36 Changes in the Raman spectra of PVOH films crosslinked on one side for (a) 15 minutes (b) 1 hour. Films were pre-heated at 40°C for 3 hours before crosslinking

Some changes occur in the Raman spectra (region $1400\text{-}600\text{ cm}^{-1}$) after PVOH film is crosslinked with GA (Fig. 3.23, Section 3.4.8), including the appearance of 4 bands in the C-H and O-H bending region (1382 , 1348 , 1331 and 1302 cm^{-1}), the decreases in the intensities of the peaks at 1148 cm^{-1} (C-O-C stretching), 857 and 922 cm^{-1} (C-C stretching). An increase in intensity and a shift to the higher wave number of the 1224 cm^{-1} peak is also taken into account. Raman spectra of PVOH films crosslinked on one side (Fig. 4.36) shows that there was a decrease in the intensities of the crystalline peaks at 1148 and 1094 cm^{-1} on treated and

untreated sides of the samples pre-heated at 40°C for 3 hours suggesting a decrease in the crystallinity. The decrease was higher in the sample crosslinked for 60 minutes. The shapes of the broad band between 1382 and 1300 cm^{-1} in the spectra collected from the treated and untreated sides of the 60-minute crosslinked films slightly changed compared to those of uncrosslinked films, specifically, a visible peak at 1331 cm^{-1} was observed in the spectra of the treated side. These changes indicated that crosslinking occurred on both sides of film crosslinked on one side for 60 minutes accompanied by a decrease in crystallinity. For those crosslinked on one side for 15 minutes, the crosslinking can be observed in the Raman spectrum of the treated side whilst it is hard to tell if it occurred on the untreated side.

For films heated at 180°C (Fig. 4.37), after being crosslinked on one side for 1 hour, the crystallite peaks at 1148 and 1094 cm^{-1} were still very sharp on the spectra of both sides indicating the retainment of the crystallinity in the films which are in agreement with the FTIR results.

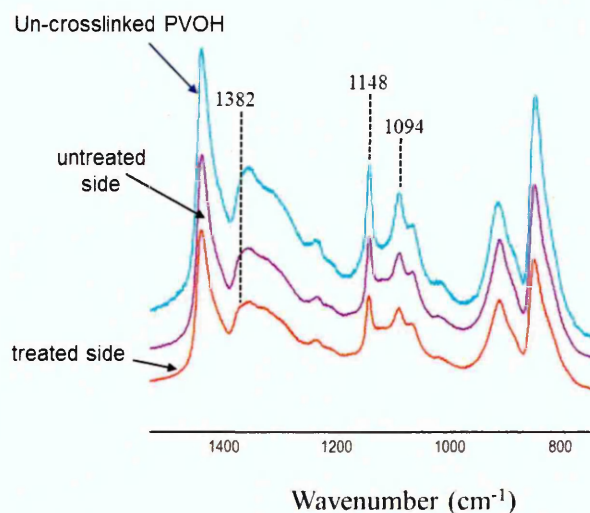


Figure 4.37 Changes in the Raman spectra of PVOH films crosslinked on one side for 60 minutes. Film was annealed at 180°C for 10 minutes prior to crosslinking

4.5.2.5 Discussion

The diffusion of the crosslinking solution into the PVOH films was investigated by ATR-FTIR. The results showed that water in the crosslinking solution could penetrate into the film and diffuse through to the other side very quickly, which were followed by the crosslinking reaction at the lower surface (that in contact with ATR crystal).

When crosslinking occurs, the O-H groups of PVOH are consumed by GA to create crosslinks which possess the ability to resist the transfer of water vapour leading to a decrease in WVTR values and swelling by water. The WVTR results showed that the one-side crosslinked PVOH films had comparable water vapour barrier properties to those of both-side crosslinked films (Fig. 4.30). When films were pre-heated at different temperatures, the crosslinking reactions occurred to a higher extent in films treated at low temperatures (40, 60, 90°C for 3 hours) than in those treated at higher temperatures (120, 150 and 180°C for 10 minutes) as evidenced by the FTIR spectra in Figs. 4.33 and 4.34. This was described as being related to the different degrees of crystallinity in the films before crosslinking. The effects of annealing on the crystallinity of PVOH31 films were discussed in Section 4.3 and it was found that the degree of crystallinity increased when the annealing temperatures increased as evidenced by FTIR (Fig. 4.8), Raman (Fig. 4.11) and XRD results (Fig. 4.12). Therefore, films treated at low temperatures prior to the one-side crosslinking reactions had lower degrees of crystallinity than those treated at high temperatures, which made it easier for the crosslinking solution to diffuse and penetrate into the films and ultimately crosslink with more O-H groups. This can explain why the improvement in the water vapour barrier properties for films treated at 40°C after one-side crosslinking was higher than those treated at higher temperatures (Fig. 4.29)

Both crosslinks and crystallinity contribute to the water and water vapour resistance of the films. The WVTR results in Fig. 4.28 showed that the water vapour barrier properties of one-side crosslinked films which were annealed at 150 and 180°C prior to crosslinking were higher than the respective films pre-heated at 40 and 60°C. Moreover, the FTIR and Raman results (Figs 4.33, 4.34

and 4.37) showed a lower level of crosslinking in films heated at high temperatures. This indicated that the water vapour barrier properties in the crosslinked films of those annealed at 150 and 180°C were mainly contributed to by the crystallinity of the films. The swelling test results in hot water also confirm this argument. When the films crosslinked for 5 minutes and pre-treated at 120, 150 and 180°C were placed in hot water (90°C), they dissolved partially, majorly or completely, respectively but for those treated at lower temperatures (40, 60 and 90°C), the respective crosslinked films became swollen and formed gels. Due to the high retainment of crystallinity in the films annealed at higher temperatures (120, 150 and 180°C) prior to crosslinking, fewer crosslinks were produced. When the films crosslinked on one side for 5 minutes were placed in hot water, the present crystallites dissolved making the films dissolve. The same reason was also applied to the films crosslinked for 15 minutes and annealed at 150 and 180°C since they became swollen in water and formed a gel sticking to the blotting paper. In the low-temperature treated films, more crosslinks were produced and supported their stability in water, i.e. did not dissolve. However, this stability was not perfect since the crosslinking occurred mainly on one side of the films which made the films easily broken and stuck to the blotting paper compared to shape retainments of the respective films in the case of both-side crosslinking (Section 3.4.5). It also resulted in the degrees of swelling in water of the one-side crosslinked films higher than those of the both-side crosslinked films (Fig. 4.32).

With 1 hour of treatment time, all the one-side crosslinked films simply swelled in hot water indicating that the crosslinking occurred effectively to protect the films from dissolution. The increase in the swelling of films annealed at high temperatures (120 to 180°C) (Fig. 4.31) indicated fewer crosslinks were present in comparison with those annealed at lower temperatures, they did possess higher crystallinity but in hot water, the crystallites were dissolved.

To summarise, the one-side crosslinking improved the water vapour barrier properties of the PVOH films such that they were comparable to those of the both-side crosslinked films. The one-side crosslinking reactions occurred more

effectively in the films annealed at low temperatures than those heated at higher temperatures (120, 150 and 180°C) due to the higher crystallinity in the latter films which hindered the penetration of the crosslinking solution. In addition, although the crosslinked films prepared at the high annealing temperatures prior to crosslinking contained fewer crosslinks in their structures, their water vapour barrier properties were higher which was ascribed by a more dominant contribution from the crystallinity of the films.

4.6 CONCLUSION

Heat treatment is an effective method to improve the water vapour barrier properties of PVOH films, thanks to the increase of the film crystallinity after annealing. The higher the treatment temperature, the lower the water vapour transmission rates and the swelling in water. The crosslinking reaction on one side of PVOH films could improve their water and water vapour barrier properties, which were very comparable to those of the both-side crosslinked films. However, the one-side crosslinking used less crosslinking solution volume than for the both-side crosslinking which helps to reduce the cost. A combination between the one-side crosslinking with GA and heat treatment can produce crosslinked films with better water vapour barrier properties than those just under heat treatment. In addition, crosslinked films of low treatment time (5 minutes) were able to dissolve in water which may contribute to the degradability of the crosslinked system.

Between PVOH films of two different molecular weights, PVOH124 exhibited higher water vapour resistance but poorer crystallinity compared to PVOH31. This was due to fewer chain ends and longer molecular chains present in the PVOH124 films, which reduced free volume (which can be related to better water vapour barrier properties) and lower degree of crystallinity, respectively. After annealing, PVOH124 films had higher crystallinity and better water vapour barrier properties. When crosslinking with GA, the PVOH124 films also exhibited higher water vapour barrier properties than crosslinked PVOH31 films.

After crosslinking, PVOH124 films annealed at 90°C showed the poorest water vapour resistance when compared with crosslinked films of PVOH124 annealed at 40°C and 180°C. PVOH124 films heated at 180°C showed the highest crystallinity and the lowest WVTR values whether crosslinked or un-crosslinked, the major contribution to these properties was believed to be due to the crystallinity of the films.

The incorporation of bentonite and plasticiser into poly(vinyl alcohol) films and subsequent chemical crosslinking

In this chapter, the addition of bentonite on the properties of PVOH films in terms of water vapour barrier properties and mechanical properties are reported. In addition, the crosslinking reaction between PVOH/Clay films and GA was also investigated.

Flexible films are often necessary in packaging. To improve the flexibility of PVOH films as well as to overcome the brittleness of PVOH/Clay films, a plasticiser is used. The effects of plasticiser on the properties of PVOH and PVOH/Clay films (10 wt% clay) were investigated. In addition, the crosslinking reactions between GA and the films containing a plasticiser are also reported.

5.1 EXPERIMENTAL

5.1.1 PVOH/Clay film preparation

The bentonite (NaMMT) used in this report was Closite[®] Na⁺ purchased from Southern Clay Products and used as received. The bentonite is predominantly sodium montmorillonite and has a cation exchange capacity value of 92.5 meq/100g.

For PVOH/Clay film preparation, firstly, a desired amount of clay was added to a round-bottom flask (RBF) containing water. The clay suspension was then mixed vigorously using a magnetic stirrer bar at room temperature. After 2 hours, PVOH granules ($M_w = 31,000-50,000$, 98-99% hydrolysed) were gradually added to the clay suspension and the temperature increased to 90°C. Stirring was continued vigorously at 90°C for a further 4 hours. Then films were cast in Petri dishes and dried at room temperature for 48 hours.

A denotation for PVOH/Clay film is NaCF.

5.1.2 PVOH/PEG and NaCF10/PEG films preparation

The concentration of each component used was based on the total solid content. Here, the plasticiser was kept constant at 20 wt% and NaMMT at 10 wt% of the dry films. Hence the denotation NaCF10/PEG represents a PVOH film containing 10 wt% clay and 20 wt% PEG.

For PVOH/PEG film preparation, a desired amount of PVOH (98-99% hydrolysed, $M_w = 31,000-50,000$, melting point = 200°C and density = 1.26 g/cm³) was added to a round-bottom flask (RBF) containing water at a weight ratio of 1:20 (PVOH : water). The mixture was stirred using a magnetic flea at 90°C for 1 hour before poly(ethylene glycol) (PEG, liquid, $M_w = 400$, melting point = 4 - 8°C, $d = 1.126$ g/mL) was added into the solution. Stirring was continued at 90°C for a further 5 hours. Films were then cast in Petri dishes and dried at room temperature for 48 hours.

To prepare NaCF10/PEG film, a desired amount of NaMMT was stirred vigorously with water in a beaker at room temperature for 2 hours. Concurrently, PVOH was dissolved in water contained in a round-bottom flask at 90°C using a magnetic flea. After 1 hour, PEG was added into the PVOH solution and the stirring continued for another 1 hour before the clay suspension was incorporated into the mixture and kept stirring vigorously at 90°C for a further 4 hours. Finally, the films were cast in Petri dishes and dried at room temperature for 48 hours.

The dry films with thickness varying from 50-60 μm were stored in a closed container at room temperature.

5.1.3 Crosslinking reaction of PVOH/Clay, PVOH/PEG and NaCF10/PEG films

Like the crosslinking reaction of PVOH films (Chapter 3), an aqueous crosslinking solution was prepared which contained GA, sulphuric acid and sodium sulphate at a ratio of 1:5:32 in molarity. Before the crosslinking reaction, all the films were dried at 40°C for 3 hours to release the majority of physisorbed water. The dry films were then immersed in the crosslinking solution which was

also at 40°C. The molar ratio between PVOH repeat units and GA was kept at 4:1. After specified lengths of time, the crosslinked films were taken out of the crosslinking solution, thoroughly washed with water and then washed with acetone. Finally, films were dried in an oven at 40°C for 48 hours.

5.2 CHARACTERISATION

The instrumental set up for sample characterisations in this chapter were described in detail in Section 2.2, Chapter 2. Table 5.1 briefly describes the sample preparations undertaken before each type of characterisation.

Table 5.1 Characterisation methods and sample preparations

No.	Techniques	Sample preparation
1	Water vapour transmission rate (WVTR)	- Before measurements, samples were conditioned in a humidity chamber set at 23°C and 85% RH for at least 20 hours before measurement (i.e. after which no change in weight was observed)
2	Swelling test	- Samples were cut into squares (2.5 x 2.5 cm) and immersed in water for 24 hours
3	Contact angle measurement (CA)	- Samples were stored in a sealed container at room temperature after film preparation
4	Fourier transform infrared spectroscopy (FTIR)	- Samples were dried at 40°C in an oven overnight before their spectra were collected.
5	Raman spectroscopy	- Samples were stored in a sealed container at room temperature after film preparation
6	X-ray diffraction	- Samples were dried at 40°C in an oven overnight before analysis
7	Dynamic mechanical analysis (DMA)	- Samples were cut into rectangular strips. Measurement areas were 4-5 mm width and 6-7 mm length. - Samples were dried at 40°C in an oven overnight before measurements

5.3 EFFECT OF BENTONITE ON THE PROPERTIES OF PVOH FILMS

The incorporation of NaMMT into PVOH films is believed to improve its water vapour barrier and mechanical properties [62,64,111]. In this study, three amounts of NaMMT were investigated, namely, 5, 10 and 20 wt% of the total solid content of which the denotations were NaCF5, NaCF10 and NaCF20, respectively. The PVOH/Clay films were clear, but slightly more opaque than the neat PVOH films. In addition, the higher the clay content, the more brittle the film became when handled.

5.3.1 WVTR results

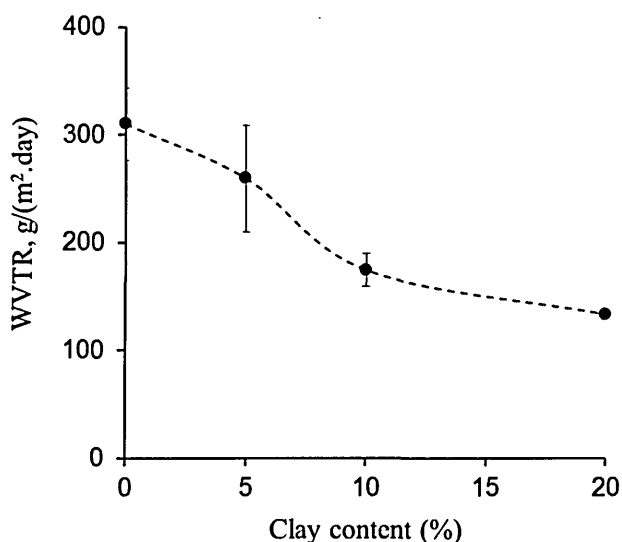


Figure 5.1 WVTR results (23°C and 85% RH) of PVOH and PVOH/Clay films as a function of clay content

When NaMMT was incorporated into the PVOH films, the water vapour barrier properties improved significantly and increased with higher clay content. It can be observed in Figure 5.1 that with 5 and 10 wt% clay loading, the improvements were about 16.3 and 43.7%, respectively. With a loading of 20 wt% clay, the WVTR value was 133.2 g/(m²·day) which was about 57% lower than that of neat PVOH film. The improvement in water vapour barrier properties when clay was present was in agreement with Mahdavi *et al.* [118]. The authors showed that

when 23 and 54 wt% MMT were loaded into PVOH films ($M_w = 85,000-146,000$), the WVTR values (at 35°C and 35% RH) decreased from 550 g/(m².day) (neat PVOH films) to 400 and 180 g/(m².day), respectively. It can be seen that with similar clay amount loaded into the films (20 wt% for herein PVOH films and 23 wt% for Mahdavi's films), the improvement in water vapour barrier properties of PVOH films herein (57%) was higher than that of Mahdavi's films (27%). While herein data show that the water barrier properties increased with increasing clay contents in the PVOH films, Yeh. *et al.* [117], on the contrary, reported an increase in clay amount could lead to a decrease in water vapour barrier properties. According to the authors, the WVTR values decreased from 440 g/(m².day) for neat PVOH film ($M_w = 50,000-55,000$, fully hydrolysed) to 250 g/(m².day) for films containing 1-3 wt% MMT while increasing the clay content to 5% and above led to an increase in WVTR values (> 350 g/(m².day) which was ascribed to the microphase separation between PVOH and clay.

5.3.2 Water contact angle results



Figure 5.2 Water droplet shapes on the surface of PVOH and top surface of NaCF10 films. The images were taken immediately after the liquid was dropped on the film surfaces

Fig. 5.2 shows that the water wettability of the PVOH film was higher than that of the NaCF10 films as evidenced by the lower contact angles values (see also Fig. 5.3). This is in agreement with Lim *et al.* [179] who reported an increase in the water contact angle of PVOH/NaMMT relative to PVOH film ($M_w = 74,800$, 98.0-99.5% hydrolysed) when increasing the clay contents up to 5 wt%.

However, a decrease in water contact angle was recorded by Pique *et al.* [151] in which they obtained a value of $34 \pm 2^\circ$ for PVOH/NaMMT 4 wt% in comparison with $57 \pm 1^\circ$ for neat PVOH film ($M_w = 85,000-124,000$, 88% hydrolysed). As demonstrated in Fig. 5.3, the contact angle values decreased linearly with the time from the moment the liquid touched the film surface. At 30 seconds after the water liquid was dropped on the film surface, the contact angle values were $51.4 \pm 9.3^\circ$ and $67.3 \pm 3.4^\circ$ for neat PVOH and NaCF10 films, respectively.

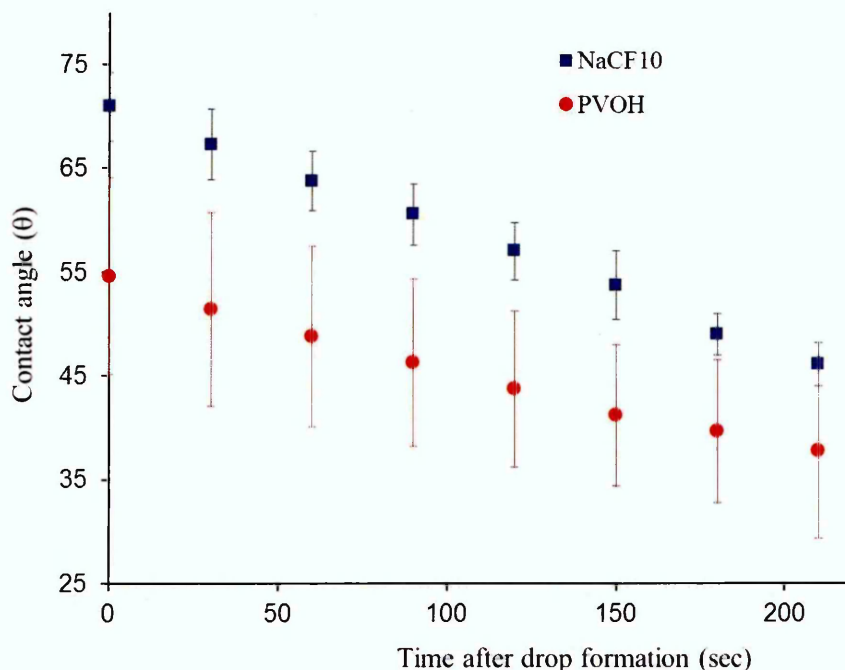


Figure 5.3 Water contact angles of PVOH and NaCF10 versus time after drop formation. The drop type was sessile and the testing atmosphere was 20-22°C and atmospheric humidity. Each value was a mean of 5-10 measurements at the same condition.

5.3.3 FTIR results

Fig. 5.4 shows FTIR spectra in the range of $4000 - 600 \text{ cm}^{-1}$ for NaMMT powder, neat PVOH film and PVOH/Clay film containing 5 wt% clay. For PVOH/Clay film, the spectra from both surfaces were collected, the bottom surface was the interface between the film and Petri dish. The assignments for the absorption bands in the spectrum of NaMMT are described in Table 5.2 which are referenced from the literature [180-186]. When 5 wt% NaMMT was incorporated

into PVOH, the 1087 cm^{-1} absorption band, assigned to the C-O stretching in the neat PVOH films, shifted to lower frequency (1083 and 1072 cm^{-1} for top and bottom spectra, respectively). Furthermore, the 986 cm^{-1} peak assigned to characteristic Si-O stretching of clay shifted to higher frequency (1045 cm^{-1}) in both spectra collected from the top and bottom surfaces of NaCF5 film. These changes indicate a strong interaction between PVOH and NaMMT.

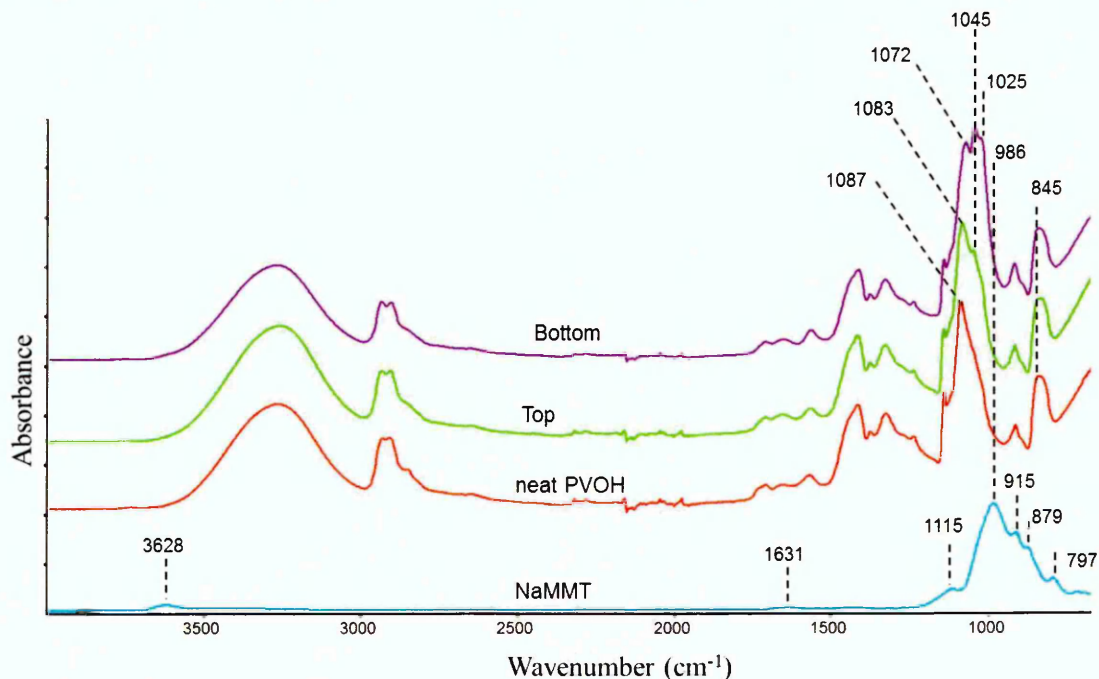


Figure 5.4 ATR-FTIR spectra of NaMMT, neat PVOH and both sides of NaCF5 films in which the bottom side is the interface between the Petri dish and the NaCF5 film.

Table 5.2 Characteristic absorption bands in the ATR-FTIR spectrum of NaMMT

Wavenumber (cm^{-1})	Assignments
3628	O-H stretching of AlOH and SiOH
1631	O-H bending of absorbed water
1115	Si-O stretching (out-of-plane)
986	Si-O stretching
915	Al-Al-OH bending
879	Al-Fe-OH bending
797	Al-Mg-OH bending

There were also differences in the absorption bands in the region 1200 - 800 cm^{-1} when comparing the spectra from the top and bottom surfaces of the NaCF5 film. The prominent 1045 cm^{-1} and 1025 cm^{-1} peaks in the spectrum collected from the bottom surface of the PVOH/Clay film, ascribed to the Si-O stretching bands [117], indicates more clay was present at the bottom surface of the PVOH/Clay film.

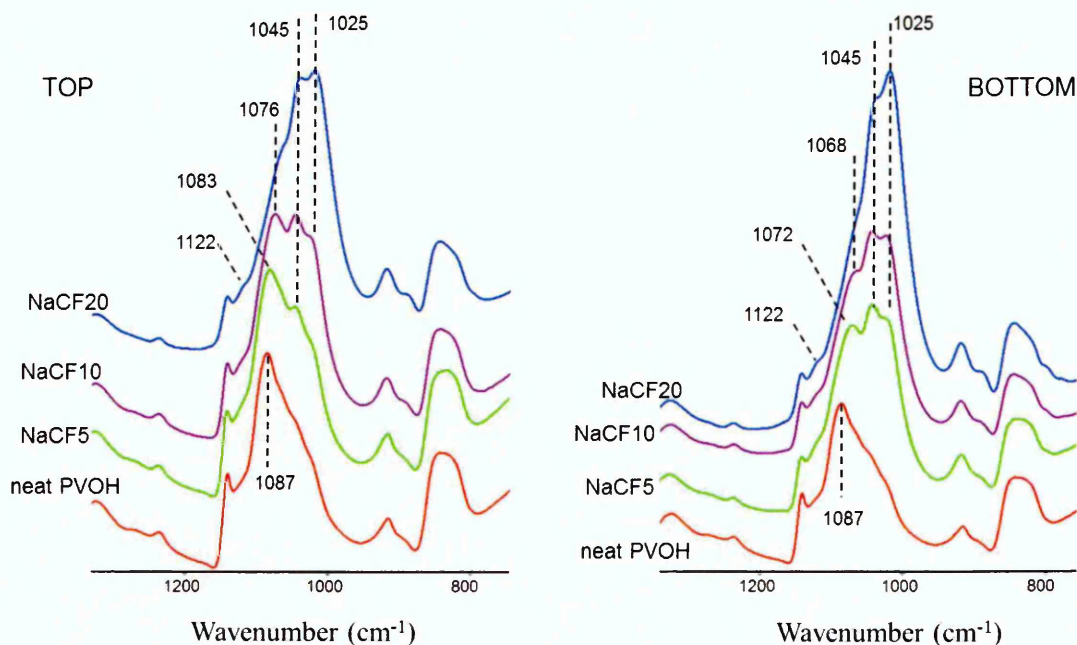


Figure 5.5 ATR-FTIR spectra of PVOH/Clay films with different clay contents. The spectra of PVOH/Clay films were collected from both sides of the films, of which the bottom side was the interface between the PVOH/Clay film and the Petri dish

Similarly, increasing the clay contents in the PVOH films resulted in a gradual shift of the C-O stretching to a lower frequency as well as increases in the intensity of the Si-O stretching at 1045 cm^{-1} and 1025 cm^{-1} (Fig. 5.5). Additionally, the shift of the C-O stretching band to lower frequency was enhanced in the spectra of the bottom surfaces compared to those from the top surfaces of the PVOH/Clay films. For example, in the spectra collected from the top surfaces, the 1087 cm^{-1} peak shifted to 1083 and 1076 cm^{-1} when clay concentration increased from 5 to 10 wt%, respectively; whereas, this peak

shifted to 1072 and 1068 cm^{-1} with the respective clay contents in the spectra collected from the bottom sides of the PVOH/Clay films. This peak was almost unresolved in the spectrum of NaCF20 due to the dominance of the Si-O stretching band due to the higher clay content.

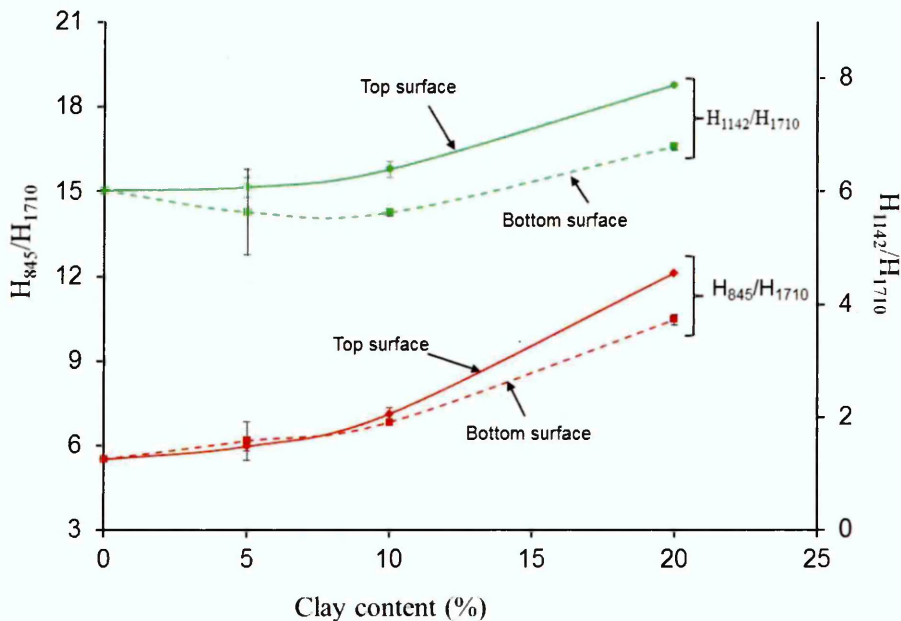


Figure 5.6 Peak height ratios H_{845}/H_{1710} and H_{1142}/H_{1710} in the FTIR spectra collected from the top and bottom surfaces of PVOH/Clay films as a function of clay content (error bars are present for all data points and some are hidden by the data meters)

The absorption bands at 1142 and 845 cm^{-1} have been reported to be proportional to the degree of crystallinity (Chapter 3, Section 3.4.7). It is noteworthy that the FTIR spectra collected from both sides of neat PVOH film gave very similar values of H_{845}/H_{1710} and H_{1142}/H_{1087} suggesting a consistency of the crystallinity through the unmodified film. For PVOH/clay films, it is difficult to evaluate the crystallinity change in the PVOH/Clay films utilising the intensity of the 1142 cm^{-1} peak relative to that at 1087 cm^{-1} due to the shift of the latter to lower frequencies in the presence of clay as well as it being almost overlapped by the band at 1045 cm^{-1} in the spectra of NaCF20. Therefore, two peak height ratios H_{1142}/H_{1710} and H_{845}/H_{1710} were used and shown in Fig. 5.6 as a function of clay content. It can be observed that the H_{845}/H_{1710} and H_{1142}/H_{1710} did not change

significantly when 5 and 10 wt% clay were present indicating no significant change in crystallinity. With 20 wt% clay loading, these ratios increased considerably showing a considerable increase in the crystallinity and the top surface exhibited higher crystallinity than the bottom surface

5.3.4 Raman spectroscopy results

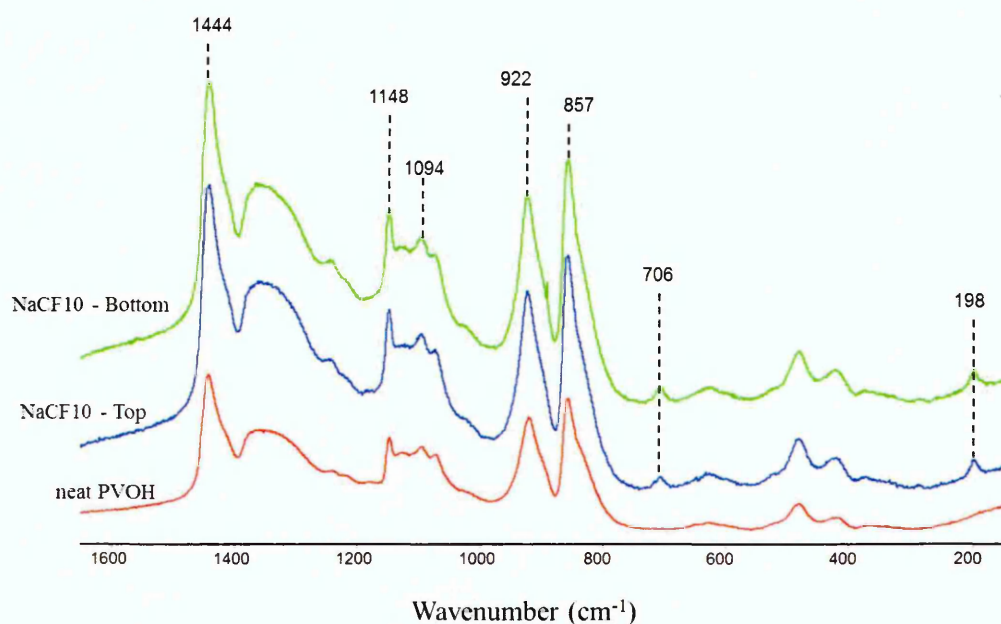


Figure 5.7 Raman spectra of neat PVOH films and NaCF10. All spectra were baseline corrected and were offset for clarity

Fig. 5.7 shows that the Raman spectra of PVOH/Clay films containing 10 wt% clay exhibit strong characteristic absorption bands of PVOH at 1444 cm^{-1} (C-H bending), 1148 and 1094 cm^{-1} (C-C and C-O stretching), 922 and 857 cm^{-1} (C-H bending and C-C stretching) (See 3.4.8). Moreover, two additional peaks at 706 and 198 cm^{-1} were present in the spectra of NaCF10 films which are characteristic of NaMMT and therefore indicative of the presence of clay in the films [187,188]. It can also be observed that there was a small increase in the intensities of the 1148 cm^{-1} peak indicating an increase in the crystallinity when clay was present in PVOH films.

5.3.5 XRD results

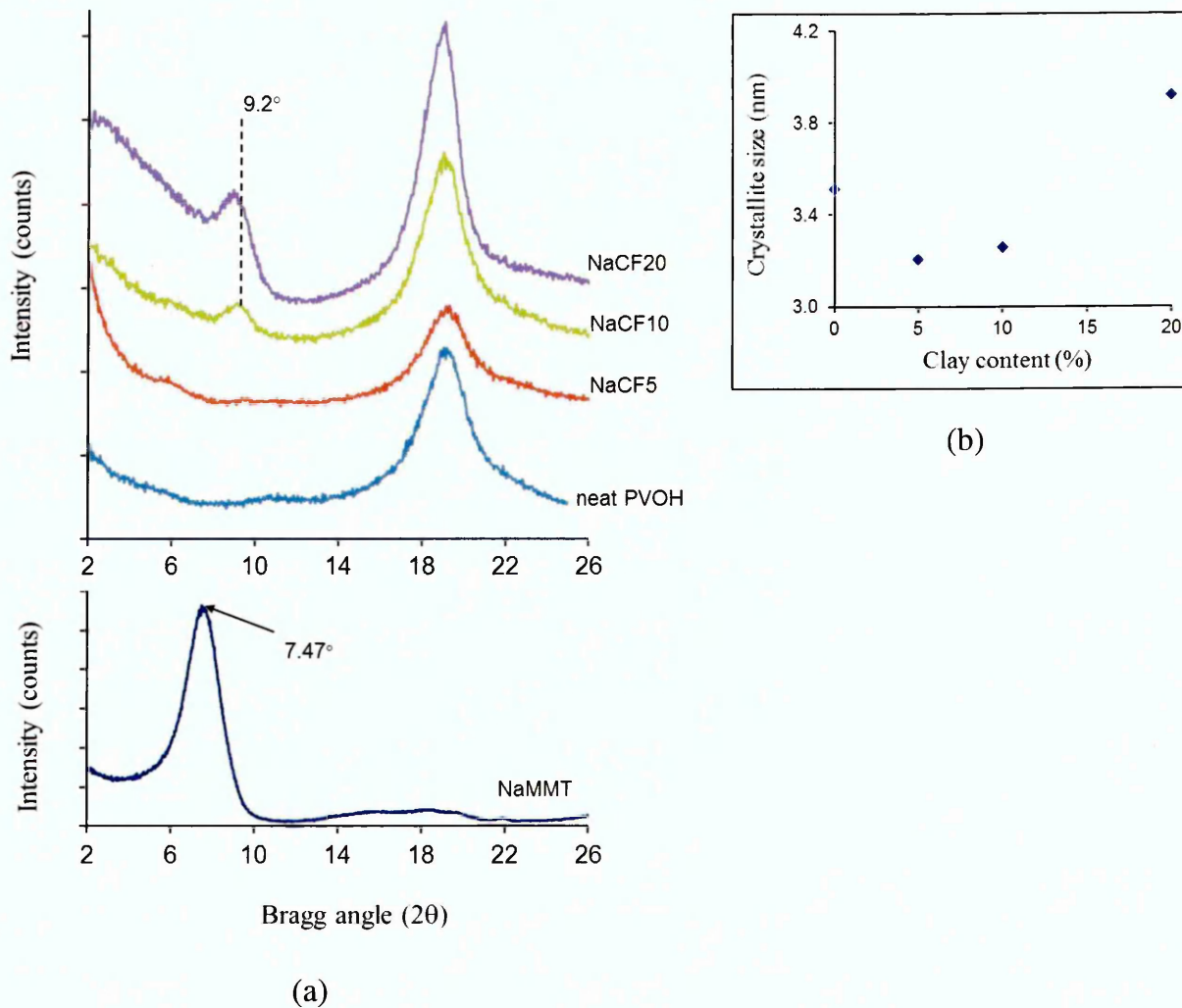


Figure 5.8 (a) XRD patterns of NaMMT, PVOH films and PVOH/Clay films with clay content varied from 5 to 20 wt%. The diffractions were taken from the top surfaces of the PVOH/Clay films

(b) Crystallite size calculated from Scherrer equation

The X-ray diffraction patterns of PVOH film, NaMMT and PVOH/Clay films containing 5, 10 and 20 wt% clay are shown in Figure 5.8a. The principle crystal diffraction peak for PVOH films at 19.2° 2θ , corresponding to a $d_{\text{spacing}} = 4.62 \text{ \AA}$, slightly shifted to lower Bragg angles when the clay loading increased from 10 to 20 wt%. Gaume *et al.* [186] also reported a shift of this peak to lower angles with increasing clay contents in the PVOH matrix while Lim *et al.* [179] described a shift to the opposite way, i.e. to higher Bragg angles. However, both studies confirmed a slight change in the morphology of PVOH with the presence of clay.

The herein data in Fig. 5.8b shows an increase in crystallite size with 20 wt% clay loading while the incorporation of 5 and 10 wt% clay resulted in a decrease of crystallite size.

NaMMT shows a sharp peak at $7.47^\circ 2\theta$ which is attributed to the basal spacing of the clay ($d_{\text{spacing}} = 11.83 \text{ \AA}$) and (001) reflection of NaMMT [62,64,179,186]. The addition of clay into PVOH resulted in producing either intercalated or exfoliated structures which depends on the clay content. The XRD pattern of NaCF5 shows no apparent peaks corresponding to the basal spacing of NaMMT except for a small shoulder around $5.7^\circ 2\theta$. The increasing baseline towards lower angle (below $4^\circ 2\theta$) reveals that a very disordered, if not exfoliated structure was present in the NaCF5 films [179].

In comparison with NaCF5, the X-ray diffraction pattern of NaCF10 exhibited a peak at $\sim 9.2^\circ 2\theta$ ($d_{\text{spacing}} = 9.6 \text{ \AA}$) which slightly shifted to lower Bragg angle ($9^\circ 2\theta$, $d_{\text{spacing}} = 9.8 \text{ \AA}$) and increased intensity in the diffractogram of NaCF20. Furthermore, the increasing towards lower Bragg angles of the baselines and the absences of the characteristic peak of clay ($2\theta = 7.47^\circ$) in their XRD diffractograms indicate that there was a mixture of both intercalated and very well dispersed clay structures present [62,108,186].

5.3.6 DMA results

The $\tan \delta$ as a function of temperature for the PVOH and NaCF10 films is plotted in Fig. 5.9. As described in Section 3.4.10, the $\tan \delta$ curve of PVOH showed two peaks at around 50°C and 120°C which were associated with the α transition (T_g) and slippage of the crystallites, respectively [134,170]. When clay was loaded into the polymer, some relaxations occurred at below 50°C , and in particular two relaxations at $\sim 10^\circ\text{C}$ and $\sim 28^\circ\text{C}$ which were assigned to γ and β transitions, respectively. The glass transition temperature of the NaCF10 was observed at 60°C , which was higher than that of neat PVOH indicating that when clay was incorporated into PVOH, the clay layers restricted the relaxation of the polymer

chains during the T_g phase due to them being in close proximity to the clay layers [101,189].

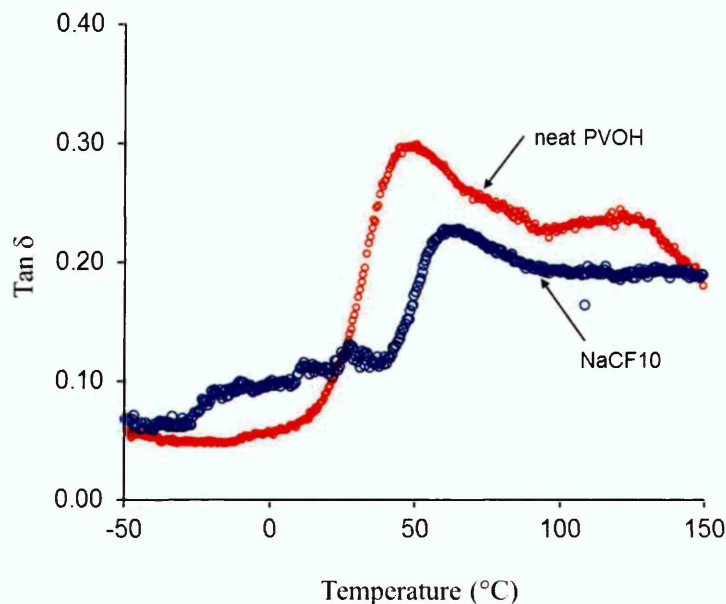


Figure 5.9 Tan δ of neat PVOH and NaCF10 films as a function of temperature.

5.3.7 Discussion

The increase in the water and water vapour barrier properties of PVOH films when incorporating clay has been reported in the literature [62,108,110,151,179]. This improvement has been ascribed to the tortuous path effect (Fig. 5.10) where the clay layers in the polymer act as impermeable barriers hindering the diffusing molecules, forcing them to follow longer and more tortuous paths resulting in the higher resistance to water and water vapour molecules [62,63,101,105,113,114,189,190]. The strong adsorption-interaction between the molecular chains and clay layers also acts to hold the matrix together and resist the penetration of water, analogous to a crosslinked system. In addition, the less polar clay presumably at the surface of the film resulted in lower wettability by water of the PVOH/Clay film surface than neat PVOH film surface, as evidenced by contact angle measurement (See 5.3.2)

When clay was incorporated into the polymer matrix, the morphology of the polymer was affected. On the one hand, some studies in the past reported an

increase in the crystallinity of PVOH film when clay was present [110,179,190,191], which was possibly due to strong specific interactions between the clay surface and polymer creating nucleating sites for the PVOH crystals [110,186,191]. On the other hand, several other authors have stated that the crystallinity of PVOH decreased after clay was added [188,192], perhaps due to the disruption of crystallites growth due to the presence of clay. Moreover, Gaume *et al.* [186] by using XRD and DSC measurements confirmed the increase in the crystallite size but not overall crystallinity in the PVOH/Clay film when compared to neat PVOH. The FTIR results herein showed a strong interaction between clay and PVOH and described changes in the degree of crystallinity utilising the peak height ratio H_{845}/H_{1710} and H_{1142}/H_{1710} (Fig. 5.6). The crystallinity did not change significantly when clay was present in the film with an amount of 5 and 10 wt%, whilst it increased significantly with clay loading of 20 wt%. In addition, a higher crystallinity on the top surface than on the bottom surface in NaCF20 was observed in Fig. 5.6 which may be due to the agglomeration and settling of clay particles at the interface in contact with the Petri dish which in turn could diminish the orientation of crystalline polymer resulting in more amorphous state [193]. Changes in morphology of PVOH when clay was present were described in XRD data in which the crystallites size increased significantly with 20 wt% clay loading (Fig. 5.8b).

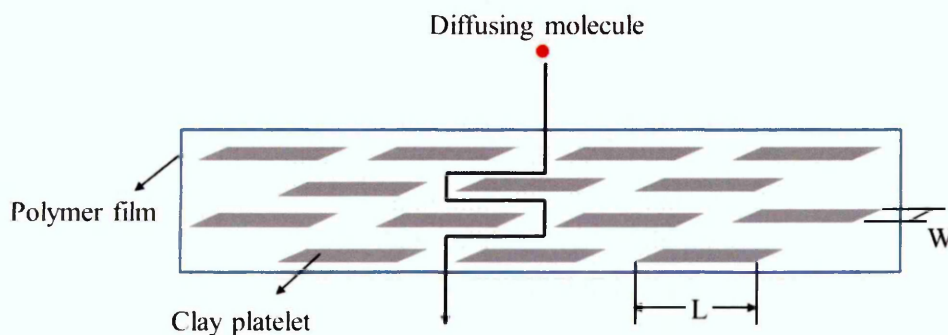


Figure 5.10 Tortuous effect - Gas/vapour finds difficulty and long way to pass through the film when nanoparticles are present.

The increase in the glass transition temperature in the PVOH/Clay film indicates a good clay dispersion and interaction with PVOH, which restricts the movement

of the polymer chains. Whether T_g increases or decreases when clay is present in a PVOH matrix is not consistent among previous studies. For example, Grunlan *et al.* [114] reported an increase in T_g of $\sim 10^\circ\text{C}$ when 10 wt% NaMMT was added to PVOH. Whereas, Yang *et al.* [188] found a decrease of 1°C in the T_g of PVOH/Clay film containing the same amount of clay. A decrease in T_g when clay was present in PVOH was also cited by Ogata *et al.* [193], in which the T_g decreased from 55 to 45°C when the clay content varied from 0 to 20 wt%.

5.3.8 Summary

In summary, the water vapour barrier properties of PVOH films improved by about 16.3%, 43.7% and 57% when 5, 10 and 20 wt% NaMMT was added, respectively. The successful interaction between PVOH and clay was proved by the FTIR results by showing a shift of the characteristic Si-O stretching band of clay and C-O stretching band of PVOH. The crystallinity of the PVOH films increased when high clay content (20 wt%) was present in the film. The glass transition temperature of the films also increased when clay (10 wt%) was added into the polymer. Since the PVOH/Clay films were quite brittle and the brittleness increased with increasing clay content, the NaCF5 and NaCF10 composites were selected for further experiments involving crosslinking with GA. The larger improvement in water vapour barrier properties for NaCF10 in comparison with NaCF5 was the reason for choosing the former.

5.4 EFFECT OF CROSSLINKING ON THE PROPERTIES OF PVOH/CLAY FILMS

5.4.1 Water and water vapour barrier properties

When PVOH/Clay films were crosslinked with GA, the water vapour barrier properties improved significantly. Figure 5.11 shows that after just 15 minutes of treatment, the improvements were 63% and 68% for NaCF5 and NaCF10 films, respectively compared to 66% for PVOH films. Similar to the WVTR results of

crosslinked PVOH films (in the absence of clay), an increase in the crosslinking reaction time resulted in negative effects on the water vapour properties for crosslinked PVOH/Clay films, especially with 24-hour-treatment. This was attributed to an increasing number of acetal linkages which were generated with increasing crosslinking times and their affinity to water molecules.

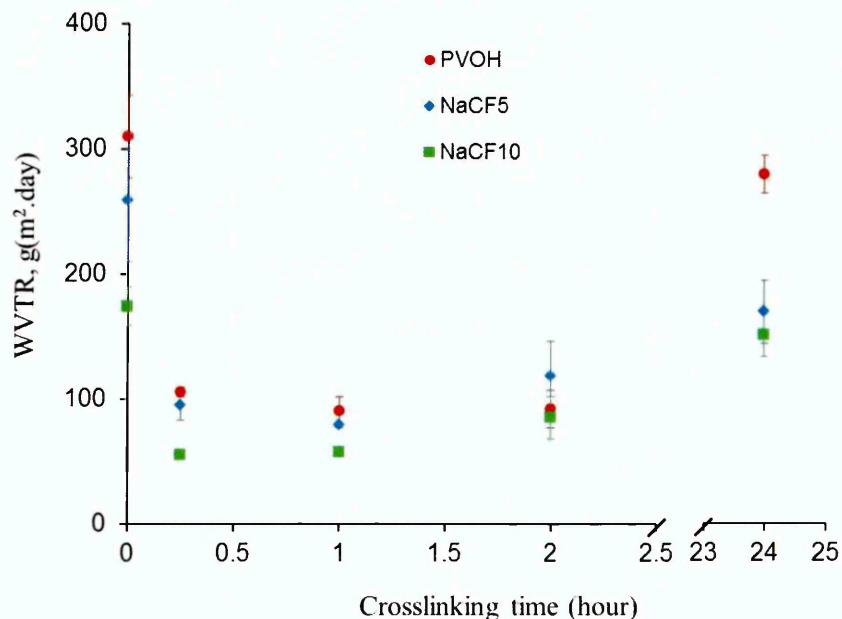


Figure 5.11 WVTR results (23°C and 85% RH) of crosslinked PVOH/Clay films (5 wt% and 10 wt% clay) compared to crosslinked PVOH.

In the crosslinked PVOH/Clay films, both crosslinks and nanoclay contribute to the water vapour barrier properties of the samples. As demonstrated in Fig. 5.11 the WVTR values of crosslinked NaCF10 were consistently lower than those of crosslinked NaCF5 and both of these were lower than the WVTR values of crosslinked PVOH films (with the exception of the 2-hour crosslinked films in which the WVTR values of crosslinked PVOH was lower than those of crosslinked NaCF5). The WVTR differences between crosslinked PVOH and crosslinked PVOH/Clay films formed with low crosslinking times were not as marked as those un-crosslinked and crosslinked for 24 hours. This is believed to be due to the tortuous effects caused by clay in which the clay particles in the polymer act as impermeable barriers hindering the diffusing molecules, forcing

them to follow longer and more tortuous paths resulting in the higher resistance to water and water vapour molecules. In addition, this effect may also hinder the penetration of GA into the films to crosslink with PVOH molecules resulting in lower number of crosslinks generated in the PVOH/Clay films than in the PVOH films when extending the crosslinking time. Indeed, Fig. 5.12 illustrates a higher degree of crosslinking in PVOH films compared to NaCF10 at all the different crosslinking times. The degree of crosslinking was calculated based on the weight gains of the films after the crosslinking reaction (See Appendix A1.2). With 24 hours of treatment, more acetal groups will be present in the crosslinked PVOH films than in the crosslinked PVOH/Clay films, which correspond to higher WVTR values in the crosslinked PVOH films.

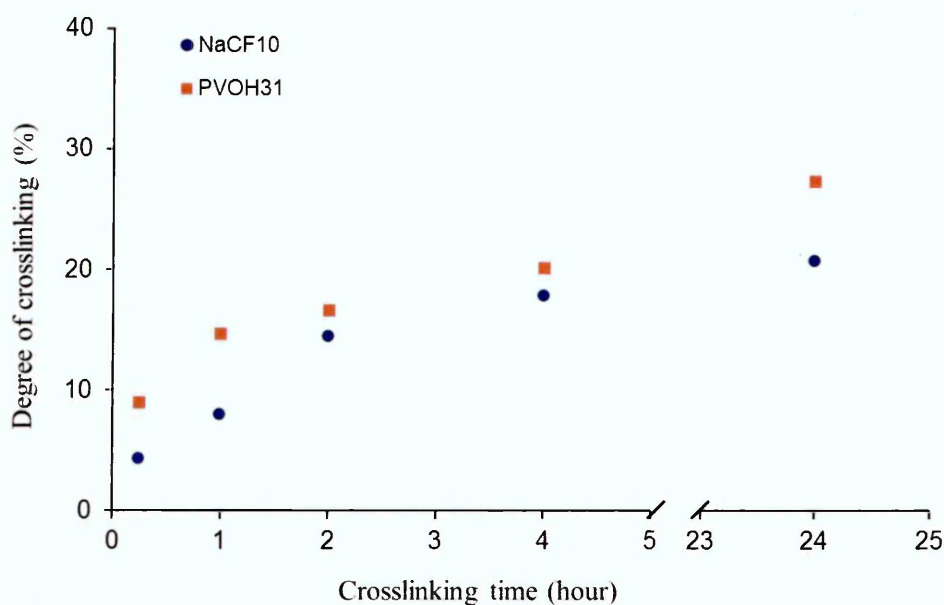


Figure 5.12 Comparison between degrees of crosslinking as a function of crosslinking time in different crosslinked films of NaCF10 and PVOH. The degree of crosslinking was calculated based on the weight gains of the films after the crosslinking reaction

When immersing the un-crosslinked PVOH/Clay films in water at 22°C for 24 hours, they dissolved completely while the crosslinked films swelled. When in hot water (90°C for 24 hours), like crosslinked PVOH films, the crosslinked NaCF5 and NaCF10 films were stable, i.e. just swollen but not dissolved, indicating that the crosslinking reaction occurred effectively in the PVOH/Clay

films, even with low crosslinking time (15 minutes). In addition, the swelling degrees in water of the crosslinked PVOH/Clay films decreased with increased clay content and were lower than those of crosslinked PVOH films despite less crosslinking occurring. Fig. 5.13 shows that with 15 minutes of crosslinking, the crosslinked PVOH films possessed a degree of swelling in hot water (90°C) of 175%, which was higher than those of crosslinked NaCF5 and NaCF10 films (156% and 124%, respectively). This indicated that although clay hindered the diffusion of the crosslinking agent into the PVOH/Clay films, the crosslinking reactions still occurred to support the resistance to water.

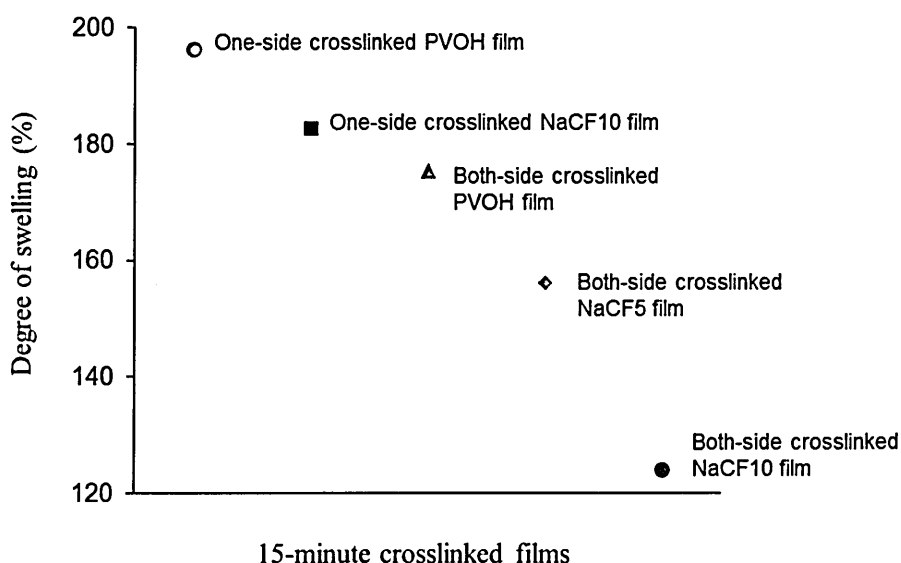


Figure 5.13 Degree of swelling in hot water (90°C) for PVOH and NaCF5, NaCF10 films after crosslinking with GA for 15 minutes

Similar to PVOH films, the crosslinking reaction appeared to occur relatively fast between the PVOH/Clay films and the GA as evidenced when investigating the one-side crosslinking of NaCF10 films for durations of 5, 15 and 60 minutes. After being immersed in hot water (90°C) for 24 hours, the NaCF10 film crosslinked on one side for 5 minutes did not dissolve; it became a gel but did not stick to the blotting paper, which differed to the respective one-side crosslinked PVOH film in which the film was easily broken and stuck to the blotting paper

(see Section 4.5.2.2). The one-side crosslinked NaCF10 films with 15 and 60 minutes of crosslinking time simply swelled in hot water.

Fig. 5.13 also shows that with the same 15 minutes of crosslinking time, the degree of swelling in hot water of the one-side crosslinked NaCF10 was 183%, which was lower than that of one-side crosslinked PVOH film (196%) and higher than the value of both-side crosslinked NaCF10 film (124%).

5.4.2 FTIR results

When NaCF10 films were immersed in the crosslinking solution, their top and bottom surfaces were crosslinked by GA (the bottom surface was the surface in contact with the Petri dish during the film formation while the top surface was the side exposed to air). When crosslinking with GA for increasing lengths of time, a decrease in the O-H stretching absorption band at 3270 cm^{-1} together with its shift to higher wavenumbers was observed on both surfaces (Fig. 5.14). The lower the intensity of the O-H stretching band, the more number of O-H groups were consumed by GA. In addition, when crosslinking time was increased, an increase in the intensity of the band at 2865 cm^{-1} was observed, which was due to the C-H stretching of GA. The results proved that the crosslinking between PVOH and GA occurred in the NaCF10 film on both top and bottom surfaces.

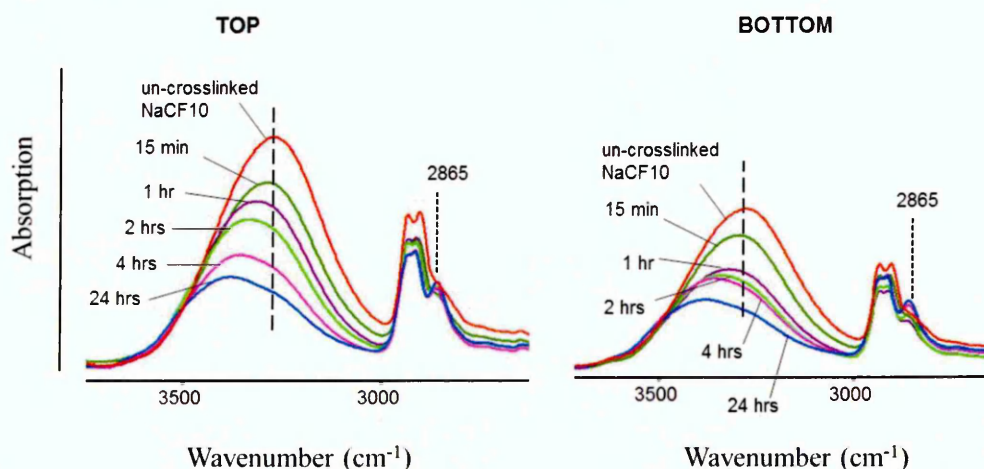


Figure 5.14 Changes in O-H stretching groups in the FTIR spectra after the NaCF10 films were crosslinked with GA at varied crosslinking times

The peak area ratio of O-H stretching band ($3700 - 2996 \text{ cm}^{-1}$) relative to C-H stretching absorption band ($2996 - 2778 \text{ cm}^{-1}$) was taken to compare the degrees of crosslinking between crosslinked PVOH, NaCF5 and NaCF10 films prepared with different crosslinking times. Fig. 5.15 shows that all $A_{(O-H)}/A_{(C-H)}$ ratios decreased with increasing crosslinking times indicating more O-H groups were consumed by GA. It is also shown that more O-H groups were consumed in the NaCF10 films than in the PVOH films. In addition, the peak area ratios of crosslinked NaCF5 and NaCF10 show that more O-H groups were consumed in the bottom sides than in the top sides. These results indicate that crosslinking occurred more on the bottom surfaces than on the top surfaces of the PVOH/Clay films and more in PVOH/Clay films than in PVOH films. Even though it has been shown that less crosslinking occurred in the clay containing films (Fig. 5.12), these FTIR results suggest that a higher portion of the crosslinking occurred at the outer surfaces of the films (note that the FTIR technique only analyses a few μm of the film). This would tie in with the fact that the clay limits the diffusion of the GA molecules into the film (due to the tortuous path effect) and enhance the crosslinking at the surfaces.

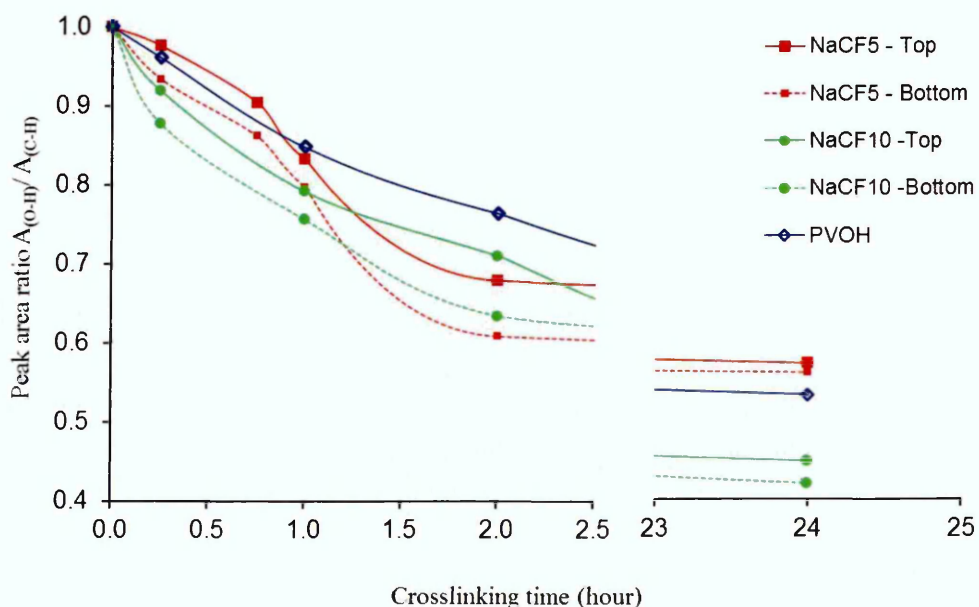


Figure 5.15 Normalised peak area ratio between O-H and C-H stretching groups of FTIR collected from crosslinked PVOH, NaCF5 and NaCF10 films as a function of crosslinking times. The values of un-crosslinked films are normalised to 1.

The 1500-800 cm^{-1} region also exhibited changes related to the crosslinking between PVOH and GA in the NaCF10 films (Fig. 5.16). Firstly, there was an increase in the C-O stretching group at 1129 cm^{-1} indicating the occurrence of the crosslinking reaction and the formation of acetal linkages. Secondly the crystalline peak at 1142 cm^{-1} decreased and therefore was not clearly present in the films crosslinked for longer times which made it impossible to determine any changes in the crystallinity after the crosslinking reaction. But the decrease of the C-C bending absorption band at 845 cm^{-1} , which was stated to be sensitive to crystallinity [99] (discussed in Section 3.4.7) did suggest a decrease in crystallinity.

The spectra of the crosslinked NaCF10 films were different when comparing the top and bottom sides. Due to more clay being present on the bottom surfaces of the NaCF10, the spectra of the bottom side showed a higher intensity for the Si-O stretching bands at 1045 and 1025 cm^{-1} .

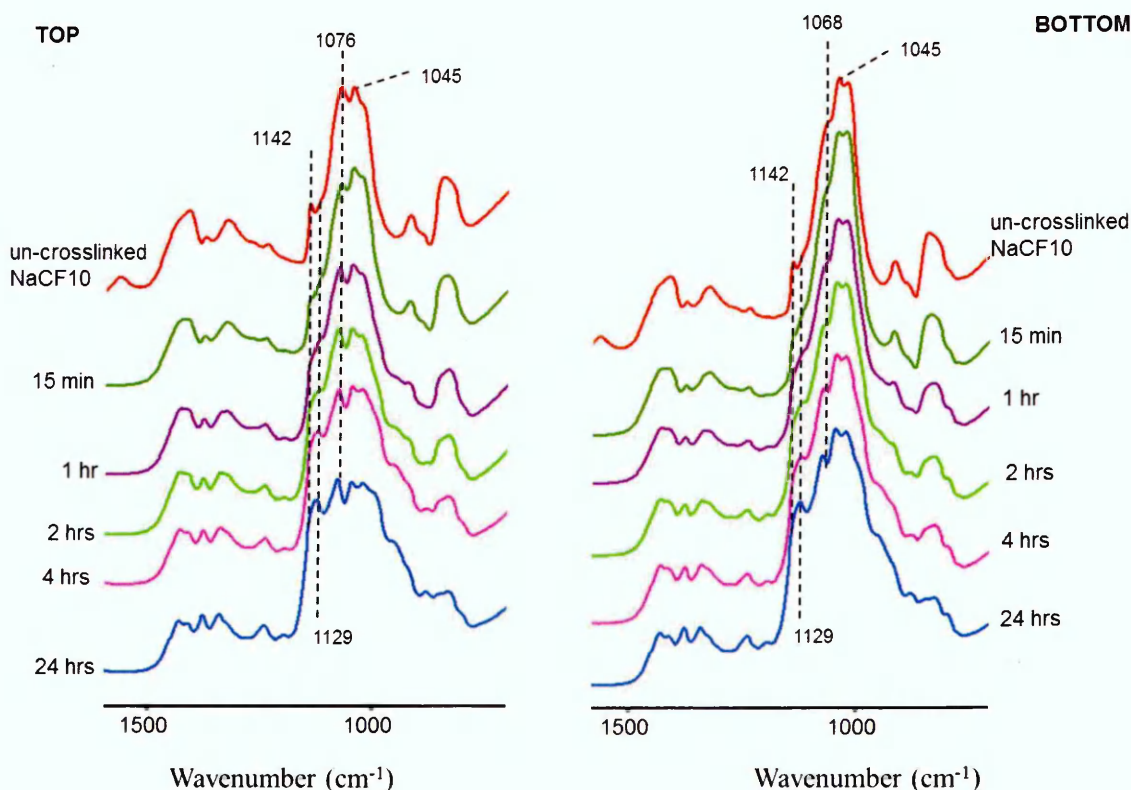


Figure 5.16 Changes in the 1500-800 cm^{-1} region in the FTIR spectra of the top and bottom surfaces after NaCF10 films were crosslinked with GA for different crosslinking times

5.4.3 Summary

GA as a crosslinking agent is able to crosslink PVOH/Clay films to produce crosslinked systems having higher water and water vapour barrier properties than either the un-crosslinked clay films or crosslinked PVOH. With the tortuous path effect, clay particles can hinder the penetration of GA into the PVOH/Clay films resulting in a lower degree of crosslinking compared to PVOH films. In addition, more crosslinking may occur at the outer surfaces of the clay containing films as shown by FTIR results. The crosslinking reaction still occurs very fast as evidenced by the stabilisation in hot water of one-side crosslinked films prepared with 5 minutes crosslinking time. The presence of clay reduces the increase in the WVTR values when exposed to high crosslinking times (for example at 24 hours) when compared to the crosslinked PVOH films.

5.5 EFFECT OF PLASTICISER ON THE PROPERTIES OF PVOH AND PVOH/CLAY FILMS

5.5.1 WVTR results

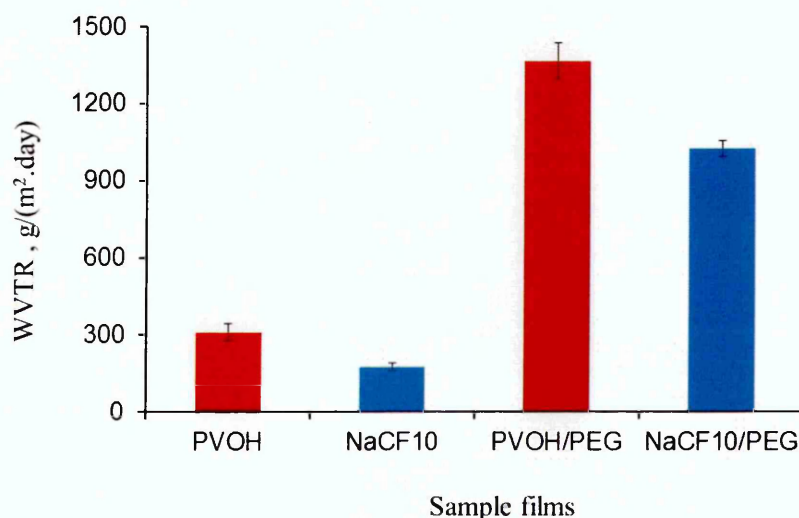
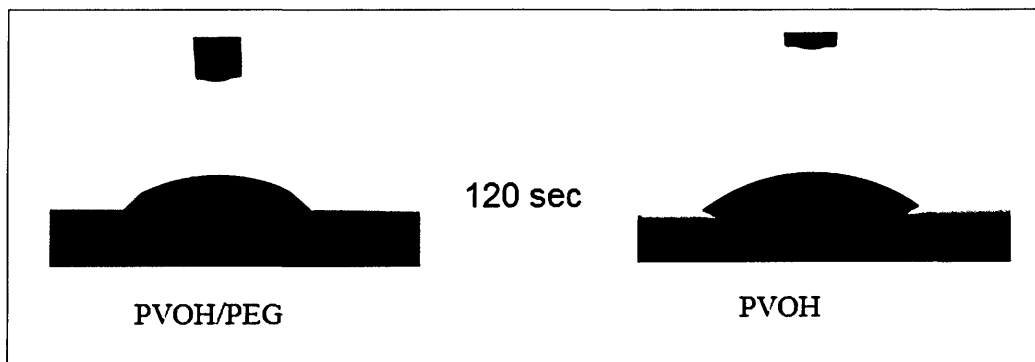


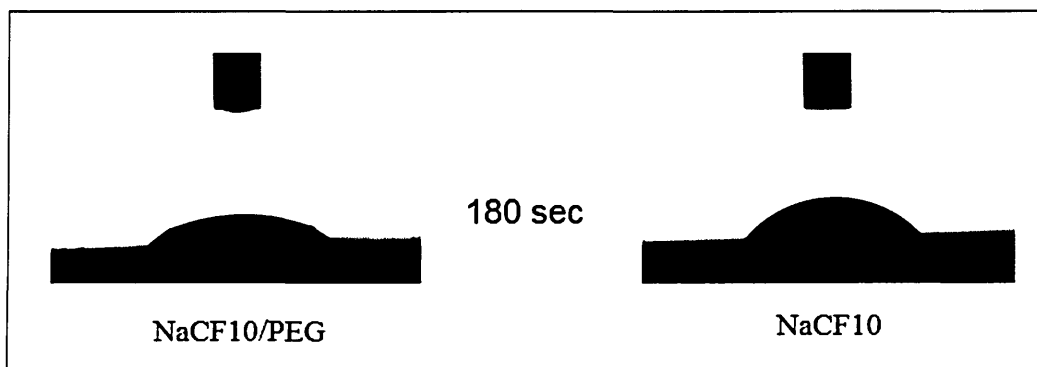
Figure 5.17 WVTR results (23°C, 85% RH) of PVOH and NaCF10 in the presence of PEG400 compared to those of un-plasticised films.

Fig. 5.17 describes the effects of PEG400 on the water vapour resistance of PVOH and PVOH/Clay films. It can be observed that with the incorporation of 20 wt% PEG400 into PVOH, the WVTR value increased to 1366 g/(m².day), which was 4.4 times higher than that of the neat PVOH film (310 g/(m².day)). Similarly, PEG400 also reduced the water vapour resistance of the PVOH/Clay films containing 10 wt% clay since the WVTR value increased to 1022 g/(m².day), which was 5.85 times higher than that without plasticiser (174.7 g/(m².day)).

5.5.2 Water contact angle results



(a)



(b)

Figure 5.18 Water droplet shapes on the film surfaces after specific lengths of time
(a) PVOH/PEG and PVOH films after 120 seconds
(b) NaCF10/ PEG and NaCF10 after 180 seconds

During the water contact angle measurements, the liquid droplet was left on the film surface for a duration of time whilst the contact angle values as well as the images of the droplet were taken every 30 seconds. One could observe that due to the effect of plasticiser, the water droplet on the surfaces of the plasticised films collapsed earlier than those on the films without plasticiser. It is shown in Fig. 5.18 that the droplet shape had deformed at 120 and 180 seconds for the PVOH/PEG and NaCF10/PEG films, respectively and so the contact angle could not be measured correctly. The droplets on the films without PEG still maintained the smooth ellipse curve shape for all the measurement times.

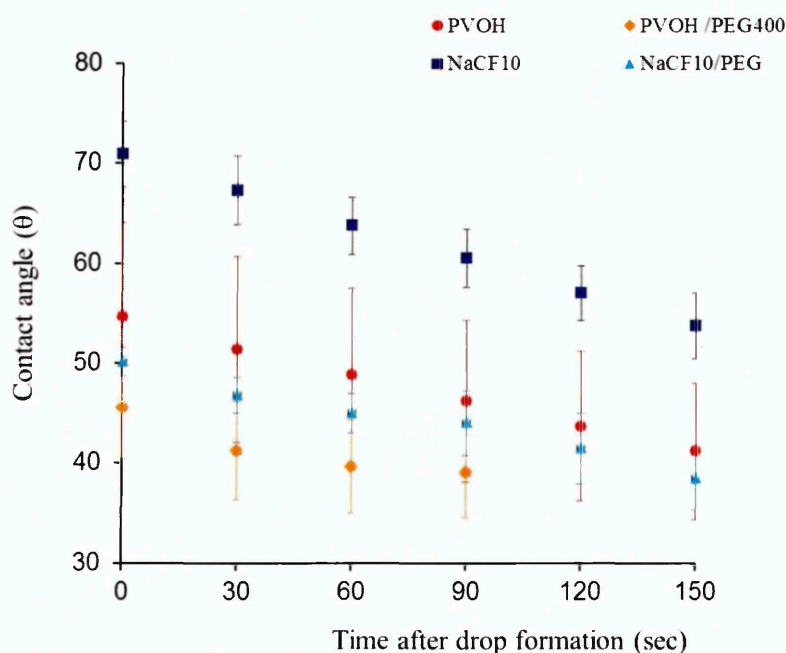


Figure 5.19 A reduction in the water contact angle values of PVOH and NaCF10 in the presence of PEG400. The contact angles were plotted as a function of time after the liquid was dropped on the film surface.

The contact angles values are described in Fig. 5.19 as a function of time after the liquid was dropped on the film surface. With 20 wt% of PEG400 present in the PVOH and PVOH/Clay films, a decrease in the contact angle values was observed. The NaCF10 film exhibited the highest contact angle values followed by those of neat PVOH film while the PVOH/PEG films showed the lowest values. When PEG was added into the PVOH/Clay film, the contact angle

decrease significantly and became even lower than those of the neat PVOH films. At 30 seconds after the water liquid was dropped on the films surface, the NaCF10 film showed a contact angle value of $67.3 \pm 3.4^\circ$ which decreased by 30% in the presence of PEG400. For PVOH, the reduction in the value was about 19.8% at the same measurement time.

5.5.3 FTIR results

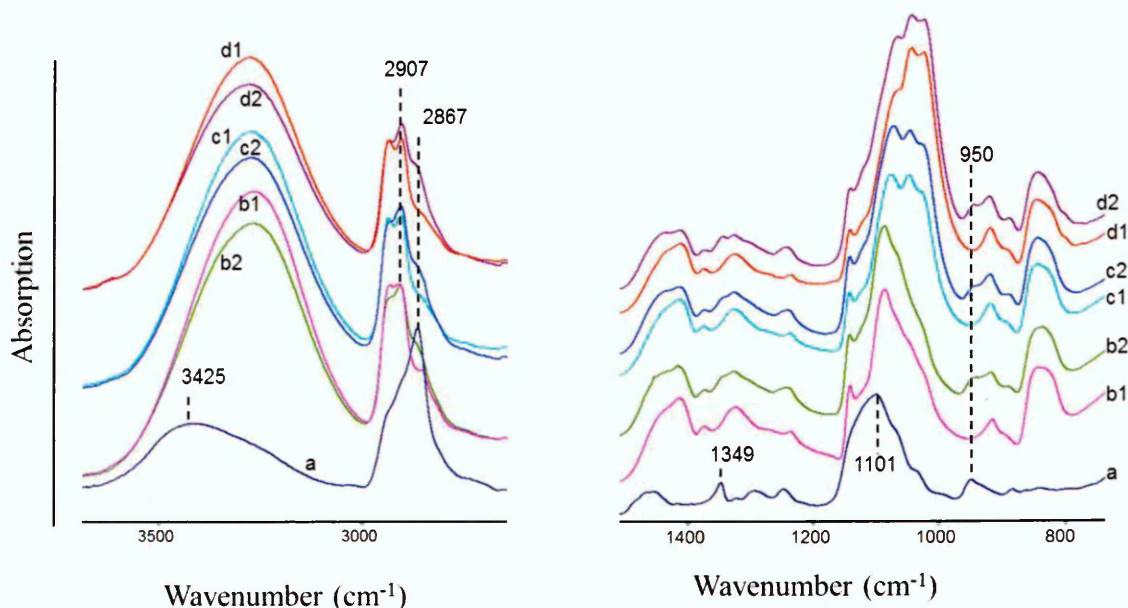


Figure 5.20 ATR-FTIR spectra of PVOH and NaCF10 films in the presence of PEG400. Spectra are offset for clarity

a - PEG400

b1 - PVOH

c1 - NaCF10 - top

d1 - NaCF10 - bottom

b2 - PVOH/PEG400

c2 - NaCF10/PEG400 - top

d2 - NaCF10/PEG400 - bottom

The FTIR spectrum of PEG400 has several characteristic absorption bands which are assigned in Table 5.3. As can be observed in Fig. 5.20, the incorporation of PEG into the polymer matrix caused a decrease in the intensity of O-H stretching band in the $3700\text{-}2990\text{ cm}^{-1}$ region and an increase in the intensity at 2867 cm^{-1} which is ascribed to the C-H stretching of PEG in the films. In addition, slight increases in the intensities of absorption bands at 2907 and 950 cm^{-1} were also

observed, which are representative of C-H stretching and C-H bending, respectively.

Table 5.3 Assignment of characteristic absorption bands in the FTIR spectrum of PEG [194,195]

Wavenumber (cm ⁻¹)	Assignment
3425	O-H stretching
2867	C-H stretching
1349	C-H bending
1101	C-O stretching
950	C-H bending

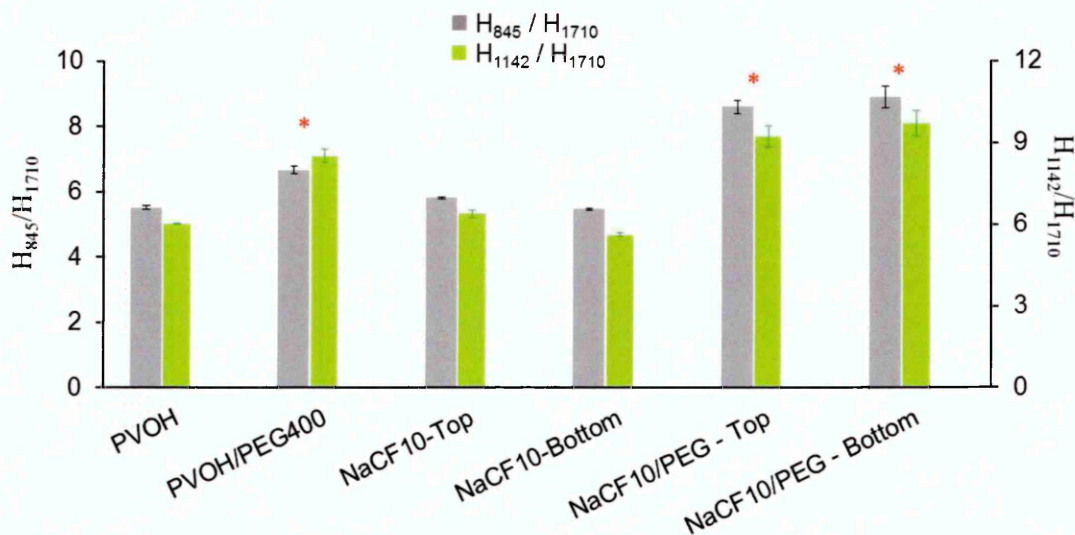


Figure 5.21 Peak height ratios H_{845}/H_{1710} and H_{1142}/H_{1710} in FTIR spectra collected from PVOH and NaCF10 films in the presence of PEG400.

The peak height ratios H_{845}/H_{1710} and H_{1142}/H_{1710} obtained from FTIR spectra of the plasticised films were compared to those of un-plasticised films and shown in Fig. 5.21. It is shown that both peak height ratios increased when PEG was present in the films indicating an increase in crystallinity.

5.5.4 Raman spectroscopy results

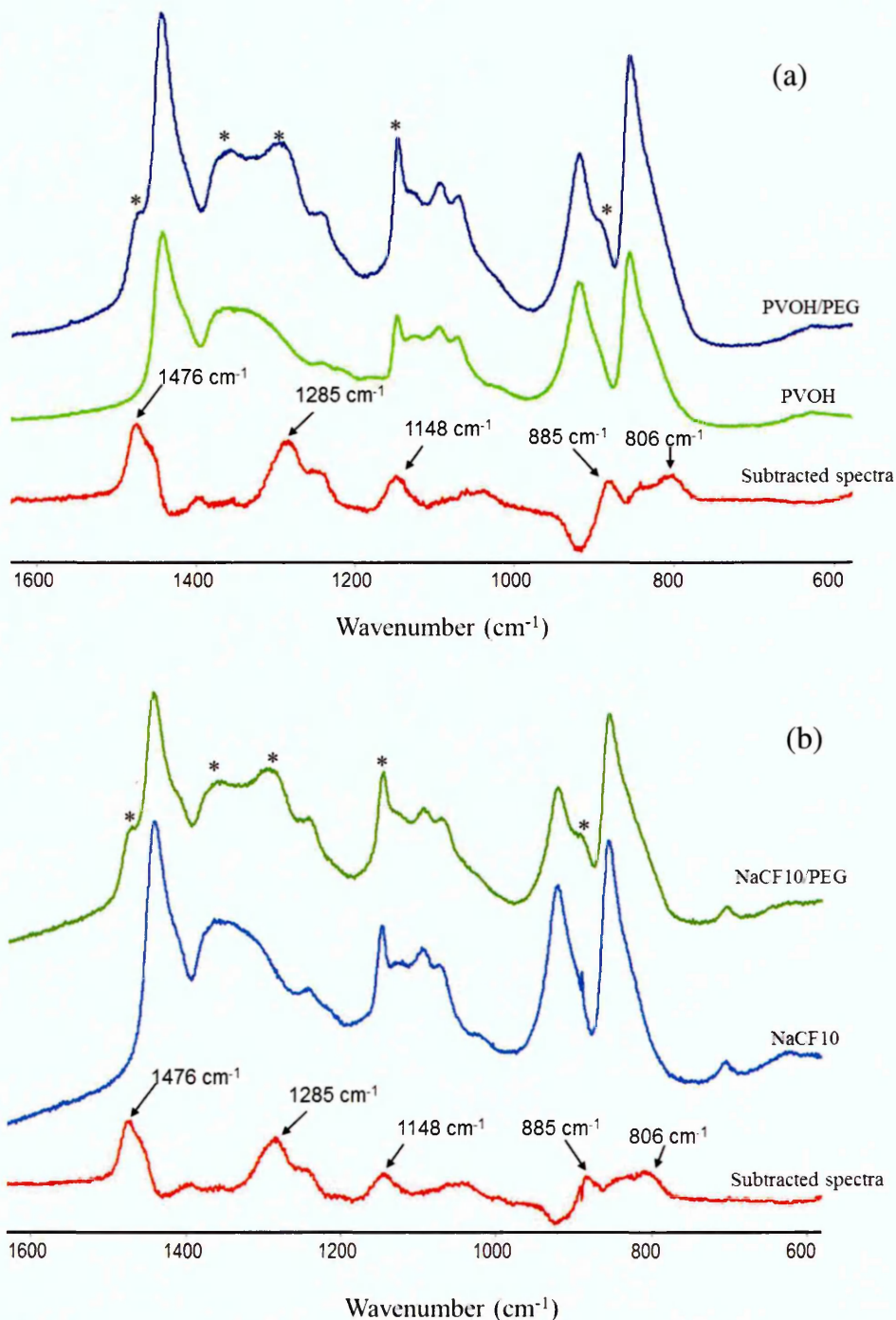


Figure 5.22 Raman spectra of films containing PEG400 in comparison with those without PEG. Subtracted spectra were operated using OMNIC software

- (a) PVOH/PEG and PVOH films**
- (b) NaCF10/PEG and NaCF10 films**

The Raman spectrum of pure PEG400 was not collected but its characteristic absorption bands were referenced from literature. Fig. 5.21 shows the Raman

spectra of plasticised PVOH and NaCF10 films compared to those without plasticiser. There were some changes related to the presence of PEG in the films which are marked by an asterisk (*). In order to compare the spectra in more detail, a subtraction of the spectrum of the plasticised film by that of the un-plasticised spectrum was performed using the OMNIC software.

The subtracted spectra displayed in Fig.5.22a and 5.22b were similar and were attributed to PEG with the characteristic absorption bands at 1476 cm^{-1} ($\text{CH}_2\text{-CH}_2$ bending vibration), 1285 cm^{-1} (CH_2 wagging and twisting vibration), 1148 cm^{-1} (C-C stretching), 885 and 806 cm^{-1} (skeleton vibration) [196-200]. This indicates a successful incorporation of PEG into the PVOH and PVOH/Clay matrix. One can observe that there was an increase in the intensity at 1148 cm^{-1} , which represents for crystallinity in the films, in the PEG containing films. This indicates that the crystallinity increases when PEG was incorporated into PVOH and NaCF10 films and is in agreement with FTIR data (Fig. 5.21)

5.5.5 XRD results

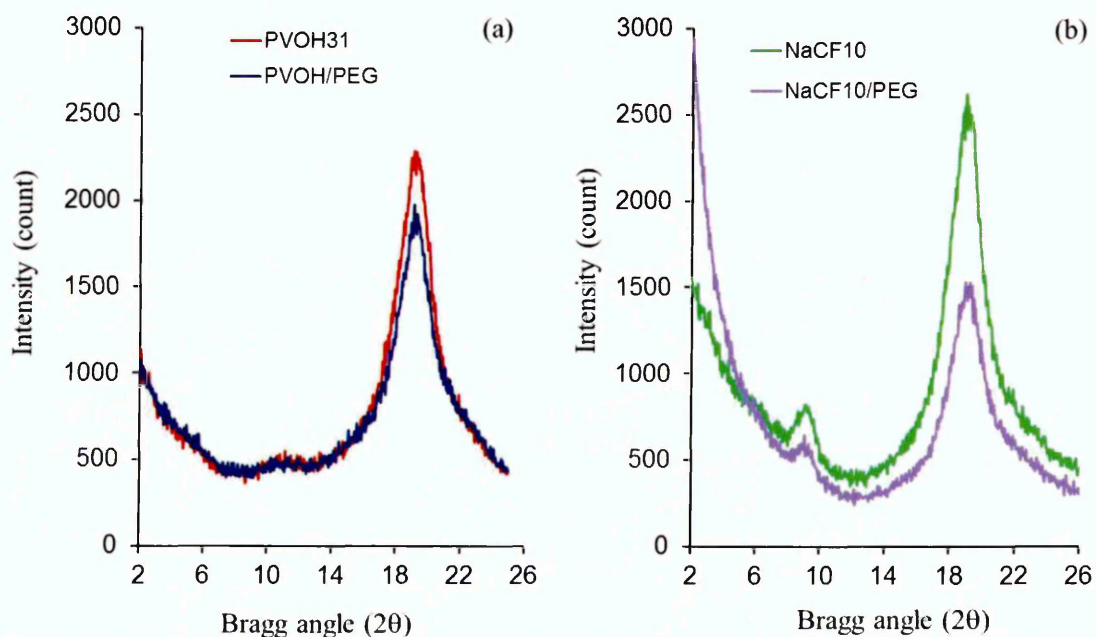


Figure 5.23 X-ray diffractions of plasticised and un-plasticised PVOH and PVOH/Clay films.

Fig. 5.23a shows similar XRD patterns for PVOH and PVOH/PEG films with one principle intense peak at $19.2^\circ 2\theta$ which characterises the crystallinity of PVOH. In Fig. 5.23b, there is a decrease in the intensity of the diffraction peak at $19.2^\circ 2\theta$ in the diffractogram of NaCF10/PEG. It is difficult to state whether the degree of crystallinity of the NaCF10 film decreased or not when PEG was present since the decrease in intensity observed in Fig. 5.23b may be due to a decrease in the amount of PVOH due to its substitution by PEG. In terms of crystallite size, a reduction in size was observed when PEG was present in PVOH films while a slight increase in crystallite size was observed for the case of NaCF10/PEG film in comparison with NaCF10 film (Table 5.4)

Table 5.4 Crystallite size of PVOH and NaCF10 films before and after incorporation of PEG400

	PVOH	PVOH/PEG	NaCF10	NaCF10/PEG
Crystallite size (nm)	3.51	3.17	3.26	3.34

5.5.6 DMA results

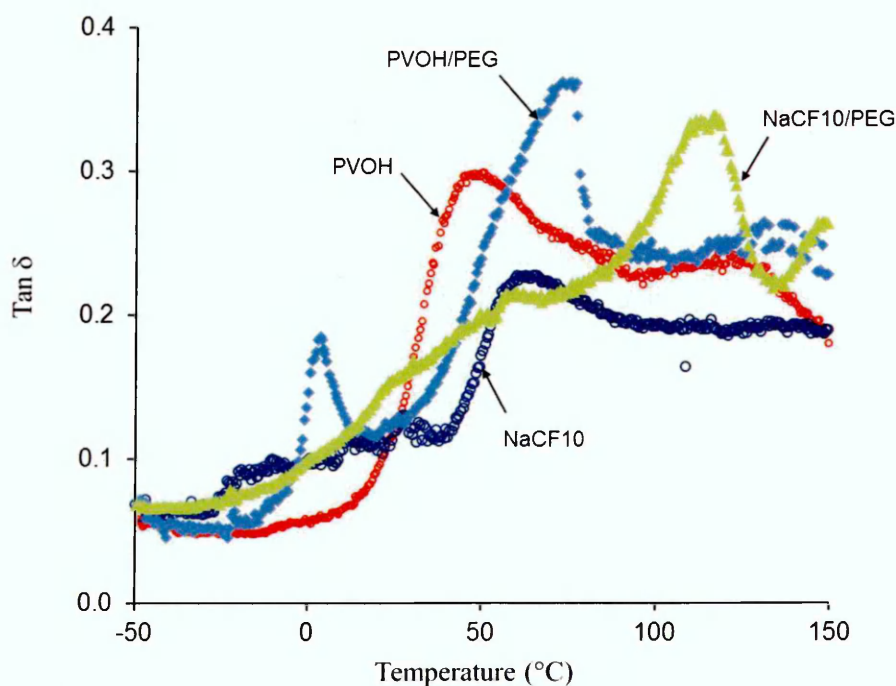


Figure 5.24 Tan δ as a function of temperature for PVOH and NaCF10 films containing PEG400 compared with those without PEG. The frequency was 1 Hz.

The $\tan \delta$ curve for the PVOH/PEG film in Fig. 5.24 shows three relaxations at 2.9, 72, and 130°C. The first relaxation (2.9°C), assigned to the β transition related to the movement of side groups (hydroxyl and acetate groups) and localised groups of several carbon atoms, is much more prominent in the PVOH/PEG film than in neat PVOH film. The relaxation at 130°C is attributed to the crystal-crystal slippage which occurs at a temperature very close to that of neat PVOH (120°C). The relaxation at 72°C represents the α transition or glass transition temperature (T_g). In theory, when a plasticiser is added to a polymer matrix, more free volume is promoted by the miscibility of plasticiser caused by an increase in the polymer-plasticiser interaction. As a result, the segmental motions in the polymer chains are facilitated (PEG acts like a grease) leading to a decrease of the glass transition temperature [201-203]. However, for the result herein, the T_g value is higher (72°C) than that of neat PVOH (50°C). An appropriate explanation for this could be due to hydrogen bonding formed between PEG and PVOH molecules which stabilises the PVOH segments and PEG molecules and interrupts the movement of the polymer chains upon heating. Li *et al.* [57] reported hydrogen bonding between PVOH and PEG400 could explain an increase in T_g values when increasing PEG400 content in PVOH ($M_w = 74,800$, $T_g = 85^\circ\text{C}$). According to the authors, when the content of PEG increased from 5 to 25 wt%, T_g increased gradually but the values were slightly lower than that of neat PVOH.

For NaCF10 film containing plasticiser, the $\tan \delta$ curve also exhibited three relaxations at 24, 59 and 115°C, in which those at 24 and 115°C are assigned to β transition and alpha star transition (T_{α}^*) related to the movement of localised groups of several backbone carbon atoms and the crystal-crystal slippage, respectively. The relaxation at 59°C is believed to be the α transition since it shifted to higher temperature (64°C) with higher frequency (10 Hz) (data not shown). It can be observed that there was no significant difference between T_g values of NaCF10/PEG and NaCF10 films.

5.5.7 Discussion

The successful dispersion of PEG into PVOH and PVOH/Clay matrix was demonstrated by the FTIR and Raman results and the films were homogeneous. According to Li *et al.* [57], when PEG was incorporated into PVOH, the interaction between the two species followed two ways: (i) PEG with low molecular weight could be easily dispersed in the polymer matrix to increase its free volume, this facilitates the segmental motions of the polymer chains and allows more diffusing paths for penetrant molecules, and (ii) PEG created a physical network with PVOH by forming hydrogen bonds with the polymer molecules. It is likely that both effects happened concurrently herein for the PVOH/PEG and NaCF10/PEG materials. The spacing effect of plasticiser and the hydrophilic nature of the polymer-plasticiser and polymer-clay-plasticiser systems made the water vapour transmission rates of PVOH and PVOH/Clay increase more than 4 times when containing 20 wt% PEG. The water wettability of the film surface also increased for the PEG-containing films as evidenced by the significant decrease in water contact angles. On the other hand, the increase in the glass transition temperature when PEG was present in PVOH film maybe due to hydrogen bonding between PEG and PVOH to support the stabilisation of PVOH segments and PEG molecule. In addition, while the FTIR and Raman results suggested an increase in crystallinity when PEG was present in PVOH and PVOH/Clay films (Figs. 5.21 and 5.22) which could be ascribed to the increase in hydrogen bonding in the films, the XRD data (Fig. 5.23) was too ambiguous to describe changes in the degree of crystallinity due to the substitution of PVOH molecules by PEG..

To have more understanding about the competition between spacing effects and hydrogen bonding effects caused by PEG400 in the films, further investigation with different PEG concentrations should be carried out in order to have a broader observation about the influence of PEG on the structures of PVOH and PVOH/Clay films.

5.5.8 Summary

In summary, PEG400 with a concentration of 20 wt% was miscible in the PVOH and PVOH/Clay matrices but its presence made the water vapour barrier properties decrease remarkably. In addition, the glass transition temperature (T_g) increased for PVOH/PEG film and did not change significantly in NaCF10/PEG film compared to their respective un-plasticised films. Two possible effects occurring concurrently in PVOH and PVOH/Clay films when PEG was incorporated were spacing effects by PEG and hydrogen bonding production between PEG and PVOH.

5.6 EFFECT OF CROSSLINKING ON THE PROPERTIES OF PLASTICISED PVOH AND PVOH/CLAY FILMS.

5.6.1 Weight change after crosslinking reaction

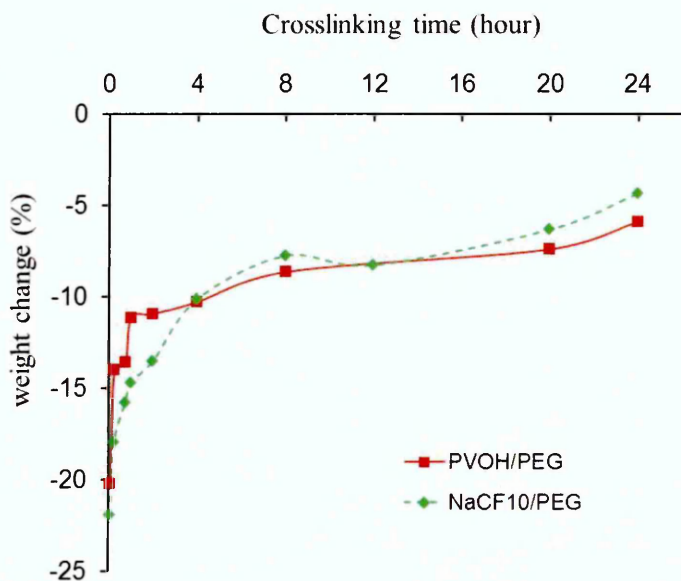


Figure 5.25 Weight changes of PVOH and PVOH/Clay films containing PEG after the crosslinking reaction with GA.

Fig. 5.25 shows that after the crosslinking reaction with GA, the samples decreased in weight. After 5 minutes of crosslinking, the weights of PVOH/PEG and NaCF10/PEG films decreased by 20% and 21%, respectively. When the

crosslinking time increased, less decrease in weight was observed indicating more crosslinks present in the films due to the increasing crosslinking reaction with GA at longer crosslinking times. It is noteworthy that the concentration of PEG400 present in the films before crosslinking reaction was 20 wt%. Therefore, the weight loss of the plasticised films after the crosslinking reaction could be mainly ascribed to the leaching of PEG from the films during the crosslinking reaction. In addition, the dissolution of some PVOH molecules in water at the beginning of the immersion may have contributed to the weight loss (See Chapter 3, Section 3.4.1). It also appeared that the presence of clay was unable to stop the leaching of PEG even though it is known to absorb very strongly to clay [204,205].

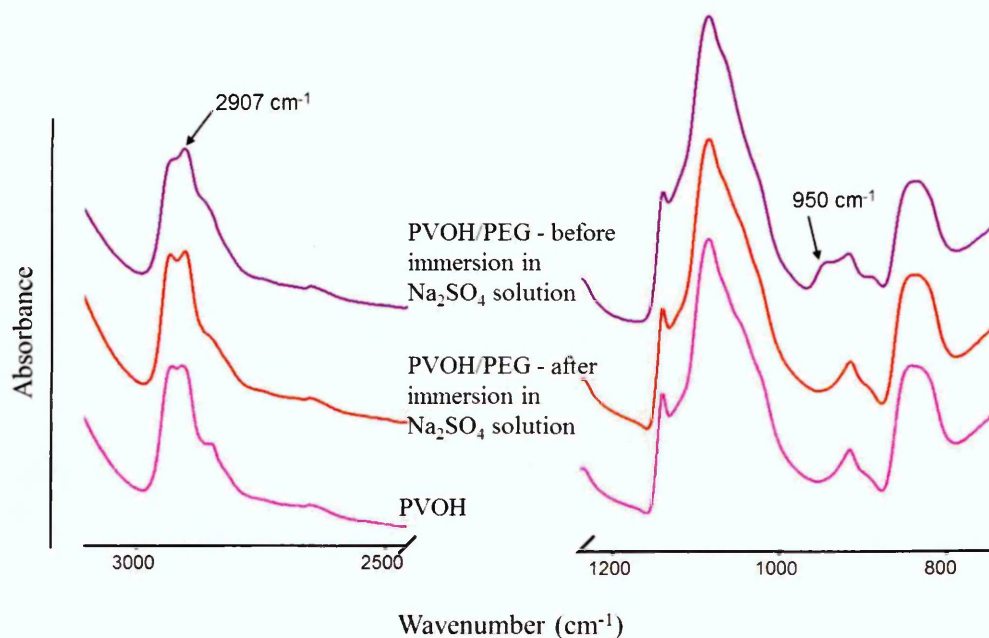


Figure 5.26 Changes in the FTIR spectra of PVOH/PEG film after immersion in sodium sulphate solution for 30 minutes without the presence of crosslinking agent and catalyst.

In order to study the loss of plasticiser during the crosslinking reaction, a piece of PVOH/PEG film was immersed in an aqueous solution at 40°C containing Na₂SO₄ without the presence of both crosslinking agent GA and catalyst (H₂SO₄). The salt:water ratio was kept the same as the ratio used in the crosslinking solution. After 30 minutes, the film was taken out of solution then washed with water and dried at 40°C for 2 days. Its FTIR spectrum was compared with the

spectra of PVOH/PEG film before the immersion and the PVOH film without PEG.

Fig. 5.26 shows that after immersing the PVOH/PEG in the solution, the 2907 cm^{-1} peak which was assigned to C-H stretching of PEG decreased in intensity. In addition, the absorption band at 950 cm^{-1} characterised as C-H bending of PEG disappeared. It can also be observed that the spectrum of the film after immersing in the salt solution was similar to that of neat PVOH. The leaching of plasticiser was also observed for PVOH film containing 20 wt% PEG of molecular weights 600 or 1,000 g/mol. After immersion in Na_2SO_4 solution without the presence of GA and catalyst, the PVOH/PEG600 and PVOH/PEG1000 films decreased in weight by 21-22%. The results confirmed the loss of PEG in the crosslinking solution as mentioned above.

5.6.2 WVTR results

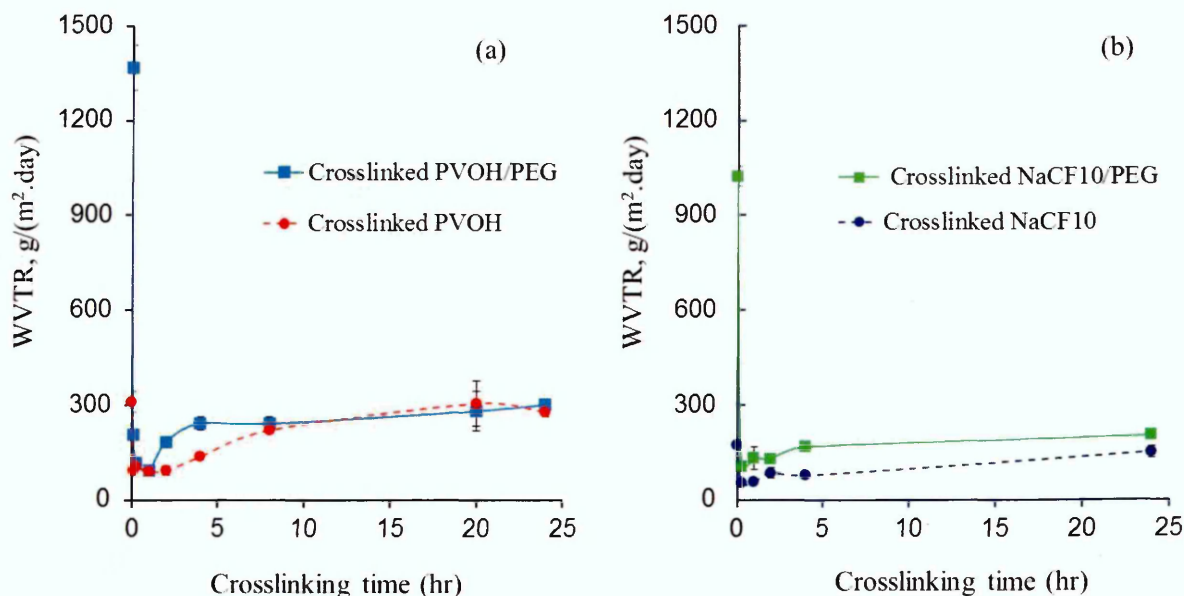


Figure 5.27 WVTR results (23°C , 85% RH) of crosslinked plasticised films and un-plasticised films at different crosslinking times
(a) Crosslinked PVOH and PVOH/PEG films
(b) Crosslinked NaCF10 and NaCF10/PEG films

It can be observed in Fig. 5.27 that after the crosslinking process, the water vapour barrier properties of the plasticised PVOH and PVOH/Clay films

improved markedly. When comparing the WVTR values of PVOH with those containing PEG for their crosslinked equivalents, the samples with PEG400 were generally higher with crosslinking time up to 8 hours (Fig. 5.27a). Similarly, the crosslinked PVOH/Clay films containing PEG exhibited a considerable decrease in WVTR values, for example, the WVTR decreased by ~90% from 1022 g/(cm².day) for un-crosslinked NaCF10/PEG films to 103 g/(cm².day) for 15-minute-crosslinked films (Fig. 5.27b). Due to the leaching of PEG during the crosslinking reaction, however, a true comparison could not be made between crosslinking with and without plasticiser. The higher WVTR values in crosslinked plasticised PVOH and PVOH/Clay films compared to their respective crosslinked films containing no PEG may be attributed to the space occupied by the PEG molecules which allowed for a greater free volume in the films thus higher WVTR values.

5.6.3 Summary

During the crosslinking reaction with GA, the PEG400 contained in PVOH and PVOH/Clay films leached out as evidenced by a decrease in weight after crosslinking. The crosslinked plasticised films possessed low WVTR values comparable to those of respective crosslinked films without PEG. However, the true effect of PEG could not be ascertained due to the leaching of PEG during the crosslinking reaction.

5.7 CONCLUSION

When 5 wt% NaMMT was incorporated into PVOH polymer, a very disordered, if not exfoliated structure was achieved and is due to similar hydrophilicity for clay and polymer. With higher clay content (10 and 20 wt%), very well dispersed structures were still present in the polymer matrix. In the PVOH/Clay films, NaMMT acts as impermeable sites to restrict the diffusion of the penetrant molecules into the films. The water vapour barrier properties improved when clay was present and increased with increasing clay content. Under visual

observation and manual handling, the PVOH/Clay films are brittle and the brittleness increased with increasing clay amount. NaCF10 films show higher improvement in the water vapour barrier properties compared to NaCF5 films and were less brittle than NaCF20 films. The T_g transition temperature of NaCF10 was higher than that of PVOH.

The crosslinking system between GA and PVOH/Clay films exhibits good barrier properties to water and water vapour due to the contributions of both crosslinks and clay particles. The crosslinking reaction in the PVOH/Clay films can occur very fast like in the case of PVOH.

When 20 wt% of PEG400 was incorporated into the PVOH and PVOH/Clay (10 wt% clay) films, the plasticiser was compatible with the polymer matrix to form homogeneous films. In addition, it contributed to form a very well dispersed clay system (if not exfoliated) in the PVOH/Clay films. However, the water vapour barrier properties decreased considerably in the presence of PEG. The glass transition temperatures were 22°C higher in the plasticised PVOH films than in the films without PEG while it almost unchanged in the case of NaCF10/PEG film. Based on observation and manipulation by hand, the plasticised PVOH and NaCF10 films were more flexible than those without plasticiser. However, after crosslinking with GA, these films became less flexible, if not brittle. PEG had less influence on the water vapour barrier properties of the crosslinked PEG-containing films as it was leached out of the films into the crosslinking solution.

Thermal stability of PVOH and its modified films

In this chapter, the thermal stabilities of PVOH ($M_w = 31,000 - 50,000$) and its modified films using thermogravimetry analysis (TGA) are reported. The TGA instrumental set up was described in Section 2.2, Chapter 2.

6.1 THERMAL STABILITY OF CROSSLINKED PVOH31 FILMS

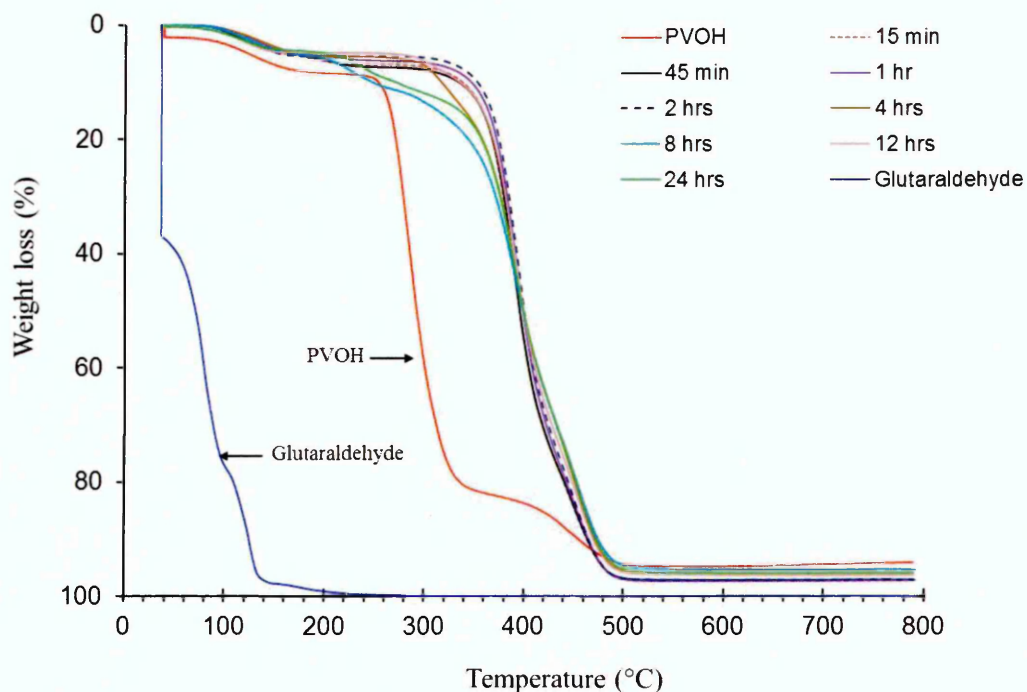


Figure 06.1 TGA thermograms of crosslinked PVOH31 films prepared using different crosslinking times in comparison with neat PVOH31 and glutaraldehyde. The heating rate was 20°C/ min under nitrogen with a flow rate of 40 mL/min. The sample was kept at 35°C for 15 minutes before following the set temperature programme.

Fig. 6.1 describes the percentage weight losses as a function of heating temperature for PVOH31, GA and crosslinked films. The majority of weight loss from GA took place between 35 and 140°C due to water evaporation since the GA solution contains 75 wt% water. GA was completely decomposed by 250°C. For PVOH, the weight loss occurring between 100-200°C was attributed to the

loss of absorbed moisture present in the films. In agreement with Peng *et al.* [167] and Li *et al.* [57], the thermal degradation of PVOH occurred in two steps with two corresponding peak maxima in derivative thermogravimetric (DTG) curves (Fig. 6.2) [167]. The first step commencing at around 220°C is described mainly as hydroxyl elimination reactions while the second step starting from 360°C is due to chain-scission reactions [206-208]. PVOH was completely decomposed by 520°C with a total weight loss of approximately 94%.

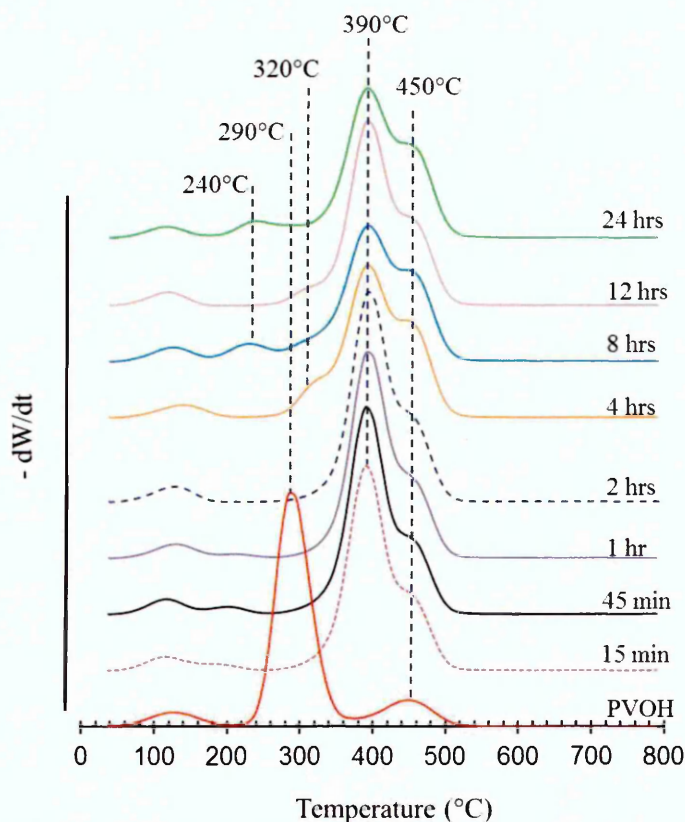


Figure 6.2 DTG curves - Thermal stability changes of PVOH31 films after crosslinking with GA for different lengths of time. Curves are offset for clarity

It can be observed in Fig. 6.2 that the main maximum (i.e. maximum rate of weight loss) at 290°C shifted to a much higher temperature of 390°C after PVOH film was crosslinked with GA showing a large improvement in thermal stability after the crosslinking reaction. There were few significant differences in peak maxima temperatures between the crosslinked films prepared using different

crosslinking times, showing that treatment of PVOH with GA was only required for a short time (15 minutes or possibly lower) to impart a significant enhancement in thermal stability.

The degradation of crosslinked PVOH films also occurred in two steps, in which the DTG peak maxima of the second degradation step were at the same temperature as that of neat PVOH film (450°C). There were small maxima (240 and 320°C) below the main degradation maxima (390°C) in the DTG curves of crosslinked PVOH films from 4 hours of crosslinking time, which were possibly due to the breaking of the pendant GA molecules (only crosslinked by one aldehyde group) on the polymer chains. The crosslinked films were completely decomposed at 520°C with the total weight loss 94-98%

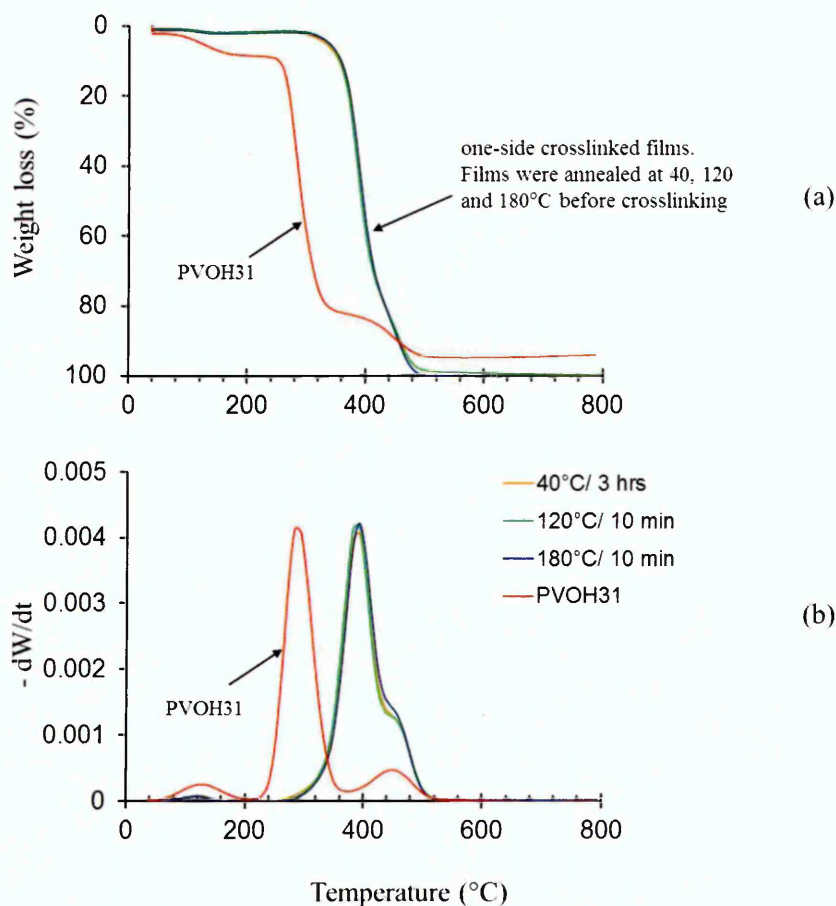


Figure 6.3 (a) TG and (b) DTG thermograms of one-side crosslinked PVOH films with 5 minutes crosslinking time. Films were annealed at 40°C/3 hrs, 120°C/10 min and 180°C/10 min before crosslinking

One-side crosslinked PVOH films also exhibited improved thermal stability compared to neat PVOH film. Fig. 6.3 illustrates the thermograms of PVOH films crosslinked by GA on one side for 5 minutes after annealing at different temperatures (see Chapter 4, Section 4.5.2). It can be observed that regardless of annealing temperatures before crosslinking, all one-side crosslinked PVOH films showed a main degradation maximum at a higher temperature (390°C) than that of neat PVOH (290°C) and at the same temperature as those crosslinked on both sides as shown in Fig. 6.2. This indicates that crosslinking PVOH with GA on one side for just 5 minutes can improve the thermal stability of PVOH film significantly and that crosslinking on either one side or both sides resulted in the same thermal stability improvement.

6.2 THERMAL STABILITY OF PVOH31 FILM TREATED WITH SODIUM SULPHATE SOLUTION

In Chapter 3, Section 3.5, treatment of PVOH31 films with sodium sulphate solution was reported. Fig. 6.4 shows the TG (a) and DTG (b) thermograms of PVOH films after salt treatment compared to those of neat PVOH films. It can be observed that there was a delay in the degradation temperature after PVOH films were treated with salt solution as evidenced by a shift of the main maximum to higher temperature (Fig. 6.4b). The maximum in the DTG curve of PVOH film at ~290°C shifted to 390°C in films treated with salt solution for 1, 2, 4 and 24 hours indicating higher thermal stability. Like crosslinked PVOH films (see Fig. 6.2), the thermograms of all the PVOH films treated with salt for different lengths of time did not show any significant differences indicating similar thermal stability between these films.

Comparing the DTG thermograms of crosslinked PVOH (one side (Fig. 6.3) and both sides (Fig. 6.2)) and salt treated films (Fig. 6.4) shows that the respective films behaved similarly when subjected to temperature since they showed the same main maxima at ~390°C. The underlying fact for these films is that they have all been treated with Na₂SO₄. It is possibly the presence of Na₂SO₄, which

acts as a barrier to heat, help to improve the thermal stability. This is quite substantial given the small amounts of salt present can improve the thermal stability of the films (see Table 3.7, Section 3.5.7, Chapter 3)

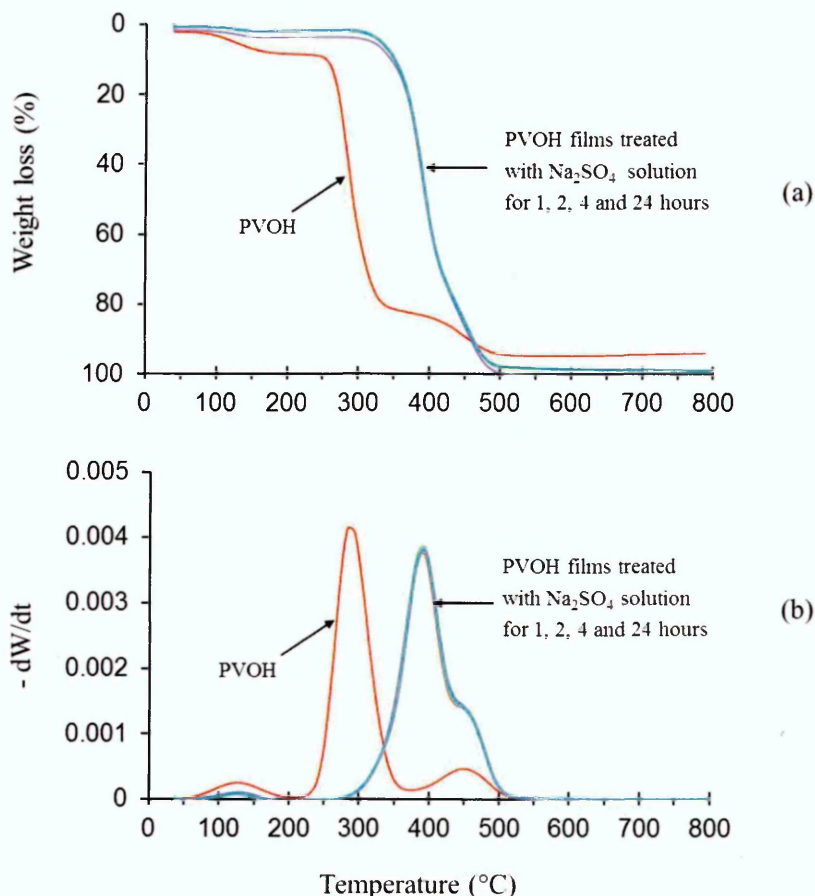


Figure 06.4 (a) TG and (b) DTG thermograms of PVOH films after treatment with Na₂SO₄ solution for different lengths of time

6.3 THERMAL STABILITY OF ANNEALED PVOH31 FILM

As reported in Chapter 4, Section 4.3.4, the TGA investigation of annealed PVOH films was mainly for demonstrating the amount of water present in the films after annealing. Fig. 6.5 shows that the main maxima in the DTG traces for all the annealed films were at the same temperature as neat PVOH film (290°C) indicating that annealing of PVOH films (i.e. the introduction of crystallinity) did not contribute to the thermal stability.

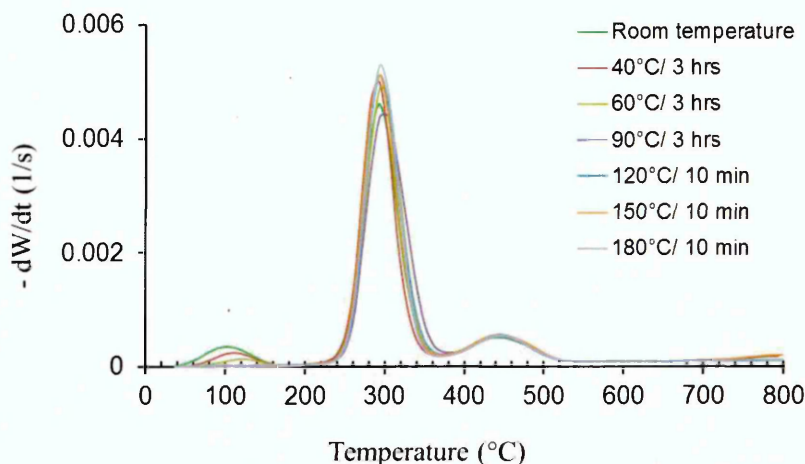


Figure 6.5 DTG thermograms of PVOH31 films after annealing at different temperatures

6.4 THERMAL STABILITY OF PVOH31 FILMS AFTER BENTONITE AND/OR PLASTICISER WAS INCORPORATED AND SUBSEQUENT CROSSLINKED BY GA

6.4.1 Thermal stability of PVOH and crosslinked films containing NaMMT.

The thermal stabilities of PVOH and PVOH/Clay films containing 5-20 wt% clay (Chapter 5, Section 5.3) were investigated by TGA and are described in Fig. 6.6. No significant weight loss was observed in the TGA curve of NaMMT indicating its good resistance to thermal degradation; whereas, for all PVOH/Clay films, their degradation occurred in two steps similar to neat PVOH in which the second step was in the same temperature range as that of PVOH film (390-520°C). The weight loss up to 200°C was due to the evaporation of water present in the films. It is shown in Fig. 6.6b that the main maximum observed in the DTG of PVOH film shifted to higher temperatures when clay was present in the film. There was no significant difference between the thermograms of NaCF5 and NaCF10 films in which the maxima were present at 300°C, whereas increasing the clay loading to 20 wt% resulted in a shift of the maximum to 315°C. As can be seen in Fig. 6.6a, the higher clay content, the more residues remained after thermal decomposition. At 520°C, the residual amounts of the

NaCF5, NaCF10 and NaCF20 were 12%, 16% and ~27%, respectively which was attributed to the residual clay and carbonaceous char from the degradation of PVOH.

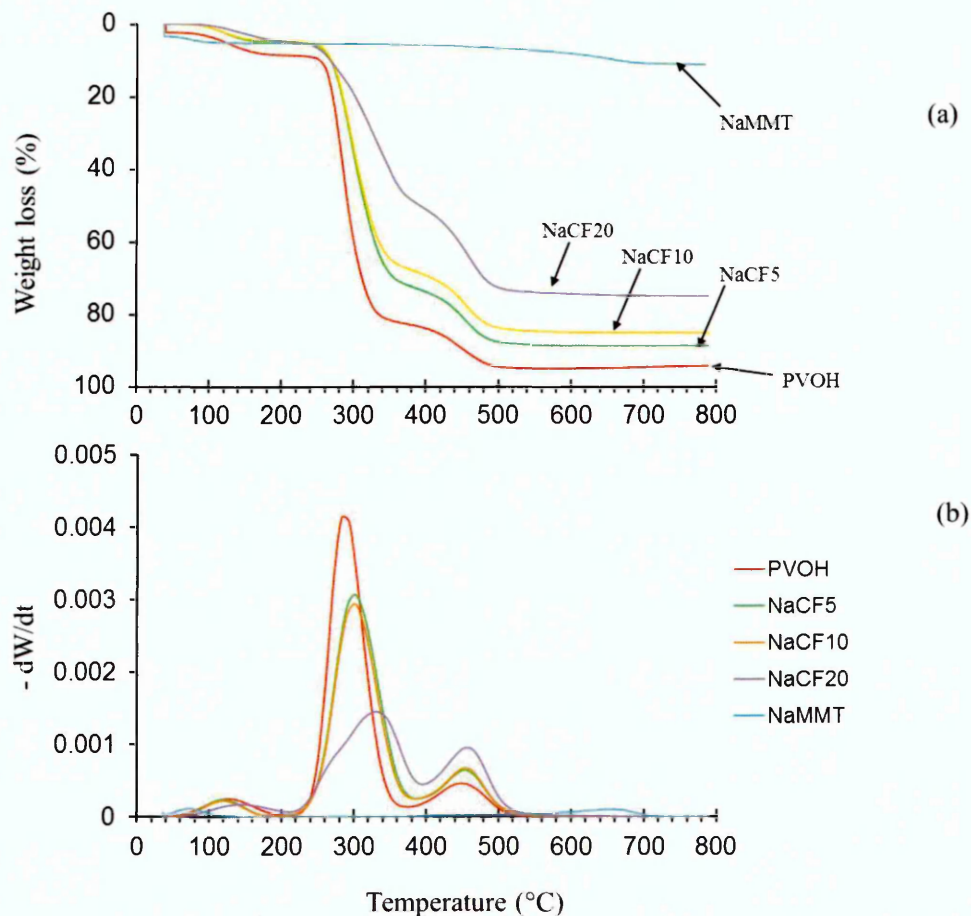


Figure 6.6 (a) TG (b) DTG thermograms of PVOH/Clay films with different amount of clay

The results indicate that more thermally stable films can be obtained with the incorporation of clay. In PVOH film, clay acts as a barrier to heat and thus slows down the heat transfer process within the polymer. It can also restrict any volatile decomposition products from leaving the polymer which contributes to retard the degradation process through the polymer [109,209]. In addition, the well dispersed NaMMT in PVOH as exfoliated and/or intercalated structures (see Section 5.3) is a possible further explanation for the improved thermal stability

since the mobility of polymer chains may be restricted and suppress the degradation reaction resulting in higher decomposition temperature.

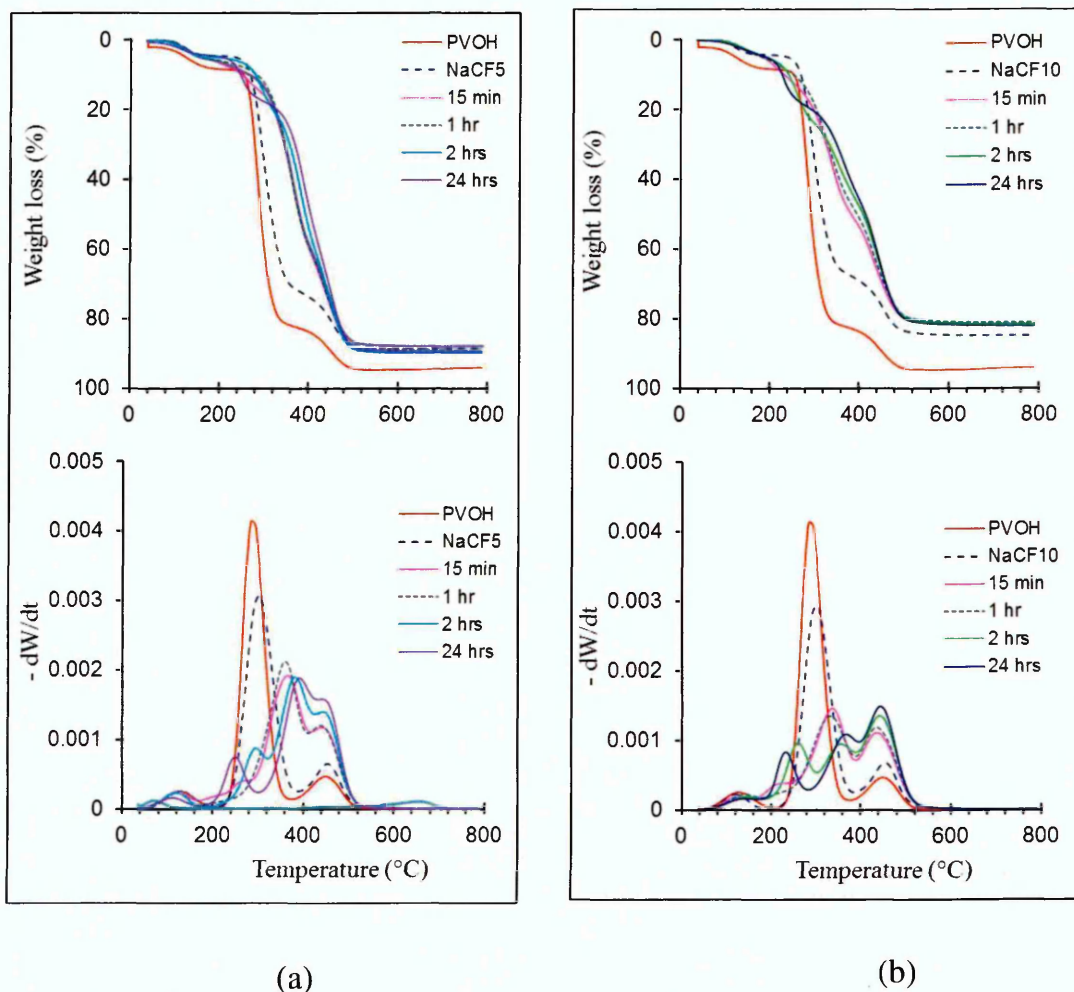


Figure 6.7 TG and DTG thermograms of (a) NaCF5 and (b) NaCF10 after crosslinking with GA with different crosslinking times

When NaCF5 and NaCF10 films were crosslinked with GA, a much greater and significant delay on thermal degradation was observed indicating better thermal stabilities (Fig. 6.7 and Table 6.1). The degradation rates (i.e. maxima intensity) were also significant lower for crosslinked PVOH/Clay films than for un-crosslinked films. The weight loss up to 200°C was attributed to the loss of absorbed water. Figure 6.7a shows that when NaCF5 film was crosslinked for 15 minutes and 1 hour, their main degradation maxima in the DTG curves were not

much different (360-370°C), the decomposition also occurred in two steps like un-crosslinked PVOH and NaCF5 films. With 2 and 24 hours of treatment time, the degradation of the crosslinked NaCF5 films occurred in three steps in addition to a shift of the main maxima to higher temperatures (380-390°C). Two small maxima appear as the first degradation step in the DTG traces of 2 and 24 hours crosslinked films of which that for the latter is at a lower temperature. This may be attributed to the breaking of pendant aldehydes which were created concurrently with crosslinks and are easily cleaved at lower temperature [53]. The longer the crosslinking time, the more pendant GA molecules will be present leading to more weight loss at the first degradation step.

For crosslinked NaCF10 films (Fig. 6.7b), the degradation of the crosslinked films was similar to those of the crosslinked NaCF5 films. To compare the thermal stability between crosslinked PVOH/Clay films and crosslinked PVOH31 films, the temperatures of each maxima and corresponding weight loss were utilised, these are described in Table 6.1. It is shown that in comparison with crosslinked PVOH films, crosslinked NaCF5 and NaCF10 films did not show higher thermal stability and decomposed at lower temperatures than crosslinked PVOH films.

In summary, when NaMMT was incorporated into PVOH, the PVOH/Clay films showed some improved thermal stability. This improvement was not significantly different between PVOH films containing 5 and 10 wt% NaMMT but became noticeable when increasing clay loading to 20 wt%. Crosslinking these films with GA for 15 minutes or 1 hour led to much greater improvement in thermal stability in comparison with un-crosslinked PVOH and PVOH/Clay films. With longer crosslinking times (2 and 24 hours), a decomposition at low temperature (200-300°C) was observed which was possibly due to grafted pendant aldehyde molecules in the main chains. However, FTIR results in Chapter 3 (Section 3.4.7) and Chapter 5 (Section 5.4.2) showed no evidence of the pendant aldehyde with crosslinking times of 24 hours or below.

Table 6.1 Degradation steps with maxima and corresponding weight losses of crosslinked PVOH, NaCF5 and NaCF10 films prepared with different crosslinking times.

	Crosslinking time	Region of decomposition					
		1		2		3	
		Peak maxima	Weight loss (%)	Peak maxima	Weight loss (%)	Peak maxima	Weight loss (%)
Crosslinked PVOH, NaCF5* and NaCF10** films	15 min			390	80.7	450	97.2
				360*	62.8*	440*	88.8*
				340**	51.3**	440**	80.6**
	1 hr			390	79.5	450	97.2
				365*	62.3*	440*	88.2*
				340**	49.1	440**	79.9**
	2 hrs	---	---	390	79.5	450	97
		290*	21.1*	380*	67.1*	450*	89.3*
		260**	24.4**	350**	47.7**	450**	80.3**
	24 hrs	240	11.5	390	63.9	450	95.6
		250*	18*	390*	63.4*	450*	88.7*
		230**	19.1**	370**	42.7**	450**	80.7**

(*) - Crosslinked NaCF5 films (**) - Crosslinked NaCF10 films

6.4.2 Effect of plasticiser on the thermal stability of PVOH and PVOH/Clay films.

Fig. 6.8 presents TG and DTG thermograms of PEG, PVOH and PVOH/Clay (10 wt% clay) films containing 20 wt% PEG400. The PEG alone exhibited one degradation step with a single temperature maximum at 350°C. Similar to the DTG curve of neat PVOH film, the DTG curve of PVOH/PEG film shows two degradation steps with its main maxima present between those of neat PVOH and PEG400 alone, which was approximately 15°C higher than that of neat PVOH film. Additionally, it can be observed that the maximum weight loss rate (i.e. maximum intensity) of PVOH/PEG was lower than that of neat PVOH film. The results are in agreement with Li *et al.* [57] who reported the possibility of hydrogen bonding between PVOH and PEG stabilising the polymer chains and

thus resulting in a higher thermal stability. Another possible explanation is that the enhancement in thermal stability is simply due to an average of the combined thermal stabilities between PVOH and PEG400.

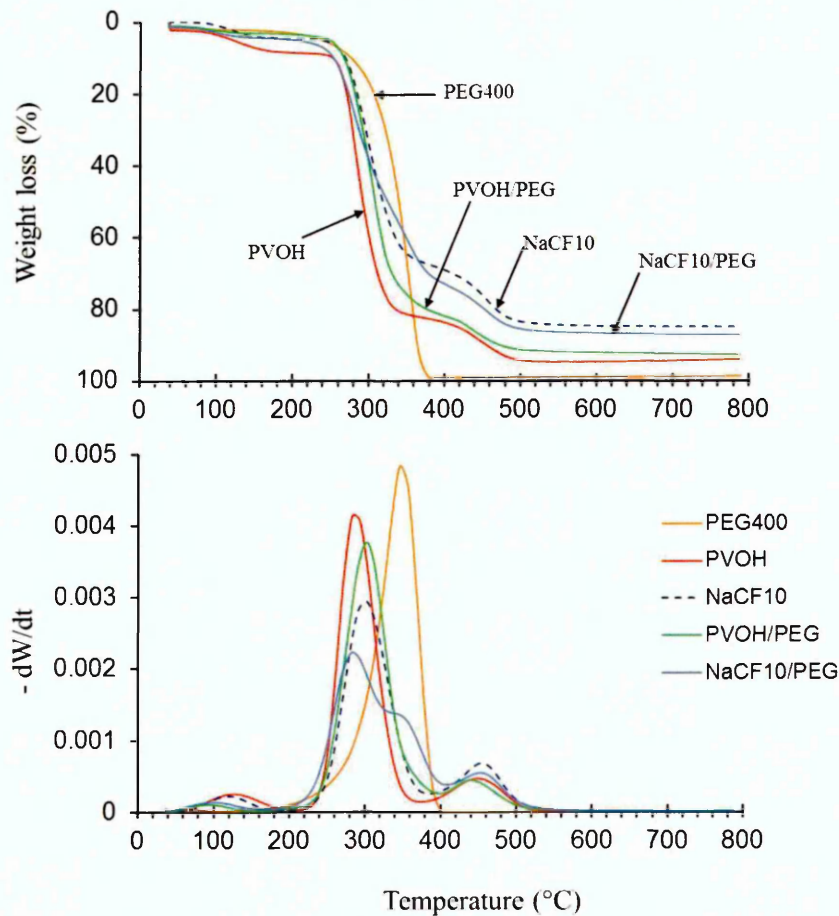


Figure 6.8 TG and DTG curves of plasticised PVOH and PVOH/Clay films in comparison with films without PEG

When 20 wt% PEG400 was present in the PVOH/Clay film containing 10 wt% clay (NaCF10/PEG), the main maximum occurred at a lower temperature (285°C) than that of NaCF10 film (300°C) indicating that degradation occurred at a lower temperature in the presence of PEG400. A maximum at 350°C was also observed in the DTG curve of NaCF10/PEG, which was also at the same position of that for PEG400. The results show that the first degradation step of NaCF10/PEG film was due PVOH present in the film whereas the shouldering peak at 350°C was attributed to the presence of PEG.

Overall, the presence of PEG in the PVOH and PVOH/PEG did not affect the thermal stability of the films significantly.

6.5 CONCLUSION

When PVOH31 film was crosslinked with GA, the thermal stability improved significantly with a shift of the main maxima by 100°C to higher temperature. The decomposition was similar for all PVOH crosslinked films whether treated on one side or both sides, or with different crosslinking times. Crosslinking PVOH films on one side for just 5 minutes imparted a significant increase in thermal stability regardless of the annealing temperature before crosslinking.

The salt treated PVOH films exhibited higher thermal stability than PVOH films and there was no significant difference between samples treated with sodium sulphate with different lengths of time. Whereas, annealing PVOH did not contribute to thermal stability improvement. The incorporation of NaMMT into PVOH31 induced slightly higher thermal stability properties. For PVOH/Clay films containing 5, 10 and 20 wt% NaMMT, the NaCF20 film showed the highest thermal stability. Crosslinking the NaCF5 and NaCF10 film with GA also help to improve the thermal stability of the films compared to those of un-crosslinked PVOH and PVOH/Clay films. However, the crosslinked NaCF5 and NaCF10 films were less thermally stable than crosslinked PVOH films.

In general, PEG400 did not affect the thermal stability of PVOH and PVOH/Clay films significantly even though its presence in these films (20 wt%) caused a slight shift of the main maxima by 15°C.

Conclusion and Future work

7.1 CONCLUSION

Relative humidity, film thickness and polymer molecular weight have considerable impact on the WVTR values of PVOH films. An increase in relative humidity led to a corresponding increase in WVTR values as well as the permeability coefficient. With low RH's of 50 and 75% at 23°C, films showed good resistance to water vapour with WVTR values below 50 g/(m².day). With 85 and 95% RH at 23°C, the WVTR values increased to 310 and 1683 g/(m².day), respectively. Increasing film thickness or molecular weight of PVOH led to a decrease in WVTR's of polymer films. The WVTR values of PVOH124 ($M_w = 124,000-186,000$) were 30% lower than those of PVOH31 ($M_w = 31,000-50,000$). The vapour permeability P was shown to increase with thickness whereas the WVTR values were proportional to *thickness*^{-x} where x = 0.8-1.

Crosslinking with GA, salt treatment with sodium sulphate solution, heat treatment and clay incorporation were utilised to enhance the water vapour barrier properties of PVOH31 films. Fig. 7.1 summarise WVTR values of PVOH31 films after being treated by the different methods. Most of the modification methods resulted in a decrease in the WVTR values, except for the incorporation of plasticiser.

❖ The crosslinking reaction with GA and salt treatment with Na₂SO₄ solution are very effective and comparable in improving the water vapour barrier properties of PVOH films in which the WVTR decreased by more than 60%. In Chapter 3, it was shown that GA was effective in reducing the WVTR's for PVOH films when using short (5 minutes) and medium (2 hours) crosslinking times and a molar ratio of 4:1 between PVOH repeat unit and GA. However, extending the crosslinking time had a negative effect on the water vapour barrier properties of the films due to an increase in the number of acetal linkages within crosslinks

which have good affinity to water. For sodium sulphate treated films, the different treatment times did not produce any considerable differences in WVTR values and so shows that the increase in WVTR values with extended crosslinking time (more than 2 hours) was due to the crosslinking GA and not an effect from the salt. With 1 hour of salt treatment time, the WVTR values were $\sim 89 \text{ g}/(\text{m}^2.\text{day})$ showing an improvement in water vapour barrier properties by 71%.

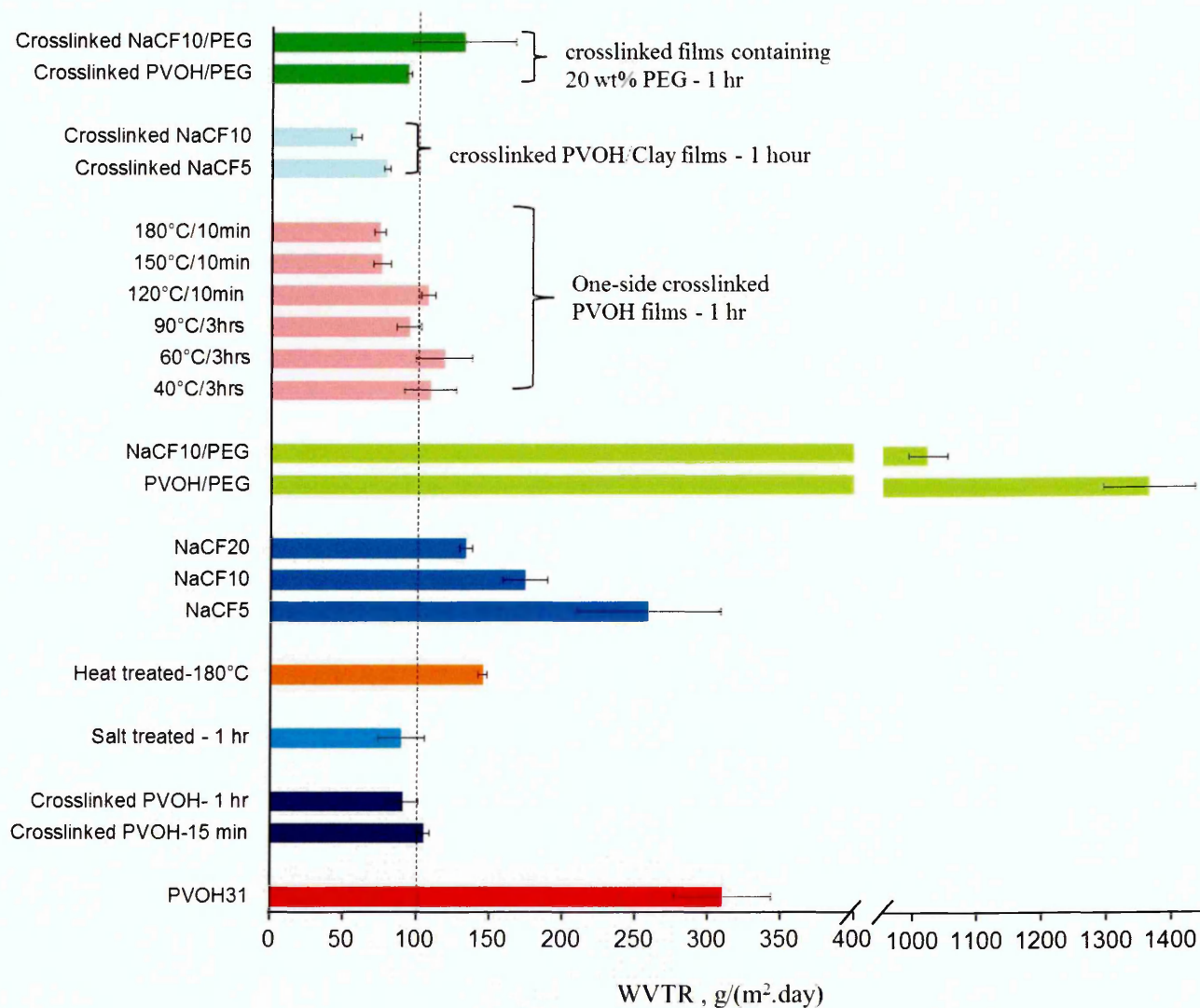


Figure 7.1 WVTR (23°C, 85% RH) values of PVOH31 films after being treated with different modification methods

The heat treatment (Chapter 4) and incorporation of bentonite (Chapter 5) can also help to reduce the WVTR values of PVOH films but by not as much as the

crosslinking and salt treatment methods. When heating PVOH film at 40°C/3hrs, 60°C/3hrs, 90°C/3hrs, 120°C/10min, 150°C/10min and 180°C/10min, the WVTR's decreased with the lowest values being obtained when annealing at 180°C (145 g/(m².day)), expressing an improvement of 53% in comparison with the untreated PVOH film (310 g/(m².day)). In PVOH/Clay films, NaMMT acts as impermeable sites to restrict the diffusion of the penetrant molecules into the films, forcing them to follow longer and more tortuous paths resulting in the higher resistance to water vapour molecules. The water vapour barrier properties improved when clay was present and increased with increasing clay content, in which the improvements were 16.3%, 43.7% and 57% when 5, 10 and 20 wt% NaMMT were added, respectively. Crosslinking the PVOH/Clay films resulted in much lower WVTR values which are comparable but slightly lower than those of respective crosslinked PVOH films and salt treated films. With 1 hour of crosslinking treatment and when compared to un-crosslinked PVOH/Clay films, the improvements in water vapour barrier properties in the crosslinked films were 69% and 67% for NaCF5 and NaCF10, respectively; whereas that for respective crosslinked PVOH films was 70%.

The series FTIR experiment showed that when in contact with one surface of PVOH film, the crosslinking solution can diffuse from the top to the bottom of the film. One-side crosslinking reaction between PVOH31 and GA was successful in improving the water vapour barrier properties of the films as well as reducing the amount of chemical used thus potentially reducing cost. Fig. 7.1 also shows that their WVTR values are comparable to those of the both-side crosslinked films. The one-side crosslinking reactions occurred more effectively in the films annealed at low temperatures (40, 60 and 90°C) than those heated at higher temperatures (120, 150 and 180°C) due to the higher crystallinity in the films annealed at high temperatures which hindered the penetration of the crosslinking solution. The water vapour barrier properties of the crosslinked films prepared at the high annealing temperatures prior to crosslinking were higher than those of the others at lower annealing temperatures despite fewer crosslinks in their structures.

The incorporation of plasticiser into PVOH film caused a negative effect on its water vapour barrier property (see Section 5.5). With 20 wt% PEG400 present in PVOH and PVOH/Clay film (10 wt% clay), the water vapour barrier properties decreased by 4.4 and 5.8 times with corresponding WVTR values of 1366 and 1022 g/(m².day), respectively. During the crosslinking reaction with GA, the PEG400 leached out as evidenced by a corresponding decrease in weight after crosslinking. The crosslinked plasticised films possessed low WVTR values comparable to those of crosslinked films without PEG. Although it was the intention for the PEG to remain in the films, its presence may have provided voids within the PVOH and PVOH/Clay films after leaching in which water may have passed more freely, however this does not seem to have been the case.

❖ PVOH and PVOH/Clay films dissolved after being immersed in water for 15 minutes. After heat treatment at different temperatures for specific lengths of time and then being immersed in water for 24 hours, PVOH films treated at 120, 150 and 180°C for 10 minutes swelled while the others at 40, 60 and 90°C for 3 hours dissolved, disintegrated or became a gel, respectively. In the case of salt treated films, all the films swelled in cold water (22°C, 24 hours) but dissolved at 45°C. The degree of swelling in water at 22°C of films treated with salt solution for 15 minutes and 24 hours were 730 and 150%, respectively, compared to 84% and 24% of the respective both-side crosslinked PVOH films.

After crosslinking with GA on both sides, the PVOH and PVOH/Clay films were stable, i.e. did not dissolve, even in hot water (90°C, 24 hours), and this was notably the case with short crosslinking times (5 minutes). One-side crosslinked PVOH and PVOH/Clay film also did not dissolve in hot water but became a gel after being plotted with paper or being stuck to the plotted paper in the case of one-side crosslinked PVOH film. However, when increasing the annealing temperatures of PVOH films prior to one-side crosslinking reaction, all the one-side crosslinked PVOH films swelled in cold water (22°C) but behaved differently in hot water (90°C). When the films crosslinked on one side for 5 minutes and pre-treated at 120, 150 and 180°C were placed in hot water, they

dissolved partially, majorly or completely, respectively but for those treated at lower temperatures (40, 60 and 90°C), the respective crosslinked films became swollen and formed gels. It could be explained by the high retainment of crystallinity in the films annealed at higher temperatures prior to crosslinking which hindered the penetration of GA resulting in fewer crosslinks being produced.

Annealing films at high temperature can induce the crystallinity and therefore improve water vapour barrier properties. However some studies have suggested that the degree of crystallinity can decrease when the films are exposed to high humid environments for a duration of time [205]. Therefore, crosslinking films on one side may be an effective measure in reducing the loss of water vapour barrier properties. In addition, the one-side crosslinked films with short crosslinking times are able to dissolve in hot water which may contribute to reprocessing/ recycling and not hinder its biodegradation.

❖ Heat treatment of PVOH films at 40°C/3hrs, 60°C/3hrs, 90°C/3hrs, 120°C/10min, 150°C/10min and 180°C/10min induced increases in the degree of crystallinity as demonstrated by FTIR, Raman and XRD results (Chapter 4). The samples annealed at 40 and 60°C were similar in their properties to unheated PVOH while the films at 180°C possessed the highest degree of crystallinity (39.2%) and also the lowest WVTR value. On the contrary, the crosslinking reaction with GA decreased the crystallinity of the PVOH films as evidenced by a decrease in the intensity of crystalline representative peaks at 1142 cm⁻¹ and 845 cm⁻¹ in their FTIR spectra. As the crosslinking time increased, there was an increase in the crosslinking degree but a decrease in the crystallinity. By using weight gain of the film after the crosslinking reaction, the maximum degree of crosslinking was achieved at 24 hours of crosslinking times with a value of 26.5%.

During the salt treatment from 1 to 24 hours, the degree of crystallinity of PVOH film did not change significantly as demonstrated by the FTIR and XRD results. No evidence of any chemical interactions between PVOH and Na₂SO₄ as well as no significant differences in terms of chemical structure between sample treated

with salt solution for different time lengths were observed using these techniques. Therefore, the considerable improvement in the water and water vapour resistance of PVOH films after salt treatment despite the low levels of salt present in the films (for example, the 4-hour salt treated PVOH film contained 187 and 118 ppm ions Na^+ and SO_4^{2-}) was possibly explained by the "salting out" effect of sodium sulphate, in which the SO_4^{2-} anion polarises and removes the water molecules that hydrogen bond between PVOH molecules thus increasing the hydrophobic interface between PVOH and water to stabilise the polymer. At the same time, it presumably facilitated the rearrangement and packing of PVOH molecules leading to better resistant to water molecules but not enough to gain higher crystallinity.

When 5% wt NaMMT was present in PVOH, a very disordered, if not exfoliated structure was achieved and is due to a similar polarity for clay and polymer. With higher clay content (10 and 20 wt%), very well dispersed structures were still present in the polymer matrix. Based on FTIR results, no significant change in crystallinity was observed when incorporating 5 and 10 wt% clay, but with 20 wt% clay loading, the crystallinity increased significantly. From XRD data, crystallite sizes were shown to increase with 20 wt% but decrease with 5 and 10 wt% clay present. Under visual observation and manual handling, the PVOH/Clay films were brittle and the brittleness increases with increased clay amount. NaCF10 films showed higher improvement in the water vapour barrier properties compared to NaCF5 films and are less brittle than NaCF20 films.

For heated and then one-side crosslinked films, both crosslinks and crystallinity contributed to the water and water vapour barrier properties of the films. Films pre-heated at lower temperatures prior to the crosslinking reactions had a lower degree of crystallinity than those treated at higher temperatures. Therefore, for those heated at low temperatures (40, 60 and 90°C for 3 hours) their water vapour barrier properties were mainly contributed to by the crosslinks. On the contrary, the one-side crosslinked films of those annealed at 150 and 180°C possessed fewer crosslinks due to their higher degrees of crystallinity which hindered the penetration and diffusion of GA to crosslink the O-H groups. However, their water vapour barrier properties were still higher than those of

lower annealing temperatures. In hot water, the films crosslinked on one side for 5 minutes and annealed at 150 and 180°C prior to crosslinking dissolved due to the dissolution of their crystallites which requires high temperature (90°C).

❖ The DMA results showed that the both-side crosslinked PVOH films had higher T_g (77.5 to 199.5°C with 5 minutes to 48 hours of crosslinking times) than neat PVOH (50°C) thus possessing a higher operating application temperature range. In addition, DMA evidence indicated a more flexible structure was present in the crosslinked films compared to the neat PVOH films. For salt treated PVOH films, higher flexibility and T_g were observed compared to that of neat PVOH film. There were no significant differences between T_g values of samples treated with salt solution for different duration of times, in which the values were about 75-80°C. In comparison with T_g values of the respective crosslinked PVOH films (127-232°C), the values of salt treated films were lower.

For heat treated films, the DMA results did not show a strong systematic trend. Films annealed at 120°C/10min had the lowest T_g temperature (55°C). Increasing the annealing temperature did not necessarily lead to an increase in the T_g value. The T_g temperature also increased when clay was added into the polymer. With 10 wt% clay loading, the PVOH/Clay film had a T_g of 60°C.

With 20 wt% PEG present in the films, the T_g increased for PVOH films (72°C) but did not change significantly in PVOH/Clay 10 wt% films when compared to their respective un-plasticised films. This may be due to hydrogen bonding production between PEG and PVOH.

❖ The TGA results in Chapter 6 showed that when PVOH31 film was crosslinked with GA, the thermal stability improved significantly with a shift of the main maxima in the DTG curves by 100°C to higher temperature. The decomposition was similar for all PVOH crosslinked films whether treated on one side or both sides, or with different crosslinking times. Crosslinking PVOH

films on one side for just 5 minutes imparted a significant increase in thermal stability regardless of the annealing temperature before crosslinking.

The salt treated PVOH films exhibited higher thermal stability than PVOH films and there was no significant difference between samples treated with sodium sulphate with different lengths of time. Again, the decomposition was similar for salt treated films and crosslinked PVOH films with a shift of the main maxima by 100°C to higher temperature. Annealing PVOH did not contribute to thermal stability improvement. The incorporation of NaMMT into PVOH31 induced slightly higher thermal stability properties. For PVOH/Clay films containing 5, 10 and 20 wt% NaMMT, the NaCF20 film showed the highest thermal stability with the main maxima in the DTG curve at 315°C in comparison with that of neat PVOH at 290°C. Crosslinking the NaCF5 and NaCF10 film with GA also help to improve the thermal stability of the films compared to those of un-crosslinked PVOH and PVOH/Clay films. However, the crosslinked NaCF5 and NaCF10 films were less thermally stable than crosslinked PVOH films.

When 20 wt% PEG was present in the films, in general, PEG400 did not affect the thermal stability of PVOH and PVOH/Clay films significantly even though its presence in these films (20 wt%) caused a slight shift of the main maxima by 15°C to either higher or lower temperature.

7.2 FUTURE WORK

The degrees of crystallinity of PVOH and its modified films in this thesis were calculated using an equation derived from the literature [37] which was based on FTIR spectra. Although XRD can be used to measure the crystallinity degree of PVOH films by deconvoluting the diffraction peaks, its application is rather complicated since PVOH is a semi-crystalline polymer without very clear defined crystalline and amorphous diffraction peaks in the XRD diffractometer. In order to substantiate or provide a more accurate evaluation of the crystallinity, other techniques are suggested to be used, including differential scanning calorimetry (DSC) and density measurements. DSC may prove troublesome

since its degradation occurs before and during the melting point, and may result in erroneous data. Ideally, standards of known crystallinity could be utilised to form a calibration for either the FTIR, DSC or XRD measurements, but obtaining such calibration is not easy to source.

It should be interesting to study the crosslinking reaction between PVOH and other crosslinkers using similar preparation methods as used in this thesis. The effect of glyoxal on the water vapour barrier properties of PVOH films has already been investigated. The preliminary results show that when PVOH31 films were crosslinked with glyoxal from 15 minutes to 24 hours, the WVTR values decreased by 75% and were not significantly different between various crosslinking times. Further assessments are required in order to evaluate whether this improvement is due to the effect of salt in the crosslinking solution or the crosslinking effect by glyoxal. Boric acid is also an alternative crosslinker that could be utilised for PVOH. Alternatively, PVOH films may be crosslinked by using electron-beam irradiation.

Sodium sulphate has proved to show a considerable effect on improving the water vapour barrier properties of PVOH films. A study about the influence of other salts such as sodium chloride, potassium chloride or potassium sulphate in comparison with the effect of sodium sulphate on the water vapour barrier properties of PVOH is recommended. Alternatively, sodium trimetaphosphate ($\text{Na}_3\text{O}_9\text{P}_3$) is also an option as it is currently used within the food industry and is non-toxic towards human.

For the incorporation of bentonite in PVOH films so far, only the clay amount of 10 wt% has been investigated more deeply than the other amounts. Other clay contents such as 5 and 20 wt% should be investigated in terms of changes in crystallinity and dynamic mechanical properties. Properties of the all PVOH/Clay films after crosslinking with GA should be analysed in order to have a substantial evaluation about the effect of clay in PVOH films. In addition, with its tortuous path effect, clay particles hinder the penetration of GA during the crosslinking reaction. Therefore, the location of crosslinks in the PVOH/Clay films could be analysed using Raman depth profile or FTIR imaging along the edge of a fractured film or microtomed section.

Due to the leaching of PEG400 (as well as PEG600 and PEG1000) during the crosslinking reaction, the crosslinked plasticised films did not possess any desired improvement in flexibility. Therefore, a more suitable plasticiser for PVOH films should be found which does not leach out during the crosslinking reaction and thus can retain any flexibility in the crosslinked products. Some suggested plasticisers include glycerol, glycerine and propylene glycol.

Study about the biodegradability of crosslinked PVOH films is required to evaluate how this property changes after crosslinking with GA. PVOH is soluble in water thus it is easily attacked and decomposed by bacteria. The fact is that the both-side crosslinked PVOH films are stable even in hot water (i.e. not dissolve) while the one-side crosslinked films swell, dissolve or form gels depending on the annealing temperature before crosslinking reaction and the length of crosslinking time. One can assume that the biodegradation will still occur because the primary linkages formed contain C-O bands and these are anticipated to be broken down by bacteria. In order to check this hypothesis, further methods for biodegradability investigation of crosslinked films should be carried out, including soil burial and enzymatic degradation tests.

The application of the different modification methods on PVOH-coated paper is one of the next logical steps in order to evaluate their influences on the water vapour transmission rates and other properties. Paper can be coated with PVOH solution standard coating, rolling or dipping in PVOH solution. PVOH coated paper can then be treated by coating methods and subjected to heat. Furthermore, all these coating techniques can be realised in an industry context.

REFERENCES

- [1] British Plastic Federation [online].
http://www.bpf.co.uk/Sustainability/Plastics_and_Sustainability.aspx#Packaging%2%A0
Last access 20 Oct 2015.
- [2] Tolinski M. *Plastics and Sustainability: towards a peaceful coexistence between bio-based and fossil fuel-based plastics.* : Wiley, 2011.
- [3] Paine F, Paine H. *A handbook of food packaging.* Glasgow: Leonard Hill, 1983.
- [4] Vroman I, Tighzert L. *Biodegradable polymers.* Materials 2009;2:307-44.
- [5] Johansson C, Bras J, Mondragon I, Nechita P, Plackett D, Simon P, Svetec D, Virtanen S, Baschetti M, Breen C, Clegg F, Aucejo S. *Renewable fibers and bio-based materials for packaging applications - a review of recent developments.* Bioresources 2012;7:2506-52.
- [6] Weber C. *Biobased packaging materials for the food industry: Status and perspectives.* A European Concerted Action 2000.
- [7] World Packaging Organisation/ PIRA International Ltda. *Market statistics and future trends in global packaging.* 2008.
- [8] Markets and Markets. <http://www.marketsandmarkets.com/Market-Reports/paper-paperboard-packaging-market-23392290.html>
Last access 20 Oct 2015.
- [9] Han J editor. *Innovations in Food Packaging, 2nd edition.* USA: Elsevier, 2014.
- [10] Zhang Z, Britt I, Tung M. *Water absorption in EVOH films and its influence on glass transition temperature.* Journal of Polymer Science Part B: Polymer Physics 1999;37:691-9.
- [11] Despond S, Espuche E, Cartier N, Domard A. *Barrier properties of paper-chitosan and paper-chitosan-carnauba wax films.* Journal of Applied Polymer Science 2005;98:704-10.
- [12] Khwaldia K, Arab-Tehrany E, Desobry S. *Biopolymer coatings on paper packaging materials.* Comprehensive Reviews in Food Science and Food Safety 2010;9:82-91.

- [13] Andersson C. *New ways to enhance the functionality of paperboard by surface treatment—a review*. Packaging Technology and Science 2008;21:339-73.
- [14] Johansson C, Clegg F. *Effect of clay type on dispersion and barrier properties of hydrophobically modified poly (vinyl alcohol)–bentonite nanocomposites*. Journal of Applied Polymer Science 2015;132:42229.
- [15] Johansson C, Clegg F. *Hydrophobically modified poly (vinyl alcohol) and bentonite nanocomposites thereof: Barrier, mechanical, and aesthetic properties*. Journal of Applied Polymer Science 2015;132:41737.
- [16] Vyorykka J, Zuercher K. *Aqueous polyolefin dispersion - for low energy polyolefin melt application*. . 12th TAPPI European PLACE Conference 18-20 May 2009.
- [17] Khwaldia K. *Water vapour barrier and mechanical properties of paper-sodium caseinate and paper-sodium caseinate-paraffin wax films*. Journal of Food Biochemistry 2010;34:998-1013.
- [18] Kittur F, Kumar K, Tharanathan R. *Functional packaging properties of chitosan films*. Zeitschrift Für Lebensmitteluntersuchung Und-Forschung A 1998;206:44-7.
- [19] Gällstedt M, Brottman A, Hedenqvist M. *Packaging-related properties of protein-and chitosan-coated paper*. Packaging Technology and Science 2005;18:161-70.
- [20] Parris N, Vergano P, Dickey L, Cooke P, Craig J. *Enzymatic hydrolysis of zein-wax-coated paper*. Journal of Agricultural and Food Chemistry 1998;46:4056-9.
- [21] Back E. *Autodispersible waxes for recyclable packaging papers. 1. Principles for wax removal after alkaline hot dispersion*. Tappi Journal (USA) 1995;78.
- [22] Visakh P, Oguz B, Guillermo P. *Polyelectrolyte: thermodynamics and rheology*. Switzerland: Springer, 2014.
- [23] Thomas S, Durand D, Chassenieux C, Jyotishkumar P. *Handbook of biopolymer-based materials: from blends and composites to gels and complex networks*. : John Wiley & Sons, 2013.
- [24] European Bioplastics. *FACT SHEET - What are bioplastics? - Material types, terminology and labels - an introduction*. 2014.
- [25] Saunders KJ. *Organic polymer chemistry: An introduction to the organic chemistry of adhesives, fibres, plastics, and rubbers*. London: Chapman and Hall, 1973.

- [26] Edwards D. *The unsung polymer: polyvinyl alcohol*
<http://www.packagingtoday.co.uk/features/featurethe-unsung-polymer-polyvinyl-alcohol/>. Packaging Today 2012.
- [27] SEKISUI. *Brochure: Selvol - Polyvinyl alcohol... A versatile performance in paper and paperboard applications*. 2011.
- [28] Kuraray.
http://www.kuraray.eu/fileadmin/Downloads/exceval/TDS_Exceval_en.pdf
http://www.poval.jp/english/poval/s_grades/sg_r.html. ;2015.
- [29] Bolto B, Tran T, Hoang M, Xie Z. *Crosslinked poly(vinyl alcohol) membranes*. Progress in Polymer Science 2009;34:969-81.
- [30] Gonzalez J, Alvarez V. *The effect of the annealing on the poly (vinyl alcohol) obtained by freezing–thawing*. Thermochimica Acta 2011;521:184-90.
- [31] Hassan C, Peppas N. *Structure and applications of poly(vinyl alcohol) hydrogels produced by conventional crosslinking or by freezing/thawing methods*. In: Anonymous Biopolymer . PVA Hydrogels, Anionic Polymerisation Nanocomposites. : Springer Berlin Heidelberg, 2000. p. 37-65.
- [32] Tang X, Alavi S. *Recent advances in starch, polyvinyl alcohol based polymer blends, nanocomposites and their biodegradability*. Carbohydrate Polymers 2011;85:7-16.
- [33] Iwaseya M, Watanabe M, Yamaura K, Dai L, Noguchi H. *High performance films obtained from PVA/Na₂SO₄/H₂O and PVA/CH₃COONa/H₂O systems*. Journal of Materials Science 2005;40:5695-8.
- [34] Tretinnikov O, Zagorskaya S. *Effect of alkali halide salt additives on the structure of poly (vinyl alcohol) films cast from aqueous solutions*. Polymer Science Series A 2013;55:463-70.
- [35] Tretinnikov O, Zagorskaya S. *Effect of inorganic salts on the crystallinity of polyvinyl alcohol*. Journal of Applied Spectroscopy 2012;78:904-8.
- [36] Bolto B, Hoang M, Xie Z. *A review of membrane selection for the dehydration of aqueous ethanol by pervaporation*. Chemical Engineering and Processing: Process Intensification 2011;50:227-35.
- [37] Tretinnikov O, Zagorskaya S. *Determination of the degree of crystallinity of poly(vinyl alcohol) by FTIR spectroscopy*. Journal of Applied Spectroscopy 2012;79:521-6.
- [38] Komiya S, Otsuka E, Hirashima Y, Suzuki A. *Salt effects on formation of microcrystallites in poly (vinyl alcohol) gels prepared by cast-drying method*. Progress in Natural Science: Materials International 2011;21:375-9.

- [39] Kuraray Specialties Europe KSE GmbH. *Brochure: Mowiol–Polyvinyl alcohol*. Germany: Frankfurt/ Main, 2003.
- [40] Korodenko G, Lipatov YS, Fabulyak F, Pugachevskii G, Tuichiyev S, Lukashov V. *Effect of sodium acetate on the structure of polyvinyl alcohol*. Polymer Science USSR 1984;26:280-6.
- [41] Sakurada I. *Polyvinyl alcohol fibers*. New York: CRC Press, 1985.
- [42] Shin J, Kim Y, Lim Y, Nho Y. *Removal of sodium acetate in poly (vinyl alcohol) and its quantification by ¹H NMR spectroscopy*. Journal of Applied Polymer Science 2008;107:3179-83.
- [43] Smirnov L, Kulikova N, Platonova N. *Infrared spectra of polyvinylalcohol*. Polymer Science USSR 1967;9:2849-56.
- [44] Haweel C, Ammar S. *Preparation of polyvinyl alcohol from local raw material*. Iraqi Journal of Chemical and Petroleum Engineering (IJCPE) 2008;9:15-21.
- [45] Bunn C. *Crystal structure of polyvinyl alcohol*. Nature 1948;161:929-30.
- [46] Bunn CW, Peiser HS. *Mixed crystal formation in high polymers*. Nature 1947;159:161.
- [47] Kenney J, Willcockson G. *Structure–property relationships of poly (vinyl alcohol). III. Relationships between stereo-regularity, crystallinity, and water resistance in poly (vinyl alcohol)*. Journal of Polymer Science Part A-1: Polymer Chemistry 1966;4:679-98.
- [48] Assender H, Windle A. *Crystallinity in poly (vinyl alcohol). 1. An X-ray diffraction study of atactic PVOH*. Polymer 1998;39:4295-302.
- [49] Peppas N. *Infrared spectroscopy of semicrystalline poly (vinyl alcohol) networks*. Die Makromolekulare Chemie 1977;178:595-601.
- [50] Peppas N, Hansen P. *Crystallization kinetics of poly (vinyl alcohol)*. Journal of Applied Polymer Science 1982;27:4787-97.
- [51] Peppas N, Merrill E. *Poly (vinyl alcohol) hydrogels: Reinforcement of radiation-crosslinked networks by crystallization*. Journal of Polymer Science: Polymer Chemistry Edition 1976;14:441-57.
- [52] Marten F. *Vinyl alcohol polymers..* In: Seidel A, Bickford M, editors. Kirk-Othmer Encyclopedia of Chemical Technology. : Wiley Online Library, 2002.
- [53] Park J, Park J, Ruckenstein E. *On the viscoelastic properties of poly(vinyl alcohol) and chemically crosslinked poly(vinyl alcohol)*. Journal of Applied Polymer Science 2001;82:1816-23.

[54] Kumar S, Majhi MR, Singh VK. *Preparation of porous magnesium by decomposing an extract known as starch soluble ($C_6H_{10}O_5$)N*. American Journal of Scientific and Industry Research 2014;5(4):120-5.

[55] Jang J, Lee D. *Plasticizer effect on the melting and crystallization behavior of polyvinyl alcohol*. Polymer 2003;44:8139-46.

[56] Lim L, Wan L. *The effect of plasticizers on the properties of polyvinyl alcohol films*. Drug Development and Industrial Pharmacy 1994;20:1007-20.

[57] Li Y, Wu W, Lin F, Xiang A. *The interaction between poly(vinyl alcohol) and low-molar-mass poly(ethylene oxide)*. Journal of Applied Polymer Science 2012;126:162-8.

[58] Krumova M, Lopez D, Benavente R, Mijangos C, Perena J. *Effect of crosslinking on the mechanical and thermal properties of poly (vinyl alcohol)*. Polymer 2000;41:9265-72.

[59] Rumyantsev M. *Influences of polymer conformation on acetalization reaction of poly(vinyl alcohol): langevin dynamics and DFT approaches*. Proceedings of the 15th International Electronic Conference on Synthetic Organic Chemistry 2011;15.

[60] Rumyantsev M, Zelentsov S, Gushchin A. *Retardation effect in acetalization of poly (vinyl alcohol) with butyraldehyde*. European Polymer Journal 2013;49:1698-706.

[61] Labuschagne P, Germishuizen W, Verryn S, Moolman F. *Improved oxygen barrier performance of poly(vinyl alcohol) films through hydrogen bond complex with poly(methyl vinyl ether-co-maleic acid)*. European Polymer Journal 2008;44:2146-52.

[62] Sapalidis AA, Katsaros KF, Kanellopoulos KN. *PVA / Montmorillonite nanocomposites: development and properties*. In: Cuppoletti J, editor. Nanocomposites and Polymers with Analytical Methods. InTech - Open access, 2011. p. 29.

[63] Bajpai A. *Document: Clay used as waterproofing material in polymer membranes*. Society of Plastic Engineers 2011.

[64] Sapalidis AA, Katsaros FK, Steriotis TA, Kanellopoulos NK. *Properties of poly(vinyl alcohol)-bentonite clay nanocomposite films in relation to polymer-clay interactions*. Journal of Applied Polymer Science 2012;123:1812-21.

[65] Zhang Y, Zhu P, Edgren D. *Crosslinking reaction of poly (vinyl alcohol) with glyoxal*. Journal of Polymer Research 2010;17:725-30.

[66] Kim K, Lee S, Han N. *Effects of the degree of cross-linking on properties of poly(vinyl alcohol) membranes*. Polymer Journal 1993;25:1295-302.

- [67] Premraj R, Doble M. *Biodegradation of polymers*. Indian Journal of Biotechnology 2005;4:186-93.
- [68] Kawai F, Hu X. *Biochemistry of microbial polyvinyl alcohol degradation*. Applied Microbiology and Biotechnology 2009;84:227-37.
- [69] Suzuki T. *Degradation of poly (vinyl alcohol) by microorganisms*. Journal of Applied Polymer Science Applied Polymer Symposium 1979;35:431-7.
- [70] Watanabe Y, Morita M, Hamada N, Tsujisaka Y. *Formation of hydrogen peroxide by a polyvinyl alcohol degrading enzyme*. Agriculture and Biological Chemistry 1975;39:2447-8.
- [71] SEKISUI. *Brochure: Polyvinyl alcohol - A versatile polymer for specialty coating applications*.
- [72] Patel A, Vavia P. *Evaluation of synthesized cross linked polyvinyl alcohol as potential disintegrant*. Journal of Pharmacy & Pharmaceutical Sciences 2010;13:114-27.
- [73] Peppas N, Merrill E. *Development of semicrystalline poly (vinyl alcohol) hydrogels for biomedical applications*. Journal of Biomedical Materials Research 1977;11:423-34.
- [74] Varshosaz J, Koopaie N. *Cross-linked poly(vinyl alcohol) hydrogel: study of swelling and drug release behaviour*. Iranian Polymer Journal 2002;11:123-31.
- [75] Jain D, Carvalho E, Banthia A, Banerjee R. *Development of polyvinyl alcohol-gelatin membranes for antibiotic delivery in the eye*. Drug Development and Industrial Pharmacy 2011;37:167-77.
- [76] National Occupational Health and Safety Commission. *Priority existing chemical No. 3 glutaraldehyde: Full public report*. Canberra: Australian Government Publishing Service 1994.
- [77] Morris J. *A formaldehyde glutaraldehyde fixative of high osmolality for use in electron microscopy*. Journal of Cell Biology 1965;27:137-9.
- [78] Kools W. *Membrane formation by phase inversion in multicomponent polymer systems. Mechanisms and morphologies*. Thesis - Universiteit Twente, Hoogstraten, Belgium 1998.
- [79] Ahmad A, Yusuf N, Ooi B. *Preparation and modification of poly (vinyl) alcohol membrane: Effect of crosslinking time towards its morphology*. Desalination 2012;287:35-40.
- [80] Yeom C, Lee K. *Pervaporation separation of water-acetic acid mixtures through poly (vinyl alcohol) membranes crosslinked with glutaraldehyde*. Journal of Membrane Science 1996;109:257-65.

- [81] Philipp W, Hsu L. *Three methods for in situ cross-linking of polyvinyl alcohol films for application as ion-conducting membranes in potassium hydroxide electrolyte*. United States Patent 1979.
- [82] Philipp W, Hsu L, Sheibley D. *In situ self cross-linking of polyvinyl alcohol battery separators*. United States Patent 1979.
- [83] Wang Y, Yang H, Xu Z. *Influence of post-treatments on the properties of porous poly (vinyl alcohol) membranes*. Journal of Applied Polymer Science 2008;107:1423-9.
- [84] Sigma-Aldrich. *Sodium sulphate - Safety data sheet*. 2012.
- [85] Büchel K, Moretto H, Werner D. *Industrial inorganic chemistry - 2nd edition*. Germany: John Wiley & Sons, 2008.
- [86] RSC - Chemistry World.
<http://www.rsc.org/chemistryworld/2015/07/sodium-sulfate-sal-mirabilis-podcast>
Last access 21 Oct 2015. 2015.
- [87] Kenichi T, Tetsuro O. *Wet spinning polyvinyl alcohol process*. United States Patent 1961.
- [88] Teruo S, Sadamaru M. *Method for preparing polyvinyl alcohol fibers employing wet spinning techniques*. United States Patent 1963.
- [89] Yamagata et al. *Process for separating polyvinyl alcohol from its solution*. United States Patent 1978.
- [90] Idris A, Zain NA, Suhaimi M. *Immobilization of Baker's yeast invertase in PVA–alginate matrix using innovative immobilization technique*. Process Biochemistry 2008;43:331-8.
- [91] Pham D, Bach L. *Immobilized bacteria by using PVA (Polyvinyl alcohol) crosslinked with sodium sulfate*. International Journal of Science and Engineering 2014;7:41-7.
- [92] Takei T, Ikeda K, Ijima H, Yoshida M, Kawakami K. *A comparison of sodium sulfate, sodium phosphate, and boric acid for preparation of immobilized Pseudomonas putida F1 in poly (vinyl alcohol) beads*. Polymer Bulletin 2012;69:363-73.
- [93] Takei T, Ikeda K, Ijima H, Kawakami K. *Fabrication of poly (vinyl alcohol) hydrogel beads crosslinked using sodium sulfate for microorganism immobilization*. Process Biochemistry 2011;46:566-71.
- [94] Zain N, Suhaimi M, Idris A. *Development and modification of PVA–alginate as a suitable immobilization matrix*. Process Biochemistry 2011;46:2122-9.

- [95] Curley C, Hayes J, Rowan N, Kennedy J. *An evaluation of the thermal and mechanical properties of a salt-modified polyvinyl alcohol hydrogel for a knee meniscus application*. Journal of the Mechanical Behavior of Biomedical Materials 2014;40:13-22.
- [96] Kim K, Lee S, Han N. *Kinetics of crosslinking reaction of PVA membrane with glutaraldehyde*. Korean Journal of Chemical Engineering 1994;11:41-7.
- [97] Wang Y, Hsieh Y. *Crosslinking of polyvinyl alcohol (PVA) fibrous membranes with glutaraldehyde and PEG diacylchloride*. Journal of Applied Polymer Science 2010;116:3249-55.
- [98] Mallapragada S, Peppas N, Colombo P. *Crystal dissolution-controlled release systems. II. Metronidazole release from semicrystalline poly (vinyl alcohol) systems*. Journal of Biomedical Materials Research 1997;36:125-30.
- [99] Lebedeva V, Distler G, Kortukova YI. *A study of the crystallization of polyvinylalcohol films*. Polymer Science USSR 1968;9:2343-51.
- [100] Mallapragada S, Peppas N. *Dissolution mechanism of semicrystalline poly (vinyl alcohol) in water*. Journal of Polymer Science Part B Polymer Physics 1996;34:1339-46.
- [101] Pavlidou S, Papaspyrides CD. *A review on polymer-layered silicate nanocomposites*. Progress in Polymer Science 2008;33:1119-98.
- [102] Olad A. *Polymer/Clay nanocomposites* . In: Reddy B, editor. Advances in diverse industrial applications of nanocomposites. Croatia: InTech, 2011. p. 113-38.
- [103] Hatzigrigoriou NB, Papaspyrides CD. *Nanotechnology in plastic food-contact materials*. Journal of Applied Polymer Science 2011;122:3720-39.
- [104] Millot G, Farrand W, Paquet H. *Geology of clays: weathering, sedimentology, geochemistry*. Berlin: Springer Berlin Heidelberg, 1970.
- [105] Okamoto M. *Biodegradable polymer/layered silicate nanocomposites: a Review*. In: Mallapragada KS, Narasimhan B, editors. Handbook of Biodegradable Polymeric Materials and Their Applications. USA: American Scientific, 205. p. 1-45.
- [106] Duncan T. *Applications of nanotechnology in food packaging and food safety: Barrier materials, antimicrobials and sensors*. Journal of Colloid and Interface Science 2011;363:1-24.
- [107] Choudalakis G, Gotsis A. *Permeability of polymer/clay nanocomposites: A review*. European Polymer Journal 2009;45:967-84.

- [108] Strawhecker K, Manias E. *Structure and properties of poly(vinyl alcohol)/Na montmorillonite nanocomposites*. Chemistry of Materials 2000;12:2943-9.
- [109] Chang J, Jang T, Ihn K, Lee W, Sur G. *Poly(vinyl alcohol) nanocomposites with different clays: pristine clays and organoclays*. Journal of Applied Polymer Science 2003;90:3208-14.
- [110] Strawhecker K, Manias E. *Nanocomposites based on water soluble polymers and unmodified smectite clays*. In: Mai Y, Yu Z, editors. Polymer Nanocomposites. USA: Woddhead Publishing Limited, 2006. p. 206.
- [111] Corobea MC, Donescu D, Petcu C, Radovici C, Serban S, Constantinescu E, Miculescu M. *Polyvinyl alcohol - Na montmorillonite nanocomposites films obtained by solution intercalation*. Journal of Optoelectronics and Advanced Materials 2007;9:3358-60.
- [112] Alexandre M, Dubois P. *Polymer-layered silicate nanocomposites: preparation, properties and uses of a new class of materials*. Materials Science and Engineering: R: Reports 2000;28:1-63.
- [113] Bharadwaj R. *Modeling the barrier properties of polymer-layered silicate nanocomposites*. Macromolecules 2001;34:9189-92.
- [114] Grunlan J, Grigorian A, Hamilton C, Mehrabi A. *Effect of clay concentration on the oxygen permeability and optical properties of a modified poly (vinyl alcohol)*. Journal of Applied Polymer Science 2004;93:1102-9.
- [115] Nielsen LE. *Models for the permeability of filled polymer systems*. Journal of Macromolecular Science—Chemistry 1967;1:929-42.
- [116] Breen A, Breen C, Clegg F, Döppers L, Labet M, Sammon C, Yarwood J. *FTIR-ATR studies of the sorption and diffusion of acetone: water mixtures in poly (vinyl alcohol)-clay nanocomposites*. Polymer 2012;53 (20):4420-8.
- [117] Yeh J, Yu M, Liou S. *Dehydration of water–alcohol mixtures by vapor permeation through PVA/clay nanocomposite membrane*. Journal of Applied Polymer Science 2003;89:3632-8.
- [118] Mahdavi H, Mirzadeh H, Zohuriaan-Mehr M, Talebnezhad F. *Poly (vinyl alcohol)/chitosan/clay nano-composite films*. Journal of American Science 2013;9:203-14.
- [119] British Standard. *Determination of water vapour transmission rate (dish method); BS 2782-8 : Method 820A*. 1996.
- [120] British Standard. *Method for determining the permeability to water vapour of flexible sheet materials used for packaging; BS 3177 : 1959*. 1959.

- [121] Machine Applications Corporation. *The humidity/moisture handbook*. Ohio, USA, 2011.
- [122] Mo C, Yuan W, Lei W, Shijiu Y. *Effects of temperature and humidity on the barrier properties of biaxially-oriented polypropylene and polyvinyl alcohol films*. *Journal of Applied Packaging Research* 2014;6:5.
- [123] Comyn J. *Polymer permeability*. London: Chapman and Hall, 1985.
- [124] British Standard. *Paper, board and pulps — Standard atmosphere for conditioning and testing and procedure for monitoring the atmosphere and conditioning of samples. BS EN 20187:1993*. 1993.
- [125] Farid O. *Investigating membrane selectivity based on polymer swelling*. Thesis - University of Nottingham 2010.
- [126] Larkin P. *Infrared and Raman spectroscopy: principles and spectral interpretation*. The United States: Elsevier, 2011.
- [127] PerkinElmer. *Brochure: FT-IR Spectroscopy—Attenuated total reflectance (ATR)*. 2005.
- [128] Lewis I, Edwards H editors. *Handbook of Raman spectroscopy: from the research laboratory to the process line*. America: CRC Press, 2001.
- [129] Whitson C. *Analytical chemistry by open learning, x-ray methods*. England: John Wiley & Sons, 1987.
- [130] Tadokoro H. *Structure of crystalline polymers*. New York: Wiley, 1979.
- [131] Dodd J, Tonge K, Currell B. *Thermal Methods: Analytical Chemistry by Open Learning*. England: John Wiley & Sons, 1987.
- [132] Widmann G. *Brochure: TA Tip - Interpreting TGA curves*. 2001.
- [133] Price D, Hourston D, Dumont F. *Thermogravimetry of polymers*. In: Meyers RA, editor. *Encyclopedia of Analytical Chemistry*. Chichester, UK: John Wiley & Sons Ltd, 2000. p. 8094-105.
- [134] Menard K. *Dynamic mechanical analysis: a practical introduction*. The United States: CRC LLC, 2008.
- [135] PerkinElmer. *Brochure: Introduction to Dynamic Mechanical Analysis (DMA) A Beginner's Guide*. 2008.
- [136] KRUSS. <http://www.kruss.de/services/education-theory/glossary/contact-angle/>
Last access 06 May 2015. ;2015.

[137] Yuan Y, Lee T. *Contact angle and wetting properties*. In: Bracco G, Holst B, editors. *Surface science techniques*. Berlin Heidelberg: Springer-Verlag, 2013. p. 3-34.

[138] KRUSS. <http://www.kruss.de/services/education-theory/glossary/drop-shape-analysis/>

Last access 07 May 2015. ;2015.

[139] Duan Z, Thomas NL. *Water vapour permeability of poly (lactic acid): Crystallinity and the tortuous path model*. *Journal of Applied Physics* 2014;115:064903.

[140] Gardon J. *Encyclopedia of polymer science and technology*. Mark, HF 1965:833-63.

[141] Sangaj N, Malshe V. *Permeability of polymers in protective organic coatings*. *Progress in Organic Coatings* 2004;50:28-39.

[142] Ashley RJ. *Permeability and plastic packaging*. In: Comyn J, editor. *Polymer Permeability*. London: Chapman and Hall, 1985. p. 269-308.

[143] Islam M, Buschatz H. *Assessment of thickness-dependent gas permeability of polymer membranes*. *Indian Journal of Chemical Technology* 2005;12:88-92.

[144] Han H, Gryte C, Ree M. *Water diffusion and sorption in films of high-performance poly (4, 4'-oxydiphenylene pyromellitimide): effects of humidity, imidization history and film thickness*. *Polymer* 1995;36:1663-72.

[145] Yang D, Koros W, Hopfenberg H, Stannett V. *The effects of morphology and hygrothermal aging on water sorption and transport in Kapton[®] polyimide*. *Journal of Applied Polymer Science* 1986;31:1619-29.

[146] Xianda Y, Anlai W, Suqin C. *Water-vapor permeability of polyvinyl alcohol films*. *Desalination* 1987;62:293-7.

[147] Mark J. *Polymer data handbook*. New York: Oxford University Press, 2009.

[148] Lange J, Wyser Y. *Recent innovations in barrier technologies for plastic packaging—a review*. *Packaging Technology and Science* 2003;16:149-58.

[149] Diversified Enterprises.

http://www.accudynetest.com/polytable_03.html?sortby=contact_angle

Last access 9 June 2015. 2015.

[150] Nechifor C, Ciobanu C, Dorohoi D, Ciobanu C. *Polymeric films properties of poly (vinyl alcohol) and poly (hydroxy urethane) in different concentrations*. *UPB Scientific Bulletin Series A* 2009;71:97-106.

- [151] Pique T, Pérez C, Alvarez V, Vázquez A. *Water soluble nanocomposite films based on poly (vinyl alcohol) and chemically modified montmorillonites*. Journal of Composite Materials 2014;48:545-53.
- [152] Buslov D, Sushko N, Tretinnikov O. *IR investigation of hydrogen bonds in weakly hydrated films of poly (vinyl alcohol)*. Polymer Science Series A 2011;53:1121-7.
- [153] Mansur H, Sadahira C, Souza A, Mansur AA. *FTIR spectroscopy characterization of poly (vinyl alcohol) hydrogel with different hydrolysis degree and chemically crosslinked with glutaraldehyde*. Materials Science and Engineering: C 2008;28:539-48.
- [154] Thermo Electron Corporation.. *OMNIC User's guide Version 7.3*. The United States of America: Thermo Electron Corporation, Madison WI 53711, 2006.
- [155] de Aragão B, Messaddeq Y. *Peak separation by derivative spectroscopy applied to FTIR analysis of hydrolized silica*. Journal of the Brazilian Chemical Society 2008;19:1582-94.
- [156] O'Haver T. *A pragmatic introduction to signal processing*. [Http://terpconnect.Umd.edu/~toh/spectrum/TOC.Html](http://terpconnect.Umd.edu/~toh/spectrum/TOC.Html) 1997.
- [157] Liang C, Pearson F. *Approximate normal vibrations of crystalline polyvinyl alcohol*. Journal of Polymer Science 1959;35:303-7.
- [158] Thomas P, Stuart B. *A Fourier transform Raman spectroscopy study of water sorption by poly (vinyl alcohol)*. Spectrochimica Acta Part A: Molecular and Biomolecular Spectroscopy 1997;53:2275-8.
- [159] Iwamoto R, Miya M, Mima S. *Determination of crystallinity of swollen poly (vinyl alcohol) by laser Raman spectroscopy*. Journal of Polymer Science: Polymer Physics Edition 1979;17:1507-15.
- [160] Badr Y, Abd El-Kader K, Khafagy RM. *Raman spectroscopic study of CdS, PVA composite films*. Journal of Applied Polymer Science 2004;92:1984-92.
- [161] HORIBA Jobin Yvon. *Brochure: Raman data and analysis - Raman Spectroscopy for Analysis and Monitoring*. 2014.
- [162] Martinelli A, Matic A, Jacobsson P, Börjesson L, Navarra M, Fernicola A, Panero S, Scrosati B. *Structural analysis of PVA-based proton conducting membranes*. Solid State Ionics 2006;177:2431-5.
- [163] Li C, Vongsvivut J, She X, Li Y, She F, Kong L. *New insight into non-isothermal crystallization of PVA-graphene composites*. Physical Chemistry Chemical Physics 2014;16:22145-58.

- [164] Socrates G. *Infrared and Raman characteristic group frequencies: tables and charts*. England: John Wiley & Sons, 2004.
- [165] Mansur H, Orefice R, Mansur AA. *Characterization of poly (vinyl alcohol)/poly (ethylene glycol) hydrogels and PVA-derived hybrids by small-angle X-ray scattering and FTIR spectroscopy*. *Polymer* 2004;45:7193-202.
- [166] Ricciardi R, Auriemma F, De Rosa C, Lauprêtre F. *X-ray diffraction analysis of poly(vinyl alcohol) hydrogels, obtained by freezing and thawing techniques*. *Macromolecules* 2004;37:1921-7.
- [167] Peng Z, Kong L. *A thermal degradation mechanism of polyvinyl alcohol/silica nanocomposites*. *Polymer Degradation and Stability* 2007;92:1061-71.
- [168] PerkinElmer. *Brochure: Dynamic Mechanical Analysis Basics: Part 2 Thermoplastic Transitions and Properties*. 2007.
- [169] Cendoya I, López D, Alegría A, Mijangos C. *Dynamic mechanical and dielectrical properties of poly (vinyl alcohol) and poly (vinyl alcohol)-based nanocomposites*. *Journal of Polymer Science Part B: Polymer Physics* 2001;39:1968-75.
- [170] Peng Z, Kong L, Li S. *Dynamic mechanical analysis of polyvinylalcohol/silica nanocomposite*. *Synthetic Metals* 2005;152:25-8.
- [171] Pshezhetskii V, Rakhnyanskaya A, Gaponenko I, Nalbandyan YE. *A differential scanning calorimetry study of polyvinyl alcohol*. *Polymer Science USSR* 1990;32:722-6.
- [172] Zhang Y, Cremer P. *Interactions between macromolecules and ions: the Hofmeister series*. *Current Opinion in Chemical Biology* 2006;10:658-63.
- [173] Betzabe Gonzalez-Campos J, Garcia-Carvajal Z, Prokhorov E, Luna-Barcenas JG, Mendoza-Duarte M, Lara-Romero J, del Rio R, Sanchez I. *Revisiting the thermal relaxations of poly (vinyl alcohol)*. *Journal of Polymer Science* 2012;125:4082-90.
- [174] Nishio Y, Manley RJ. *Cellulose-poly (vinyl alcohol) blends prepared from solutions in N, N-dimethylacetamide-lithium chloride*. *Macromolecules* 1988;21:1270-7.
- [175] George S, Thomas S. *Transport phenomena through polymeric systems*. *Progress in Polymer Science* 2001;26:985-1017.
- [176] Berens A, Hopfenberg H. *Diffusion of organic vapors at low concentrations in glassy PVC, polystyrene, and PMMA*. *Journal of Membrane Science* 1982;10:283-303.

- [177] Rosen S. *Fundamental principles of polymeric materials*. USA: John Wiley & Sons, 1982.
- [178] Meares P. *Polymers: structure and bulk properties*. England: Van Nostrand Reinhold, 1965.
- [179] Lim M, Kim D, Han H, Khan S, Seo J. *Water sorption and water-resistance properties of poly (vinyl alcohol)/clay nanocomposite films: Effects of chemical structure and morphology*. *Polymer Composites* 2015;36:660-7.
- [180] Madejová J. *FTIR techniques in clay mineral studies*. *Vibrational Spectroscopy* 2003;31:1-10.
- [181] Schroeder P. *Infrared spectroscopy in clay science*. In: Rule A., Guggenheim S., editors. *Clay Minerals Society Workshop Lectures*. USA: The Clay Mineral Society, 2002. p. 181-206.
- [182] Bora M, Ganguli J, Dutta D. *Thermal and spectroscopic studies on the decomposition of [Ni {di (2-aminoethyl) amine} 2]-and [Ni (2, 2': 6', 2''-terpyridine) 2]-Montmorillonite intercalated composites*. *Thermochimica Acta* 2000;346:169-75.
- [183] Leite I, Soares A, Carvalho L, Raposo C, Malta O, Silva S. *Characterization of pristine and purified organobentonites*. *Journal of Thermal Analysis and Calorimetry* 2010;100:563-9.
- [184] Kevadiya BD, Patel HA, Joshi GV, Abdi SH, Bajaj HC. *Montmorillonite-Alginate composites as a drug delivery system: Intercalation and in vitro release of diclofenac sodium*. *Indian J Pharm Sci* 2010;72:732-7.
- [185] Silva S, Braga C, Fook M, Raposo C, Carvalho L, Canedo E. *Application of infrared spectroscopy to analysis of chitosan/clay nanocomposites*. In: Prof. Theophile T, editor. *Infrared Spectroscopy-Materials Science, Engineering and Technology*. Croatia: InTech, 2012. p. 43-62.
- [186] Gaume J, Taviot-Gueho C, Cros S, Rivaton A, Therias S, Gardette J. *Optimization of PVA clay nanocomposite for ultra-barrier multilayer encapsulation of organic solar cells*. *Solar Energy Mater Solar Cells* 2012;99:240-9.
- [187] Frost R, Rintoul L. *Lattice vibrations of montmorillonite: an FT Raman and X-ray diffraction study*. *Applied Clay Science* 1996;11:171-83.
- [188] Yang C, Lee Y, Yang J. *Direct methanol fuel cell (DMFC) based on PVA/MMT composite polymer membranes*. *Journal of Power Sources* 2009;188:30-7.
- [189] Ray S, Okamoto M. *Polymer/layered silicate nanocomposites: a review from preparation to processing*. *Progress in Polymer Science* 2003;28:1539-641.

- [190] Sancha R, Bajpai J, Bajpai A. *Studies on transport of vapor and solute molecules through polyvinyl alcohol-based clay containing nanocomposites*. Polymer Composites 2011;32:537-45.
- [191] Döppers L, Breen C, Sammon C. *Diffusion of water and acetone into poly (vinyl alcohol)-clay nanocomposites using ATR-FTIR*. Vibrational Spectroscopy 2004;35:27-32.
- [192] Yu Y, Lin C, Yeh J, Lin W. *Preparation and properties of poly (vinyl alcohol)-clay nanocomposite materials*. Polymer 2003;44:3553-60.
- [193] Ogata N, Kawakage S, Ogihara T. *Poly (vinyl alcohol)-clay and poly (ethylene oxide)-clay blends prepared using water as solvent*. Journal of Applied Polymer Science 1997;66:573-81.
- [194] Shameli K, Bin Ahmad M, Jazayeri S, Sedaghat S, Shabanzadeh P, Jahangirian H, Mahdavi M, Abdollahi Y. *Synthesis and characterization of polyethylene glycol mediated silver nanoparticles by the green method*. International Journal of Molecular Sciences 2012;13:6639-50.
- [195] Kumar T. *Fourier transform infrared spectrometric determination of polyethylene glycol in high-density polyethylene*. Analyst 1990;115:1597-9.
- [196] Yamini D, Venkatasubbu GD, Kumar J, Ramakrishnan V. *Raman scattering studies on PEG functionalized hydroxyapatite nanoparticles*. Spectrochimica Acta Part A: Molecular and Biomolecular Spectroscopy 2014;117:299-303.
- [197] Jin Y, Sun M, Mu D, Ren X, Wang Q, Wen L. *Investigation of PEG adsorption on copper in Cu²⁺-free solution by SERS and AFM*. Electrochim Acta 2012;78:459-65.
- [198] Krishnan K, Krishnan R. *Raman and infrared spectra of ethylene glycol*. Proceedings of the Indian Academy of Sciences, Section A 1966;64:111-22.
- [199] Kozielski M. *Characterization of materials by Raman scattering*. ACTA PHYSICA POLONICA SERIES A 2007;111:343.
- [200] Koenig J, Angood A. *Raman spectra of poly (ethylene glycols) in solution*. Journal of Polymer Science Part A-2: Polymer Physics 1970;8:1787-96.
- [201] Gnanou Y, Fontanille M. *Organic and physical chemistry of polymers*. USA: John Wiley & Sons, 2008.
- [202] Woishnis W, Ebnesajjad S. *PDL handbook: Chemical resistance of thermoplastics*. USA: Elsevier, 2011.
- [203] Stevens M. *Polymer chemistry*. New York: Oxford University Press, 1990.

[204] Clegg F, Breen C, Khairuddin. *Synergistic and Competitive Aspects of the Adsorption of Poly (ethylene glycol) and Poly (vinyl alcohol) onto Na-Bentonite*. The Journal of Physical Chemistry B 2014;118:13268-78.

[205] Khairuddin. *Clay-poly(vinyl alcohol) nanocomposites: Competitive adsorption of poly(vinyl alcohol) and plasticisers onto Na-bentonite*. Thesis - Sheffield Hallam University 2011.

[206] Yang C. *Synthesis and characterization of the cross-linked PVA/TiO₂ composite polymer membrane for alkaline DMFC*. Journal of Membrane Science 2007;288:51-60.

[207] Gilman JW, VanderHart DL, Kashiwagi T. *Thermal decomposition chemistry of poly (vinyl alcohol)*. ACS Symposium Series 1994;599:161-85.

[208] Holland B, Hay J. *The thermal degradation of poly (vinyl alcohol)*. Polymer 2001;42:6775-83.

[209] Fischer H, Gielgens L, Koster T. *Nanocomposites from polymers and layered minerals*. Acta Polymerica 1999;50:122-6.

Calculations for determining the crosslinking solution volume and degree of crosslinking

A1.1 Crosslinking solution volume for crosslinking reaction

The desired amount of crosslinking solution used for each crosslinking reaction was calculated based on the ratio of PVOH repeat unit ($-\text{CH}_2-\text{CHOH}-$) to glutaraldehyde (GA) and the initial weight of PVOH films taken before the reaction [1]

According to the equation of the crosslinking reaction between PVOH and GA, four hydroxyl groups or four repeat units of PVOH react with one GA molecule (Fig. 2.5)

Symbols

m_{PVOH} - Mass of PVOH (dry film)

M_{unit} - The molar mass of one repeat unit ($-\text{CH}_2-\text{CHOH}-$) of PVOH, which has a value of 44.

n_{PVOH} - The number of moles of untreated PVOH (dry film), equal to the total ($-\text{CH}_2-\text{CHOH}-$) repeat units in the film

$$n_{\text{PVOH}} = \frac{m_{\text{PVOH}}}{M_{\text{unit}}} = \frac{m_{\text{PVOH}}}{44} \quad (1)$$

n_{GA} - The number of moles of GA in the crosslinking solution

$C_{\text{M(GA)}}$ - Concentration of GA in the crosslinking solution, which has a value of 0.03 mol/L

V_{CR} - The required volume of crosslinking solution

$$V_{\text{CR}} = \frac{n_{\text{GA}}}{C_{\text{M(GA)}}} = \frac{n_{\text{GA}}}{0.03} \quad (2)$$

❖ For a ($-\text{CH}_2-\text{CHOH}-$) repeat unit/ GA ratio = 4/1, the $n_{\text{GA}} = n_{\text{PVOH}} / 4$

$$V_{CR} = \frac{m_{PVOH}}{44 \times 4 \times 0.03} = 189 \times m_{PVOH} \text{ (mL)} \quad (3)$$

❖ For a (-CH₂-CHOH-) repeat unit/ GA ratio = 4/0.5, the $n_{GA} = (n_{PVOH} \times 0.5)/4$

$$V_{CR} = \frac{0.5 \times m_{PVOH}}{44 \times 4 \times 0.03} = 94.5 \times m_{PVOH} \text{ (mL)} \quad (4)$$

❖ For a (-CH₂-CHOH-) repeat unit/ GA ratio = 4/2, the $n_{GA} = (n_{PVOH} \times 2)/4$

$$V_{CR} = \frac{2 \times m_{PVOH}}{44 \times 4 \times 0.03} = 378 \times m_{PVOH} \text{ (mL)} \quad (5)$$

A1.2 Degree of crosslinking

The degree of crosslinking between PVOH films with GA is defined in terms of the number of moles of hydroxyl groups or repeat units in the PVOH films:

$$d_{CR} = \frac{n_{OH}^0 - n_{OH}}{n_{OH}^0} \times 100 \quad (6)$$

Where:

d_{CR} - degree of crosslinking

n_{OH}^0 - the number of moles of hydroxyl groups in PVOH film before the crosslinking reaction

n_{OH} - the remaining number of moles of hydroxyl groups in PVOH film after the crosslinking reaction

Therefore, $(n_{OH}^0 - n_{OH})$ is the number of moles of O-H groups consumed by GA during the crosslinking reaction, which is 4 times higher than the number of moles of GA used, if both aldehyde groups are consumed in the reaction.

Thus

$$\begin{aligned}
n_{\text{OH}}^0 - n_{\text{OH}} &= 4 \times (\text{number of moles of consumed GA}) \\
&= 4 \times \frac{\text{mass of consumed GA}}{\text{molar mass of GA}} \\
n_{\text{OH}}^0 - n_{\text{OH}} &= 4 \times \frac{\text{mass of consumed GA}}{100.12} \quad (7)
\end{aligned}$$

Assuming that no PVOH was lost during the crosslinking reaction due to dissolution, which is unexpected, the increase in weight of PVOH films after the crosslinking reaction is equal to the amount of GA consumed in the reaction.

Thus

Mass of consumed GA = weight increase of PVOH films

$$\Delta m = m - m^0$$

Where m^0 and m are masses of PVOH film before and after crosslinking reaction

From Eqs. (6) and (7),

$$d_{\text{CR}} = \frac{4 \times \left(\frac{\Delta m}{100.12} \right)}{\left(\frac{m^0}{44} \right)} \times 100 \quad (8)$$

Where 44 and 100.12 are the molecular masses of one PVOH repeat unit ($-\text{CH}_2-\text{CHOH}-$) and GA, respectively.

Since the PVOH films were dried in an oven at 40°C for 48 hours after the crosslinking reaction, they contained almost no water. However, the initial weight of PVOH film prior to crosslinking, m^0 , did not take into account the mass of water present in the films. According to TGA data, after drying at 40°C for 3 hours, the average amount of water present in PVOH films is ~ 4.8 wt%. Therefore, the actual value of PVOH mass before the crosslinking reaction was $0.952 \times m^0$.

From the Eq. (8), we have the degree of crosslinking:

$$d_{CR} = \frac{4 \times \left(\frac{\Delta m}{100.12} \right)}{\left(\frac{(1 - 0.048) \times m^0}{44} \right)} \times 100 \quad (9)$$

REFERENCE

- [1] Kim K, Lee S, Han N. *Effects of the degree of cross-linking on properties of poly(vinyl alcohol) membranes*. Polymer Journal 1993;25:1295-302.

APPENDIX 2

Permeability coefficient calculation

$$P = \frac{(\text{Water vapour transmission rate}) \times (\text{Film thickness})}{\text{Driving pressure}} \quad (1)$$

Or

$$P = (\text{WVTR}) \times \frac{\ell}{(p_1 - p_2)} \quad (2)$$

Where

- P permeability coefficient
- WVTR water vapour transmission rate
- ℓ film thickness
- p_1 pressure of water vapour in the environment on the top side of the film.
- p_2 pressure of water vapour in the under side of the tested film within the Payne cup.

As the water vapour transmission rate analyses were conducted in a large humidity chamber, the water vapour pressure in the under side of the film in the Payne cup was negligible in comparison with the water vapour pressure of the testing environment, i.e. $p_2 \rightarrow 0$.

To calculate p_1 , the equation using the relative humidity is used:

$$\text{RH}(\%) = \frac{p_1}{p_s} \times 100 \quad (3)$$

Where p_s = pressure of saturated water vapour at the experiment temperature, which can be found using tabulated data, i.e. in the CRC Handbook of Chemistry

and Physics [1]. If the data at a desired temperature is not provided, the saturated water vapour pressure can be calculated based on the interpolation method.

For example, the pressure of saturated water vapour at different temperatures is provided below:

Temperature (°C)	20	25	30	40
Pressure (MPa)	2.339×10^{-3}	3.167×10^{-3}	4.247×10^{-3}	7.385×10^{-3}

By interpolation, the pressure of saturated water vapour at 23°C has a value of 2.974×10^{-3} MPa.

Therefore, if the WVTR test is conducted at 23°C, 85% RH, the water vapour pressure is obtained from Eq. (3), which is $p_1 (=0.85 \times p_s) = 2.528 \times 10^{-3}$ MPa.

Then Eq.(2) is used to calculate the permeability coefficient if the WVTRs and film thicknesses are known.

REFERENCE

[1] Haynes W editor. *CRC Handbook of Chemistry and Physics, 94th Edition*. The United States: CRC Press, 2013.

APPENDIX 3

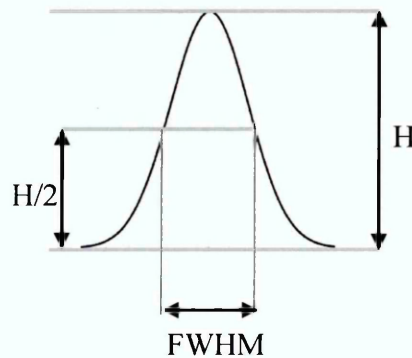
Crystallite size calculation

Crystallite sizes of PVOH and its modified films were calculated using XRD diffractograms and Scherrer's equation [1]:

$$L = \frac{K \times \lambda}{FWHM \times \cos(\theta)} \quad (1)$$

Where

- L crystallite size (diameter of crystallite), in Å
- λ X-ray wavelength, here $\lambda = 1.54$ Å (Cu-tube)
- θ Bragg angle, in *degrees*
- FWHM full width at half maximum for the corresponding peak, in *radians*. FWHM was calculated based on the original XRD diffractogram using X'pert Data Viewer software.



K - a Scherrer constant. The value of K varies depending on the how the peak width is defined, the crystallite shape and the crystallite-size distribution [2]. As Bunn [3] reported the monoclinic structure of unit cells of PVOH, it can be assumed that the PVOH crystal is spherical in shape with cubic symmetry. In this case the common value for K is 0.9 [1].

REFERENCES

- [1] Waseda Y, Matsubara E, Shinoda K. *X-ray diffraction crystallography: introduction, examples and solved problems*. Berlin: Springer, 2011.
- [2] Langford JI, Wilson A. *Scherrer after sixty years: a survey and some new results in the determination of crystallite size*. *Journal of Applied Crystallography* 1978;11:102-13.
- [3] Bunn C. *Crystal structure of polyvinyl alcohol*. *Nature* 1948;161:929-30.